



Grant Agreement No.: 226479

SafeLand

Living with landslide risk in Europe: Assessment,
effects of global change, and risk management strategies

7th Framework Programme
Cooperation Theme 6 Environment (including climate change)
Sub-Activity 6.1.3 Natural Hazards

Deliverable D2.2

Examples of international practice in landslide hazard and risk mapping.
Assessing the state of art of landslide hazard and risk assessment
in the P.R. of China

Work Package 2.1 - Harmonisation and development of procedures for
quantifying landslide hazard

Deliverable/Work Package Leader: ITC

Revision: 1 – draft

October 2010

Rev	Delivery responsible	Controlled by	Date
0	ITC	NGI	JULY 2010
1	ITC	NGI	OCTOBER 2010

SUMMARY

As a contribution to the FP7 SafeLand project which aims to consolidate and developing good practices of landslide risk management in Europe, we organized a workshop in the Chengdu University of Technology on April 13 and 14, 2010, with the aim to assess the state of art of landslide hazard and risk assessment in the P.R. of China. For achieving this objective, Chinese experts in landslide hazard and risk assessment were invited to give presentations and write a chapter for a report which would form one of the deliverables for the EU FP7 SAFELAND project. The report will also be published as a book in China

Note about contributors

The following organisations and individuals contributed to the work described in this deliverable.

Lead partner responsible for the deliverable:

Faculty of Geo-Information Science and Earth Observation (ITC), University of Twente.

Deliverable prepared by:

Cees van Westen (ITC) and

Xuanmei Fan and Runqiu Huang (State Key Laboratory on Geohazard Prevention, Chengdu University of Technology, China).

Partner responsible for quality control:

NGI

Deliverable reviewed by:



UNIVERSITY OF TWENTE.

Faculty of Geo-information Science and Earth Observation,

University of Twente



State Key Laboratory of Geo-hazards Prevention,
Chengdu University of Technology

TABLE OF CONTENTS

CHAPTER 1	GENERAL INTRODUCTION	4
	<i>Cees Van Westen</i>	
1.1	Background	4
1.2	Main objective of the report.....	6
1.3	Chapter content preview	6
CHAPTER 2	LANDSLIDE HAZARDS IN CHINA: AN OVERVIEW	9
	<i>Runqiu Huang</i>	
2.1	Introduction	9
2.2	Distribution of landslides in China	12
2.3	Main triggering factors and typical landslides in China	16
2.4	Genetic mechanism of large-scale landslide in China.....	31
2.5	Landslide risk zoning and mitigation strategies in China	40
2.6	Conclusions	44
CHAPTER 3	LANDSLIDE INVENTORY MAPPING IN CHINA	50
	<i>Shuren Wu, Jusong Shi & Ping Sun</i>	
3.1	Introduction	50
3.2	Landslide inventory mapping projects in China.....	52
3.3	Landslide inventory methods.....	55
3.4	Landslide inventory database	61
3.4	Conclusion and potential challenges	62
CHAPTER 4	REMOTE SENSING APPLICATIONS FOR LANDSLIDE RESEARCH IN CHINA.....	64
	<i>Chuan Tang & Xuanmei Fan</i>	
4.1	Introduction	64
4.2	Application of remote sensing in landslide inventory	65
4.3	Application of remote sensing in large scale landslide study	67
4.4	Application of remote sensing technology in landslide monitoring	70
4.5	Application of remote-sensing in landslide risk assessment	72
4.6	Conclusions	74
CHAPTER 5	MEDIUM AND LARGE SCALE LANDSLIDE HAZARD ASSESSMENT IN CHINA.....	77

Kunlong Yin & Lixia Chen

5.1 Introduction	77
5.2 Terms and basic assumptions	78
5.3 Methods of mathematical models and GIS application.....	78
5.4 Illustrations	84
5.5 Conclusions	98
CHAPTER 6 METHODS FOR LOCAL SCALE HAZARD ASSESSMENT	101

Hengxing Lan, Hongjiang Liu & Shengwen Qi

6.1 Introduction	101
6.2 Methodology.....	102
6.3 A case study	107
6.4 Conclusions and discussions	112
CHAPTER 7 LANDSLIDE EARLY WARNING AND MONITORING.....	115

Qiang Xu

7.1 Introduction	115
7.2 Landslide monitoring in China	116
7.3 Early warning of landslides in China	124
7.4 Conclusions	137
CHAPTER 8 NATURAL TERRAIN LANDSLIDE RISK MANAGEMENT- EXPERIENCE AND PRACTICE IN HONG KONG.....	139

K.C. Ng, K.K.S. Ho & T.H.H. Hui

8.1 Introduction	139
8.2 Hong Kong's Slope Safety System	140
8.3 Landslide Risk Management	142
8.4 Landslide Inventories	144
8.5 Strategy Managing Natural Terrain Risk	147
8.6 Susceptibility and Hazard Zoning	149
8.7 Studies of Notable Natural Terrain Landslides	157
8.8 Rainfall-Landslide Correlations for Natural Terrain	160
8.9 Application of Digital Technology	161
8.10 Natural Terrain Landslide Risk Assessment	163
8.11 Qualitative Risk Assessment	165

8.12 Impetus to the Use of Quantitative Risk Assessment In Hong Kong	170
8.13 Assessment of Mobility of Natural Terrain Landslide Debris.....	173
8.14 Quantification of Landslide Consequence	176
8.15 Global QRA of Natural Terrain Landslides.....	179
8.16 Site-Specific QRA.....	180
8.17 Potential Effects of Climate Change.....	190
8.18 Concluding Remarks.....	191
CHAPTER 9 EARTHQUAKE INDUCED LANDSLIDES: THE CASE OF WENCHUAN EARTHQUAKE	199
<i>Cees van Westen, Tolga Gorum, Xuanmei Fan, Runqiu Huang, Qiang Xu & Gonghui Wang</i>	
9.1 Introduction	199
9.2 Methodology and input data	201
9.3 General Distribution Characteristics of Co-seismic Landslides	207
9.4 Analysis of Relations with Seismic and Geo-environmental Factors	211
CHAPTER 10 DISCUSSION AND CONCLUSIONS	223
<i>Runqiu Huang, Cees van Westen, Xuanmei Fan, Qiang Xu, Niek Rengers, Chuan Tang</i>	
ACKNOWLEDGEMENTS	226
APPENDIX 1 OVERVIEW OF LANDSLIDE ORGANIZATIONS IN CHINA	227
APPENDIX 2 LIST OF WORKSHOP PARTICIPANTS.....	229

CHAPTER 1 GENERAL INTRODUCTION

Cees Van Westen

Faculty of Geo-information Science and Earth Observation, University of Twente, Netherlands

1.1 Background

Landslides represent a major threat to human life, property and constructed facilities, infrastructure and natural environment in most mountainous and hilly regions of the world. Statistics from The Centre for Research on the Epidemiology of Disasters (CRED) show that, on average, landslides are responsible for a small percentage of all fatalities from natural hazards worldwide. The socio-economic impact of landslides is underestimated because landslides are usually not separated from other natural hazard triggers, such as extreme precipitation, earthquakes or floods. This underestimation contributes to reducing the awareness and concern of both authorities and general public about landslide risk. However, events such as the 2008 Wenchuan Earthquake have shown that individual triggering events can cause many victims of landslides. As a consequence of climate change and increase in exposure in many parts of the world, the risk associated with landslides is growing. Climate change, increased susceptibility of surface soil to instability, anthropogenic activities, growing urbanization, uncontrolled land-use and increased vulnerability of population and infrastructure as a result, contribute to the growing landslide risk.

China is a country with regions that have a high landslide risk. Landslides threaten lives and properties in 30 provinces, resulting in an estimated 700 to 1000 deaths and damages of properties exceeding \$10 billion RMB annually. In order to reduce the damage caused by landslides, the Chinese government has taken the following measures since 1999: (1) Nationwide landslide investigation and risk zoning; (2) Detailed mapping for high risk zones of landslide hazards; (3) Stabilization and mitigation on major landslides; (4) Weather-based regional landslide hazard warning; (5) Geohazard risk assessment on infrastructure construction; (6) Education and training for geohazard mitigation.

As a contribution to the FP7 SafeLand project which aims to consolidate and developing good practices of landslide risk management in Europe, we organized a workshop in the Chengdu University of Technology on April 13 and 14, 2010, with the aim to assess the state of art of landslide hazard and risk assessment in the P.R. of China. For achieving this objective, Chinese experts in landslide hazard and risk assessment were invited to give presentations and write a chapter for a report which would form one of the deliverables for the EU FP7 SAFELAND project. The report will also be published as a book in China.

SafeLand is a Large-scale integrating Collaborative research project funded by The Seventh Framework Programme for research and technological development (FP7) of the European Commission. The project team is composed of 25 institutions from 13 European countries. More information can be found on <http://www.safeland-fp7.eu/Introduction.html>.

SafeLand will develop generic quantitative risk assessment and management tools and strategies for landslides at local, regional and European scales and establish the baseline for the

risk associated with landslides in Europe, to improve the ability to forecast landslide hazard and detect hazard and risk zones. Part of the research focuses on reviewing existing landslide databases and proposing improvements for delineating areas at risk in agreement with the EU Soil Thematic Strategy and its associated Proposal for a Soil Framework Directive, and for achieving interoperability and harmonization in agreement with the INSPIRE European Directive.

The definitions of some basic terms that will be used frequently in the following chapters are as below:

Landslide risk: regarding to Varnes (1984)'s definition, it is expressed as "the expected number of lives lost, persons injured, damage to property and disruption of economic activity due to a particular damaging phenomenon or a given area and reference period". When dealing with physical losses, (specific) risk can be quantified as the product of vulnerability, cost or amount of the elements at risk and the probability of occurrence of the event with a given magnitude/intensity;

Landslide hazard: is expressed as probability of occurrence within a reference period (e.g., year, design period of a building). Hazard is a function of the spatial probability, which is actually the **landslide susceptibility** (related to static environmental factors such as slope, strength of materials, depth, etc.) and the temporal probability, related indirectly to some static environmental factors like slope and hydraulic conductivity and directly to dynamic factors like rain input and drainage (van Westen et al., 2005);

Vulnerability: is defined as the degree of loss to a given element or set of elements at risk (see below) resulting from the occurrence of a natural phenomenon of a given magnitude. It is expressed on a scale from 0 (no damage) to 1 (total loss).

There are various methods of landslide hazard and risk assessment, which can be generally classified into qualitative and quantitative, or direct and indirect. Qualitative methods are subjective, ascertain susceptibility heuristically, including direct field geomorphological analysis (Verstappen, 1983) and use of index or parameter maps (also defined as Expert Evaluation Approaches, Leroi (1996); Soeters and Van Westen 1996). Quantitative methods produce numerical estimates, including statistical analysis (bivariate analysis and multivariate analysis, Carrara, 1991; Van Westen et al., 1997, Castellanos Abella and Van Westen, 2008); geotechnical models (deterministic and probabilistic, Chowdhury, 1976; Baldelli et al., 1996; Van Westen et al., 1997); ; and neural networks (Lees, 1996 and Cómez and Kavzoglu, 2005).

There is a need to develop methods for landslide hazard and risk assessment, and landslide risk management that are up to date, effective and uniform. In several parts of the world experts are reviewing the methodology for landslide hazard and risk assessment. For instance in Europe, the Safeland project, funded by the European Commission, is aiming to harmonize such methodology in Europe, and learn from other areas. Also in the P.R. of China there is a need to harmonize the methodology for landslide hazard and risk assessment.

1.2 Main objective of the report

The objective of the report is to assess the state of art of landslide hazard and risk assessment in the P.R. of China. For achieving this objective, we organized a workshop in Chengdu university of Technology on April 13 and 14, 2010. Chinese experts who have a large experience in landslide hazard and risk assessment were invited to give presentations and write a chapter for main aspects of this report. The list of participants is shown in Appendix 2.

Nowadays, various scales of landslide hazard and risk assessment programs or projects are being carried out for different purposes. Nationwide landslide inventory are carried out for creating a comprehensive landslide database, which is very helpful for landslide hazard and risk management. Medium scale landslide hazard and risk assessment are also carried out for landslide prevention and development planning by local authorities. Large scale and detailed landslide investigation and hazard assessment mainly serve for constructions (like hydropower station, railway and highway etc.), mitigation, early warning, etc. The report reviews almost all the aspects with regard to landslide hazard and risk assessment, the ongoing government activities and the latest policies. Topics that are treated are: landslide hazards in China: an overview; landslide inventory mapping in China; Remote Sensing applications for landslide research in China; Medium and large scale landslide hazard assessment in China; Methods for local scale hazard assessment; National scale vulnerability assessment; Landslide early warning and monitoring of landslides; Natural Terrain Landslide Risk Management- Experience and Practice in Hong Kong; Earthquake induced landslides: the case of Wenchuan earthquake. The last chapter "Discussion and conclusions", presents the results of a discussion forum during which the experts were asked to outline their views on how to optimize landslide hazard and risk methodologies in China.

1.3 Chapter content preview

The chapter content preview intends to give you a whole picture of this report.

Chapter 2: Landslide hazards in China: an overview, aims to present the framework of landslide problems in China, socio-economic impact, major events, regions with major landslide problems, main causes and formation mechanism, legislation, organization of landslide institutions and their responsibilities.

Chapter 3: Landslide inventory mapping in China, aims to present the state of the art in the development of landslide inventories. Which types of inventories are available in China, how are they made, how stored, how maintained and who is in charge?

Chapter 4: Remote Sensing applications for landslide research in China, aims to show the applications of Remote Sensing to landslide work in China. Which satellite systems are used, GPS use in landslide studies, InSAR, LiDAR, photogrammetry, automatic landslide mapping, landslide monitoring etc.

Chapter 5: Medium and large scale landslide hazard assessment in China, aims to present the input data requirements and the methods that are used on medium (1:25,000 – 1:100,000)

and large scales (> 1:10,000) to derive landslide susceptibility maps, and hazard maps. The use of physically-based models, use of statistical analysis, run out models, is discussed.

Chapter 6: Methods for local scale hazard assessment, shows the application of physically based models for rockfall hazard and risk assessment.

Chapter 7: Landslide early warning and monitoring of landslides, aims to present an overview of early warning methods that are used for landslide warning, e.g. using weather forecasts, rainfall thresholds, and other methods at regional and large scales, including instrumentation at site investigation level.

Chapter 8: Natural Terrain Landslide Risk Management- Experience and Practice in Hong Kong, comprehensively presents state-of-the-art methods that are applied in Hongkong for landslide susceptibility, hazard zoning, risk assessment and management using qualitative and quantitative methods.

Chapter 9: Earthquake induced landslides: the case of Wenchuan earthquake, presents the results of the work done after the Wenchuan earthquake, in terms of the mapping of the co-seismic landslides, the relation between landslides and seismic, geological and terrain factors and landslide dams.

Chapter 10: Discussion and conclusions, presents the results of a discussion forum during which the experts were asked to outline their views on how to optimize landslide hazard and risk methodologies in China.

Reference

- Baldelli, P., Aleotti, P., Polloni, G., 1996. Landsliding-susceptibility numerical mapping at the Messina Strait crossing site, Italy. In: Proc VII Int Symp on Landslides, Trondheim, June 1996, 1, pp.153–158
- Carrara, A., Cardinali, M., Detti, R., Guzzetti, F., Pasqui, V., Reichenbach, P., 1991. GIS techniques and statistical models in evaluating landslide hazard. *Earth Surface Processes and Landforms*, 16, pp.427–445
- Castellanos Abella, E.A. and Van Westen, C.J., 2008. Qualitative landslide susceptibility assessment by multicriteria analysis: a case study from San Antonio del Sur, Guantánamo, Cuba. *Geomorphology* 94, pp. 453-466
- Chowdhury, R.N., 1976. The Mechanism of Natural Slope Failures in the Greater Wollongong Area of New South Wales. *Search, Sydney*, 7, No.9, pp. 396–97
- Cómez, H. and Kavzoglu, T., 2005. Assessment of shallow landslide susceptibility using artificial neural networks in Jabonosa River Basin, Venezuela. *Engineering Geology* 78, pp.11-27
- Lees, B.G., 1996. Neural networks applications in the geosciences: an introduction. *Computer and Geosciences*, 22, pp.955–957
- Leroi, E., 1996. Landslide hazard – Risk maps at different scales: objectives, tools and developments. In: Proc VII Int Symp Landslides, Trondheim, June 1996, 1, pp. 35–52
- Soeters, R., Van Westen, C.J., 1996. Slope stability: recognition, analysis and zonation. In: Turner AK, Shuster RL (eds) “Landslides: investigation and mitigation”. Transportation Research Board – National Research Council, Special Report 247, pp. 129–177

- Van Westen, C.J., Rengers, N., Terlien, M.T.J. and Soeters, R., 1997. Prediction of the occurrence of slope instability phenomena through GIS-based hazard zonation. *Geologische Rundschau*, 86, pp. 404-414
- Van Westen, C.J., T.W.J. van Asch, and Soeters, R., 2005. Landslide hazard and risk zonation—why is it still so difficult? *Bull Eng Geol Env*, DOI 10.1007/s10064-005-0023-0
- Verstappen, H.T., 1983. *Applied geomorphology: Geomorphological survey for environmental development*. Elsevier Scientific Publishing Co., Amsterdam

CHAPTER 2 LANDSLIDE HAZARDS IN CHINA: AN OVERVIEW

Runqiu Huang

State Key Laboratory of Geohazards Prevention, Chengdu University of Technology, China

2.1 Introduction

Landslides occur frequently and widely distributed in China. There are over one million landslides in China mainland, and most landslides occurred in the first slope-descending zone along the in eastern margin of Tibet plateau and the second slope-descending zone along the Yangtze River. The triggering factor of landslide changes with the areas in China. In southwestern part of China, rainfall is the most important triggering factor. In northwestern part of China, landslides always occur in March or April in early spring, which were mainly induced by snow melting. In the conjunction part of Tibet Plateau and southwestern area, most landslides are triggered by intensive earthquake. In high altitude regions such as Qinghai-Tibet plateau and Tian Mountain in the Xinjiang province, the global climate change cause the temperature and snow line rose and the glacier retrogressed, which are all the triggering factors of landslides. The typical geo-mechanism models of large-scale landslides in rock mass are shown as following: the “three sections” mode (i.e. sliding-tension cracking-shearing), “retaining wall collapse” model, “translational landslide” model in near horizontal strata, large-scale toppling model in counter-inclined strata, and the creep-bending-shearing model, etc.. Each model corresponds to some specific rock structure conditions and deformation processes. China is a high landslide risk country; landslides threaten lives and properties in 30 provinces, resulting in an estimated 700 to 1000 deaths and damages of properties exceeding \$10 billion RMB annually. In order to reduce the damage caused by geohazards, Chinese government has taken the following measures since 1999: (1) Nation-wide landslide investigation and risk zoning; (2) Detailed mapping for high risk zones of landslide hazards; (3) Stabilization and mitigation on major landslides; (4) Weather-based regional landslide hazard warning; (5) Geohazard risk assessment on infrastructure construction; (6) Education and training for geohazard mitigation.

During the last century economic loss and fatalities due to landslides have increased. They are invariably related to unscientific construction activities by human and change in global climate such as El Niño (AU., 1998; Yin et al., 2000; Schuster et al., 2001). In mountainous areas landslides are second most destructive natural hazard after earthquake (Li et al., 1999; United states geological survey, 2000). They are more frequent in young tectonic mountains such as Rocky and Andes mountain chain in American continent (Parise et al., 1999; Collison et al., 2000; Mauritsch et al., 2000; Staub, 2001; Raetzo et al., 2002; Radbruch-Hall et al., 1983), hills of Japan and Taiwan, and Himalayas of South Asia (Yamagishi et al., 2000; Lin et al., 2002; Bhasin et al., 2002).

Since 1980s landslide hazards have increased in China and probably due to the increase of construction activities and the climate change. At present, except Shandong Province, serious landslides happened in all over of China, especially in the Yunnan, Guizhou, Sichuan, Chongqing,

Tibet in Western China; the Western Hubei, western Hunan, Shaanxi, Ningxia and Gansu. The average rate of fatalities caused by landslides is approx.1000 deaths per year during last 20 years. Besides loss of lives, landslides also induced serious losses of infrastructures such as factories, mines, transportation routes, hydropower stations and so on (Li, 1992; Schuster, 1996; Yin, 1999; Wang, 1999; Duan, 2000; Jiang, 2000; Yin, 2001).

Large landslides always caused destructive damages and fatalities, due to their large affected areas and great energy generated by the collapsed rocks that cracked from the native rock, with the high-speed and long run out distance. The landslides also have the “collapse-slide-flow” deformation characteristic (Crosta, 2001, Brückl, 2001). Hence a lot of literatures focus on the large landslide research (Schuster, 1996; Voight et al., 1992; Baum et al., 2001; Wu et al., 1989; Zhong, 1999; Chen et al., 1991; Jin, 1998; Xu et al., 1992; Zhang et al., 2001; Sun, 2000; Yin, 2000; Huang et al., 2005; Lin et al., 2002). For example, Surte soil landslide occurred in September 1950 in Sweden, which destroyed 40 buildings and interrupted the traffic system. Its volume was $400 \times 10^4 \text{ m}^3$. Vaiont reservoir slide in Italy in October 1950 killed 2500 to 2600 people with the total volume of $2.7 \times 10^8 \text{ m}^3$ (Voight et al., 1992). Helens volcano at Washington in United States broke out in May 1980, which caused the large collapse-slide-flow disaster with the total volume of $600 \times 10^4 \text{ m}^3$. Heavy rainfall by Mitch hurricane in August 1998 induced El Berrinche deep-layer landslides on Honduras. Earthquake triggered landslides in Salvador in January and February 2001 with the total volume of $75 \times 10^4 \text{ m}^3$ caused more than 500 fatalities (Baum et al., 2001).

According to the statistic results from China Geology Survey (CGS), there are over one million landslides occurred in China mainland, and among them 34 000 are large-scale ones. Landslides kill hundreds of people and cause over 20 billion RMB economic loss every year. Some of the best known are: earthquake-triggered landslide (1902) in Haiyuan, Ningxia; Diexi landslide along Min river in Sichuan (1933); Lugong, landslide (1965) in Yunan; Jipazi landslide (July, 1983) along Chang river; Saleshan landslide (March, 1983) in Gansu, Xikou landslide (July, 1989) in Huayingshan, Sichuan; Touzhai landslide (September, 1991) in Zhaotong, Yunnan; Laojinshan landslide (June, 1996) in Yuanyang, Yunan; Badu landslide (July, 1997) along the railway from Nanning to Kunming; Yigong landslide (April, 2000) in Bomi, Tibet; Tiantai village landslide (September, 2004) in Sichuan. These were the large landslide with volume of more than $2 \times 10^6 \text{ m}^3$. Table 1 gives details of some of the well known landslides in China.

Table 1 Large-scale catastrophic landslides in China since the 20th Century

Landslide name	Location	Occurrence date	Volume (10^4 m^3)	Slope forming material and type	Triggering factor	Loss
Coseismic landslide	Haiyuan, Ningxia	16.12.1920	-	Loess		675 landslides resulted in 40 slide lakes, many villages destroyed, and 0.1 million fatalities reported
Diexi landslide	Maoxian, Sichuan	25.08.1933	21000	Triassic metamorphic rock	Diexi earthquake	Damage towns and villages, 6800 fatalities, landslide dam failure took 8000 lives
Chana landslide	Gonghe, Qinghai	7.02.1943	25000	Stratum of Tertiary	Thaw	Zana Village destroyed, 114 fatalities

D.2.2: Assessing the State of Art of Landslide Hazard and Risk Assessment in the P.R. of China

Lugong landslide	Gonglu, Yunnan	22.11.1965	39000	Basalt of Permian		5 villages buried, and 444 fatalities
Tanggudong landslide	Along Yalong River, Sichuan	8.06. 1967	6800.0	Weathered slate of Triassic		Damed Yalong River for 9 days, flood of volume 57000 m ³ /s resulted after dam failure
Yanchihe Rock-fall	Yichang, Hubei	03.06. 1980	150.0	Near level layered slope	Underground mining	Destroying mining area, and deaths of 284 persons
Jipazi Landslide	Yunyang, Chongqing	18.07. 1982	1500	colluvial (old slide debris)	Rainstorm	Obstructed Yangtse River -sea route for 7 days, and economic loss of 100 million Yuan
Saleshan landslide	Dongxian, Gansu	07.03.1983	3100	Loess covering, mudstone of Tertiary	freeze-thaw	Death of 237 people
Xietan landslide	Zigui, Chongqing	12.06.1985	3000	Colluvial (old slide debris)	Rainfall	-
Zhongyangcun landslide	Wuxi, Chongqing	10.01.1988	765.0	Limestone	Rainstorm	Deaths of 33 people
Tiexi landslide	Xide, Sichuan	02.09.1988	4.0	Accumulative formation	Rainstorm	train derailed
Xikou landslide	Huaying, Sichuan	10.07.1989	100.0	weathered carbonate rock	Rainstorm	Deaths of 221 persons
Touzhai landslide	Zhaotong, Yunnan	23.09.1991	900	Highly weathered basalt	Long-term creep	Deaths of 216 persons
Jiguanlin Rock-fall	Wulong, Chongqing	30.04.1994	424.0		Underground mining, rainfall	A 10 m high water level fall formed, wave height varied from 1 to 5 m, flow intermitted for half hour, 5 boats sank, direct economic loss was 100 million Yuan.
Huangci landslide	Lanzhou, Gansu	Jan. 1995	200.0	Loess		displaced 1000 people
Erdaogou landslide	Badong, Chongqing	10.06.1995	60.0	high weathered rock	Flood	Deaths of 5 persons
Oldjinshan landslide	Yunyang, Yunnan	01.06.1996	500.0		Mining	Deaths of more than 200 persons
Yankou landslide	Yinjiang, Guizhou	18. 07.1996	1500.0	Layered limestone	Toe removal due to quarrying	65 m high landslide dam created with 8-km-long barrier lake
Shachonglu landslide	Guiyang, Guizhou	04.12.1996	2.0		Toe removal due to slope cutting	35 fatalities
Yigong landslide	Bomi, Tibet	09.04.2000	28000	-	Snow melt	Barrier lake formed, reservoir region submerged
Shuangliu landslide	Shibao, Gulin	06.06.2000	2.0		Rainstorm	Death of 10 persons
Yingjiang landslide	Ying River, Yunnan	14.08.2000	0.2	Mixed granite residual soils	Rainstorm	Death of 13 persons
Lanping landslide	Lanping, Yunnan	03.09.2000	2000		Rainstorm	Displaced 5000 persons
Qianjiangpin landslide	Three Gorges Reservoir	13.07.2003	2400	Sandy layer	Reservoir induced	Death of 14 persons, economic loss of 57350 thousand Yuan

Tiantai village landslide	Xuanhan, Sichuan	05.09.2004	2500	Gentle bedding sandy mudstone slope	Rainstorm	Displaced 1255 persons, 23 m high landslide dam formed along with 20 km long barrier lake
Danba landslide	Danba, Sichuan	March, 2005	220	Accumulative formation landslide	anthropogenic activity	Buildings destroyed, loss of 10.66million Yuan
Wulong landslide	Wulong Chongqing	05.06.2009	500	limestone	anthropogenic activity	10 people died, 64 missing, and 8 wounded

2.2 Distribution of landslides in China

China is a country with a vast mountain area, which occupies 69% of the national land area. Mountainous towns take up around half of the total number of towns in China and mountainous people occupy 50% of the total population. Landslides are widely distributed in the mountainous areas. From Figure 1 about the distribution of landslides from 2004 to 2009 (excluding landslides induced by the Wenchuan Earthquake), we can see that landslides concentrated in the southwestern, northeastern and middle mountainous regions of China, such as Yunnan, Guizhou, Sichuan and Chongqing in the southwestern China; Hunan, Hubei, and Shanxi in the middle China; Zhejiang, Fujian, Guangdong, Guangxi and Anhui in the eastern China. Whereas, there are a small number of landslides occurred in provinces such as Hebei, Shandong, Jiangsu and Xinjiang and Inner Mongolia.

The complex terrain and topography caused a lot of landslides in China. The characteristics of terrain and topography are: the continent of China is composed by the Qinghai-Tibet plateau, Yun-Gui plateau in the west, mountainous area in the middle, and plain near sea in the east, which depict the three-level terrace picture of the terrain in China. The slope-descending zones are formed. The altitude is reduced sharply from the west to the east, especially in the region among the Qinghai-Tibet plateau, Yun-Gui plateau and Sichuan basin. The typical terrain in this region are high mountains and canyons, which are formed by the deep incision of rivers originated from Qinghai-Tibet plateau, such as Jinsha River and its branches (Yalong River, Dadu River, Minjiang River), and Lancang River, Nujiang River.

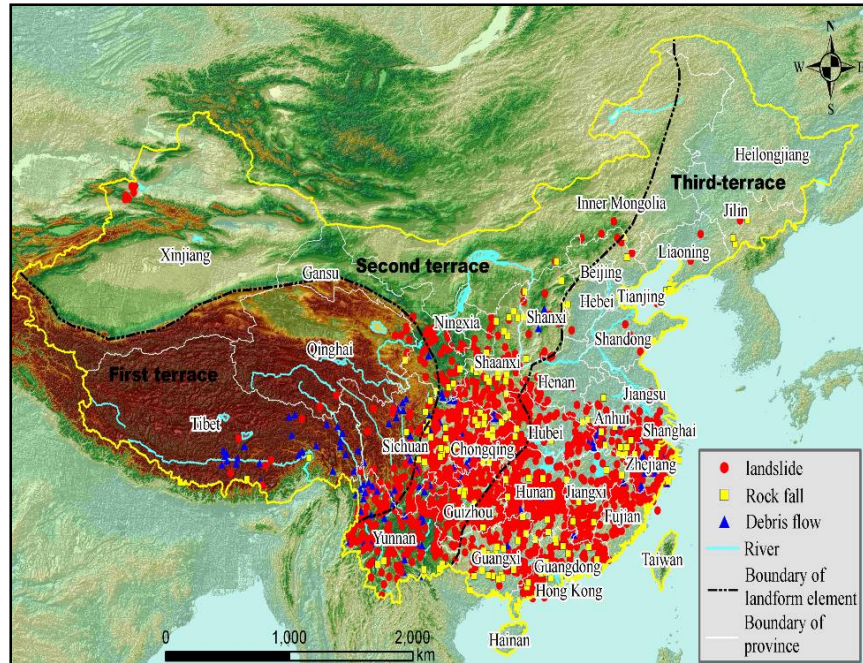


Figure.1 Distribution of landslides occurred during 2004 to 2009 (Landslides induced by Wenchuan Earthquake are not included)

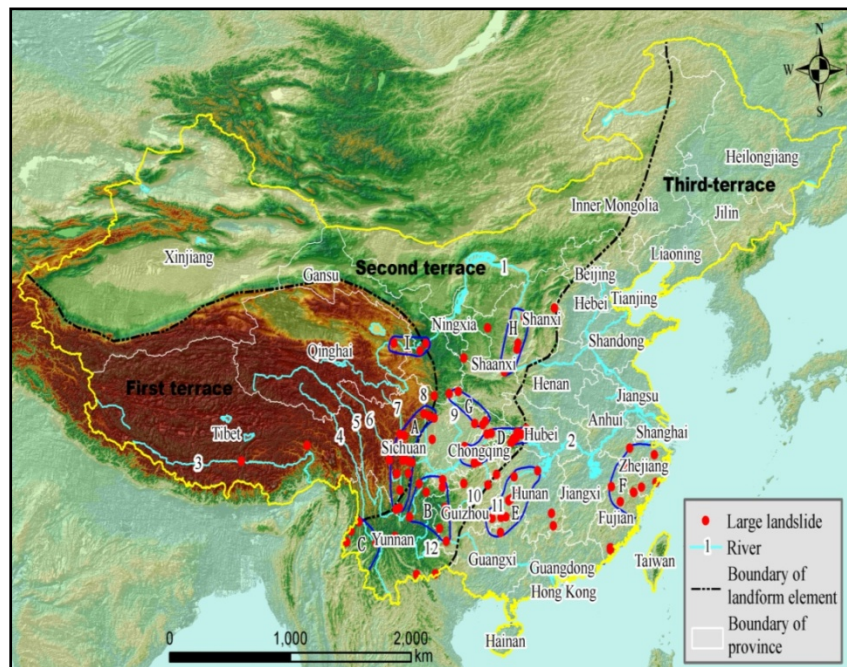


Figure.2 Distribution of catastrophic landslides in China since 20th century (1.Yellow River; 2.Yangtze River; 3.Yarlung Zangbo River; 4.Lantsang River; 5.Jinsha River; 6.Yalong River; 7.Dadu River; 8.Min River; 9.Jialing River; 10.Wu River; 11.Yuan River; 12.Pearl River (Nanpan River) (Landslides triggered by Wenchuan Earthquake are not included)

Figure 2 shows 107 large-scale landslides which had happened since the 20th century, resulting in the casualties of over 10 persons or economic loss of more than 5 million Chinese

Yuan in the mainland of China. It indicates that most large-scale landslides occurred in the first slope-descending zone along the eastern margin of Tibet plateau and the second slope-descending zone along the Yangtze River. In the eastern coast area of China, tropical storms may trigger a large number of landslides, but their scale is quite small. Among the 107 large-scale landslides, 75 landslides (70%) occurred in the first slope-descending zone of continental landform along the eastern margin of Qinghai-Tibet plateau; 17 landslides in the middle Hunan province and the middle mountainous area of Guangxi province; and 13 landslides in the mountainous areas of Zhejiang and Fujian province. Through further analysis, it is found that these landslides are distributed in the following 9 units of different terrain and geology.

A: Western Sichuan Plateau: this region is located between the Qinghai-Tibet Plateau and the Sichuan Basin, being the transitional area from the first step to the second step with the average elevation of 4000 to 4500 meters and the most important morphological mutation belt. It is also the high-frequency of geohazards such as collapses, landslides and debris flows, due to its complex geological structure, intense neotectonic movement and active internal and external motive force. In recent years, with the advance of Western development in China, a large number of hydropower stations and transportation roads are built in this area, inducing and activating many geohazards. The life and property damage caused by geohazards in this area tends to increase. From Figure 3, it is observed that large-scale landslides are mainly distributed in the vicinity of rivers such as the upstream of the Minjiang river and its branches, middle and downstream of the Dadu river and its branches, downstream of the Yalong river as well as middle and downstream of the Jinsha river. The geohazards in this area are featured with large scale and complex mechanism, so it is difficult to prevent and treat them.

B: Yunnan-Guizhou Plateau: this area is located in south-western China, including the eastern Yunnan and the western Guizhou. With the elevation ranging from 1000 to 2000 metres, it belongs to Yangtze platform. The terrain is rugged with high-lying northwest and low southeast. The strong tectonic movement accounts for the high development of geohazards in this region such as collapses, landslides, debris flows and Karst collapses, etc..

C: Western mountainous area in Yunnan: This region belongs to Gondwana Plate, with the average elevation of above 3500 meters. It also belongs to the high and extremely high mountainous zones, through which the deep rivers such Lancangjiang and Nujiang flow. Owing to the complex geological environment, active tectonic movement, great effects of large faults such as Nujiang Fault and Lancangjiang Fault and strong volcanic activity in Cenozoic Era, large-scale geohazards often occurred here. Besides, as this area is rich in water resources, many hydropower stations have been built here this year, producing more risks of geohazards.

D: Three Gorges Reservoir region-western mountainous area in Hubei: this region is situated between Chongqin (in the midstream area of Yantze River) and Yicang city of Hubei. Geohazards mainly develop in the trunk stream of Yantze River and branches of Wujiang and Qingjiang. In recent years, influenced by the water storage of Three Gorges Reservoir, the risks of geohazards tend to increase and many large-scale old landslides have been activated.

E: Western Hunnan-northern Guangxi: this region is in the transition belt between Yun-Gui Plateau and Chiang-nan Hilly Region and also in the transitional zone from the second step

to the third step in topography, with the average elevation between 600 and 1500 meters. Rainstorm is the main triggering factor of landslides in this area and most of the landslides are small-scale landslides.

F: Eastern coastal mountain area: this region contains hill area of southwest Zhejiang province and northeast Fujian province. It belongs to subtropical monsoon climate zone with an annual rainfall of 200-2 200 mm. Landslides occur mainly from July to September because of typhoon.

G: Qinba Mountain area: as the ridge of China's mainland, it played an important role in the formation and evolution of China's mainland. It is also an important weather boundary in China and a typical compound orogenic belt of unique characteristics. Shallow landslides with the maximum depth of 15 to 20 m are widely distributed in this area.

H: Midstream of Yellow river: This region is located in the juncture between the Shanxi and Shaanxi province, belonging to loess hilly terrain. Loess collapses and landslides frequently occurred in this area.

I: Upstream of Yellow River: this region is located at the border of the Qinghai province and Gansu province and in the transitional zone from the second step to the third step in topography. It belongs to loess plateau terrain. The main triggering factor of geohazards in this area is the melting of ice and snow.

Table 2 Landslide distribution zoning results of Mainland China

Zone	Location	Main Triggering factors	Characteristics
A	Western Sichuan plateau	Global climate changes, Rainfall ,earthquake, construction of hydro-power stations and roads	Landslides are concentrated in the middle reaches of the Min River, Dadu River, Yalong River, most of which are deep seated landslides
B	Yunnan-Guizhou plateau	Rainfall, construction of hydro-power stations and roads	Most landslides are landslides and rock falls
C	Western Yunnan	Rainfall ,earthquake, construction of hydropower station	Landslides are concentrated in the downstream of the Nu River and Lancang River, most of which are deep seated landslides
D	TGPR-Western Hubei	Rainfall,construction of hydro-power stations and roads	Landslides are concentrated in the middle reaches of the Yangtse Rive,most of which are catastrophe landslides
E	Western Hunan-Northern Guanxi	Rainfall, human activities	Landslides are concentrated in the Yuan River Basin, most of which are small ones.
F	Eastern costal mountain area	Rainfall , human activities	There are many landslides in this area with the features of suddenly happening ,small size and high risk
G	Qing-ba Mountain area	Rainfall ,earthquake, human activities	The main type of this area is shallow landslides
H	Midstream of Yellow river	Rainfall , Slope toe cutting, irrigation in loess plateau	The main type of this area is loess landslides
I	Upstream of Yellow river	Global climate changes, Rainfall , earthquake, human activities	The main type of this area is loess landslides

2.3 Main triggering factors and typical landslides in China

2.3.1 Main triggering factors of landslides in China

The global climate change is one of the main triggering factors of landslides. The Qinghai-Tibet plateau and Qinling Mountain range separated China into two totally different climate zones from the south to the north. The climate in southern part of China is controlled by the warm and wet air current from the Indian Ocean. Therefore, the southern part experiences heavy rainfall frequently in summer. The rainfall intensity is up to 200 to 300 mm per day. Landslides were induced by the extreme climate, especially in the Yunnan, Guizhou and Sichuan province, southwest of China. However, it is very cold in winter in northwestern part of China, which is influenced by the monsoon climate. The capillary water level in the loess slope rose and seasonally froze in the winter. The thaw of the frozen part in spring triggered many large loess landslides. The triggering factor changes with the areas, but it has following general rules.

In southwestern part of China, the intense rainfall is the most important landslide triggering factor. The rainfall intensity index (RII) can be described by the rainfall amount within 24 hours. Wang & Zhang's study (1986) on the landslides induced by the strong rainfall in 1982 Sichuan in basin indicates that the RII is about 240 mm. Most authors present RII between 200~240 mm in the southwestern part of China. Because high RII always appears in July and August, over 75% landslides induced by rainfall occur in this period.

In northwestern part of China, it is dry. Most area is covered by loess or losses deposits. Generally, the underground water table is quite low, but in the long and chilly winter, the moisture will move up to the overlying soil due to the capillarity, and form a frozen belt. With the spring's coming, it becomes warm gradually and the frozen belt in soil will be melted. Consequently, a saturated and soften cushion will be formed near the underground water table. More often and more unfavorably, it will appear at the base of a slope. A landslide is easy to occur if there is any other human-made disturbance on this occasion. Therefore, human-induced landslides always appear in March or April of early spring (Wang and Zhang,1999).

In the conjunction part of the Tibet Plateau and the southwestern regions, most landslides are triggered by intensive earthquakes (Huang and Wang, 1988). Essentially, this area corresponds to the east margin of Tibet Plateau, which is a very active geodynamics boundary consisted of a series of regional active faults resulted from quickly uplift of Tibet Plateau since Pleistocene. For example, a lot of evidences show that at least 16 earthquakes over 7 Ms magnitude have happened along Xuanshuihe active fault since 1800, with the largest one in this area. Earthquake-induced landslides widely spread in this area, especially along the big rivers such as the Jinsha River (upper reach of the Yangtze River), Minjiang River and Dadu River, etc. Moreover, rivers were often blocked by the landslides, and some huge rockfill dams and reservoir were formed. The residual lacustrine deposit found along the bank has a maximum thickness of 300 m and about 600 veins, which reveals that the reservoir had existed for a very long time.

In high altitude regions such as Qinghai-Tibet plateau and Tian Mountain in Xinjiang, the

global climate change caused the temperature and snow line rose and the glacier retrogressed, which are the main triggering factors of large landslides. According to the statistic, since 1980's 70 percent of large-scale catastrophic landslides are related to the extreme climate conditions or climate changes, and 50 percent are induced by direct intensive rainfalls (Fig. 3).

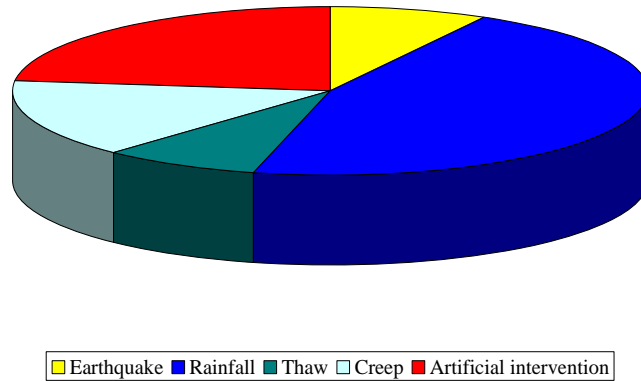


Figure.3 Main triggering factors of large-scale landslides in China

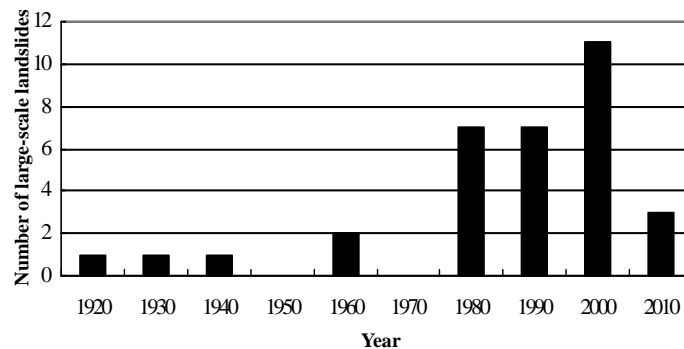


Figure.4 Large-scale landslide frequency changes with time in China

The increase of anthropogenic activities is the main reason caused large-scale catastrophic landslides in China since 1980's. With the development of society, the influences of human activities to the environment are more and more serious. The frequency of the occurrence of large scale landslide has the ascending trend (Figure.4). The data from Table 1 show that 50 percent of the large-scale landslides are directly or indirectly related to human activities. It is very obvious in the western part of China, since 1990's when the policy of accelerating the construction and development of western part of China was carried out. Tens of large engineering activities were centralized in this area.

2.3.2 Typical landslides in China

(1) Landslides around Minjiang River triggered by the Diexi earthquake

Diexi is located on the left bank of Minjiang River in Mao County, Sichuan, about 249 km from Chengdu. On 25 August 1933 at 15:53 hrs an earthquake with the moment magnitude of 7.5 occurred in Diexi. The earthquake triggered numerous landslides along either bank of the Min River, particular around epicentral region of Shawan, Diexi, Jiaochangba, Houerzhai and Longchi (Figure. 5). Landslides destroyed ancient county of Diexi, Shawan, Jiaochangba,

Houzerzhai, Longchi and 21 nearby Qiang Villages. Totally, 6,865 people died and 1,925 injured. About 11 lakes were formed due to river damming by landslides, of which Dahaizi and Xiaohaizi were the biggest. During the earthquake, landslides from Guanyin and Yinping cliffs located on either side of Min River, north of Jiaochangba, dammed the Min river and resulted in a 800 m long, 170 m wide and 255 m high dam. The dam still persists and has a storage capacity of $7.3 \times 10^7 \text{ m}^3$ of water (Zhong, 1999). The Xiao haizi barrier lake is located at the downstream of Da haizi barrier lake. Both of them are formed by the Jiaochang landslide and converged with each other.

45 days after the earthquake, due to high rainfall and after shock, seven landslide dams along Songping valley and Baila village breached. The water in the Min River overtopped and breached Dahaizi dam on 9 October 1933 at 7 pm. The flood water was reached to a height of more than 60 m at Dadian and 12 m at Guanxian, and at Dujiangyan the discharge was measured as $10\,200 \text{ m}^3/\text{s}$. The flood itself had resulted more than 8000 fatalities (Li, 2002).

Structurally, Diexi is located at a trigonal belt bounded by folded zones of the Songpan-Ganzi syncline, Longmenshan fracture zone and syncline foldbelt of Qinling. The area has also numerous compact linear and arc overturned folds and reverse faults. Geologically the bedrock is composed of metamorphic rocks of the Devonian, Carbonic, Permian and Triassic system. The main rock type includes sandstone, marble, phyllite and slate.

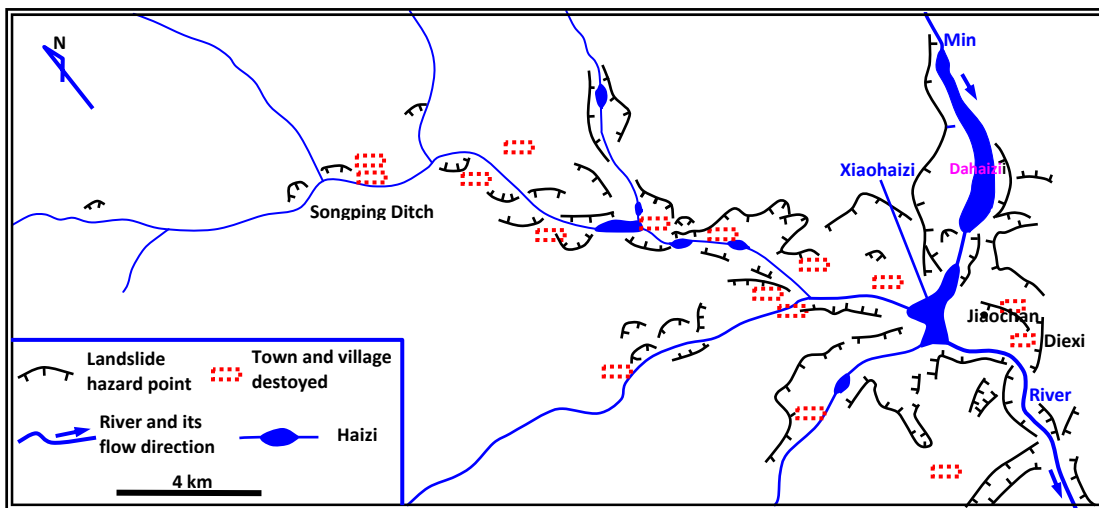


Figure.5 Landslide and rockfalls distribution induced by strong earthquake at Diexi-Songping belt in 1933 (Source: Huang et al. from Sichuan Earthquake Bureau, 2002)

The Jiaochang landslide is the largest landslide among all the landslides triggered by the Diexi earthquake. The present slopes are covered by landslide materials. Jiaochang landslide is located on the left bank of the Minjiang river. The talus extends for 1400 m with the elevation difference of 315 m and an average width of 900 m. The landslide debris covered approximately 1.5 km^2 area and has a volume of $2.1 \times 10^8 \text{ m}^3$. The average thickness is about 170 m and has wide front and a narrow after-edge with gradient varying from 15 to 35 degrees. At upper part of the Xiaohaizi landslide, Quaternary lake deposits are exposed while the base consists of metasandstone, crystalline limestone and phyllites.

(2) Tanggudong slide along Yalong river

On 8 June 1967 at 9 am a landslide occurred on the right bank of Yalong river at Tanggudong, one km from Xiari village, Bosihe, Yajiang, Ganzi (Chai, 1988 and 1989; Wu et al., 1996; Leng et al., 2002). The landslide had a length of 1900 m, maximum width of 1300 m and height of 1030 m and covered an area of 1.7 km^2 . The estimated volume was approximately $6.8 \times 10^7 \text{ m}^3$. The scar of the slide is still visible and can be identified in recent images. The debris was composed of deeply weathered black argillaceous slate and heavy-film sandstone from Xikang Group, Triassic System. The slide might be contributed to the removal of toe part of the slope due to bank erosion by Yalong River.

Tanggudong landslide formed a huge slide dam by blocking Yalong River. The dam was 200 m long, 3050 m wide and had height of 355 m at left and 175 m at right bank of Yalong River. The resulted reservoir extended upstream for about 30 km up to Luocuo and had storage capacity of $6.8 \times 10^8 \text{ m}^3$. Hence, the discharge of the river in the downstream of the dam decreased shapely, even there was no water flow in the downstream. The water level in the 200 km to 300 km area in the downstream reached the lowest value in the whole year. Finally the dam breached on 17 June 1967 at 2 pm and resulted in a big flood. Heights of the flood water were measured as 48 m about 10 km downstream of the dam, 30 m in Jinhe, Yanyuan County, 20.4 m near hydrological station in Luning and 16.6 m in Shiwen hydrological station, Miyi (Figure. 6). The rise of water in Yalong river also resulted in increase of water level in its tributaries such as Jinsha and Yangtse river. Water level of the hydrological station at Huili County rose to additional 12.4 m, at Pingshan Hydrological Station near Xiangjiaba it went up to 6.87 m and at Yinbin it was measured as 2.86 m . The maximum discharge was estimated as $57 \text{ 000 m}^3/\text{s}$ just after the failure. Peak discharges measured at lower Guili, Nuning, Deshi and Pingshan hydrological stations were 23600, 23100, 19900 and $6091 \text{ m}^3/\text{s}$ respectively. The whole dam failure process approximately lasted for 12 hours.

(3) Jipazi landslide



Figure.6 Tanggudong landslide dam and its backwater scope

In July 1982 a wide area around Chongqing and Yunyang (about 270 km downstream of Chongqing along Yangtze River) experienced continuous heavy rainfall, bringing an accumulated precipitation of 633.2 mm in 1 month. During the rainfall, slow movement was observed on Jipazi slope on the left bank of Yangtze River around 20:00 on 17 July, and 6 h later, it shifted to rapid failure, reaching a maximum velocity of 12.5 m/s. About $2.3 \times 10^6 \text{ m}^3$ of displaced mass slid into Yangtze River, giving a run out distance of about 200 m. The landslide had a length of about 1.6 km, covering area of 0.77 km^2 approximately with a maximum thickness of 93.7 m and volume of $15 \times 10^6 \text{ m}^3$ (Figure.7).



Figure.7 Jipazi landslide on Yangtze River (1982)

The landslide did not result into any fatality but destroyed more than 1,700 houses. The rock debris filled the riverbed by 40 m and blocked the ship route in Yangtze River for 7 days. The total loss by this landslide reached more than 12 million US dollars.

Jipazi landslide was a part of old Baota landslide. Its maximum thickness is 93.7 m. The upper portion consists of silt and clay, while middle part has clay layer including block of rocks and gravels of Quaternary age. The inner most layer is composed of bedded cataclastic rocks, which formed the sliding surface. The landslide is caused by the reactivity of the old Baota landslide. The sliding body also contains parts of bedding rocks.

The sliding zone (0.2–1.0 m thick) was composed by amaranthine silty clay with cataclastic sandstones. The dip angle of the slide plane ranged from 6° to 8° . The bedding

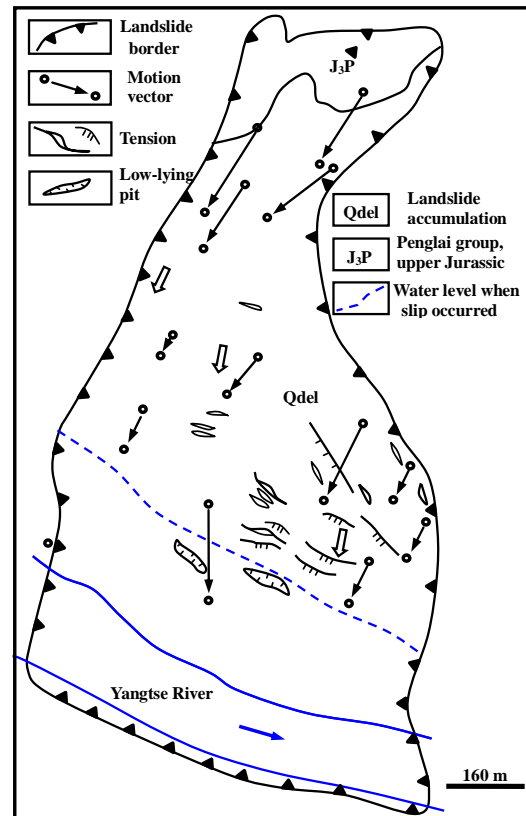


Figure.8 Geological map of Jipazi landslide (Source: from Zhang, 2000)

covered an area of approx 1.3 km². The back scarp has a width of 750 m and a height of 220 to 240 m with slope varying from 45° to 75°. The toe of the rupture surface was not clearly discerned. The landslide can be classified into two parts from the rear to the front. There are many troughs and ridges in the rear part. The main trough is located in the front of the back scarp. It is 250 m to 300 m long and 50 m to 60 m wide. Its bottom altitude is 2020 m. There is a long ridge paralleled with the trough and back scarp. Its altitude is 2080 m, composed of the NW inclined mudstone. The dip angle of the mudstone is 10°. The front part of the landslide has a lot of hummocks with the height of 5 m to 10 m, which paralleled to each other. In this part the original slope was covered by mudstone debris and loess with a height of 8 to 50 m. The sand pebble layer lying on the first terrace was found undisturbed and thus the failure plane can be inferred above the first terrace. The sliding plane was estimated to be through the horizontal mudstone layer below 120 m loess deposits (Figure. 10).

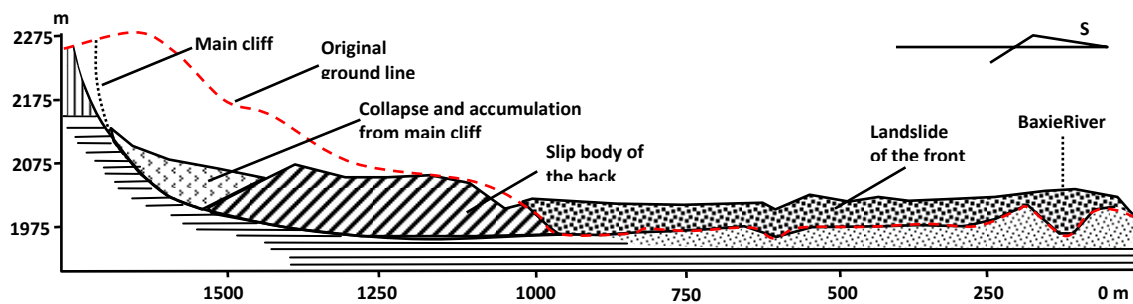


Figure. 10 Geological profile of Saleshan Landslide (Source: Zhang et al., 1994)

To summarize, Saleshan landslide developed in the mudstone slope covered with 120-m-thick loess. The deformation characteristics of the rear part of the landslide are attributed by rotational sliding. The front part transformed into debris flow. Even though, the landslide occurred in a very short time, but before that it experienced a long-term slowly creeping process.

(5) Xikou landslide in Huayingshan

On 10 July 1989, a landslide was triggered by heavy rainfall in Xikou Town of Huaying City, Sichuan Province. The landslide destroyed four villages, killing 221 people, and causing a direct economic loss of more than 0.75 million US dollars. The maximum rainfall intensity was recorded as 88.6 mm/h during the day when the landslide occurred. Before the landsliding, sporadic rock falls were noticed, and a rock block even hit the house of a farmer. Later on, a large landslide occurred. The displaced landslide mass shifted from sliding to flow, and the whole movement lasted approximately 60 s.

Two scar faces can be identified. Figure 11 presents a longitude section of this landslide. The total source area extends for 193 m from the altitude of 655 to 848 m. The main scar extends from 655 to 790 m and the secondary scar from 790 and 848 m. The main scar dips at 47° towards north-west and its width varies between 75 m and 110 m at upper and lower part, respectively. The altitude of the toe part of the source area is 655 m. The shape of the sliding plane looks like a “spoon”. The lengths of outcrops of the bedding in the upper area and in the lower area are 210 m and 165 m respectively. The volumes of main and secondary slide were

estimated as $1.8 \times 10^5 \text{ m}^3$ and $2 \times 10^4 \text{ m}^3$ while the final volume of the accumulated debris was approx. $1 \times 10^6 \text{ m}^3$.

The landslide has the double-deck structure: The upper part is composed by the carbonatite of Cambrian system and Ordovician system, which is hard and strong, while the lower part is soft and weak. These two parts are divided by the fault F7 (see Figure. 11). The sliding zone in the upper part was developed along the contact surface between the strong and weak weathered strata. Its lower part was composed of the shale, mudstone, and sandstone of Silurian System. From upper to lower parts, the source area can be divided into six sections based on the characteristics of rock structure, i.e., (I) layered block-crack structure, (II) thick-layer structure, (III) layered structure, (IV) layered shattered structure, (V) shattered structure, and (VI) brecciated texture. The brecciated texture is actually the breccia formed by renewed cementation of fault crush zone.

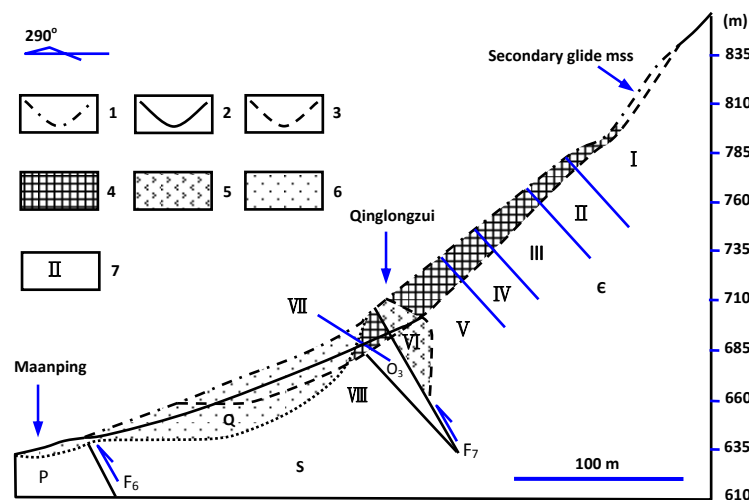


Figure.11 Schematic diagram of geological structure of Xikou landslide

1. Original topography; 2. Topography after sliding; 3. sliding plane
4. Strong weathering zone
5. Calcareous breccia
6. Colluvial deposit from Quaternary
7. Rock structure zoning (I-VI, see in the above text; VII layer limestone of Ordovician; VIII mudstone and shale of Silurian)

(6) Touzhai landslide

At 6 pm on 23 September 1991 a large landslide occurred on the upslope of Touzhaigou village located on Panhe area, 30 km away from Zhaotong, Yunan province. The slide originated at 2300 m above m.s.l. and the displaced mass travelled down slope along the Touzhai valley at a very high velocity. After it collided with the lateral walls of the valley and changed sliding directions for three times, the displaced mass stopped at the mouth of Touzhai valley at an altitude of 1820 m. The whole event lasted 3 min. All the houses on the travel path had been destroyed. Two hundred sixteen people were killed, and the direct property loss reached about 1.5 million US dollars (Zhong, 1999 and Zhang et al., 1994) (Figure. 12).

The source area is 400 m long and 300 m wide, and the displaced landslide mass from the source area was approximately $4 \times 10^6 \text{ m}^3$. However, the final deposited mass reached approximately $9 \times 10^6 \text{ m}^3$, i.e., a great volume of debris was entrained from the travel path. The landslide contains mixture of soil and rock debris. The displaced mass traveled about 3,000 m,

with a maximum width of 230 m and an average depth of 10 m on the deposit area. Figure 13 presents a longitudinal section along the main traveling path. As shown, the landsliding occurred on relatively gentle slope. The source area slope about 14° , while traveling path on the lower part sloped approximately 4.4° .

Geologically Touzhai landslide is located on the west flank of Panhe syncline. Rocks exposed near the slide zone include Emeishan basalt of Permian age ($P_2\beta$), sand shale of Xuanwei Group of Permian age (P_2x) and sand shale of Lower Triassic (T_1). The source area is 400 m long and 300 m wide and is located in $P_2\beta$ (Figure. 13). The source area was located in $P_2\beta$ and contained strongly weathered basalt of 1 m thick. As shown in Figure 13, the slip surface on the source area contains three sections, where AB section is interring laminar slip surface composed of weathered volcanic tuffs, BC section has hard and smooth surface, dipping 38° towards 110° , and CD section is the main resisting part against the downslope shear force. The basaltic surface is coarse, weathered and stratified. The displaced mass consisted of approximately 10% of big rocks (1.5–5 m in diameter) and 90% of mixture of gravel (less than 20 cm in diameter) and clayey soils. More detailed information of its triggering and movement mechanisms can be obtained from Huang and Xu (2008).

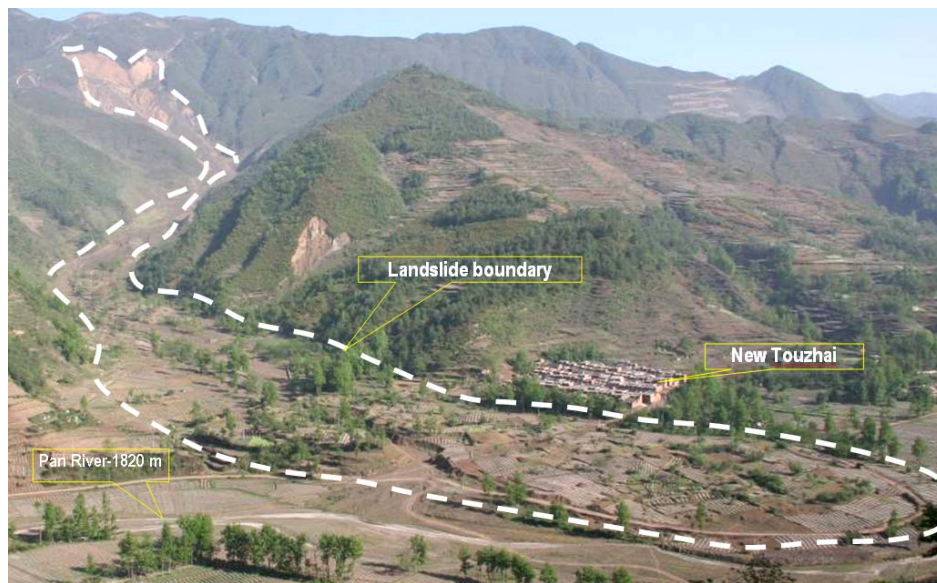


Figure. 12 Touzhai landslide—debris flow (Source: Zhong, 1999 and Chen et al., 1991)

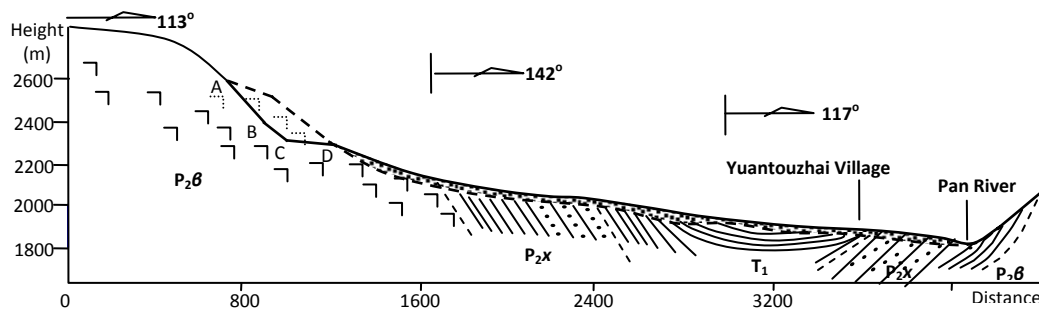


Figure. 13 Geological profile of Touzhai landslide

(7) Yigong Landslide in Tibet

At 8:05 pm on 20 April 2000, a super large landslide occurred at Zhamu Creek in Yigong, Pomi, Tibet. 30 million m^3 of rock material detached from an altitude of 5000 m above msl and flow along the Zhamu Creek with a maximum velocity of 44 m/s. The total sliding process lasted 3 min. The sliding mass entrained a lot of materials from the toe of lateral slopes of the valley. Therefore, a large number of small secondary slides had been triggered. The displaced mass travelled for 8 to 10 km and blocked Yigong Zhamu Creek, forming a landslide dam and the Yigong barrier lake. The dam was 4.6 km long, 3 km wide and 60-110 m high. Its volume was estimated as $3 \times 10^8 m^3$. As seen in Figure.14 (Yin, 2000), the landslide itself has a length of 3 km and width of 8.5 km. Yigong landslide is reported as the largest landslide in China in recent 100 years.

Yigong landslide can be divided into three zones based on the dynamic and deposition characteristics (Figure.14), which are the source zone, the transportation zone and the accumulation zone. The source zone (I) is the landslide source area with an altitude ranging from 4300 m and 5500 m above msl in Zhamu Creek. The volume of the source rock mass was estimated as 0.3×10^8 to $0.4 \times 10^8 m^3$. The transportation zone (II) contains: II-1 (steep, accelerating section) and II-2 (gentle slope section).

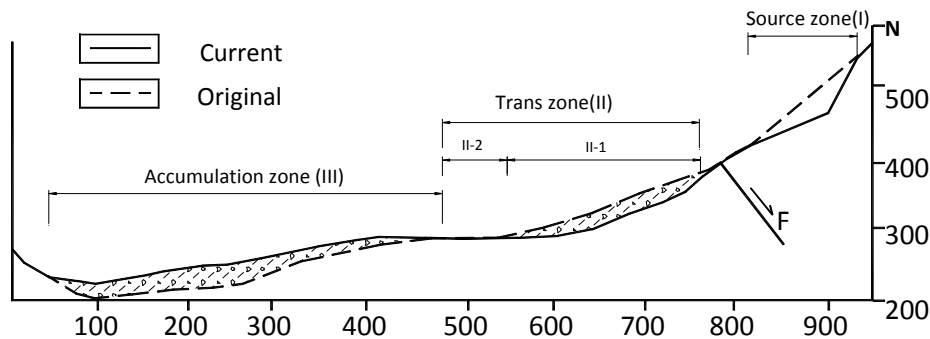


Figure. 14 Engineering geological profile of Yigong large-scale landslide.

There are a lot of deposition cones distributed in the front of the accumulation zone, which are a kind of the unique micro-morphologic landscape. Liquefaction phenomena can be observed in the field through some obvious evidences, like sand pits, which are similar to the ones caused by earthquake. 75% to 95 % of the trees in the margin of accumulation zone were pulled out from the roots or cut off in the middle. All of the damaged trees were laid down in the same direction, which might be caused by the air-blast generated by the very high speed landslide. There was a 0.5 cm to 1.0 cm thick layer of mud covered on the surface of both the damaged and undamaged trees. This kind of mud was called "blast-spattered mud". It's another evidence of the blasting effect.

The Yigong landslide is a multi-event, which initiated as a rock slide and then developed into a debris flow travelled a very long distance and finally blocked a river, forming a huge lake. Later on, the dam breach caused catastrophic damages to the downstream. The landslide was triggered by the freezing and thawing of ice and snow in rock fissures. The landslide fell down for 3000 m, disintegrating into loose debris and continuing moving along the Zhamu Creek. Due to the huge kinetic energy and sudden loading to old deposits in the creek, the pore water pressure increased sharply, which resulted in the liquefaction and reduced the shear strength

to near zero. That's why the landslide has a extremely high velocity and very long run out distance.

(8) Tiantai village landslide in Sichuan

In September 2004, heavy rainfall fell on many places in Xuanhan, Sichuan. The rainfalls on third, fourth, and fifth of September were 15.9, 122.6, and 257.0 mm, respectively. At 15:00 on the fifth of September, cracks were observed on the road located at the right back of Qian River in Yihe village, Tiantai Town. Subsequently, some houses near the road began to incline toward and fell into the river. The landslide was a retrogressive one. The whole process of the movement lasted 8 h. Around 23:00, the toe part of the landslide reached the river, followed by other parts. This landslide was 1,200 m long, 1,600 m wide, and 23 m thick in average. Its volume is about $25 \times 10^6 \text{ m}^3$. The altitude of the toe of the rupture surface varied from 380 to 424 m, which was 30–35 m higher than the river bed. The landslide damaged 2,983 houses and facilities in 1.2 km^2 area, making 1,255 people homeless. Some 2 million m^3 of debris moved into the river, forming a natural dam that was 1500 m wide and 20 m high. The temporary reservoir had a capacity of 60 million m^3 . The rising water flooded another village and river banks on the upstream, such that 19,360 persons had to be evacuated immediately. The direct economic loss was about 14.5 million US dollars.

The slope of the landslide varies from 10° to 33° , and the cliff developed along the river is 30 to 40 m high. The slope is composed of red silt-sandy mudstone, siltstone and fine-grained gray sandstone belonging to Suining Formation Jurassic. The general strike direction is 110° to 120° with dip varying between 5° to 10° . The slopes are cataclinal i.e. rock is dipping in the direction of the slope. There are four gullies developed on the main body of the landslide, which are Yujiahe gully, Maliushu gully, Liangshuijing gully and Dahe gully (from south to north). The gradient of valleys varies from 15.3% to 19.7% (Figure.15).

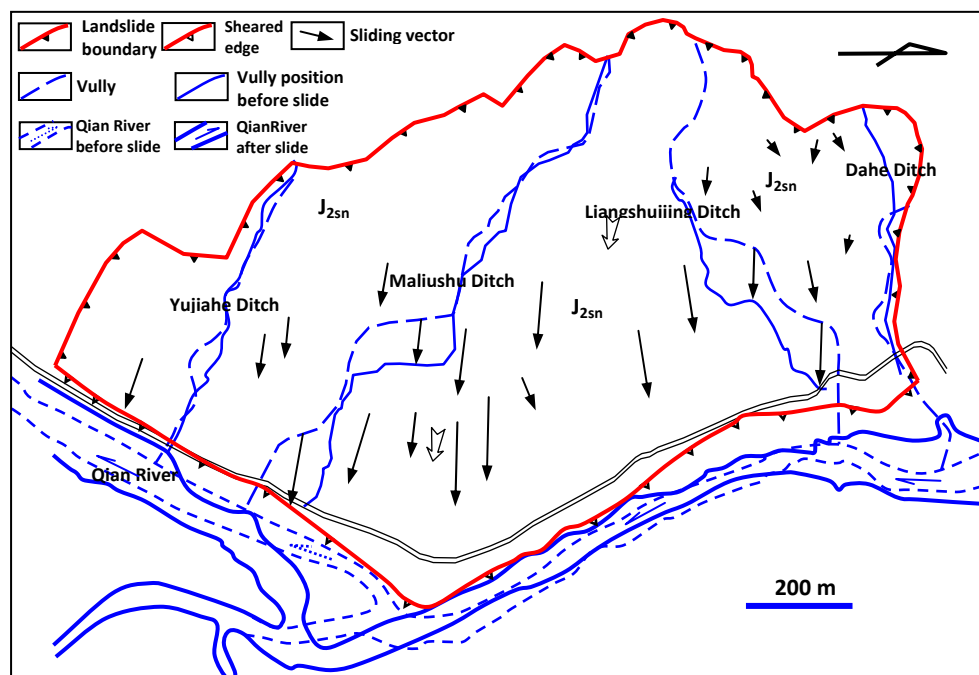


Figure. 15 Geological map of Tiantai village landslide

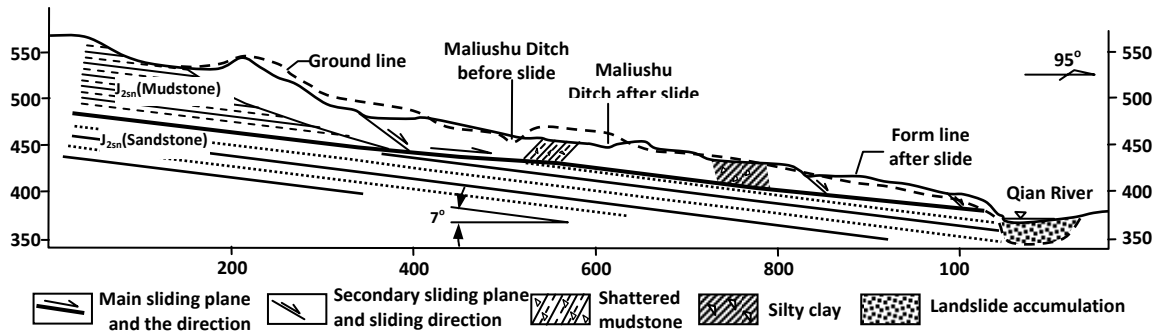


Figure. 16 Geological profile of Tiantai village landslide

Beneath a cover of cultivated soil and colluvium (3 to 5 m thick) is 20 m thick mudstone horizon. The sliding plane is located close to the junction with the underlying sandstone beds. The dip angle of the sandstone beds varies from 8° to 10° . The sliding plane contains brown silty clay with thickness varying from 20 to 30 cm (Figure.16). The altitude of the back-edge is from 520 m to 570 m. The height of the scarp in the rear varies from 15 m to 35 m.

The characteristics of Tiantai village landslide are shown as follows: (1) the dip angle of the sliding plane was very gentle; (2) the thickness of the landslide is not very large (10 to 20 m on the flanks and 20 to 30 m in the middle); (3) the displaced landslide mass formed into several blocks by the cracks on the surface; (4) the creep deformation of the landslide before completely failure is long (lasted more than 8 hrs), but the failure time is very short; (5) there are only minor changes in original slope angle after the slide; (6) the deformation of the landslide was retrogressive.

Based on detailed investigation, we finally found out that the intense rainfall was the key triggering factor. The landslide occurred when the heavy rain hit it. The rainfall infiltrated into the slope through the cracks, which also made the cracks become larger and deeper. The underground water also generated the uplift water pressure along the sliding plane. So the deformation and failure process contains three stages: the rainfall infiltrated stage, the cracks development stage and the slide stage. There were a lot of tectonic joints and weathering cracks in the slope, which provide paths for rainfall seeped into the slope. The water mainly flew through the cracks and the interface between the mudstone and sandstone. The water can not be drained out immediately, so the uplifting pressure was generated, which made resistance decreased sharply. When the crack water pressure reached a certain value, the slope would began to split, then the water pressure dissipated and drove the slope to break up and move forward.

(9) Danba landslide in Sichuan

Danba is located at an altitude 1864 m within a narrow valley on the right flank of Dajin River, in Ganzi, Sichuan. The town has a population of 11 000 spread within 2.5 km^2 . In August 2002, some signs of movements such as tension cracks, were observed on the slope above the town. The slope movement became more serious on August of 2004, and the downslope movement of slope as a whole was becoming obvious. The landslide is 200m to 250m wide, 290m long, 30m thick, and about $2.2 \times 10^6 \text{ m}^3$ in volume. The observed displacement on the beginning of February 2005 showed a rate of 2–3 cm/day in average with a maximum rate of 5

cm/day. On 14 March 2005, the toe part of the landslide showed outward extensive deformation and local failures occurred on some areas, leading to the collapse of some houses. At this time, the accumulative displacement of the slope ranged from 70 to 100 cm. Obviously, if the landslide occurs in total, the capital of Danba County will be badly destroyed. Furthermore, the landslide will block the river, threatening the people who live in the upper and lower streams of Dadu River (Figure.17).

Physiographically Danba is located in the eastern part of Qinghai-Tibet Plateau. The area is characterized by neotectonic movements and heavy erosion by Dajin river, thus it provides a favorable condition for development of a landslide. Geologically the area exposes garnetiferous mica schist including biotite granulite of Fourth Formation-complex (S_{mx}^4) of Moaxian Group, Silurian System. The overburden material consists of old landslide debris (Q_4^{del}), rock fall deposits (Q_4^{col+dl}) and morainic deposits (Q_4^{fgl}) (Figure. 18). The area lacks surface springs thus indicating possibility of deep groundwater table.

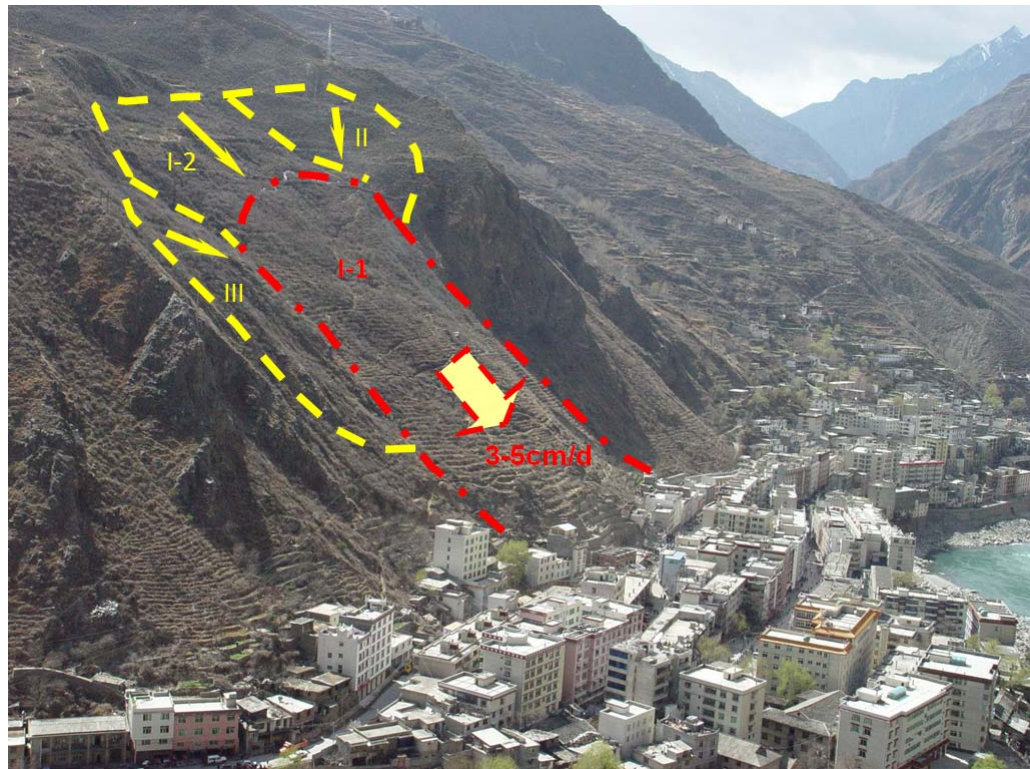


Figure. 17 Danba Landslide

Field data indicate that slip surface of Danba landslide is located within the colluvial layer with a dip of 30° . The thickness of landslide mass ranges from 20 to 35 m. Several tension cracks with a total length of more than 1,500 m have been developed on the surface of the landslide. The landslide mainly consisted of big rock blocks, and the sliding surface was along the interface of the bedrock. Field monitoring of landsliding revealed that the sliding mass can be divided into three regions (Regions I, II, and III) as shown in Figure. 18.

Region-I constitutes the main part of the landslide covering $5.5 \times 10^4 \text{ m}^2$ area and volume of $1.7 \times 10^6 \text{ m}^3$. The slope has an average angle of 30° . However, the toe part slopes 50° to 70° ,

showing the terrace landforms. The landslide debris in this region is 290 m long and 150-200 m wide, with slip direction of 353° . The thickness at the front part varies from 6 to 28 m. Landsliding with great displacement led to the damage on both the houses and streets that locate at the slope foot. Region II was located on the left side of the back of the landslide, and covered an area of 6000 m^2 . Main dip direction was 20° , and the slope angle ranges from 20° to 30° . The volume was $1.5 \times 10^5 \text{ m}^3$, with the thickness of 15 to 20 m. The deformation was mainly localized on the vicinity of back scarp and also along the tension fissures on the side edges. This region had greater displacement rate than Region I. Region III located on the right side of the landslide. It was 50-85 m wide and 180 m long, covering an area of $1.4 \times 10^4 \text{ m}^2$. The mean thickness of the slide mass was 25 m with the gradient of 30° to 45° .

Recognizing the risk of this landslide, countermeasures were conducted by putting counter pressure on the toe part, installing prestressed anchors on the main body, and local cutting. Totally 269 prestressed anchors were installed with their prestressed force being 1,300 kN and length being 40–52m(the bonding lengths were 8–10 m). The volume of cut landslide mass from the upper part of the slope was $1,800 \text{ m}^3$. These measures provided remarkable reinforcement effect.

Danba Landslide belonged to reactivated ancient landslide. Human activities might have played a key role on the reactivation. Since 1998, many buildings had been built on the toe part of the slope. Excavation and cut of the slope increased the free surface of the toe part of the slope, elevating its instability. From March to October of 2004, a large-scale re-building of a big street immediately below the slope expanded the free surface of the steep slope further. This absolutely decreased the supporting force of the slope foot, accelerating the movement of the slope. Therefore, it is of great importance to understand landslide potential of this kind of slopes for the mitigation of landslide hazards with the urbanization, especially for developing area.

(10) Wulong landslide in Chongqing

On June 5, 2009, a catastrophic rockslide-debris flow occurred at the crest of the Jiweishan Mountain in Wulong, Chongqing, China. Approximately five million cubic meters of limestone blocks slid along a weak interlayer of bituminous and carbonaceous shale. The source mass descended from the upper part of the slope rapidly, crossing a 200-m wide and 50-m deep creek in front of it. Blocked by the opposite steep creek wall, the sliding mass changed its direction and traveled a further 2.2 km along the creek in debris-flow mode, finally forming a large accumulation zone with an average depth of 30 m. This is one of the most catastrophic

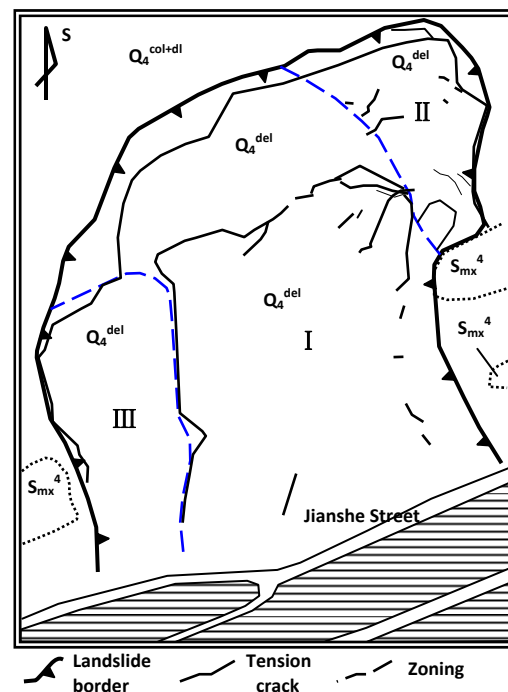


Figure. 18 Engineering geological map of Danba Landslide

rockslide events in recent years in China. It buried 12 houses and the entrance of an iron mining tunnel where some 27 miners were working inside. Ten people died, 64 missing, and eight wounded.

The Wulong rockslide-debris flow occurred at the crest of the Jiweishan Mountain, Wulong County, Chongqing, China, where an iron mine is located. Its location is shown in Figure. 19. The Jiweishan range extends along the SN direction. The eastern flank of it is a 50–150-m cliff (Figure. 20). The peak and tip of Jiweishan Mountain at elevations of 1,442 and 1,000 m asl, respectively, giving a height difference of 442 m. The source area of the rockslide is 720 m long, up to 125 m wide, and covers an area of 84,000 m², involving five million cubic meters of rocks.

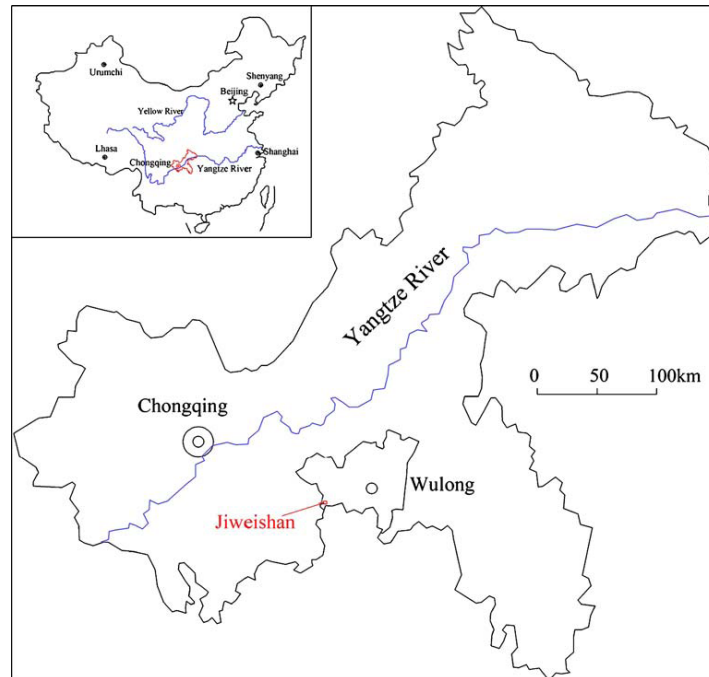


Figure. 19 Location map of Wulong landslide

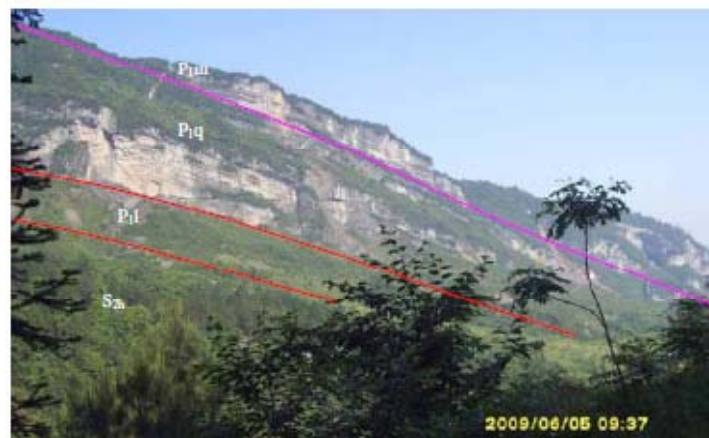


Figure. 20 Pre-slide overview of the source area of the Wulong rock slide-debris flow with the boundary lines of different strata

Field survey and a lot of local people's accounts indicated that the deformation of the Jiweishan mountain has a long history. Local people claimed that they found a crack on the surface of the east-facing cliff in 1960s. In 1999 a professional geological reconnaissance team found the aperture width of this crack has developed to 1.5 m, which can be described as the cavernous crack. In September 2001, some small scale rock falls occurred in the southern part of the cliff in the source area, which drew the attention of a geological team. The local government evacuated 871 people from the potential dangerous area in 2001. After 2005, the rock fall scale increased and began to extend to the north of the cliff progressively. In July and August 2007, the local geo-hazards management department organized a professional geological team to carry out the geo-hazards investigation of the Jiweishan mountain again. Through this investigation, a 1000 m long, 10 m wide, 15-20 m high rock avalanche zone along the eastern cliff with a volume of about 200 000 m³ was defined. At about 3:00 pm on June 5 2009, after a long term creep deformation, approximate 5 million m³ rock mass slid along the weak interlayer overlying on the P₁q strata.

The key block in the front of the source area plays a significant role in controlling the deformation of the rock slide at the beginning. Because there is an EW striking free surface in front of it, it failed first driven by the great deformation strain released after a long term accumulation. Then the rock mass that was cut into blocks by the almost NS and EW striking joint sets behind it began to slide retrogressively. After dropping from a 50 m high cliff, the sliding materials attained large kinetic energy, running up to the opposite slope, entraining a large number of materials from the bilateral creek slopes. It finally transformed into a debris flow, and travelled for a very long distance at a high speed. The velocity of Wulong landslide was calculated to be 42.5 m/s, which suggests that it is a extremely rapid rock slide, according to the classification proposed by Cruden and Varnes (1996). Due to its very large velocity, the air blast and flow-type traveling phenomena were produced during the sliding process.

2.4 Genetic mechanism of large-scale landslide in China

2.4.1 The three section mechanism: sliding-tension and cracking-shearing

Sliding-tension and cracking-shearing mechanism includes three deformation and failure stages, which are the "creeping" along gentle inclined cataclinal structural planes, the "tension cracking" in the rear and "shearing failure" of the "lock section" (resistant part) in the middle. This kind of deformation and failure mechanism was first observed near the Longxia hydropower station, Yellow River. The Zana and Longxi landslides were the representative ones in this area (Zhang et al., 1990). Later on, this mechanism was also found in Laxiwa hydropower Station along the Yellow River and Yanchi phosphor mine in Hubei (Huang, 1993 and 1996). The sliding-tension and cracking-shearing mechanism is very typical, which is controlled by the near horizontal structural planes at the foot of the slope. It is also a main kind of mechanism causing large-scale and high speed landslides in China

Landslides with this mechanism usually occur in the following slopes: (1) slopes that are consisted of brittle rocks, and have the near horizontal or inclined cataclinal structural planes at the foot of slopes; (2) slopes that are composed by hard rocks with the thin weak interlayers.

The deformation and failure processes are as follows:

(1) During formation process of slopes, the relief rebound deformation caused the epigenetic deformation along the gentle structural planes at the foot of the slope and generated the tension stress zone and tension cracking in the head of landslide, especially in the high stress zone (Figure. 21).

(2) Under the long-term effect of the slope gravity, the slopes creep constantly along the gentle structural planes and cause the cracks in the head developed to the deep insides (Figure. 21). Thus, the slope can be divided into three parts: the creeping part, tension cracking part and the “lock section” (resistant part which is like a lock to restrict the slope deformation) between the former two parts. The “lock section” is crucial for the slope stability. The stresses of the resistant part are accumulated with the deformation development of the creeping and cracking.

(3) When the depths of the cracks in the rear reach a certain value, the gradual accumulative stresses in the “lock section” will cause the slope began the progressive failure stage. Finally, the “lock section” will be broken by the shearing force. Meanwhile brittle failure of the slope will occur. Because this kind of slope usually has large potential energy, the sliding speed is very high.

For this kind of slope, its stability is mainly determined by the “lock section” (resistant part). Therefore, the counter measure for this kind of landslide is preventing the development of the cracks in the rear or enhancing the resistant strength in the front of the slope.

Due to the special deformation and failure mechanism, the morphology of the slip surface looks like a “spoon” or “shovel”, containing three segments: the gentle dip angle segment along the strata or structural plane; the steep (>60°) segment crossing the strata in the rear and the curved segment between the former two segments.

Based on the case study on Laxiwa Hydropower Station along the Yellow River, Huang (1991) used visco-elastic-plastic finite element method to analyze the deformation process of the secular, as we mentioned above, and proposed a threshold for (Huang, 1993):

$$K \geq K_c = (1 + C \cdot \text{tg} \varphi_i \cdot \text{ctg} 2\alpha) / (1 - C \cdot \text{tg} \varphi_i \cdot \text{ctg} 2\alpha) \quad (1)$$

Where $K = \sigma_1 / \sigma_3$; α is the angle between the normal of the structural plane and σ_1 ; φ_i is the long-term strength index, $C = \text{tg} \varphi_i / \sin 2\alpha$.

Zhang et al. (1983) also found a threshold, according to the critical depth of the crack in the rear. The critical depth can be expressed as:

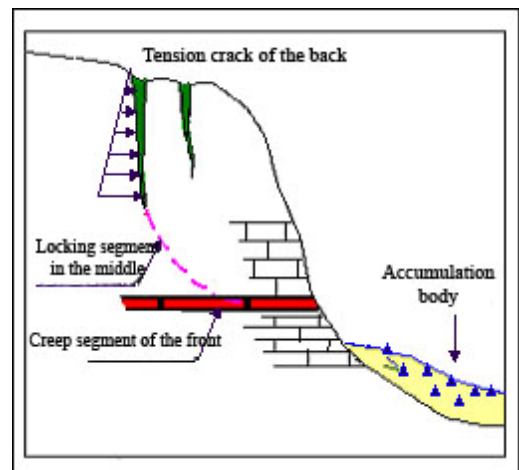


Figure. 21 Creep-tension–shearing mechanism of a landslide (three-section mechanism)

$$H_{cr}=0.5763H- 27.0992 \quad (2)$$

Huang et al. (1991) presented an equation to evaluate the slope stability:

$$K = \beta K_m \quad (3)$$

where, K is the slope stability coefficient under the effect of the resistant part, K_m is the slope stability coefficient based on the supposed sliding plane, β is the over loading coefficient considering the failure of the resistant part, which can be obtained by physical model tests or numerical modeling.

2.4.2 Retaining wall collapse mechanism

Xikou landslide in Sichuan province and Touzhai landslide in Zhaotong, Yunnan province as aforementioned are representative ones for the “retaining wall collapse” mechanism. The basic characteristics of this kind of landslides are: there is a comparatively rigid part in the middle or front part of the slope. The strength of the rigid part is very high, so it plays a role like a “retaining wall” (a resistant part). This rigid part usually suffers very large force caused by the deformation of the upper slope. Thus, it plays a very important role in maintain the stabilities of slopes (Huang et al., 1993 and 2002). With the deformation development, the abruptly brittle shearing failure of the rigid part will occur. Finally the high speed landslide will happen. The concept model of this kind of slope is shown in Figure.22 (Huang, 1996).

(1) The strengths in the slope are quite different from the upper to the lower parts: the upper (head) of the slope is hard, while the lower (front) part is soft, which are bounded by the strong rigid part (resistant part).

(2) The rigidity of the lock section is much higher than that of soft base below. Therefore, the lower base enduring the load transferred from the upper part of the slope is limited. It means that the lock section is like a retaining wall, which suffered the most of the sliding force from the upper slope.

Consequently, the stress concentration occurs in the rigid part. With time goes by, the soft base below was being compressed, and slowly crept toward the free face. The stress concentration is aggravated. When concentrated stress becomes larger than the strength of the rock mass, a abruptly brittle failure of the rigid part, will occur, which will cause the failure of landslide.

Visco-elastic-plastic nonlinear finite element method was used to simulate and validate the above mechanism as follows (Huang, 1996):

(1) The surface displacement in the middle of the slope is less than that in the upper part and lower part of the slope. The secular deformation in the upper part of the slope can reach several tens centimeters, while the deformation of the lock section is small. The deformation of

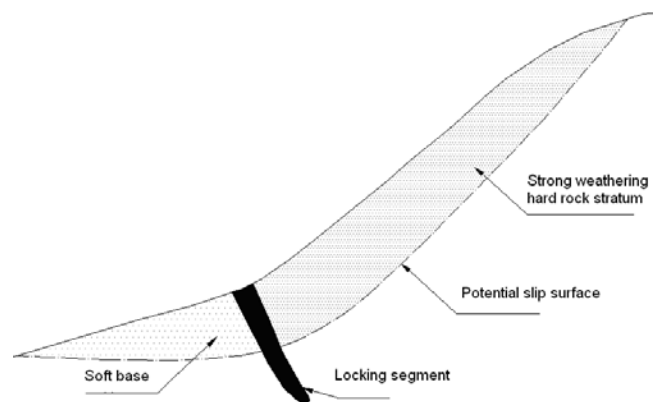


Figure. 22 A conceptual model of retaining wall collapse landslide mechanism (Source: Huang, 1996)

the upper part will be restricted by the lock section, whilst the stresses and strain caused by the sliding force of the upper part will be accumulated in the rigid part.

(2) Accumulation and transmission of the stress: maximum and minimum principle stresses of different parts of the slope varied with time which can be seen in Figure. 23. It shows that the stress in the lock section (the rigid part) increased with time. The stress of the lower part (the soft base) did not change with time. Contrastly, the stresses decreased after a period of time, when the stress in the lock section increased. This means the reduced stress in the lower part caused the stress increase of the rigid part. In Figure.23 (b), the minimum principle stress of the rigid part showed the decline trend. When the maximum principle stress rose, the minimum principle stress went down, which had a negative effect on the slope stability. The minimum principle stress in the lower part fluctuated with time within a small range, but the decreased trend is obvious.

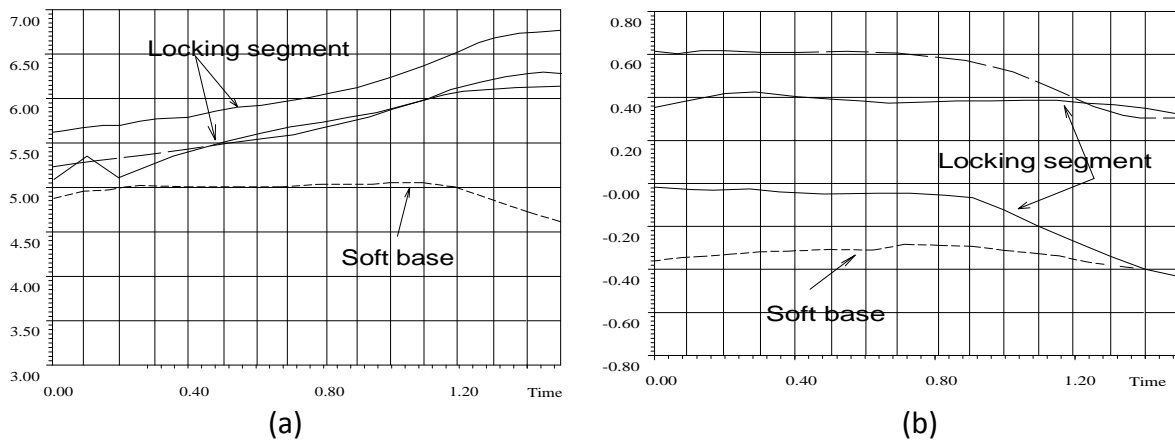


Fig. 23 (a) Relationship curves between maximum principal stress and time; (b) Relationship curves between minimum principal stress and time

2.4.3 Translational mechanism in the near horizontal strata

Translational landslides usually develop characteristically in nearly horizontal bedrock composed of sandstone and mudstone. The main trigger factor of translational landslide is the heavy rainfall. They mainly failed due to the combination effect of the static water pressure and the uplift pressure (Zhang et al., 1994 and Wang et al., 1983). The sliding plane probably develops along the interface of the mudstone and sandstone. Some cracks or troughs can be observed in the rear of the landslide. The widths of the cracks and troughs indicate the horizontal displacement of the landslide. The landslide is always cut into several blocks by the cracks. The deformation process of translational landslide is gradual and retrogressive.

Translational landslides are common in China, particularly in the mudstone and sandstone strata of Jurassic and Triassic system in the Three Gorges reservoir area and the Sichuan basin. The volume of this kind of landslide varies from 10^4 m^3 to 10^9 m^3 . Tons of translational landslides were triggered by heavy rainfall in July 1981 in Sichuan basin. Besides, there are also a lot typical ones distributed in the Wanzhou old town, Three Gorges reservoir area and eastern part of Qinghai.

When the heavy rainfall hit the landslide area, the water will infiltrate into the cracks in the slope and cause high hydrostatic pressure and uplift pressure along the sliding plane. When the water level in the cracks reached a certain value, the landslide will be pushed forward by the combination of the hydrostatic pressure and uplift pressure (Figure. 24).

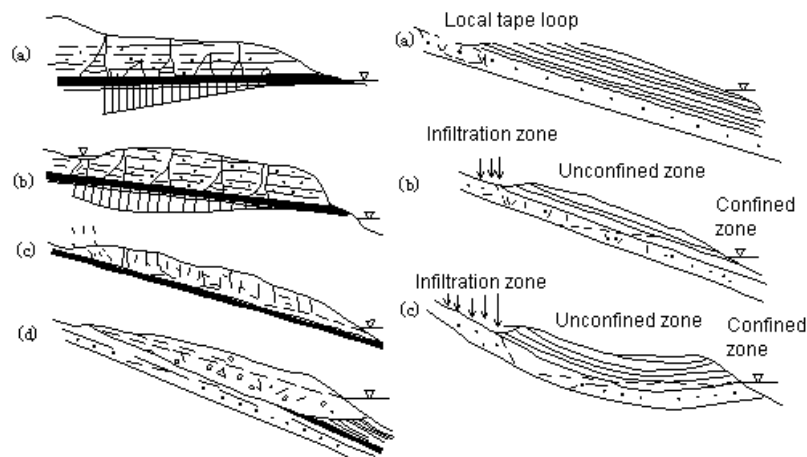


Figure.24 Hydrodynamics model of consequent rocky slopes (Source: Zhang et al., 1994)

The left: hydrodynamic model in unsaturated-season variation zone: (a) and (b) filling water in cracks (shadow curves denote pore water pressure distribution); (c) Infiltration, phreatic water; (d) Phreatic water. The right: hydrodynamic model in interlaminar aquifer: (a) Weak circular artesian water, (b) and (c) Strong circular artesian water

The genetic mechanism of translational landslide is shown in Figure.26. The limit equilibrium criterion for translational landslides has been proposed by Zhang et al. (1994).

$$h_{cr} = \frac{1}{2 \cos \alpha} \left[L^2 \operatorname{tg}^2 \phi + 8 \frac{W}{\gamma_w} \cos \alpha (\cos \alpha \operatorname{tg} \phi - \sin \alpha) \right]^{1/2} - \frac{L}{2 \cos \alpha} \operatorname{tg} \phi \quad (4)$$

Where h_{cr} = the critical water head value; w = the weight of a 1 m wide slide block (t/m); α = the dip angle of the sliding plane (a downslope dip gives a positive value, an upslope dip gives a negative value), $0^\circ < \alpha < 10^\circ$; L = the length of the slide block; ϕ = the friction angle of the sliding plane; γ_w = the bulk density of water, $\rho_w g$.

If $\alpha = 0$, the above equation can be wrote as

$$h_{cr} = \frac{1}{2} \left[L^2 \operatorname{tg}^2 \phi + 8 \frac{W}{\gamma_w} \operatorname{tg} \phi \right]^{1/2} - \frac{1}{2} \operatorname{tg} \phi \quad (5)$$

The hydrostatic pressure and the uplift pressure will dissipate quickly when the landslide began to slide. Thus the sliding blocks stopped. The width of the trough or cracks in the rear indicates the displacement of the landslide. Based on the investigation of the translational landslides triggered by heavy rainfall in Sichuan, it can be seen that the widths of the trough varied from several meters to server ten meters, which are the natural drainage of groundwater.

Based on the analysis of the genetic mechanism of translational landslide, the further researches on the Tiantai village landslide in Xuanhan, Sichuan were carried out. According to the deformation and failure characteristics of Tiantai village landslide, it was defined as the multi-translational landslide. The hydrostatic water not only acted at the back side of the landslide, but also caused the high artesian groundwater pressure which forced the groundwater to infiltrate into the cracks in the slope and thus generated the hydrostatic water pressure in these cracks (Figure.25). Once the landslide began to slide, the water pressure will dissipate. Meanwhile the landslide will break up into many sliding blocks. This is the genetic mechanism of multi-translational landslide.

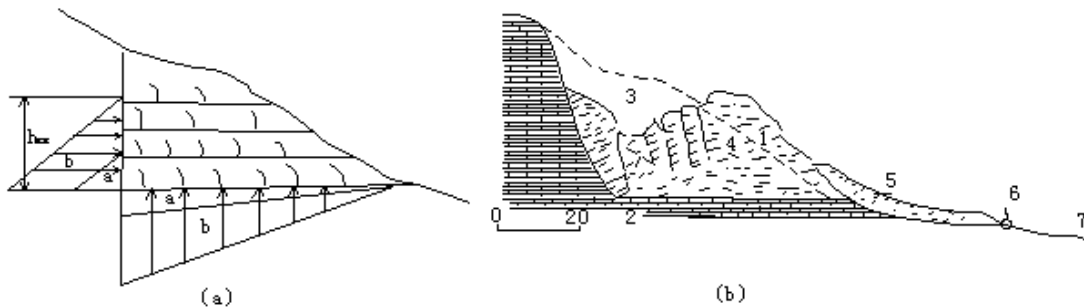


Fig. 25 Translational model of landslide occurrence induced by heavy rainfall (Source: Zhang et al., 1994)

(a) Genetic mechanism analysis: a and b are separately distributions of pore water pressures under the conditions of common and heavy rainfalls (b) Honghuatang Landslide of Longquan Mountain in Chengdu: 1—Original slope surface; 2—Siltstone and fine sandstone and mudstone of Cretacic; 3—Trough in the rear; 4—Sliding block; 5—Collapse zone of the front part; 6—Springs; 7—Debris flow

2.4.4 Toppling deformation mechanism in counter-inclined strata

Few people believe that large-scale landslide can occur in the counter-inclined rock strata slope. They think that the toppling deformation can only occur in the superficial part (from the surface to several meters deep place) of the counter-inclined slope (Zhang et al., 1994 and Wang, 1992). In recent twenty years, however, 200 to 300 meter deep bending and toppling deformation occurred in the Southwest of China, and this deformation resulted in occurrence of very large-scale landslides. For example, large toppling deformation occurred in the Triassic metamorphic sandstone and slate slopes with 10 km wide along Yalong River. The deformation area is located on the left bank of first stage Jinping Hydropower Station. Its depth is near 300 m. It can also be seen that the rock slopes located on the both banks of the river toppled toward the river in the upstream, 10 km away from the station (Figure. 26). The toppling deformation of the slopes formed two large landslides: the hydropower station landslide and the Jiaba landslide (Figure.27).

The slope is very steep, near vertical. The strata dip to 85° - 87° towards the N 10° to 30° E. The bottom of the strata is mainly composed of dark gray thin lamellar sandy slate of Triassic. The middle and top part of the strata is mainly composed of the grayish-green thin lamellar schist, marble with a little of sandstone. According to the data from the horizontal tunnel (ZD1#), the toppling of the strata was very intense.

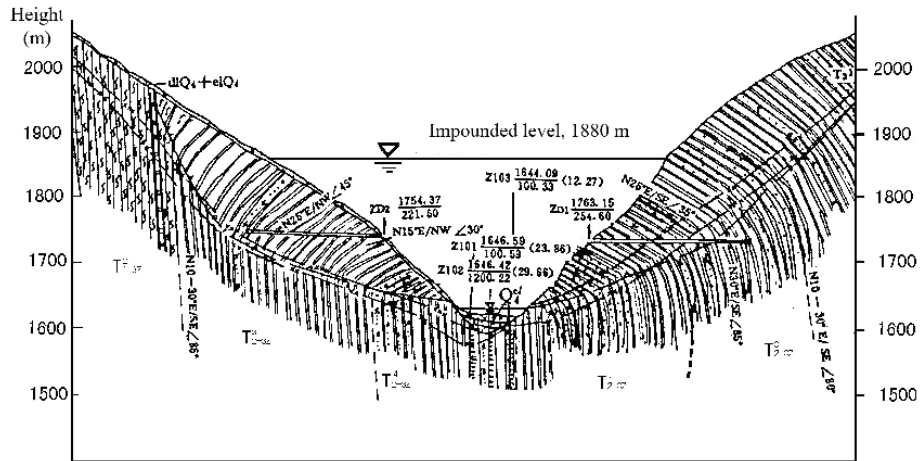


Figure. 26 Engineering geological profile of hydrological station dam site in Yalong River (unit : m) (Source: Wang et al., 1995)

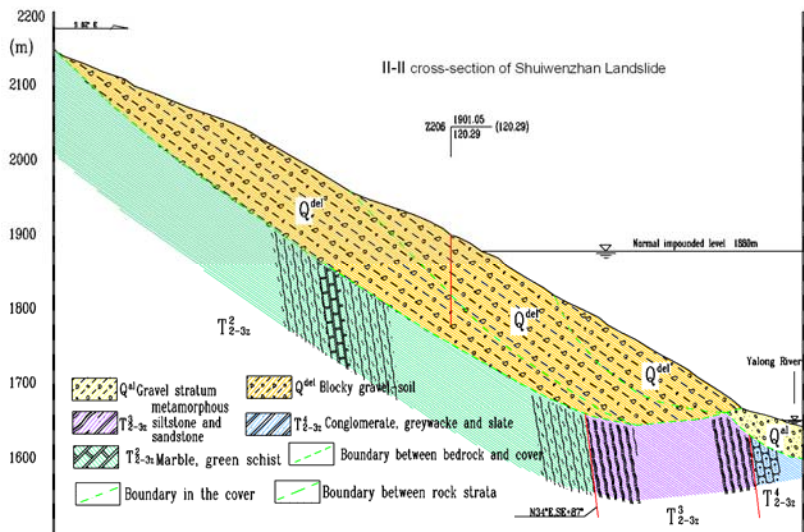


Figure. 27 Engineering geological profile of hydrological station at Yalong River landslide near the dam site (unit: m)

Similar toppling deformation phenomena was also found in the strata composed by the metamorphic sandstone and slate in Miaowei hydropower station on Lancang River. The dip angle of the strata changed gradually from the initial uprightness to 40 degrees. The horizontal and vertical depth of the toppling deformation area was around 200 m and 100 m respectively. Due to a large-scale toppling deformation, gentle platform and multilevel tension collapse zone were formed.

Another large-scale toppling slide occurred on the top of Yinshuigou clastic accumulation in Xiaowan hydropower Station. The strata are composed of the granite gneiss. It was confused that usually the granite gneiss is attributed to blocky structure. It means that the probability of toppling deformation in granite strata is very slim. However, in this area the granite gneiss was cut into steep layers across the River. In fact, the structure of the rock mass has been totally

changed by the tectonic structure and the fault F7 (towards EW). The granite gneiss with original massive structure has become the layer structure rock mass with the weak slate. That's why the large-scale toppling deformation can occur in this area.

Toppling deformation outcrops in the Xiaowan hydropower Station area were revealed by ground excavation and drainage tunnels (Figure. 28), which has following typical characteristics:

(1) The depth of the deformation zone were 150 to 200 m, and about 200 m, respectively.

(2) The deformation had the obvious ductile characteristics, which affected large area with intense toppling features. The dip angle of the rock strata varied from vertical to horizontal, which was caused by the the weak slate in the strata that sharply reduced the rigidity of the rock mass.

(3) The deformation had the obviously zonation characteristic. According to the deformation intensity, the slope can be divided into A, B, C and D four zones from inner part to outside part of the slope (Figure.28).

In brief, several conclusions can be drawn, as follows:

(1) Occurrence of large-scale toppling deformations in counter inclined lamellar rock slope is closely related to the strength and thickness of the rock. The toppling deformation usually occurs in approximately perpendicular weak lamellar strata. In fact, toppling deformations towards the free face were found in all steep slate and schist strata. The toppling degree and scale varied from one slope to another slope.

(2) Generally, all large-scale toppling deformation failures were formed through long incubating process. During the process, the rock strata can have large flexible bending deformations before failure. The failure can only happened, when the deformation accumulated to a certain threshold value. In other words, the formation of the sliding plane is completely caused by the evolution of the slope. Therefore, most slopes have the distortion phenomena, but only a small number of them can evolve into landslides. Once the landslides are formed, probably they will be large and deep slides, due to the long-term deformation.

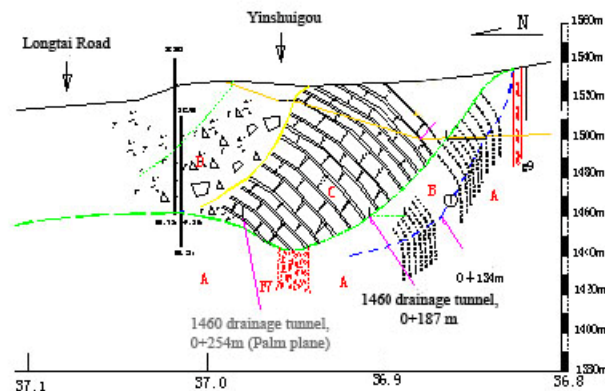


Figure. 28 Toppling deformation structure at Xiaowan Hydropower Station on Lancang river

A —Near vertical rock mass; B —Toppling loose rock mass; C —Toppling and falling accumulation; D —Colluvium;
 ① —The most curving cross section

(3) It is common that the toppling failure occurred in the steep hard thick-layer rock strata. Usually, its deformation depth is not large, ranging from 30 to 40 meters. The deformation characteristics and slope stability of the soft flexible rock strata and the hard lamellar rock strata are quite different. The former has a long deformation time from the beginning to the slope failure, and the degree of toppling can be very large. Besides, the slope stability is also not low during the deformation process. In contrast, the latter fails in very short time since the slope begins to deform. Thus, the stability is comparatively low.

2.4.5 Sliding-bending-shearing mechanism of consequent lamellar rock slope

During the past 20 years, a large number of researches on failure mechanism of consequent lamellar rock slopes were made (Zhang et al., 1994; Loky et al., 1978 and Broadbent et al., 1971). The consequent lamellar rock slopes can be classified into two categories, according to the dip angle of the slip surface. For the first category, its dip angle of the slip surface is less than the slope angle, so the outcrop of the potential slip surface will be observed in the slope or revealed by excavation. Its deformation mechanism is relatively simple, which supposed to be the creep-sliding along a potential slip surface. It is easy to identify the position of its slip surface and the corresponding stability condition. Such kind of slopes may fail suddenly. Identifying the position of the potential slip surface and monitoring the slope deformation during construction are very important for these slopes. For the other category, its dip angle of the potential slip surface is larger than the slope angle. Large-scale landslides always belong to this category. Its slip surface can't be found in the slope, hence it is hidden underneath the foot of the slope. The formation of the slip surface needs a long secular deformation process. The potential damage caused by this type of slopes is much larger than that of the first category as aforementioned. The most effective mitigation measure of this kind of slope is strengthening and protecting the resistant parts of the slope.

The conceptual model of cataclinal lamellar rock slope can be concluded as "sliding-bending-shearing" or "sliding-shearing" (Zhang et al., 1994 and Huang et al., 2002). According to the different deformation characteristics, the slope can be divided into two parts: the sliding part in the head and middle of slope (*Zone I* in Figure.29) and the bending-swelling part in the lower (front) part (*Zone II* in Figure.29). The sliding force is mainly from *Zone I* due to the gravity, which acts on the lower part of the slope (*Zone II*). The slide can't outcrop in *Zone II*, because the dip angle of the slip surface is larger than the slope angle. The deformation is restricted in *Zone II*. As a result, the slope will bend and swell in the front. It is obvious that once the bending-sweeling deformation in *Zone II* is aggravated, *Zone II* (the resistant part) will be broken by shearing, which will lead to the landslide. The resistant force of the bending-swelling part is the controlling factor of the slope stability.

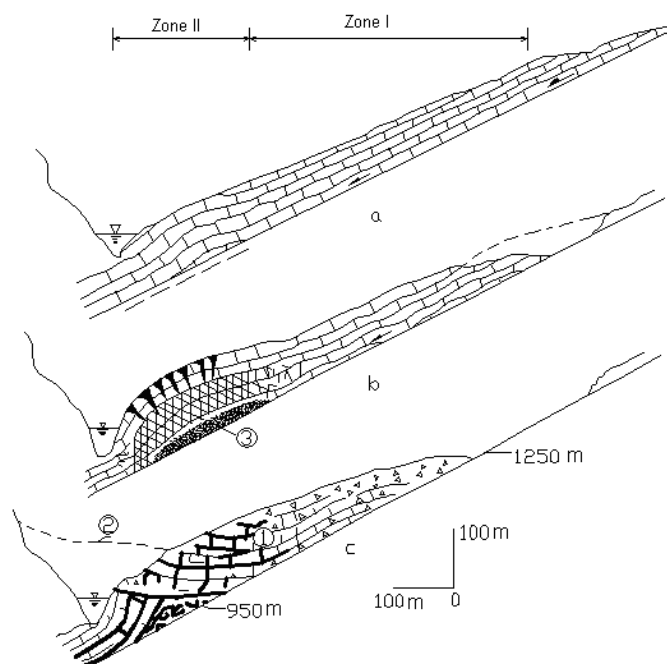


Figure. 29 Deformation and failure conceptual model of cataclinal rock slopes (From Zhang et al., 1994, modified)

2.5 Landslide risk zoning and mitigation strategies in China

China suffers severe landslide hazards every year. Landslides threaten people's lives and properties in 30 provinces, resulting in an estimated 700 to 1000 deaths and more than \$10 billion RMB economic loss annually (Yin, 2004). In order to reduce the damage caused by landslides, Chinese government has taken the following counter measures since 1990:

2.5.1 Nation-wide landslide investigation and risk zoning

Since 1999, China has completed a landslide mapping program with the scale of 1:500,000. A landslide database was built, including detailed geological information of 55 000 landslides, 13 000 rockfalls and 17 000 debris flows. More specific investigations and risk zoning of landslides have been ongoing since 1999, which covers landslide-prone areas in about 1500 counties. The main task of this program is to investigate the potential landslides, provide an emergency preparedness plan, as well as establish warning systems. About 150 000 potential landslides have been identified, and 80 000 of them are monitored. This program, called "monitoring and preventing by masses", has been proved to be very efficient for landslide mitigation (Yin, 2004). The success rate of landslide prediction and warning is obviously rising since the mapping and risk zoning plan was carried out (Table 3). Figure.30 presents the fatalities caused by landslides in China's mainland from 1995 to 2009. Before 2000, there were almost 1157 people per year killed by landslides, but after 2000, the number was 781, which obviously decreased.

Table 3 Number & losses of landslides and successfully predicted landslides in China mainland during 2001-2009

Year	Number of landslides	Fatalities	Economic loss (10 ⁸ RMB)	successfully predicted Landslides	Number of survivals (10 ⁴)	Avoided economic loss (10 ⁴ RMB)
2001	5793	908	35.0	231	0.4	0.86
2002	48000	1016	51.0	703	1.9	2.36
2003	13832	868	48.7	697	3.0	-
2004	13555	858	40.9	722	4.8	4.53
2005	17751	682	36.5	500	1.1	3.41
2006	102804	774	43.2	478	2.1	2.39
2007	25364	679	24.8	920	3.8	5.50
2008	26580	757	32.7	478	2.1	3.22
2009	10840	486	17.7	209	1.4	1.64
average	29391	781	36.7	549	2.3	3.5

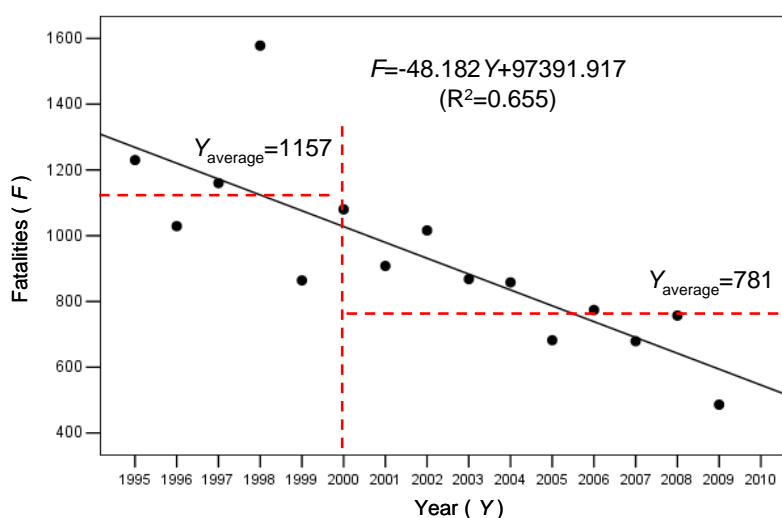


Figure.30 Fatalities caused by landslides in China's mainland from 1995 to 2009

Table 4 shows the statistical results of life and economic loss caused by large-scale landslides in the abovementioned nine landslide concentration zones from 2001 to 2009. As shown in this table, the casualties in D zone are most serious, while the economic loss in A zone is very large. In order to quantify the landslide risk in different areas, a risk index was created, which is expressed as Equation 6. In Equation 6, in order to combine the fatality and the economic loss, one fatality is assumed to be represented by 2 million RMB. As shown in Table 4 and Figure 31, landslide risk is ranked into four levels: very high, high, medium and low. Although the risk zonation is simple, the results fit the practical risk situation in China very well.

$$\text{Risk} = \text{Fatalities} * 200 + \text{Property loss} \quad (6)$$

Table 4 Statistical table of life and property damage caused by large-scale landslides in the abovementioned 9 landslide concentration zones during 2001 to 2009

Zone	Landslide number	Fatalities	Economic loss (10 ⁴ RMB)	Integrated index	Risk
A	13	164	25911	58711	Very high
B	4	114	0	22800	High
C	4	88	1000	18600	Medium
D	7	215	8000	51000	Very high
E	17	76	15463	30663	High
F	11	148	5928	35528	High
G	4	0	14771	14771	Medium
H	5	55	2800	13800	Medium
I	3	7	2060	3460	Low
Sum	68	867	75933		

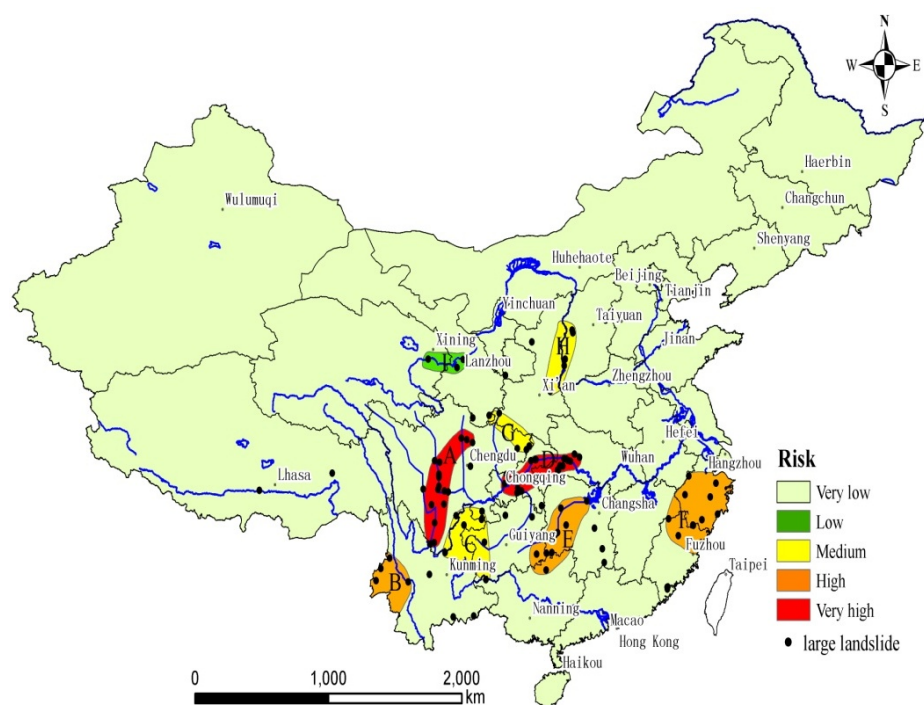


Figure.31 Landslide risk map of China

2.5.2 Detailed landslide mapping for high risk zones

Both the landslide triggering factors and mechanism in China are very complicated. More detailed surveying and mapping for landslides in the high risk zones have been carried out on the base of landslide geological conditions. The landslide triggering factors, such as rainfall, earthquake, and human activities are comprehensively analyzed. This survey program is based on 1:50 000 scale. Detailed landslide inventory and distribution map were produced, which provide us with a lot of information, including landslide susceptibility, geological and geo-

environment conditions, their impacts of construction projects, such as dams and pipe lines etc in the high risk zones. These documents will be used as guidance for risk assessment for urban development and relocations. In China, the landslide hazard reduction work is usually organized by central or local governments. Therefore, geologists' suggestions are very important for decision makers. Through the landslide hazard and risk maps created by experts, the people in the government can understand the critical issues better and make right decisions (Yin, 2004).

2.5.3 Mitigation for some major landslides

Since "International Decade of Natural Disaster Reduction Program" started in 1990, more than 200 major landslides that severely threatened the cities, main rivers, and other key public facilities have been stabilized. The Three Gorges Project is one of the largest water resources development programs in the world. The resettled population of the Three Gorges Reservoir area is about 1.2 million. During the first phase from 1993 to 1997, 82 000 people were resettled, and 550 000 populations were resettled in the second phase of the project from 1997 to 2003. Till 2009, over 600 000 people were resettled during the third phase of the project. The resettlement is a big challenge for government, because it is difficult to find suitable construction land in the reservoir area. Sometimes people have no alternatives except moving to landslide-prone areas. A systematic landslide mitigation project has been carried out since 2001, which aimed to protect and stabilize the dangerous slopes, rockfall deposits as well as to solve the engineering problems that we encountered when the large-scale excavation and filling were carried out (Yin, 2004).

2.5.4 Weather-based regional landslide hazard warning

In 2003, the Ministry of Land Resources (MLR) and China Meteorological Administration (CMA) signed a cooperative agreement on operating a weather-based geohazard warning service during the raining seasons. CMA provides rainfall data, and MLR will make forecast for geo-hazard occurrence, and release warning announcement through China Central Television (CCTV) after broadcasting daily weather forecast. In the same way, the local cooperative agreements have also been signed by local provincial governments. The weather-based warning system is part of the landslide prevention program of "monitoring and prevention by masses". According to incomplete statistics in 2004, over 700 landslides were successfully predicted and warned, and 46 000 persons were evacuated from dangerous areas. On August 24, 2004, MRL and CMA jointly proposed a 4-5 class landslide warning system in the coastal areas in Zhejiang and Fujian Province, before the "Aily" Typhoon coming on 25-26 August. Two days later, the typhoon brought 400-600 mm rainfall, which triggered hundreds of landslides, but nobody was injured or killed, because tens of thousands of people were evacuated from the dangerous region (Yin, 2004).

2.5.5 Risk assessment of landslides caused by the construction of infrastructures

The construction of infrastructures in the western mountain areas of China has caused a lot of landslides. According to the latest statistics, about 80% of the landslides are induced by

inappropriate construction activities. In 1999, the Ministry of Land Resources issued that before a project starts, the government needs first to evaluate the possible geo-hazards that might be caused by this project. It is a compulsory policy to prevent the inappropriate anthropogenic activity induced landslides. The largest project related to landslide risk assessment in China is the natural gas pipeline project, which links the Xinjiang Autonomous Region to Shanghai. The 4200 km long pipeline comes through various complicate geological and geomorphologic areas, which pose significant constraints on the pipe alignment and construction. The beforehand potential landslide hazard assessment of this project is very helpful for avoiding many major hazards that may threaten the project (Yin, 2004).

2.5.6 Education and training for geohazard mitigation

In China, the development in rural areas is behind that in the urban areas. People in rural areas are much more vulnerable than those in the urban areas, due to their low incomes and poor knowledge on landslide prevention. The Ministry of Land Resources of China organized a series of training courses in 19 provinces in 2006. Three million people joined in the course and learned some fundamental knowledge on how to carry out appropriate activities to avoid human activity-induced geo-hazards, simple methods of landslide monitoring and early warning, emergent evacuation and rescuing actions, etc. A large number of landslides had been successfully warned and avoided in the raining season in 2007, which reflects that the public training and education have a good effect on landslide hazard prevention (Yin, 2004).

2.6 Conclusions

(1) Landslides occur frequently in China, especially large-scale landslides. In the western part of China, the large-scale landslides are notable for their scale, complex formation mechanism and serious destruction.

(2) The general terrain and topography in China somehow determine the landslide distribution. The continent of China is composed by the Qinghai-Tibet plateau, Yun-Gui plateau in the west, mountainous area in the middle, and plain near sea in the east, which depict the three-level terrace picture of the terrain in China. The slope-descending zones are formed. The altitude is reduced sharply from the west to the east, especially in the region among Qinghai-Tibet plateau, Yun-Gui plateau and Sichuan basin. The typical terrain in this region are high mountains and canyons which are formed by the deep incising of rivers originated from Qinghai-Tibet plateau, such as Jinsha River and its branches (Yalong River, Dadu River, Minjiang River), Lancang River and Nujiang River.

(3) The plate tectonics movement in China is very active, comparing to the other countries in the world. Due to the intense plate collision between Indian Ocean Plate and Eurasian Plate and continual uplifting of Qinghai-Tibet plateau, the geological endogen in the crust transfers from the west to the east, affecting numerous areas, including the far away middle and eastern parts. The intensive interactions between the endogenic and epigenetic geological process cause serious dynamic change of the high steep slopes, which are resulted in the development

of large-scale landslides. Strong earthquakes are also common in this area and repetitive seismic activities make the slopes unstable and very fragile.

(4) The triggering factor changes with the areas in China. In the southwestern part of China, rainfall is the most important triggering factor, while in the northwestern part, landslides always occur in March or April, which were mainly induced by snow melting. In the conjunction part between Tibet Plateau and southwestern area, most landslides are triggered by strong earthquakes. In high altitude regions such as Qinghai-Tibet plateau and Tian Mountain in Xinjiang, the global climate change cause the temperature and snow line rose and the glacier retrogressed, which are the triggering factors of large landslides. Meanwhile, human activity is also one important triggering factor.

(5) The genetic mechanisms of large-scale landslides are very complicated. The large-scale landslides can be classified into three types: rock landslide, soil landslide, and unconsolidated debris landslide. Except the unconsolidated debris landslide, the former two types have more complex deformation mechanism.

① The mechanisms of large-scale landslides can be grouped into several typical types: sliding-tension and cracking-shearing, “retaining wall collapse” model, translational sliding in near horizontal strata, large-scale toppling deformation in the counter-inclined strata, as well as the creep-shearing model of cataclinal rock strata. Every type has its specific deforming evolvement and failure mechanism, occurring in different geological environments. Detailed landslide investigation and understanding landslide genetic mechanisms are very important and fundamental for making the mitigation measures.

② Large-scale rock landslides always occurred with the abrupt brittle failure of “lock section” (the resistant part) of slope. The lock section plays an important role in restricting the landslide deformation and improving the stability of landslide. It is also the key to evaluate and prevent the landslide disasters.

(6) China has accomplished a nation-wide landslide investigation and mapping program started since 1999, and also has successfully carried out a number of large-scale landslide prevention projects since the early 1990s, with particular attention to the Three Gorges reservoir area and the cities under rapid development in the western part of China. The weather-based landslide forecast system has been established that covers the landslide prone zone in the national wide.

Acknowledgement

The author would like to thank Xu Zemin for arranging some parts of representative landslide cases; Prof. Xu Q for offering some of landslide cases and other colleagues for their critical suggestions.

References

- Au S.W.C. Rain-induced slope instability in Hong Kong. *Engineering Geology*, 1998, 51 (1): 1~36
- Baum R. L., Crone A. J., Escobar D. & Harp E. L. et al. Assessment of Landslide Hazards Resulting from the February 13, 2001, El Salvador Earthquake -- A Report to the Government of El Salvador and the U.S. Agency for International Development. *U.S. Geological Survey Open-File Report 01-0119*, Version 1.0, 22 p., 2001.
- Bhasin R., Grimstad E. & Larsen J. O. et al. Landslide hazards and mitigation measures at Gangtok, Sikkim Himalaya. *Engineering Geology*, 2002, 64(4): 351~368
- Broadbent, C. D. and Ko, K. C. Rheology aspects of rock slope failure. Proc. of 13th Symp. on Rock Mechanics, 1971, Illinois, pp537-572.
- Brückl E. P. Cause-Effect Models of Large Landslides. *Natural Hazards*, 2001, 23(2-3): 291-314.
- Cai Z. X.. On characteristics of soil and water loss and related policies of control in upper reaches of Changjiang River. *Discovery of Nature*, 1988, (4): 97-104
- Cai Z. X.. The study on slide disaster and its countermeasure. *Journal of Catastrophology*, 1989, (1): 74-77
- Chen Z. S., and Kong J. M.. A catastrophic landslide of Sept. 23, 1991 at Touzhaigou of Zhaotong, Yunnan Province. *Journal of Mountain Research*, 1991, 9(4): 265~268
- Collison A., Wade S. & Griffiths J. et al. Modelling the impact of predicted climate change on landslide frequency and magnitude in SE England. *Engineering Geology*, 2000, 55(3): 205~218
- Crosta G.B. Failure and flow development of a complex slide: the 1993 Sesa landslide. *Engineering Geology*, 2001, 59 (1-2): 173~199.
- Cruden DM and Varnes DJ (1996) Landslides types and processes. In Turner, AK and Schuster RL (Editors), *Landslides Investigation and Mitigation: Transportation Research Board, US National Research Council, Special Report 247*, Washington, DC: 36-75
- Duan Y. H.. Basic characters of geo-hazards and its development trend in china. *Quaternary Sciences*, 1999, 19(3): 208~216
- Duan Y. H.. Present state, trend and countermeasure of geological hazards in Chinese West. *Economic research reference*. 2000, (58): 12~18
- Hang Z. Y., Huang R. Q.. Epigenetic recreation of rockmass structure and time-dependent deformation, In: Proc. of the 6th Cong. of IAEGE, A. A. Balkema, 1990. pp. 2065-2072.
- Huang R. Q. Full-course numerical simulation of hazardous landslides and falls. In: Proc. of the 7th Inter. Symp. on Landslides. A. A. Balkema, 1996. pp1134-1140
- Huang R. Q., Wang S. T., and Zhang Z. Y., et al. Shallow earth crust dynamics process and engineering environment research in Western China. Chengdu: Sichuan University Press, 2002
- Huang R. Q., Zhao S. J., and Song X. B.. The formation and mechanism analysis of Tiantai landslide, Xuanhan County, Sichuan Province. *Hydrogeology and Engineering Geology*, 2005, 32 (1), 13-15
- Huang R. Q., Deng R. G., et al. Full simulation process for high slope substance moving. Chengdu: Chengdu University of Technology Press, 1993
- Huang R. Q.. Studies of the geological model and formation mechanism of Xikou landslide. In: Proc. of the 7th Inter. Symp. on Landslides. A. A. Balkema. 1996. pp1671-1678

- Huang R.Q., Chen L.S., Human induced landslide in China: mechanism study and its implications on slope management, *Chinese Journal of Rock Mechanics and Engineering*, 2004, 23(16): 2766-2777
- Huang R.Q., Wang Z.R., Xu Q., A study of failure rules of anti-dip strata slopes, *Advance of Engineering Geology* (No.2), Chengdu: Southwest Jiaotong University Press, 1994:47-51
- Huang R.Q., Xu, Z.M., Touzhaigou landslide, Zhaotong, Yunnan Province (1991). In: Huang, R.Q., Xu, Z.M. (eds), *Catastrophic landslides in China*. Chinese Science, China, 2008: 307-340
- Huang R.Q., Zhang Z.Y., Wang S.T., Research on rock structure and epigenetic reformation, *Hydrogeology and Engineering Geology*, 1994, 21(4): 17-21
- Huang R.Q., Zhang Z.Y., Wang S.T., Symtematic engineering geology studying of the stability of high slope, Chengdu University of Technology Press, 1991
- Huang Z. Z, Tang R. C., and Liu S. L.. Re-discussion of the Seismogenic Structure of the Diexi Large Earthquake in 1933 and the Arc Tectonics on Jiaochang, Sichuan Province. *Earthquake Research in China*, 2002, 18(2): 183~192
- Huang, R Q, Wang S T. Rolling friction mechanism for high speed motion of a landslide[A]. In: Proceedings of the 5th International Symposium on Landslides[C]. Rotterdam: A. A. Balkema, 1988, 673~678
- Jiang C. S.. Present state and prevention of China's geological disasters. *Chinese Geology*, 2000, (4): 3~5
- Jin D. S.. Laojinshan Landslide in Yuanyang, Yunnan Province. *The Chinese Journal of Geological Hazard and Control*, 1998, 9(4): 98~101,80
- Leng L., and Leng R. H.. Flood in Yalong River and its historical lesson. *Sichuan Water Conservation*, 2002, (2): 42~44
- Li N.. Landfall-landslide blocking river disasters and its prevention measures in Yunnan Province[C]. Commission of Proceedings of Landslides ed. Proceedings of Landslides(No. 9). Beijing: China Railway Publishing House, 1992: 50-55
- Li T B, Chen M D, and Wang L S. Real-time following prediction of the landslides. Chengdu: Chengdu University of Technology Press, 1999.
- Li Y. C.. On-the-spot record of Diexi Earthquake. *Literary History World*, 2002, (6): 39~42
- Lin D. M., Pi L. Y. Huang H. L. et al. Study on engineering-geological conditions for landslide at Badu k343 section Nankun railway and control on it. *Journal of Engineering Geology*, 2002, 10(2): 220~224
- Lin P. S., Lin J.Y. & Hung J. C. et al. Assessing debris-flow hazard in a watershed in Taiwan. *Engineering Geology*, 2002, 66(3-4): 295~313
- Lo, K. Y. and Wai, R. S. C.. Time dependent deformation of shaly rocks in southern Ontario. *Cana. Geotech. J.*, 1978, Vol.15.
- Mauritsch H. J., Seiberl W. & Arndt R. et al. Geophysical investigations of large landslides in the Carnic Region of southern Austria. *Engineering Geology*, 2000, 56 (3-4): 373~388
- Parise M. & Wasowski J. Landslide Activity Maps for Landslide Hazard Evaluation: Three Case Studies from Southern Italy. *Natural Hazards*, 1999, 20(2-3): 159~183
- Radbruch-Hall D.H., Colton R. B. & Davies W. E. et al. Landslide Overview Map of the Conterminous United States. *United States Geological Survey Professional Paper* 1183, 1983

- Raetzo H., Lateltin O. & Bollinger D. et al. Hazard assessment in Switzerland - Codes of Practice for mass movements. *Bulletin of Engineering Geology and the Environment*, 2002, 61: 263~268
- Schuster R. L. & Lynn M. H. Socioeconomic Impacts of Landslides in the Western Hemisphere. *U.S. Geological Survey Open-file Report*, 01-9276, 2001
- Schuster R.L. The 25 most catastrophic landslides of the 20th century, in Chacon, Irigaray and Fernandez (eds.), *Landslides, Proc. Of the 8th International Conf. & Field Trip on Landslides*, Granada, Spain, 27~28 Sept. Rotterdam: Balkema, 1996
- Staub I. B. A methodology for the mapping and analysis of "debris-flow initiation" hazard - application to the Bragousse torrent (France). *Bulletin of Engineering Geology and the Environment*, 2001, 59(4): 319~327
- Sun D. Y.. Project regulation of Badu Landslide in Nan-Kun Railway. Beijing: Chinese railway press, 2000.
- Sun T., Chen Y.. Application of finite element technique to analyzing the slope stability—evaluation the stability of the Jiaochang talus slide in Tianlonghu Hydropower Station. *Sichuan Water Power*, 2001, 20(1): 28~31
- The U.S. Geological Survey. Landslide hazards. *USGS Fact Sheet* Fs-071-00, 2000
- Varnes D.J. and Savage W.Z.. The Slumgullion Earth flow: A Large-Scale Natural Laboratory, U.S. Geological Survey Bulletin 2130. Washington: United States government printing office, 1996(available at: <http://pubs.usgs.gov/bul/b2130/>).
- Voight B. & Faust C. Frictional heat and strength loss in some rapid landslides: error correction and affirmation of mechanism for the Vaiont landslide. *Geotechnique*, 1992, 42: 641~643.
- Wang J D, Zhang Z Y. Systematic Engineering Studies of Typical Loess Landslides with High Speed Motion[M]. Chengdu: Sichuan Science and Technology Publishing House, 1999.
- Wang L S, Zhang Z Y, Li Y G, et al. Rainstorm rock slides and their stability problem in the construction at Sichuan basin [A]. In: Proceedings of the 5th International Congress of IAEG[C]. Rotterdam: A. A. Balkema,1986,2 047~2 056
- Wang L. S., Zhao Z. Y.. The basic geological mechanism model of slope rock body deformation and destruction. *Hydrological and Engineering Geology*. 1983
- Wang S. J. The deformation mechanism and process research of Jinchuan strip mine slope. *Chinese Journal of Geotechnical Engineering*, 1992, 14(1): 1~7
- Wang S. J.Tasks and future of engineering geology. *Journal of Engineering Geology*, 1999, 7(3): 195~199
- Wang S. T., Huang R. Q., and Li Y. S... Key engineering geology problems and research on Jinping Hydropower Station in Yalongjiang River. Chengdu: Chengdu University of Science and Technology Press, 1995.(in Chinese)
- Wu C., Ran H. X., Zhen Y. H., et al. Hydrograph of the dam-break flood of the reservoir formed by mountain collapse in Ya Longjiang, *Journal of Hydrodynamics(A)*, 1996, 11(6): 646~652
- Wu W. J., Wang S. Y.. The mechanism of Saleshan Landslide. National landslide conference—landslides. Chengdu: Sichuan Science and Technology Press. 1989, pp. 184-189.
- Xu B. D., Pan H. T.. The effect of coal mining on Kengkou and Hancheng Power Plants slope[C]// Commission of Proceedings of Landslides ed. Proceedings of Landslides (No. 9). Beijing: China Railway Publishing House, 1992: 1-9

- Xu D.J, Chen C.X, Liu X.W, et al., Study on prediction of rock slopes , Chinese Journal of Rock Mechanics and Engineering, 1999, 18(4): 369-372
- Yamagishi H. Recent Landslides in Western Hokkaido, Japan. *Pure and Applied Geophysics*, 2000, 157(6-8): 1115~1134
- Yin S. L., Han Z. S., and Li Z. Z.. Progress of landslide researches in the world. *Hydrogeology and Engineering Geology*, 2000, (5): 1~4
- Yin Y. P.. A review and vision of geological hazards in China. *Management Geological Science and Technology*, 2001, 18(3): 26~29
- Yin Y. P.. The research on characteristics of rapid huge landslide in Yigong River in the Bomi, Tibet and disaster relief. *Hydrogeology and Engineering Geology*, 2000, (4): 8~11
- YIN Yueping, Initial study on the hazard-relief strategy of geological hazard in China. *The Chinese Journal of Geological Hazard and Control*. Vol.15. 2004(2): 1~6.
- Zhang Z. Y., Liu H. C., et al. Key engineering geology problem and research on Longyangxia Hydropower Station of Huanghe River. Chengdu: Chengdu University of Technology Press, 1990
- Zhang Z. Y., The present status, technical advance and development trends of landslide remedial measures. *Journal of Geological Hazards and Environment Preservation*, 2000, 11(2): 89~97
- Zhang Z.Y., Liu H. C.. A special case history of the environmental impact by underground mining —the mechanism and control measures of the ground upheaval deformation of hancheng power plant. *Earth Science Frontiers*, 2001, 8 (2): 285~295
- Zhang Z.Y., Wang S.T., Wang L.S., Principle of engineering geology analysis, 1994
- Zhong L. X. Case study on significant geohazards in China. *The Chinese Journal of Geological Hazard and Control*, 1999, 10(3): 1~10

CHAPTER 3 LANDSLIDE INVENTORY MAPPING IN CHINA

Shuren Wu, Jusong Shi & Ping Sun

*Key Laboratory of Neotectonic Movement & Geohazard, Ministry of Land and Resources
Institute of Geomechanics, Chinese Academy of Geological Sciences, Beijing, 100081, China*

3.1 Introduction

Landslide inventory mapping is the basis of landslide risk assessment. How to build a complete landslide inventory database and real-time updating and database maintenance, how to keep the landslide inventory data availability, reliability and timeliness (updated) are the key problems of landslide risk assessment and management. Since the nineties of the 20th century, China has carried out national environmental geological survey of the major rivers and major geohazards along important lifelines at 1:500000 scale, especially on landslide investigation. Since 1999, Ministry of Land and Resources launched a national mountainous or hilly county (city) geohazard investigation and zoning project, which not only includes landslide, but also include land subsidence, ground fissure, ground collapse. The project ended in 2008. The geohazard warning information systems in 1640 counties were completed, which preliminary revealed the national landslide distribution characteristics in China. Landslide prone areas and high hazard level areas were depicted, meanwhile a basic landslide public monitoring and elemental early warning systems were set up, which effectively reduce the loss caused by geohazards. The first national geohazard inventory database was established. In recent years, landslide hazard survey and inventory database construction have made significant progress in China, mainly in:

① For river basin development, flooding control, water resources and hydropower development, China carried out landslide inventory in the major river basins. With the construction of major projects (such as large-scale hydropower stations, railway, oil or gas pipeline), China carried out engineering geological survey of the affected engineering construction sites or the route of lifelines, finished landslide mapping and established the corresponding landslide early warning information system. The most typical example is Geohazard Monitoring and Early Warning Information Systems in the reservoir region of Three Gorges Project, which are based detailed landslide inventory database;

② Since 1999, Ministry of Land and Resource organized national "County geohazard survey project" and built a corresponding Geohazard database (CGHIS), which is the most comprehensive landslide inventory database, including geological environment factors with uniform standard of landslide data attribute, structure and contents of the database;

③ Since 2005, China Geological survey started 1:50 000 landslide survey project has been carried out, including the high resolution remote sensing image interpretation, field investigation and comprehensive detailed studies for county geohazards investigation. This work provided detailed and professional landslide inventory data for the national wide landslide inventory database;

④ A number of research work on landslide study supported by Ministry of Science and Technology or other funding, including landslide early warning information system, landslide inventory database structure, quantitative methods for landslide risk assessment etc., to some extent, provided effective methods or technology for landslide inventory mapping in China.

⑤ Since December 1st, 1999, the implementation of Geohazard Hazard Assessment for important engineering construction sites greatly promoted landslide investigation and inventory. Meanwhile, a series of standards or norms correspond to the needs of engineering construction type, such as *Water Resources and Hydropower Engineering Geological Investigation specification*, *Geotechnical Engineering Investigation Standards*, *Railway Engineering geological exploration norm* and etc., those standards have a clear requirement for landslide investigation and exploration methods and technology in different phase of engineering construction, provide a detailed inventory technical requirements and means of methods;

⑥ Responding to major or unexpected landslide hazard events, landslide emergency mapping and landslide field inspection before raining season were organized by Ministry of Land and resource and departments at all levels of government respectively, by using ground survey, remote sensing survey and exploration or those methods combination. This work contributes a lot to the data update of landslide inventory database and also provides the up-to-date landslide data and information.

Landslide investigation and inventory mapping varied with different departments for different needs with different specifications, standard or norms, such as *Geotechnical Engineering Investigation Standards*, *Water Resources and Hydropower Engineering Geological Investigation specification*, *Railway engineering geological investigation norms*, *Specifications for engineering geology exploration for Landslide preventions*. The fall, landslide and debris flow survey are defined by these specifications with the main contents and technical requirements corresponding to different stages of engineering construction. Landslide risk management is one of the mandates of Ministry of Land and Resource. National wide landslide inventory is based on geohazard survey projects mainly at 1:100000 and 1:50000 scale, which are organized by China Geological Survey. And those projects are providing none-profit public service. China Institute of Geo-Environment Monitoring is in charge of landslide inventory database construction and maintenance. China geological survey, related government agencies and companies involved in landslide survey or mapping are in duty bound to provide landslide inventory data and documentaries. Based on a general introduction of China's current public services projects for landslide inventory mapping including purpose, achievements and methods used, this chapter will introduce technical guideline and framework of landslide survey at 1:50000 scale with emphasis on landslide inventory methods from data collection and analysis, remote sensing image interpretation, ground survey mapping and engineering survey and other methods for landslide mapping application with Baoji city landslide survey as a case study. Following a brief introduction of China landslide inventory database technical guidelines, the landslide field inventory form and technical processes of inventory database of will be focused on, database software tools and the contents of database as well. Finally, this chapter will discuss the potential challenges and problems of China landslide inventory and database

construction from data accuracy, completeness, accessibility, updating and sharing, compatibility and integration of different data, data visualization and availability and etc..

3.2 Landslide inventory mapping projects in China

There are 6 types of projects related to landslide inventory mapping in China as follows. Each type of project will be brief introduced from the main objects, purpose, coverage and achievements as follows.

3.2.1 1:100000 County geohazards investigation

From 1999 to 2005, in order to identify the characteristics of the national geohazard distribution, to reduce casualties and property losses, Ministry of Land and Resource carried out geohazard investigation in 700 counties (cities) which have suffered serious loss due to geohazards. This investigation covers 45% of the total number of counties (cities) in mountainous or hill region with an area of 2.08 million square kilometers, accounting 32% of mountainous or hilly area. 440 million population were involved. Based on the achievements of county landslide investigation and mapping, China Institute of Geo-Environment Monitoring carried out comprehensive studies and landslide inventory database integration. The rule of landslide spatial distribution, major geohazards distribution and related consequence were revealed, meanwhile the landslide prone areas were delineated. Finally a national geohazard database was created.

The 700 counties (cities) geohazard investigation the counties geohazard investigation has achieved good economic and social benefits. Ministry of Land and Resources approved a state special finance funding project- Geohazard survey in hilly and mountainous areas. From 2006 to 2008, MLR carried out geohazard survey of the other 940 mountainous or hilly counties (cities) , which accounted 55% of the total number of counties (cities) in mountainous or hill region with an area of 4.42 million square kilometers, accounting 68% of mountainous or hilly area. 350 million population were involved.

At the end of 2008, a total of 1,640 counties nationwide geohazard survey at 1:100 000 scale was completed, It recorded 176,452 spots in total, including 75 821 landslides, 31384 rock falls, 20305 debris flows, 37104 potential unstable slopes, 9269 ground collapses, 2542 ground fissures, 27 ground subsidences (according to the China Geological Environmental Monitoring Institute, ended in April 2010).

The object of county geohazard investigation in China is to carry out geohazard inventory mapping, delineate geohazard prone areas and dangerous areas, construct geohazard information system, establish and improve public geohazard monitoring and early warning network, make effort to geohazard prevention, losses reduction and life or property protection. The main tasks are as follows:

① Geohazard investigation and inventory, including rock falls, landslides, debris or mud flows, ground subsidence, ground fissures, collapses. Ascertain their distribution, size, structure characteristics, controlling factors, etc;

② Potential unstable slope near the towns, factories, mines, major transportation lines, important engineering facilities investigation;

③ Geohazard information system construction, including geohazards susceptibility assessment and geohazard prone and dangerous areas delineation, geohazard prevention plan and zoning , to assist local governments to establish public monitoring and early warning network and to make geohazard mitigation plans;

④ Geohazard mitigation training for local staff according to the achievement of the county geohazard investigation and guiding geohazard monitoring and early warning.

3.2.2 1:50 000 Geohazards survey and mapping

Based on the national county geohazards investigation, China Geological Survey started 1:50 000 scale landslide investigation and mapping project since 2005. According to geology structural difference in China, the project was divided into 3 separate parts, which are the Northwest loess plateau, the Southwest mountainous area and the Hunan, Hubei, Guangxi mountainous regions. The detailed investigation, mapping and explorations on landslides, rock falls, flow types slides and potential unstable slopes were carried out, in order to provide basic geological data for geohazard prevention. The main tasks are:

① to carry out geological surveys, analyzing structure and soil conditions of landslides, falls, debris flows, identifying their development, mechanism, evaluation and prediction of their development trend, as well as creating the environmental engineering geology mapping;

② to carry out the geohazard investigation and inventory, understanding their distribution, size, structural characteristics, controlling factors and triggering factors, and evaluating their hazard and consequence.

③ to carry out the investigations on potential unstable slopes and other geohazards that are close to cities, towns, factories, mines, major transportation lines, important engineering facilities, major rivers, important scenic areas and key traditional areas, and estimate their hazard and consequence.

④ according to the mitigation planning, finding new sites for emergency relocation and carrying out landslide hazards assessment for construction land and preliminary assessment of its suitability;

⑤ to collect meteorological and hydrological data and carry out hydrogeological conditions survey and analysis the impact of precipitation on slides, falls and debris flows, and consequently creating the meteorological geohazard early warning zonation;

⑥ to assist local governments to establish public geohazard monitoring and early warning network , and make the prevention and emergency work plans for important geohazards;

⑦ to establish a geohazard information system and carry out geohazard assessment including susceptibility and hazard assessment and mapping.

Till the April 2010, China Geological Survey has completed detailed geohazard survey in 88 counties, which covers the main geohazard high susceptibility basin or project sites, providing professional geohazard survey and hazard zoning data, the achievements are as follows:

① The work in the Northwest Loess Plateau region was coordinated with Xi'an geological survey center and has completed the detailed geohazard investigation, mapping and data updating in 47 counties (cities) totally. So far 18 857 landslides were investigated, including 8922 potential landslides, 4204 slides, 1118 rock falls, 1112 debris flows, 2413 potential

unstable slopes, and 75 other types). Among them, there are 1478 fatal potential geohazards and 1910 recently inventory ones. The geohazard investigation provided more accurate data and technical support for the local government's geohazard prevention and mitigation planning.

② The work in Southwest Mountainous region was coordinated with Chengdu geological survey center and has completed the detailed geohazard investigation in 28 counties (cities) totally from 2005 to 2009. In total, 12 957 landslides were investigated, among which there are 4367 recently investigated spots compared to the 1:100 000 county geohazards investigation.

③ The work in the mountainous regions in Hunan, Hubei and Guangxi province was coordinated with Wuhan geological survey center and has completed detailed geohazard investigation in 13 counties (cities). 4713 geohazards were investigated in total, including 2710 slides, 846 falls, 64 debris flows, 863 potential unstable slopes, 205 ground collapses, 7 ground fissures.

3.2.3 Landslide investigation in the important national project regions

For different needs of national important project planning, site or route selection, design, construction and safe operation, a lot of geological survey and geotechnical engineering investigation were carried out. Landslide mappings in project site, reservoir region or along the route of railways, highways, oil and gas pipeline were finished. The most representative region is the Three Gorges reservoir area. Ministry of Land and Resource , Ministry of Water Resources, Ministry of Communications, the Three Gorges Construction Committee of Immigration, Local Government and other relevant departments at all levels, have done a lot of work in order to control and prevent geohazards in Three Gorges reservoir area. Since the 1990s, Ministry of Land and Resource and the Committee on the Yangtze River of Ministry of Water Resources have conducted extensive investigation for the stability of reservoir bank and geohazard assessment in the Three Gorges region. Especially in the construction phase of the Three Gorges Project, quite a lot of site engineering geological investigations for towns, resettlement site selection geological survey work were carried out. Since 1999, the first 13 counties geohazard investigations in Three Gorges area were carried out with systematically landslide inventory database and large scale engineering geology exploration of major towns and cities site in the reservoir region for geohazard prevention. Since 2001, the implementation of geohazard centralized prevention project in Three Gorges reservoir area, Hubei and Chongqing finished 465 landslides engineering works and 216 km reservoir bank protection works. Since 2006, large scale landslide survey and monitoring in TGP area were carried out. Aerial photos covered 40,000 km², and 3D virtual environment of the TGP area were completed. Geohazard Monitoring and Early Warning Information Systems in the reservoir region of Three Gorges Project were established.

3.2.4 Geohazards hazard assessment for new planning construction site

From December 1st, 1999, landslide hazard assessment must be carried out for the urban construction in geohazard-prone area, and other engineering construction may induce geohazards, in the phase of site selection. The achievement of the geohazard assessment must be validated by provincial administrative departments related to geology or mineral resources and as a prerequisite for the approval of construction land. If the construction didn't meet the

criteria, the land administrative departments shouldn't handle pre-construction land inspection and approval procedures. According to Ministry of Land and Resource *Geohazard Hazard Assessment technical requirements (Trial)*, engineering construction in geohazard-prone areas must carry out geohazard hazard assessment in the feasibility study stage. Cities, villages and towns planning in geohazard-prone areas must also carry out geohazard hazard assessment for planning site. Geohazard hazard assessment should assess the possibility that the engineering construction might be affected by geohazards and the possibility that the construction might induce geohazards. Meanwhile specific mitigation measures should be proposed as well. The main contents of geohazards hazard assessment in the construction site are: to clarify the environmental and engineering geological conditions; to provide prevention measures and proposals, and make a construction site suitability assessment.

3.2.5 Research work or thesis

Most of the scientific research work related to landslide inventory mapping is supported by the National Natural Science Foundation, Ministry of Science and Technology or the relevant ministries funding. Besides, master and doctoral theses from university also contribute a lot, such as Chengdu University of Technology has made fruitful work on spatial prediction of landslide, geohazard information systems, geological disaster prevention and control. Since 2006, the Key Project National Eleventh Five-Year Technology Support Program -Geological Hazards Assessment Study is about the geohazard survey and risk assessment mapping in Baoji, Yan'an and other places. It's a very typical example of landslide inventory mapping and landslide risk assessment and zoning in China.

3.2.6 Landslide emergence mapping

Responding to major or unexpected landslide hazard events, landslide emergency mapping and landslide field inspection before raining season are organized by Ministry of Land and resource and departments at all levels of government respectively, by using ground survey, remote sensing survey and exploration or those methods combination. This work contributed a lot to the data update of landslide inventory database and also provided the up-to-date landslide data and information. After the 2008 Wenchuan earthquake, Ministry of Land and Resources (CGS) carried out the rapid earthquake-induced landslides/dammed lake mapping and inventory by making use of the high-resolution remote sensing survey and imagery interpretation with the combination of field investigation. Landslide typology and potential impact assessment with a focus on major catastrophic landslides were studied. Susceptibility assessment of potential landslides and debris flows near the sites where the residents were temporarily relocated were analyzed. In the landslide emergency mapping, 9517 landslides were recorded in the Wenchuan earthquake region, including the detailed investigation on 31 large scale landslides that caused 4996 direct fatalities and 34 dammed lakes that threatened about 700,000 people at the downstreams.

3.3 Landslide inventory methods

Landslide inventory maps are compiled at different scales (from the local scale to the national scale) by making use of a variety of techniques or methods: the remote sensing

imagery interpretation, geomorphologic field mapping, engineering geological slope investigations, exploration and the examination of historical archives. These techniques are often used with the combination with others. With the variation of different purpose and investment, different measures were used. In China, the national wide landslide inventory is none-profit public service. The scale of landslide mapping is quite different from the intensity of landslide hazard and risk. In this chapter, landslide inventory methods will be introduced, according to the technical guideline for landslide survey at 1:50 000 scale created by China Geological Survey and Baoji prefecture-level municipality landslide survey will be take as case study.

3.3.1 Technical guideline introduction

The final draft of the technical guideline for landslide investigation at 1:50 000 scale was finished in March 2007, which is divided into 14 chapters, including the scope, references regulations and documents, general principles, basic requirements, survey grade, regional geological environment survey, slide investigations, fall survey, debris flow investigation, potential unstable slope investigation, basic investigation methods, basic principles for landslide hazard assessment and mapping, project design and final report, quality control and inspection measures, the achievement acceptance and so on. The guideline has attachments, including different type landslide field inventory forms and documentary.

3.3.2 Framework of landslide investigation at 1:50 000 scale

The framework of landslide investigation at 1:50 000 scale is as follow (Fig.1), which includes landslide inventory methods and project sequence. Two systems: landslide information system and landslide monitoring and early warning system, as well as three levels of assessment and mapping: landslide susceptibility, hazard and risk assessment and mapping are contained in Fig.1.

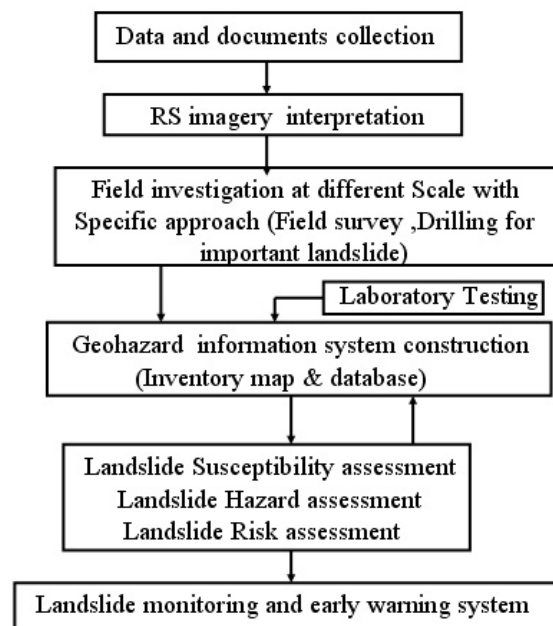


Figure.1 Framework of 1:50000 landslide hazards investigation of China Geological Survey

3.3.3 Historical records and documentaries collection and analysis

The basic method for landslide investigation with a scale of 1:50 000 is historical records and documentaries collection and analysis, the following historical records and documentaries are required:

(1) Basic environmental and geological conditions and triggers, including: meteorology, hydrology, topography, stratigraphy, tectonics, earthquakes, hydrogeology, engineering geology as well as human engineering and economic activities.

(2) Landslide documentaries and records, including: time, type, size, loss and its investigation, exploration, monitoring, treatment and rescue, relief work etc.

(3) Relevant social, economic information, including: population and economic status, development and other basic data, such as towns, water utilities, transportation, mining, engineering, ecology, distribution of industrial and agricultural construction, national economic construction planning, ecological environment construction plan, all natural and human resources and their development status and planning.

(4) Landslide prevention planning and regulatory from all levels governments and relevant departments, including landslide monitoring and prevention system and information.

3.3.4 Remote sensing imagery landslide interpretation

High resolution satellite remote sensing imageries are used for landslide interpretation and environmental background data acquisition in the 1:50 000 scale landslide mapping project, which can be a great contribution for the rapid changing building or infrastructure data update. The main objective of RS imagery interpretation is to identify the type, size and spatial distribution of slide, fall, flow and potential unstable slopes, to delineate the boundary of slides and their affected area, to analysis the geological background and element at risk as well. Multiple sources of satellite imageries were used for the landslide interpretation of Baoji city. The most popularly used imageries are SPOT5 and Quick Bird. Some advance approaches were applied for landslide identification such as hill shade superposition with DEM data, satellite image, 3D virtual environment. As one of the achievement of landslide interpretation, each landslide has a unique form for image characteristics description, the spatial information and landslide attributes can be identified, and also description of field inspection results (Fig.2).

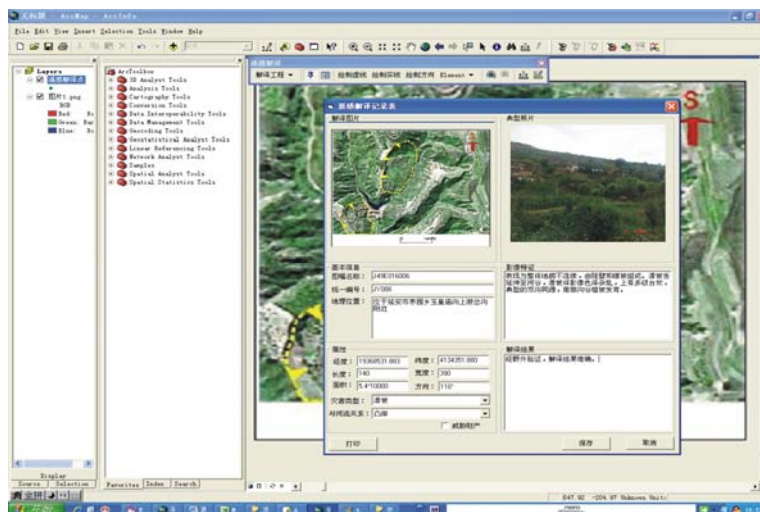


Figure. 2 Landslide image interpretation form and software

3.3.5 Landslide field investigation and data acquisition

According to the difference of environmental geological conditions and geohazards density, the survey area is divided into general and important survey area. The investigation is carried out in accordance with the accuracy of three different scales: the 1:10 000 scale survey near urban or high density geohazards areas; 1:50 000 scale survey in important survey area and 1:100 000 scale investigation. Landslide field investigation includes the RS interpretation field verification, on-site investigation and mapping. For the on-site investigation of each landslide, the field survey data sheet (as shown in Table 1) should be filled. The data sheet covers following information: landslide location, type of moment, state of activity, landslide geometry, geological setting, lithology, land use, causes, analysis of landslide mechanism, elements at risk, damages, investigation process and remedial measures for risk reduction. Ground mapping includes using large scale topographic maps to delineate landslide boundary in field, engineering geological investigation and landslide profile mapping. Field data acquisition in 1:50 000 scale geohazard investigation can be finished in the field with handy computer with field data collection software and GIS spatial data layers. The landslide field survey data sheet can be put in database by records. The recorded landslide can be automatic located by wireless Bluetooth GPS and put a point in the landslide data layer with conjunction to the record.

Table 1 slide field survey data sheet

Project name: _____ Map name: _____ Map No.: _____

Name	Province County (City) Town Village Team										
Field No.	Time	<input type="checkbox"/> Ancient		Position	GC	Long.	° ' "	Elevation (m)	Top		
Unique No.		<input type="checkbox"/> Old				Lat.	° ' "		Toe		
City No.		<input type="checkbox"/> New				Y M D	H M				
Type	<input type="checkbox"/> Processed <input type="checkbox"/> Traction			Material	<input type="checkbox"/> Rock <input type="checkbox"/> Stone block <input type="checkbox"/> Soil						
Landslide environment characteristics	Geoenvironment	Stratum lithologic character			Geological structure		Microtopography		Groundwater type		
		Lithology	Era	Dip/Angle	Position	Seismic intensity	<input type="checkbox"/> Steep scarp <input type="checkbox"/> Steep slope <input type="checkbox"/> Gentle slope <input type="checkbox"/> Platform		<input type="checkbox"/> Pore water <input type="checkbox"/> Crevice water <input type="checkbox"/> Karst water		<input type="checkbox"/> Underwater water <input type="checkbox"/> Confined water <input type="checkbox"/> Upstream water
				∠							
	Geographical condition	Precipitation (mm)			Hydrography						
		Annual	Daily maximum	Maximum	Flood level(m)	Low water level(m)	Location relative to river				
							<input type="checkbox"/> Left bank <input type="checkbox"/> Right bank		<input type="checkbox"/> Concave bank <input type="checkbox"/> Convex bank		
Original slope	Altitude (m)	Slope degree (°)	Slope structural type		Control structural plane						
			<input type="checkbox"/> Soil <input type="checkbox"/> Fragmentary rock <input type="checkbox"/> Carbonatite		Type	<input type="checkbox"/> Bed plane <input type="checkbox"/> Schistosity plane <input type="checkbox"/> Joint/crack plane			Attitude	∠	
										∠	

	Slope shape	<input type="checkbox"/> Crystalline rock <input type="checkbox"/> metamorphite		<input type="checkbox"/> Gentle layered slope <input type="checkbox"/> Forward slope <input type="checkbox"/> Transverse slope <input type="checkbox"/> Oblique slope <input type="checkbox"/> Inverse slope <input type="checkbox"/> Special slope	<input type="checkbox"/> Contact plane of cover and bedrock <input type="checkbox"/> Intralayer disturbed layer <input type="checkbox"/> Tectonic disturbed layer <input type="checkbox"/> Fault <input type="checkbox"/> Old sliding surface					
		<input type="checkbox"/> Convex <input type="checkbox"/> Concave <input type="checkbox"/> Flat <input type="checkbox"/> Step								
landslide characteristics	geometry features	Length(m)	Width(m)	Thicknes (m)	Area(m ²)	Vol.(m ³)	Scale	Angle (°)	Attitude (°)	
						<input type="checkbox"/> Huge <input type="checkbox"/> Oversized <input type="checkbox"/> Large <input type="checkbox"/> Medium <input type="checkbox"/> Small				
		Plane shape				Section shape				
		<input type="checkbox"/> Hemicycle <input type="checkbox"/> Rectangle <input type="checkbox"/> Lingula <input type="checkbox"/> Anomaly				<input type="checkbox"/> Convex <input type="checkbox"/> Concave <input type="checkbox"/> Linear <input type="checkbox"/> Step <input type="checkbox"/> Complex				
	Structure features	sliding mass features					Sliding bed features			
		Lithology	Structure	Gravel content (%)	Size(cm)		Lithology	Era	Dip/Angle	
		<input type="checkbox"/> Identifiable <input type="checkbox"/> Disorder			<input type="checkbox"/> ≤5 <input type="checkbox"/> 5~10 <input type="checkbox"/> 10~50 <input type="checkbox"/> >50				_/_	
		Features of sliding surface and sliding belt								
		Shape	Burial depth(m)	Dip direction (°)	Dip angle(°)	Thickness (m)	Name of sliding belt soil		Property	
	<input type="checkbox"/> Linear <input type="checkbox"/> Arc <input type="checkbox"/> Step <input type="checkbox"/> Wave					<input type="checkbox"/> Clay <input type="checkbox"/> Silty caly <input type="checkbox"/> Pebbly clay				
Ground water	Burial depth(m)	Outcrop			Supply type					
		<input type="checkbox"/> Rising water <input type="checkbox"/> Fall water <input type="checkbox"/> Spilling point			<input type="checkbox"/> Rainfall <input type="checkbox"/> Surface water <input type="checkbox"/> Man-induced <input type="checkbox"/> Snowmelt					
Land use		<input type="checkbox"/> Dry land <input type="checkbox"/> Paddy field <input type="checkbox"/> Grass land <input type="checkbox"/> Shrub <input type="checkbox"/> Forest <input type="checkbox"/> Bareness <input type="checkbox"/> Building								
Deformation activity	Deformation signs	Name	Position	Feature			Earliest occurrence time			
		<input type="checkbox"/> Tensile fissure <input type="checkbox"/> Shear fissure <input type="checkbox"/> Ground swell <input type="checkbox"/> Ground settlement <input type="checkbox"/> Spalling <input type="checkbox"/> Tree skew <input type="checkbox"/> Build deformation <input type="checkbox"/> Muddy water infiltration								
	Deformation stage	<input type="checkbox"/> Initial creep <input type="checkbox"/> Acceleration deformation <input type="checkbox"/> Severe deformation <input type="checkbox"/> Failure <input type="checkbox"/> Rest								
Landslide mechanism	Dominate factor	<input type="checkbox"/> Natural factor <input type="checkbox"/> Man-induced factor <input type="checkbox"/> Combined factor								
	Natural	<input type="checkbox"/> Rainfall <input type="checkbox"/> Earthquake <input type="checkbox"/> Flood <input type="checkbox"/> Collapse load								
		Geological	<input type="checkbox"/> Joint most developed <input type="checkbox"/> Structural surface angle parallel to slope <input type="checkbox"/> Structural surface angle less than slope angle <input type="checkbox"/> Soft base <input type="checkbox"/> Aquifar with underlying confining bed <input type="checkbox"/> Soil/rock <input type="checkbox"/> Broken weathering rock/bedrock <input type="checkbox"/> Strong/weak weathered interface							
		Landform	<input type="checkbox"/> Steep slope <input type="checkbox"/> Slope toe erosion <input type="checkbox"/> Over load accumulation							
		Physical	<input type="checkbox"/> Weathering <input type="checkbox"/> Thawing <input type="checkbox"/> Expanding <input type="checkbox"/> Shear strength reduction <input type="checkbox"/> Pore pressure rised <input type="checkbox"/> Flood erosion <input type="checkbox"/> Water level lowered <input type="checkbox"/> Earthquake							

D.2.2: Assessing the State of Art of Landslide Hazard and Risk Assessment in the P.R. of China

	Man-induced factor	<input type="checkbox"/> Slope steep cutting <input type="checkbox"/> Slope toe excavation <input type="checkbox"/> Load <input type="checkbox"/> Impounded level change <input type="checkbox"/> Forest vegetation destruction <input type="checkbox"/> Blast vibration <input type="checkbox"/> Mine digging <input type="checkbox"/> Drainage pond leakage <input type="checkbox"/> Irrigation seepage <input type="checkbox"/> Indiscriminate discharge of waste water						
Hazard analysis	Resurrection triggers	<input type="checkbox"/> Rainfall <input type="checkbox"/> Earthquake <input type="checkbox"/> Artificial load <input type="checkbox"/> Excavation slope toe <input type="checkbox"/> Slope toe erosion <input type="checkbox"/> Slope toe infiltration <input type="checkbox"/> Slope cutting <input type="checkbox"/> Weathering <input type="checkbox"/> Unload <input type="checkbox"/> Flowing pressure <input type="checkbox"/> Blast vibration						
	Present stability condition	<input type="checkbox"/> Stable <input type="checkbox"/> Rather stable <input type="checkbox"/> Unstable	Development trend		<input type="checkbox"/> Stable <input type="checkbox"/> Rather stable <input type="checkbox"/> Unstable			
Consequences analysis	History loss	Deaths (Person)	Damage house	Damaged road(m)	Damaged trench(m)	Other hazard	Direct loss	Indirect loss
		Disaster degree	<input type="checkbox"/> Oversized <input type="checkbox"/> Large <input type="checkbox"/> Medium <input type="checkbox"/> Small					
		Objects	<input type="checkbox"/> County <input type="checkbox"/> Town <input type="checkbox"/> Residential <input type="checkbox"/> School <input type="checkbox"/> Mine <input type="checkbox"/> Factory <input type="checkbox"/> Reservoir <input type="checkbox"/> Power plant <input type="checkbox"/> Farm <input type="checkbox"/> Irrigation channels <input type="checkbox"/> Forest <input type="checkbox"/> Highway <input type="checkbox"/> Rivers <input type="checkbox"/> Railway <input type="checkbox"/> Transmission line <input type="checkbox"/> Communication facilities <input type="checkbox"/> Defense facilities <input type="checkbox"/> Others					
Induced disaster	Element at risk	Type		Affected area		Loss		
		People		Property				
		Level	<input type="checkbox"/> Huge <input type="checkbox"/> Large <input type="checkbox"/> Medium <input type="checkbox"/> Small					
Monitoring recommendations		<input type="checkbox"/> Regular visual inspection <input type="checkbox"/> Install simple monitoring facilities <input type="checkbox"/> Ground displacement monitoring <input type="checkbox"/> Deep displacement monitoring						
Control recommendations		<input type="checkbox"/> Group monitoring	<input type="checkbox"/> Village-level monitoring <input type="checkbox"/> Town-level monitoring <input type="checkbox"/> County-level monitoring <input type="checkbox"/> City-level monitoring <input type="checkbox"/> Provincial monitoring <input type="checkbox"/> National monitoring <input type="checkbox"/> Traffic monitoring					
		<input type="checkbox"/> Professional monitoring	<input type="checkbox"/> County-level monitoring <input type="checkbox"/> City-level monitoring <input type="checkbox"/> Provincial monitoring <input type="checkbox"/> National monitoring					
		<input type="checkbox"/> Removal	<input type="checkbox"/> Partial removal <input type="checkbox"/> Full removal					
		<input type="checkbox"/> Engineering work	<input type="checkbox"/> Crack filling <input type="checkbox"/> Surface drainage <input type="checkbox"/> Underground drainage <input type="checkbox"/> Cut decompressing <input type="checkbox"/> Slope protection <input type="checkbox"/> Anti-press slope toe <input type="checkbox"/> Retaining <input type="checkbox"/> Anchorage <input type="checkbox"/> Grouting <input type="checkbox"/> Planting trees and grass <input type="checkbox"/> Terracing <input type="checkbox"/> Drain <input type="checkbox"/> Reduce vibration <input type="checkbox"/> Biotechnology					
		<input type="checkbox"/> Emergency eliminate						
		<input type="checkbox"/> Warning sign						
Remote sensing point	<input type="checkbox"/> Yes <input type="checkbox"/> No	Survey points	<input type="checkbox"/> Yes <input type="checkbox"/> No	Mapping Points	<input type="checkbox"/> Yes <input type="checkbox"/> No	Groups monitoring points	<input type="checkbox"/> Yes <input type="checkbox"/> No	
Photo record					Video record			
Field record								
Fig.	Plane map				Profile			

3.3.6 Landslide exploration

There are several methods for landslide exploration, with regard to the characteristics of landslides and the purpose of the exploration. The most commonly used methods are drilling and geophysical exploration. In Baoji city landslide survey project, drilling was used to find the slip surface of the deep-seated loess slide and the structure characteristics of slide mass, combined with the high-resolution shallow artificial seismic exploration and high density resistivity survey, which are used for detecting the slip surface of the buried fault and deep-seated Loess landslide (Fig.3). The Landslide exploration based on 1:50000 scale must submit a report including the inventory of the drilling core, landslide geometry and structure characteristics, stability assessment and prevention measures.

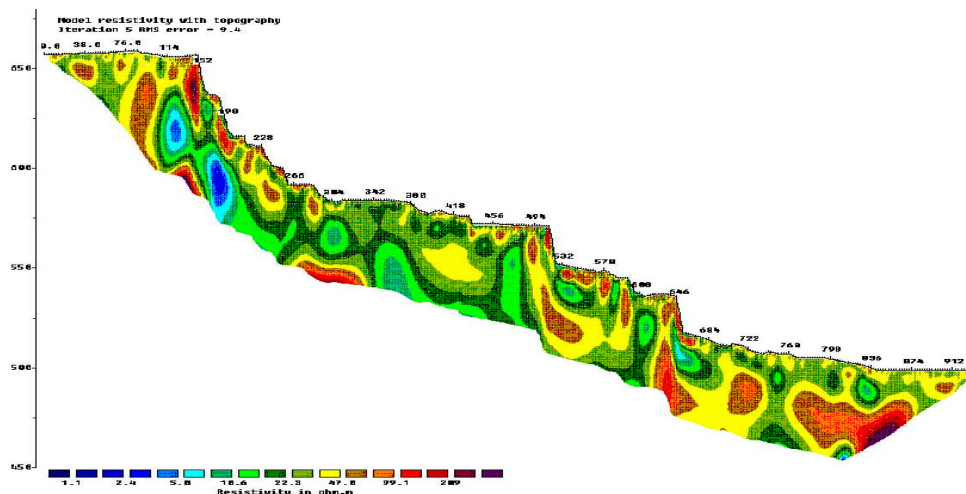


Figure.3 Main exploration line high-density resistivity inversion imaging with topographic correction

3.4 Landslide inventory database

The first national landslide inventory database in China is the geohazard information system for 1:100 000 scale county geohazard investigation project, which started in 1999. China Institute of Geo-Environment Monitoring was in charge of the database construction, data collection and maintenance. The database is based on domestic GIS software-MAPGIS platform and Microsoft Access database, which contained vector layers of landslides and an alphanumeric archive of attributes (GHIS). The relational alphanumeric database scheme is based on the Field Landslide Data Sheet (Table.1). With the aim of homogenize and integrate the landslide data over the whole territory, China Institute of Geo-Environment Monitoring developed some software components for geohazard inventory data input, data management and quality inspection, which can be download at <http://www.cigem.gov.cn/>, and technique guidelines for landslide inventory database, cartography standard and manuals as well. The technical guidelines for landslide inventory database construction in counties (cities) geohazards investigation project defined the content of the database and provide the structure of spatial data, geohazard database, data formats, layers, rule of naming, metadata and etc.

3.4.1 Workflow of landslide inventory database construction

The workflow of landslide inventory database construction of the China geological survey landslide investigation project normally includes three steps: field data acquisition, data input and management, data submission. The most important step is the field data acquisition, which was made by using handy computer (laptop) system with digital format *Field Landslide Data Sheet* and *GIS system* with digital topographic and geological maps. Different type of landslide was put in different map layers and inventory data was stored in different table. Each type of landslides has its own data sheet with the attribute including: location, type, volume, time of occurrence, surrounding environment, geometry, possible mechanism analysis, potential life or property loss, and each landslide has its own unique index ID, which is a code whose values uniquely identify each landslide over the whole China territory. The code links to the alphanumeric attributes to the geographic features. The next step is data input, which can be only data transfer from the handy computer or manually input the paper field landslide data sheets and GIS layers into the database with the help of data input software. It provided digital format data sheet and GIS system in computer and also provided data management functions. Once the county landslide inventory database was finished, it will be submitted to China Institute of Geo-Environment Monitoring as a prerequisite for approval of the end of the project.

3.4.2 Contents of landslide inventory database

The contents of landslide inventory database contain the following aspects of data and information:

- ① General information: the general information about which company or organization carried out the landslide inventory and who were involved in this project.
- ② Spatial Feature Dataset: vector GIS layers including landslide, contour line, drainage, geological maps, building, road and railway networks etc.
- ③ RS imagery: related to satellite imagery and landslide interpretation form;
- ④ Landslide inventory data: Access the format of landslide data sheet;
- ⑤ Survey data: landslide geometry ground survey data and profile;
- ⑥ Exploration data: Inventory of drilling core, method, proposals for exploration, report of exploration etc.;
- ⑦ Public Early Warning network information: methods of warning and who will be involved and etc;
- ⑧ Report: the final report of the landslide investigation project;
- ⑨ Project documentary: the proposal, planning and design report;
- ⑩ Related documentary: annual report, budget etc.

3.4 Conclusion and potential challenges

3.4.1 Conclusion

In recent years, landslide inventory mapping and inventory database construction have made significant progress in China. Ministry of Land and Resource carried out the whole

national landslide inventory mapping and database construction at 1: 100 000 scale, developing related guidelines for landslide mapping and software for database construction. Landslide inventory mapping becomes more and more important in China, and the landslide inventory method and database construction have Chinese characteristics.

3.4.2 Potential challenges

Although landslide inventory mapping and inventory database construction have made significant progress in China in recent years, there are five potential challenges as follows:

① Data quality and completeness

Landslide inventory data quality heavily depends on the skill and the experience of the investigators, the complexity of the study area, the completeness and reliability of the available information, also the methods used and the scale of landslide mapping. How to ensure and enhance the data quality and completeness is the great challenge in China.

② Available and up-to-date data acquisition

Due to the climate change, economic activities and earthquake, each year there are more than 10 000 landslide events in China. How to maintain the landslide inventory database, and get available and up-to-date landslide data is a difficult work.

③ Public sharing

Nowadays, landslide inventory database is not accessible for public, due to national security laws. How to promote and spread out the landslide information to national and local institutions, research institutes, geologists, engineers and citizens is still on the long way to be solved.

④ How to integrate all kind of landslide inventory data, maps and database?

There are quite a few landslide inventory mapping in China with different scale, accuracy, data and map format.

⑤ How to enhance spatial data analysis and visualization functions? How to make data understandable for public?

Landslide inventory database in China is based on MAPGIS software, which is not friendly for public and weak on data analysis and visualization function compared to ArcGIS. We need a simple and clear navigation software to make data understandable for public, to help the users to check and use the landslide inventory together with other vector layers and raster layers.

CHAPTER 4 REMOTE SENSING APPLICATIONS FOR LANDSLIDE RESEARCH IN CHINA

Chuan Tang¹ & Xuanmei Fan^{1,2}

¹State Key Laboratory of Geohazards Prevention, Chengdu University of Technology, China

²Faculty of Geo-information Science and Earth Observation, University of Twente, Netherlands

4.1 Introduction

The remote sensing can quickly provide the reliable up-to-date information over a large geographical area. Thus the remote sensing technology is a very critical information technology means to carry out landslide research. With the gradual perfection of remote sensing technology theory, and the gradual increasing of spatial resolution, time resolution and spectrum resolution of remote sensing imagery, the remote sensing technology has become one of the most important means to carry out landslide inventory, dynamic monitoring, early warning, and damage evaluation.

In 1980, China started to use the remote sensing data to carry out landslide research, during the early feasibility research stage of Ertan large-scale hydropower station construction in Southwestern China. The aerial photographs were used to investigate the landslide distribution, scale and its development environment on the dam site and reservoir area. On the basis of the results, the slope stability of the dam site and reservoir bank was evaluated, providing fundamental data for decision making (Wang, 2007). Since the mid-80s, the aerial photographs had been widely used in route selection and feasibility research for railway and highway. The landslide distribution along alternative construction lines were carried out mainly relied on visual interpretation and judgment of aerial photo that formed a fairly matured technical method system and widely applied at that stage (Zhuo, 2002). The regional landslide hazard distribution map was mainly on the medium scale (1:50,000 to 1:200,000) at this time. It is undoubted that landslide research keeps progress with the application of remote sensing technology, especially the rapid development of high spatial resolution of satellite imagery, commercial satellites continuously launched in succession, that provide a rich source of image as data source. At present, the general high definition image of China mainly includes SPOT5, IKONOS, Quickbird, etc., and its highest spatial resolution of panchromatic band is respectively 2.5m, 1.0m and 0.61m. The common features of these image data with both high-resolution panchromatic band, multi-spectral data is provided by a certain multi-source data fusion, so that can be both high resolution and rich color information of the fused image, which can improve target identification and classification of the level (Li, etc., 2007). At present, remote sensing technology is not only widely used for carrying out regional landslide survey but also individual landslide survey. For example, the nationwide 1:100,000 scale of "Cities and Counties Geological Hazard inventory and zonation" and 1:50,000 geological hazard inventory and zonation work are all required of taking full advantage of using of remote sensing methods for landslide identification and analysis. A keystone project, named "Key Technologic Research on Major Geological Hazard Monitoring and Early Warning and Emergency Response", stressed the

utilization of remote sensing and GIS technology for landslide identification, monitoring and early warning, and risk assessment and management (Shi et al., 2008). This chapter describes the status of remote sensing application in landslide research in China, mainly focusing on an overview of landslide inventory, monitoring and assessment through cases.

4. 2 Application of remote sensing in landslide inventory

Landslides represent the main geomorphic process. As a special geomorphic process, landslide can be reflected by remote sensing images through its shape, color, texture and structural features. Therefore, the boundary, size, and morphology of the landslide, can be directly derived from interpretation of the remote sensing imagery. Thus, landslide inventory including its dimension, type and impact factors can be carried out through a systematic and comprehensive investigation. Since 1999, Ministry of Land and Resources of China (China Geological Survey) launched a project of "Inventory of urban geological hazards in China". The project plans to find out that there were more than 1,500 counties suffering from potential geological hazards. Landslide hazard zonation was mapped and mitigation plans were completed based on landslide inventory. Nearly 800 counties have been implemented till 2007. Therefore, this plan acquired great achievements in landslide prevention and control. Remote sensing was also executed during the survey and zonation of geological hazards in some counties. With the Landsat-7 ETM satellite remote sensing data as the main source of information, the 1:100,000 scale interpretations on type, dimension and distribution characteristics of geological hazards assist and support the conventional field investigation. For example, in 2005, Department of Land Resources of Sichuan Province deploys an inventory of geological hazards using remote sensing data, which covered a total area of 60,658 km² in 25 counties. The study areas are mainly focused on landslide prone areas in Western Sichuan Province. For instance, Chengdu University of Technology (CDUT) used the ETM image of Luding County, which cover an area of 2168km², indentified 34 landslides and 133 debris flow gullies (Fig.1). Because of the advantages of ease acquisition and the cost-effectiveness, ETM satellite data has been widely used in small and medium scale landslide investigation in China (1:500,000 to 1:100,000).

In 2005, China launched 1:50,000 scale geological hazard investigation in landslide prone areas, and developed a corresponding investigation criterion named "The investigation guideline on landslides, rockfalls and debris flow hazards" (1:50,000). This guideline emphasizes the necessity and requirement of remote sensing survey, which the main objectives are utmost extracting information and data from remote sensing images for various kinds of geological hazards, analyzing the formation and spatio-temporal distribution of geohazards, compiling the corresponding inventory map of regional geological hazards, and providing data to the geological hazards survey. According to the survey contents and accuracy requirements, TM / ETM and high-resolution remote sensing satellite data (SPOT, IKONOS, Quickbird) are used as the primary information source for landslide inventory. The resultant inventory maps of geohazards are mapped in 1:50,000 scale.

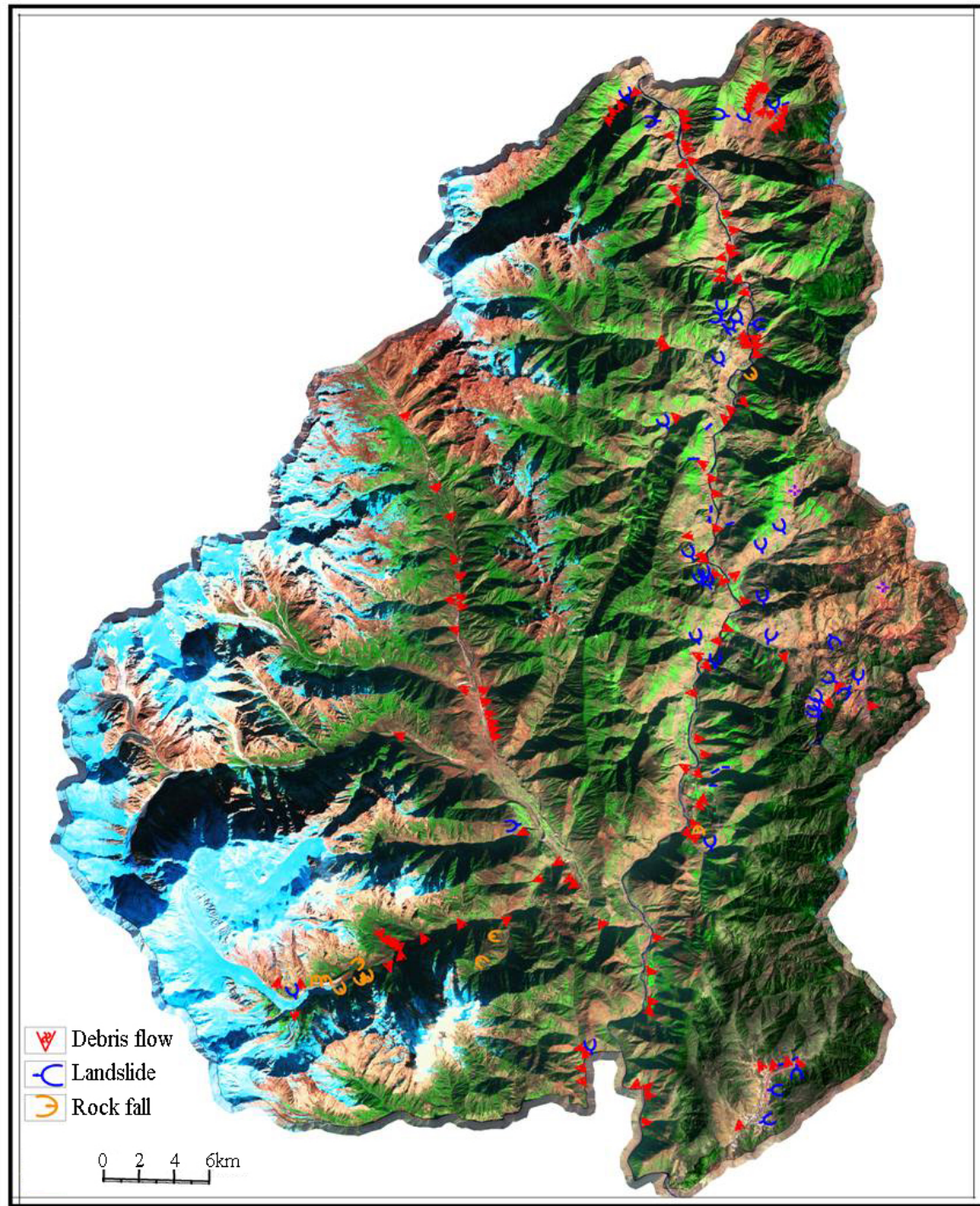


Figure.1 Inventory of landslides in Luding County of Sichuan, China based on interpretation of ETM imagery

After the Wenchuan Earthquake, remote sensing technology is more widely used in the identifications of earthquake-induced landslides. Huang et al. (2008) promptly accomplished the earthquake-induced landslide inventory map, which includes 11,308 landslides within 16 seriously-hit counties (Fig.2) by adopting the post-earthquake remote sensing data of ALOS

instance, Jipazi Landslide of the Yangtze river in July 1982, Saleshan Landslide in Gansu province in March 1983, Xikou Landslide in Huayingshan of Sichuan province in July 1989, Touzhaigou Landslide in Zhaotong of Yunnan province in September 1991, Laojinshan Landslide in Yuanyang of Yunnan province in June 1996, Badu Landslide of the Nanning-Kunming Railway in July 1997, Yigong Landslide in Bomi of Tibet in April 2000, and Xuanhan Landslide in Sichuan province in July 2004 (Huang, 2007).

With the development of high resolution satellite remote sensing, the high resolution satellite imagery is also widely used for large scale landslide survey to promptly derive the topographical characteristics and spatial information of the landslide. For example, at 8 pm in the evening of 9 April 2000, a massive landslide occurred and lasted for about 10min in Zhamunong valley, Yigongzhangbu river in Bomi County of Tibet, and the remote sensing imagery was used for the landslide survey and information derivation. The landslide traveled about 8 km along the transportation zone, making an elevation difference of about 3330 m. The landslide blocked Yigongzhangbu River (riverbed elevation 2190m in lower reaches), and the debris deposition zone was about 2500m in length and 2500m in width, covered an area of about 5 km². The thickest part reached 100m and the average thickness is about 60m. Its volume is about 218-310×10⁸ m³ (Yin, 2000). Lv, et al. (2002) adopted the TM and SPOT satellite remote sensing data to survey the formation and geomorphological characteristics of the Yigong landslide, monitor and analyze the change situation and submerged area of the Yigong lake in each phase after the landslide, that provided important information to a comprehensive understanding on the causes of landslides and dynamic changes of the barrier lake (Fig.3). After Wenchuan Earthquake, Ministry of Science and Technology of China, Ministry of Land Resources of China captured aerial remote sensing data on the period of May 16 to 28 in the worst-hit Wenchuan earthquake area by adopting high-altitude remote sensing platform equipped with advanced remote sensing sensors. These high resolution remote sensing data were used for detailed survey and risk assessment of nearly 50 large scale earthquake-induced landslides, focusing on extracting spatial information such as geometric shape, slide cover, sliding distance and the accumulation characteristics, and analysing landslide formation environments and conditions, potential risks and trends. For example, Wang, et al. (2008) interpreted the location and distribution of 52 barrier lakes formed by large scale earthquake-induced landslides by making use of these remote sensing data. One of the typical examples is Tangjiashan Landslide and the concomitant of the barrier lake. As a notable result of Wenchuan Earthquake, the volume of Tangjiashan landslide was 20.5million m³ forming the natural dam with length of 800m (along the river direction), longitudinal width 612m, maximum height 108m, and area about 30×10⁴ m² (Hu et al., 2009). Since the short observation cycle time of Fuwei No.2 of Taiwan satellite, the first effective optical remote sensing images of Beichuan area, one of the worst-hit area in Wenchuan earthquake, was obtained in the morning of May 14, 2008, and the Tangjiashan landslide and the large scale barrier lake was firstly discovered from the Fuwei satellite image. Fig. 4 shows basic characteristics of Tangjiashan landslide and the barrier lake, as well as the catastrophic Wangjiayan landslide and the New Beichuan Middle School collapse are also included in this figure, which were derived from the remote sensing data of Ministry Land and Resource of China. The Wenchuan earthquake also induced a large number of long-runout rock avalanches. Their source area, flow path and accumulation area

can be accurately identified through the utilization of high resolution remote sensing data (Xu et al.). Figure 5 shows the dynamic process of Donghekou landslide in Qingchuan County.

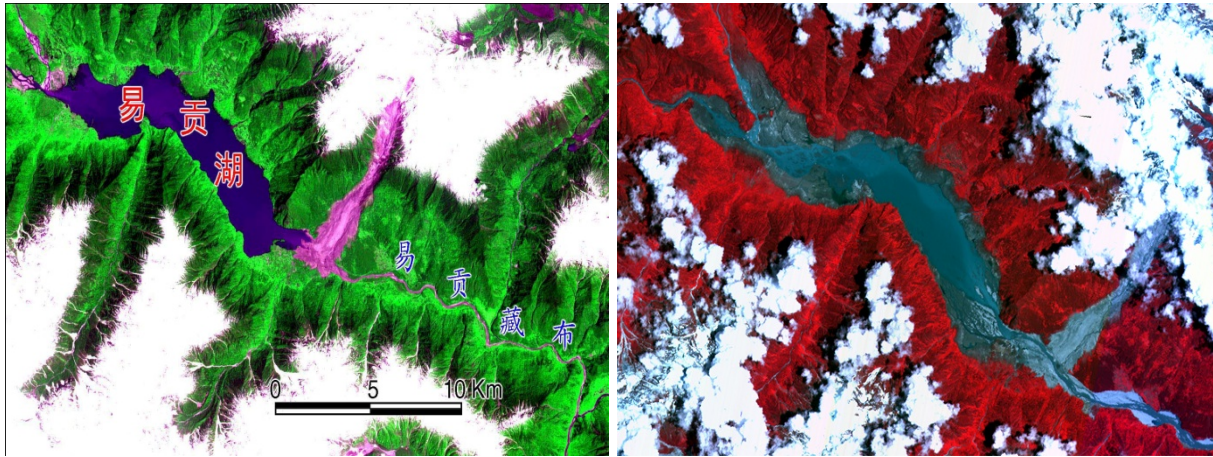


Figure. 3 Remote-sensing image of Yigong Landslide and Lake(the left picture is SPOT-4 image shot on May 4, 2000, showing the spatial position and features of Yigong Landslide and its barrier lake; the right one is SPOT-2 image taken on June 17, 2000, reflecting the characters of Yigong Lake after the dam break on June 10. It can be seen that the water had diminished obviously and the flood situation had been alleviated

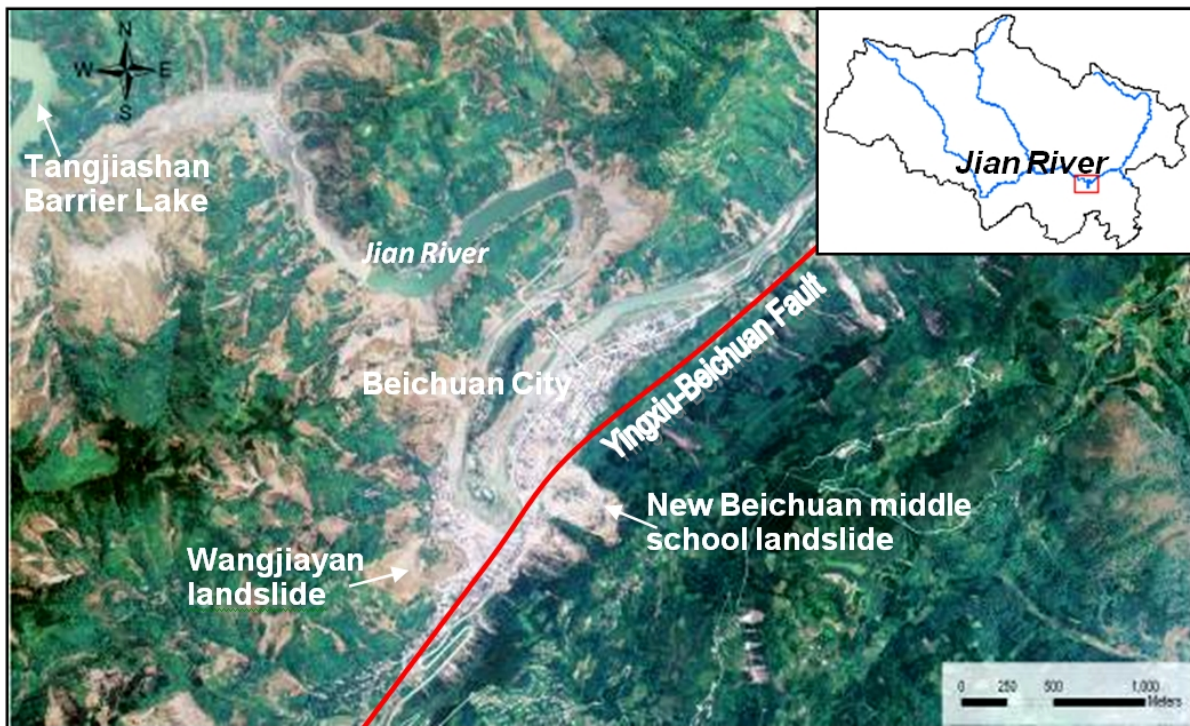


Figure. 4 Aerial photograph taken on May 18, 2008 indicating the location of Tangjiashan landslides and the barrier lakes as well as Wangjiayan landslide and New Beichuan middle school landslide

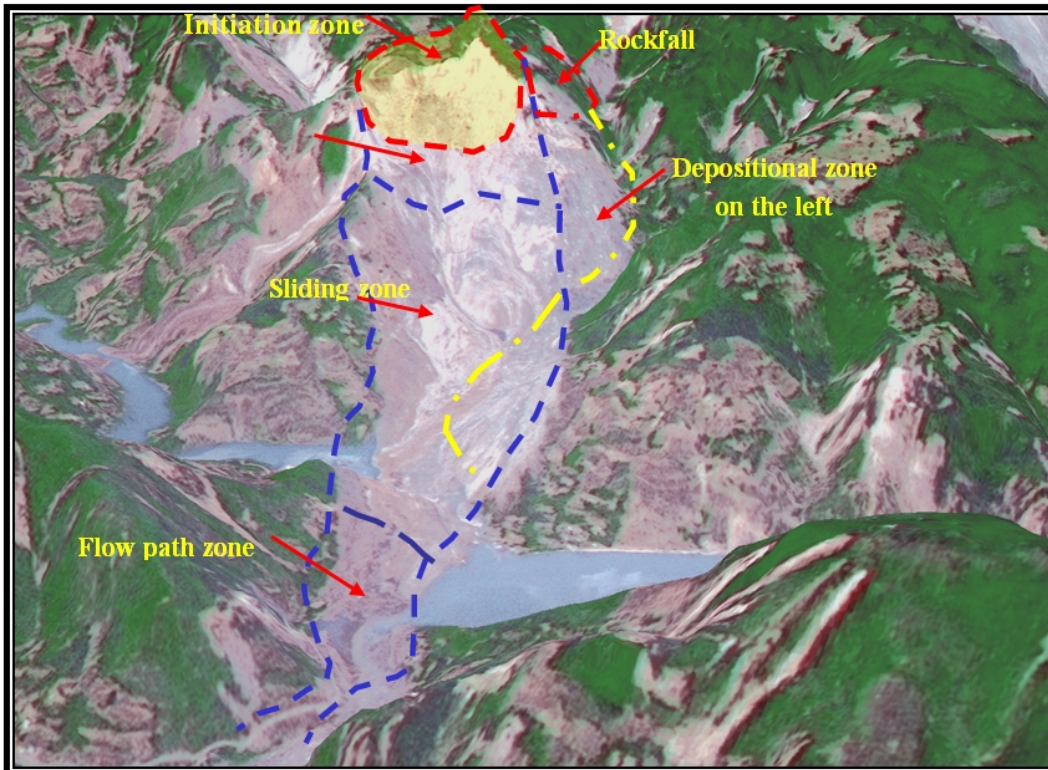


Figure.5 3D Aerial photograph indicating the dynamical process of Donghekou landslide triggered by the Wenchuan earthquake in Qingchuan County

4.4 Application of remote sensing technology in landslide monitoring

In the past decade, a lot of attentions have been paid to apply the remote sensing technology in landslide monitoring in China, especially in the dynamic monitoring of landslide displacement with time, sliding speed, morphological changes, which provided reliable data for landslide prediction and hazard evaluation. High resolution remote sensing images are mainly used to study the geometry of landslides and INSAR technology is mainly adopted to analyze the deformation and movement rule of landslide (Ouyang et al.2005). Emerging as a kind of microwave remote sensing technology, INSAR developed rapidly in recent years and became a research focus among international remote sensing field. With this technology, the ground deformation and large-scale landslides within a certain period can be monitored. Its earliest study can be dated back to 1995, when a few landslides were studied in France, and then in Italy, Canada, Germany, etc (Squarzoni et al., 2003; Tarchi et al., 2003; Singhroy et al.,1998). However, China started late in the study of landslide monitoring by INSAR and the successful application cases are few. During 2001 to 2005, owing to the efforts of CDUT, ESA and BRGM, the study on application of INSAR in landslide monitoring in the Three Gorges Reservoir Region had been conducted and some progress had been made (Deng and Huang,2003).

In China, multi-temporal and high-accuracy remote sensing images played a very important role in the investigation and monitoring of large landslides in recent years (Wang, 2006; Jiang, 2006; Shi, 2008). Wang (2007) utilized remote sensing data of 11 time phrases on 5 different platforms to permorm monitoring of Yigong Landslide and barrier lake in Tibetan region. Jiang et al. (2006) employed remote sensing data of ETM, CBERS-2 and Radarsat to conduct the monitoring of large scale landslide and barrier lakes in Pali River area of Tibet plateau in June, 2006. They rapidly obtained the important information including landslide location, barrier lake area and storage, etc., and then offered an early dam-break flood warning. Yang et al. (2005) adopted the integration technology of multi-temporal TM, SPOT, ERS-SAR and RADARSAT images to monitor and assess the effects of geohazards on Three Gorges Project and thus provided scientific support for prevention and control of geohazards.

In recent years, great progress has been made in monitoring of regional landslides using remote sensing. Based on the data of Formosat-2 satellite in Taiwan, Lin et al. (2006 and 2009) had performed the landslide monitoring continuously before and after Chi-Chi Earthquake in 1996 for more than ten years. The quantitative analyses of the changes in the area of landslides triggered by heavy typhoon were carried out. Meanwhile the impacts of the strong earthquake on landslide evolution are also evaluated.

The Wenchuan earthquake not only induced serious co-seismic landsliding but also strongly contributed to the landslide activity during the heavy rainfall that occurred 4 months after the earthquake. Tang et al. (2010) selected a study area in Beichuan with a total area of 150 km² to monitor the landslide evolution after the earthquake. The interpretation of the SPOT5 image taken after the 24 Sep, 2008 rainstorm shows that in the study area 823 new landslides occurred after the rainstorm. This number is 68% of landslides in this region that were induced by the earthquake. The new landslide surface area is $617.1 \times 10^4 \text{ m}^2$, which occupies 46.6% of the total area of the co-seismic landslides (Fig.6). This study reveals that the extensive fissuring of rock slopes due to the earthquake still poses a potential hazard in the region, as the slopes are very susceptible to future landsliding under extreme rainfall conditions.

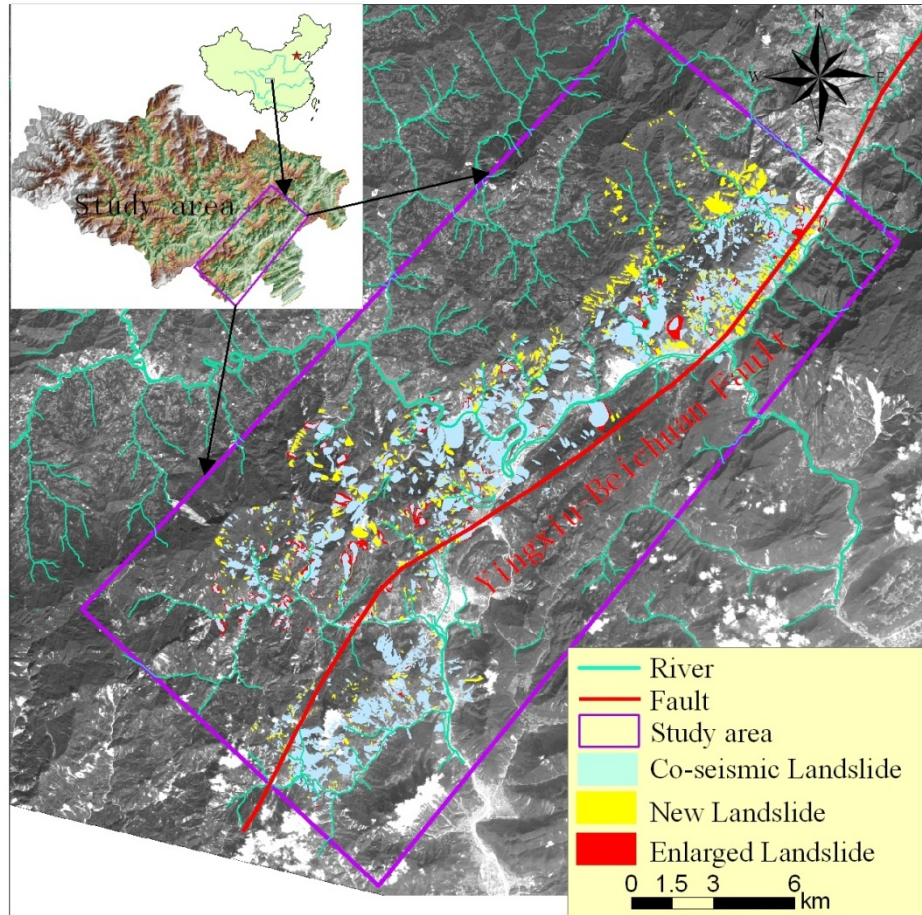


Figure.6 Monitoring result of landslides triggered by the earthquake and subsequent rainfall in the SPOT 5 imagery. Landslides are mainly located along the surface rupture traces of co-seismic faults and along the Jian River. They are concentrated on the hanging wall of the fault zone.

4.5 Application of remote-sensing in landslide risk assessment

Landslide risk assessment has become a fundamental tool in risk management as an integral part of landuse planning in the disaster prone areas. Therefore, evaluation of risks associated with landslides is an important challenge to develop proper disaster management policies. Recent developments in the use of earth observation which have been applied for improved landslide inventory mapping, landslide susceptibility and hazard assessment, elements at risk mapping, and finally landslide vulnerability and risk assessment.

The risk assessment of landslide hazard involves many aspects, such as landslide inventory, landslide hazard mapping, vulnerability mapping and risk mapping (Tang, 2004). Remote sensing technology may contribute significantly to the whole process of landslide risk assessment. Landslide inventory and mapping rely on the spatial data of landslide distribution, which is identified by remote sensing imagery. In the meantime, remote sensing has provided important data sources for the acquisition of environmental factors for hazard assessment. The vulnerability is defined as the degree of loss to a particular element or set of elements at risk

caused by a potential damage phenomena with a given intensity. The quantitative analysis of vulnerability is complicated. Remote sensing techniques can be effectively applied to assess landslide vulnerability quantitatively. To some extent, land cover changes also influence the vulnerability to landslide. Therefore the use of satellite imageries in updating land cover maps is important.

Tang et al. (2006) selected Dongchuan Town of Yunnan Province, China as a case study to approach an integrated methodology for urban debris flow risk assessment. Procedure of the methodology involved debris flow hazard zonation, urban vulnerability evaluation and risk assessment. We analyzed land-cover types for vulnerability to debris flow hazard in the study area. In this study a remotely sensed image of high spatial resolution was used as the data source to interpret the urban land use types. Subsequently the interpreted results were used as the calculation basis for monetary estimation. The remotely sensed data source used for land use type interpretation was an American commercial QUICKBIRD satellite imagery with the highest spatial resolution. Its panchromatic resolution is 0.61m and its multi-spectral resolution consists of four wavebands (red, green, blue and near infrared). Such a high spatial resolution image at a large scale can sufficiently meet the needs of urban land use interpretation. On the image all buildings in the city and its direct surroundings were digitized, as well as the land parcels, the roads and other infrastructure. This resulted in a digital parcel map. Each polygon was described in the field by a team of surveyors, making use of checklists for the in-situ collection of data on hazard and vulnerability.

According to the main land-use types of the study area and with reference to the Chinese land-use classification scheme, we highlighted buildings, roads, green lands, public gardens, agricultural fields, forest lands and so on. On the basis of spatial features and spectral characteristics and applying such factors as the object's shape, size, figure, shadow, location and lamination as indicators of interpretation, the information of land use, quantity and spatial distribution were derived. The emphasis is on loss estimation of urban buildings, roads, public gardens and green areas. As the used single remote sensing image does not allow to interpret the number of stories of buildings accurately, we undertook in-situ investigation and collected data for the number of stories of buildings in the study area, and then integrated this information with the data obtained from interpretation so as to provide the basis for the estimation of the value of urban buildings (Fig.7).

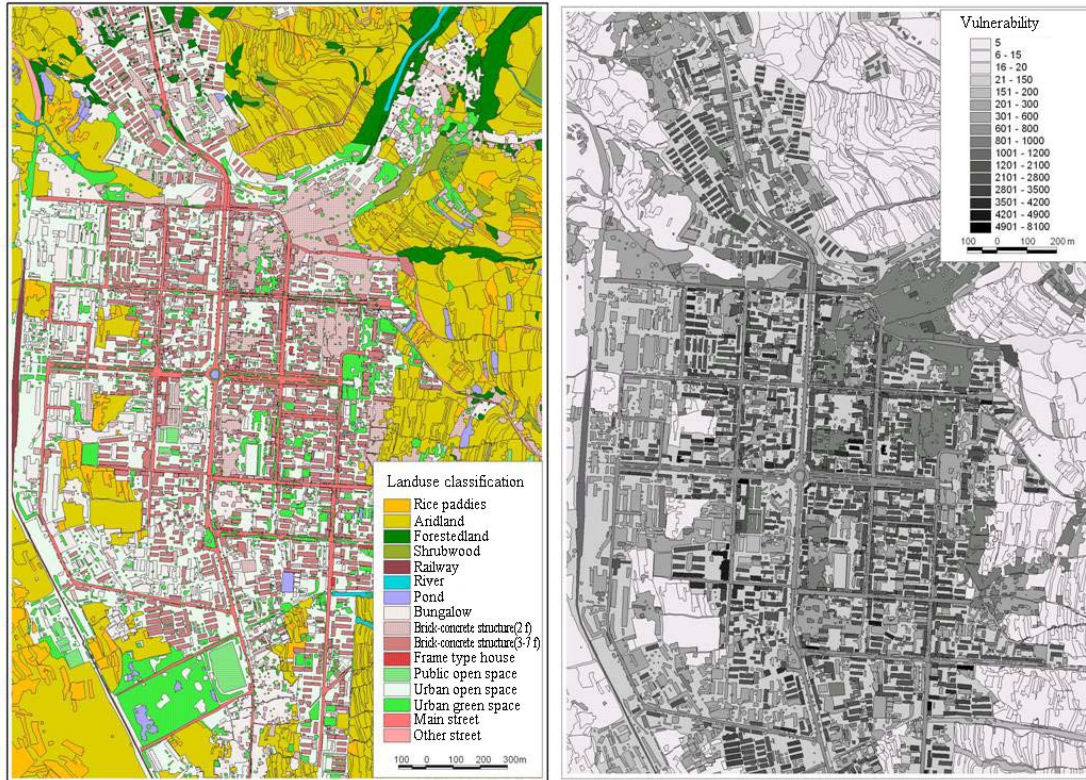


Figure.7 Urban land use map (left) and vulnerability map (right) based on an interpretation of Quickbird imagery

This interpretation and classification with help of high spatial resolution remote sensing imagery enabled us to compile a map at 1:2000 scale. We then inputted these data into ArcGIS for classification data and map compilation purposes. Comparison of the total built-up surface area determined from the topographical map and the area classified in the QUICKBIRD image provided an assessment of the accuracy of the classification which turned out to be very good.

4.6 Conclusions

The application of remote sensing technology in the study of landslides in China has a history of more than 30 years. As the main means of landslide inventory, remote sensing technology played a vital part in the investigation and risk assessment of landslides in large-scale engineer construction. With the rapid development of remote sensing technology, especially the utilization of high-resolution satellite data, it had become an indispensable means of landslide detection and identification, monitoring and assessment. Since 1999, remote sensing technology has been used to identify and evaluate regional landslides for national geohazard inventory and hazard zonation of 1:100,000 and 1:50,000 scale. Besides, it has also been widely adopted to investigate the landslide hazard in the major construction of hydro-power station, highway and railway, etc. The application of multi-temporal and high-accuracy remote sensing images plays an important role in inventory and monitoring of catastrophic landslides in recent years. High resolution satellite images can supply reliable data source for the quantitative evaluation of landslide hazard, vulnerability and risk.

References

- Chigira M, Wu X, Inokuchi T, Wang G. Landslides induced by the 2008 Wenchuan earthquake, Sichuan, China. *Geomorphology*. 2010. doi: 10.1016/j.geomorph.2010.01.003
- Dai F C, Xu C, Yao X, Xu L, Tu X B, X. B. Gong X B. Spatial distribution of landslides triggered by the 2008 Ms8.0 Wenchuan earthquake, China. *Journal of Asian Earth Sciences*. 2010. doi:10.1016/j.jseaes.2010.04.010.
- Deng Hui, Huang Runqiu. INSAR technology in geological hazard and topographic application. *Mountain*. 2003, 21(3): 373-377.
- Huang Runqiu, Li Weile. "5.12" Wenchuan earthquake triggered the development and distribution of geological hazards research. *Rock Mechanics and Engineering*. 2008, 27(12): 2585-2592.
- Huang Runqiu, Chinese large-scale landslide and its mechanism Since the 20th century. *Mechanics and Engineering*. 2007, 26(03): 433-454.
- Hu Xiewen, Lv Xiaoping, Huang Runqiu, etc. Tangjiashan big ditches mud-rock flow characteristics and main disaster evaluation. *Rock mechanics and engineering*. 2009, 28(4): 850-858.
- Jiang Weiguo, Zhang Songmei, Li Jing, Li Jiahong. Based on RS and GIS Tibetan parry river landslide monitoring. *Natural disasters*, 2006, 15(4) :24~27.
- Lv Jietang, Wang Zhihua, Zhou chenghu. Tibet YiGong landslides dammed the satellite remote sensing monitoring methods were discussed. *Earth*, 1999, 42(4):111-173.
- Lin C W, Liu S H, Chang W S, Chen M M. The impact of the Chi-Chi earthquake on the subsequent rainfall induced landslides in the epicentral area of central Taiwan. *Proceeding of international conference in commemoration of 10th anniversary of the Chi-Chi earthquake*, 2009, 336-338.
- Lin C W, Liu S H, Lee S Y, Liu C C. Impacts on the Chi-Chi earthquake on subsequent rain-induced landslides in central Taiwan. *Engineering Geology*. , 2006, 86(2-3):87-101.
- Li Tiefeng, Xu Yueren, Pan Mao, Cong Weiqing, Wen Mingsheng, Lian jianfa. Based on the image of SPOT5 rainfall type landslide remote sensing research shallow. *Journal of Peking University (natural science edition)*. 2007, 43(2):204~210.
- Ouyang Zuxi, Zhang Zongrun, Ding Kai, Shi Jie Shan, Chen Ming Jin, Mao Xing Ming. Based on the 3S technology and ground deformation observation of the Yangtze gorges landslide monitoring system of typical. *Rock mechanics and engineering journal*. 24(18):3203~3210.
- Shi Jusong, Wu Shuren, Shi Ling. Remote sensing research progress in the application of landslide hazards. *Lun Ping geology*. 2008, 54(4):505-515.
- Squarzoni C, Delacourt C, Allemand P. Nine years of spatial and temporal evolution of the La Valette landslide observed by SAR interferometry[J]. *Engineering Geology*, 2003, 68(1-2): 53-66.
- Singhroy V, Mattar K E, Gray A L. Landslide characterization in Canada using interferometric SAR and combined SAR and TM images. *Advances in Space Research*, 1998, 21(3):465-476.
- Tang Chuan, Discussed by Landslide risk figure compiled. *Journal of natural disasters*. 2004, 13(3):8-12.

- Tang Chuan, Ding Jun, Qi Xin. Wenchuan earthquake high-intensity rainstorm landslide activity of remote sensing a dynamic analysis. *Earth science - China university of geosciences*. 2010, 35 (2): 317-323.
- Tang Chuan, Zhu Jing. Disaster risk assessment by city of mud flow. *Scientific advances of water*. 2006, 17(3):67-71.
- Tarchi D, Casagli N, R Fanti. Landslide monitoring by using ground-based SAR interferometry: an example of application to the Tessina landslide in Italy. *Engineering Geology*, 2003, 68(1-2): 15-30.
- Van Westen C, Gorum T, Fan X, Huang R, Xu Q, and Tang C. Distribution Pattern of Earthquake-induced Landslides Triggered by the 12 May 2008 Wenchuan Earthquake. 2010. EGU2010-4437.
- Wang Shixin, Zhou Yi, Wei Chengjie, etc. Wenchuan earthquake dammed secondary disaster danger evaluation of remote sensing. *Journal of remote sensing*. 2008,12(6):900-907.
- Wang Zhihua. Digital landslide technique which used in tiantai landslide investigation. *Journal of geotechnical engineering*.2006,28(4):516-520.
- Wang Zhihua, New progress of remote sensing and landslides in china. *Land resources of remote sensing*. 2007,4(74):7-11.
- Xu Qiang, Huang Runqiu. Kinetics characteristics of large landslides triggered by May 12th Wenchuan earthquake. *Journal of Engineering Geology*, 2008, 16(6): 721–729.
- Yang Wunian, Pu Guoliang. Geological disasters in remote sensing image information processing and monitoring and evaluation in The Yangtze gorges. *Geological journals*. 2005. 79(3): 423~430.
- Yin Yueping. The feature and the giant of BoMi Tibet YiGong high-speed landslide disaster. *Hydrogeological and engineering geology*. 2000.(4):8-11.
- Zhuo Baoxi. Judgment and application in Engineering geology remote sensing. Beijing: China railway Press. 2002.

CHAPTER 5 MEDIUM AND LARGE SCALE LANDSLIDE HAZARD ASSESSMENT IN CHINA

Kunlong Yin¹ & Lixia Chen²

¹School of Engineering, China University of Geosciences, Wuhan, Hubei, China

²Institute of Geophysics and Geomatics, China University of Geosciences, Wuhan, Hubei, China

5.1 Introduction

In the past 20 years, the fatal landslides occurred frequently in China. The present status of landslides in China is that although the level of theory research and prevention techniques is largely improved, but landslide disasters are still becoming more and more serious. Over four hundreds of counties, ten thousands of villages in China were affected by landslides, rock falls, earth flows, and other types of geo-hazards. Nevertheless, not all the potential hazards can be controlled by treatment projects, because of the absence of economic and technique abilities. So the other efficient way to solve this problem is to do hazard zonation and risk assessment work, finding out the areas with high probability or risk for landslide occurrence. The results can be credible reference for land planning, hazard controlling, hazard management and decision making.

Since 80's in last century, Varnes proposed the definitions and principles for hazard zonation. Great progresses have been made in this field. Soeters and van Westen (1996, 1997) summarized the methods for landslide hazard susceptibility assessment. The methods are divided into four categories: inventory, heuristic, statistical, and deterministic approaches. And the susceptibility is usually obtained by these models, based on the analysis of various landslide influencing factors, which directly or indirectly related to landslide occurrence (geomorphologic parameters, lithology, geological structure, underground water table etc.). For example, Carrara et.al (1982, 1991) used multivariate method by GIS technology to assess the susceptibility of landslides in Central Italy, considering relevant geological and geomorphologic factors. Van Westen (2008) reviews the use of spatial information on environmental factors and the methods for obtaining them, aiming at landslide susceptibility assessment. Leonardo Ermini, Filippo Catani and Nicola Casagli (2005) applied artificial neural network with GIS technology for to the susceptibility assessment of landslide in Northern Apennines (Italy). In recent years, many case studies are discussed all over the world by geologist and engineers, which mainly relate to different models, factors evaluation, GIS application, etc. (Anbalagan,1992; Cascini,2008; Chung, Fabbri, Westen,1995; Corominas, Moya,2008; Fell,2008; Kamp,2008;Yin,2007; Saha,2005; Sharma,2009; Westen,2006). In China, almost all the provinces, such as Hongkong, Yunnan, Hubei, Zhejiang, etc., have relative researches and applications (Dai, 2001; Liu, Li, Wen, 2004; Xie, Zhang, Xu, 1995; Xie, Cheng, Fan, 2005; Wang, Zhang, Sun, 2005; Yin, Liu; Yin, Zhu, 2001).

This chapter is aimed to review the methodology of medium and local scale landslide hazard zonation in China. Two cases are also introduced.

5.2 Terms and basic assumptions

The term 'hazard' means the probability of occurrence within a specific period of time and within a given area of potentially damaging phenomena, ie., a landslide (Varnes et al.,1984). And the term 'zonation' applies in general sense to division of the land surface into areas and ranking of these areas according to degrees of actual or potential hazard from landslides or other mass movements on slopes. Therefore, the term 'hazard zonation' can be understood as the attempt to identify where landslides may occur over a given region on the basis of a set of relevant environmental characteristics.

In the process of hazard zonation, a key assumption of the research is that slope failures in the future will be more likely to occur under geologic, geomorphic, and hydrologic conditions which led to past and present slope movements (Varnes et al., 1984; Carrara et al., 1991, 1995).

5.3 Methods of mathematical models and GIS application

5.3.1 Evaluation factors

The mechanism analysis and factors recognition are of primary importance, when assessing the probability or susceptibility of slope failure within a specified time and within a given area. The analogy method of engineering geology can then be used correctly and the precision of zoning results can be ensured. The factors in affecting slope failure can be grouped into two categories: (1) the static factors (also named controlling factors) which are relatively static in a given time and control the geology environment, slope stability, slope magnitude, failure type, et al. mainly including slope gradient and aspect, elevation, geological structures, lithology or soil properties; and (2) the dynamic factors (also named triggering factors) which may change over a very short time span and can accelerate the slope failure, such as heavy rainfall, earthquakes, human engineering activities. It is very important that different combination of static factors and dynamic factors may induce different landslide process.

5.3.2 Mapping units

Mapping unit is an important basis for variable values selection or even hazard evaluation, which directly influences the precision of zonation result. Usually, there are three methods: grid cells, slop units and Polygon mesh units.

Grid cells, preferred by raster-based GIS users, divide the territory into regular squares of pre-defined size, which become the mapping unit of reference (Guzzetti, et al., 1999). The cell size is mostly controlled by map scale and geography coordinate. Each cell is assigned a value for each evaluation factor taken into consideration by over laying a stack of factor maps.

Slope units, automatically derived from high quality DTMs, partition the territory into regions between drainages and ridges. The slope size is mostly controlled by natural topography and geology condition. Each unit is assigned local morphometric variables and evaluation factors, which are evaluated according to the genetic mechanism of slopes.

Polygon mesh units, synthetically derived from the principle of grid cells and slope units, divide the territory into regions between drainages and ridges but with equal width (Fig.1). The method of regular grid cells is suitable for small scale hazard evaluation. But if the method is used for medium and large scale hazard evaluation, natural slopes would be artificially divided into multi segments.

Because the slope deformation and instability is derived from systemic destroy of the whole slope, grid cells method would destroy the integrity of slopes and finally influence the zonation results. To both satisfy the rationalization in geology and randomness in statistics, the method of polygon mesh units is chosen for medium and large scale landslide hazard zonation. This method is more complicated than the other two, but it has clearer geological meaning.

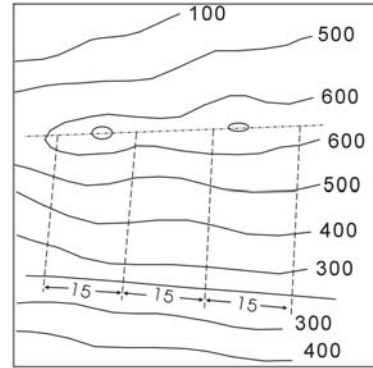


Figure.1 Sketch map of Polygon mesh units division

5.3.3 Mathematical models

Numerous methods for landslide zoning have been developed until now, which can be classified into three categories: deterministic models, statistic models and information model (Yan, et al., 1989). The former two models can also named white-box and black-box model. From the point view of grey control system theory, information model can also be regarded as grey-box model. Statistic models and information models are the points of discussion in this chapter.

(1) Statistic models

Statistic models are based on the analysis of instability factors of the past and present landslide occurrences, aiming to build up the relation of landslide and related factors or the relation of various factor combinations. Various multivariate statistical techniques have been applied, such as linear or logistic regression analysis, discriminant analysis, clustering analysis and neural net works. Regression analysis is aiming to determine the relation of landslide occurrence and the related factors. The factor with greater regression coefficient is suggested to have greater contribution for landslide. Discriminant analysis is based on the establishment of discriminant function. The level of factor contribution for landslide is reflected by the discriminant coefficient. While clustering analysis is not to directly determine the relation of landslide and related factors, it analyzes different factor combinations and the relation with different types of landslide hazard.

In various statistic models, logistic regression analysis is very useful, because the dependent variable is binary. The dependent variable for this analysis is the absence or presence of a landslide. The advantage of logistic regression analysis over other multivariate statistical models including multiple regression analysis and discriminant analysis is that the dependent variable can have only two values—an event occurring or not occurring and that

predicted values can be interpreted as probability since they are constrained to fall in the interval between 0 and 1 (Dai, Lee, et al., 2002).

Assuming that there are n units in hazard zoning area, k independent variables, x_1, x_2, \dots, x_k , affecting landslide occurrences, a vector of X is defined as $X = (x_1, x_2, \dots, x_k)$. Each variable is binary with values of 1 (presence) or 0 (absence). If x_k is a continuous variable (such as slope), some classes are established and each class (such as slope ranging from 1° to 10°) is regarded as an independent variable. If x_k is a categorical variable (such as lithology), each class of the variable is equal to 1 if the variable type is present in a zoning unit i and 0 otherwise. Only one class of the variable can be present in a unit. The conditional probability of landslide occurrences can be represented by $P(y=1|X)$. The logit of the multiple logistic regression model (Hosmer, Lemeshow, 2000) is:

$$\log it(y) = a_0 + a_1 X_1 + a_2 X_2 + \dots + a_k X_k$$

Where a_0 is the constant of the equation, and a_1, a_2, \dots, a_k are the coefficients of variables x_1, x_2, \dots, x_k . Then the predicted probability $P(y=1|X)$ of unit i can be expressed in logistic regression model:

$$\hat{P}_i = \frac{1}{1 + \exp(-(a_0 + a_1 X_{i1} + a_2 X_{i2} + \dots + a_k X_{ki}))} \quad (1)$$

(2) Information model

Information model is based on the mathematical theory of communication, which is proposed by Shannon C.E. in 1948. Landslide probability is represented by the decrease of information entropy when landslide occurs. The information value $I(y, x_1, x_2, \dots, x_k)$ of landslide y supplied by attribute x_1, x_2, \dots, x_k is calculated according to conditional probability:

$$I(y, x_1, x_2, \dots, x_k) = \log_2 \frac{p(y | x_1, x_2, \dots, x_k)}{p(y)}$$

It is very difficult to determine the probabilities of $p(y | x_1, x_2, \dots, x_k)$ and $p(y)$, but it becomes easier if the landslide inventory map and attribute maps are divided into units, then superposed.

It is assumed that the study area is divided into n units, and landslides occurred in N_0 units. After detailed analysis of landslide mechanism, factor combination x_1, x_2, \dots, x_k is thought to be the optimal one for landslide occurrence. And there are M units with the same factor combination but only M_0 units have landslide occurrence under this condition. According to the principle of prior probability, the information value $I(y, x_1, x_2, \dots, x_k)$ can be calculated by the following formula .

$$I(y, x_1, x_2, \dots, x_k) = \log_2 \frac{M_0/M}{N_0/N}$$

If the information value is calculated by area ratio of units, the above formula can be changed into:

$$I(y, x_1, x_2, \dots, x_k) = \log_2 \frac{S_0/S}{A_0/A} \quad (2)$$

Where A is the total area of units in the zoning area; A_0 is the area of units where landslide occurs; S is the area of units with factor combination x_1, x_2, \dots, x_k ; S_0 is the area of units where landslide occurs under the condition of factor combination x_1, x_2, \dots, x_k .

(3) Artificial Neural Network

The artificial neural network is composed of large number of artificial neurons similar with natural neural cells. It is a huge information processing system in which the processing works by the interaction between neurons. Nowadays, it has been applied in various research fields. In large number of neural networks, the Back Propagation Neural Network (BP) is the most popular one. This kind of neural network is trained by using the back propagation algorithm. And the learning algorithm performs a gradient descent optimization on the weights linking the nodes in each layer. The neural network is simple use and shows to be robust and gives good results in most cases.

The BP is generally composed of three layers: input layer, hidden layer and output layer. The hidden layer could be one or multi-layer. Numbers of neurons is in each layer and they are connected by weights. The prediction approaches are shown in Fig.2. The process of the model can be divided into two: training process and prediction process. The training process consists of forward propagation of input data and back propagation of errors. In the process of forward propagation, the input data is processed from input layer to hidden layer and finally to output layer, but the neurons in each layer only has effect in the next layer. If the output data is not in accord with the expected results, the output error should be calculated and be put into the process of back propagation of errors to minimize the final error by modifying the weights of neurons in each layer. The prediction process is a learning course in which the unknown samples are input and only forward propagation process works.

In the application of the neural network model, the success of prediction depends on the rationality of training samples. Generally, the training samples should contain all the status of the prediction objects as full as possible. When the model is used in landslide hazard zoning, a network can be successfully constructed by the standard input samples in sample area, and it can then be used in the predictive area. The input data is the hazard influencing factors which may be binary state variables or detailed numeric variable. Because of the difference of variable units and orders of magnitude, the variables must be normalized in advance. In output layer, the results can be expressed by different hazard stability classes (stable, potentially unstable, unstable) or by detailed numeric value (stability coefficient, failure probability).

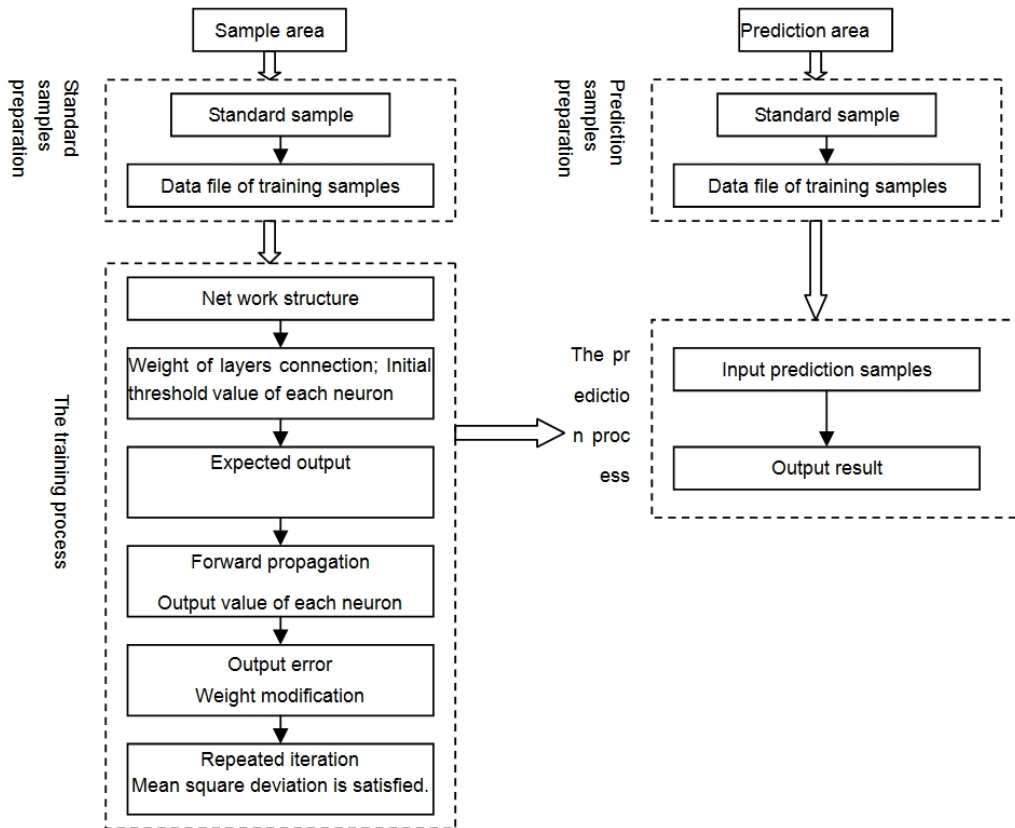


Figure.2 Prediction process of BPNN

5.3.4 Evaluation of hazard zonation results

The validation and precision of quantitative landslide hazard susceptibility should be evaluated, which is an important difference from qualitative hazard zonation. The error in zonation results comes from two items: error of landslide unit and error of stability slope unit. Usually, the former error is taken into consideration but the latter one is ignored. But perfect precision evaluation should eliminate these two errors.

A general distribution curve for hazard susceptibility prediction value is shown in Fig.3, which is similar to normal or partial normal distribution.

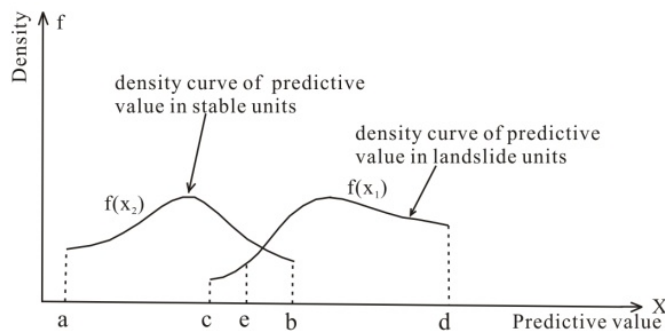


Figure.3 Density curve of landslide prediction value

It is assumed that $f(x_1)$ and $f(x_2)$ are the prediction value density distribution functions separately for landslide units and stability slope units. In these function curves, distribution interval of prediction value is (a,d), in which stability unit prediction value interval is (a,b) and landslide unit is (c,d). Point e is the critical value to partition landslide and stability slope. Theoretically, point c, e and b should be superposed, which means that the prediction precision is 100% and all of the prediction value for landslide are greater than critical value e under the condition of no inaccurate information imported. In fact, point c, e and b is not superposed. The segment of $f(x_2)$ in interval (e, b) not only includes prediction values, but also contains errors. As the curves show that all the prediction values have two kinds of errors, one is the errors A_1 of landslide units and the other is A_2 of stability slope units. According to the principle of probability multiplication, the prediction precision A can be express as:

$$A = A_1 \cdot A_2 = \int_e^d f(x_1)dx \cdot [1-m] \int_e^b f(x_2)dx \quad (0 < m < 1)$$

If it is transformed into exponential type, it is

$$A = \int_e^d f(x_1)dx \cdot [\int_a^e f(x_2)dx]^n \quad (0 < n < 1)$$

And if n is an experience value 1/3, the prediction precision can also be expressed by test probability:

$$A = \frac{M_1}{N_1} \times \left(1 - \frac{M - M_1}{N - N_1}\right)^{1/3} \quad (3)$$

Where, N is the total number of units in study area; N_1 is the number of landslide units; M is the number of units with prediction value over e; M_1 is the number of units which are both landslide and the prediction values are over e.

While if the precision is directly tested by the landslide occurrences in study area, precision A can be:

$$A = C/B \quad (B \geq C) \quad (4)$$

Where B is the number of units where landslides occur; C is the number of units in which landslides occur and prediction values are over critical value e.

5.3.5 GIS application

Because of the function of spatial analysis and mapping, GIS technology has been quickly developed in landslide hazard assessment and risk management now. From 80's in last century to today, GIS technology is applied in data management, multi-resource digital map plotting, digital elevation model or digital terrain model, hazard evaluation model analysis and decision-making support system. Traditional technology of GIS in landslide hazard is mainly applied detailedly in:

A. Hazard information management. Keane, James(1992), Bahar, Irwan (1988), Bliss & Norman (1998) used GIS approach to manage historical hazard data.

B. Hazard assessment with other evaluation models. Matula (1987), Lekkas (1995), Randall (1998), Dhakal, Amod & Sagra (1999), Yin & Yan (1989,1996 and 2001) applied GIS and hazard

evaluation models to obtain hazard susceptibility. Yin, Zhang, et al (2002) used GIS approach to assess landslide and debris-flow risk by adopting information model in China at the scale of 6 000 000.

C. Hazard assessment and risk management. Ellene (1994), Leroi (1996), Bunza (1996), Castaneda-Oscar-E (1998), Atkinson (1998), Michael (2000), Aleotti (2000) has developed information and decision making systems aimed at hazard risk evaluation and controlling. It is worth to be pointed out that a GIS-based geo-hazard monitoring and warning system has been developed and would be applied in the Three Gorges reservoir, China. The system can provide effective hazard warning information for local government, finally mitigating the losses of lives and properties in the area.

It is no doubt that GIS is a good tool for landslide hazard risk assessment and management. But it does not mean that the technology can completely replace the work of hazard data collecting, necessary field investigation and laboratory test. Oppositely, the result of hazard risk assessment is credible only when GIS technology is applied based on deep recognition of landslide mechanism.

5.4 Illustrations

5.4.1 Medium scale landslide hazard zonation

(1) Hazard zonation of Wanzhou city in the Three Gorges reservoir, China

Wanzhou city is located in the middle segment of the Three Gorges reservoir, China (Fig.4). Two urban districts of the city, Longbao and Tiancheng, are located on four ancient landslides including Taibaiyan, Diaoyanping, Pipaping and Caojiezi (Fig.7). These ancient landslides have evolved to be many secondary landslides or instable slopes induced by natural disintegration and human activities. In addition, these slopes are located on the bank of Yangtze River, where the construction and operation of the Three Gorges Dam have caused many engineering geology problems, due to the big rise and fluctuation of water level, such as riverbank reformation, river bank collapse or erosion and landslide, To decrease the losses of human lives and properties by landslides, the study aims to assess hazard susceptibility and provide landslide hazard maps for risk management in future.

① Geological settings

The geomorphology of the study area belongs to structure-erosion and erosion-low mountain relief, including floodplain, terrace and structure-erosion. A syncline with axial direction NE60° passes through the area.

The bedrock of the study area is dominated by Jurassic rocks, which mainly consists of amaranth sandstone, grey-white feldspar-quartz sandstone with amaranth muddy siltstone, silty mudstone and mudstone. Two kinds of soft interlayer were discovered in this stratum :(1) a soft interlayer of mudstone with high content of montmorillonite: The thickness of the layer ranges from 3cm to 80cm. It is very easy to be soft and expand when encountered with water, which induced the shear strength to become very low; and (2) a soft interlayer of amaranth

mudstone with high content of illite: the interlayer is mainly exposed on the surface of the mudstone and the thickness of which is no more than 1cm or even only 1mm (Fig.5-6).

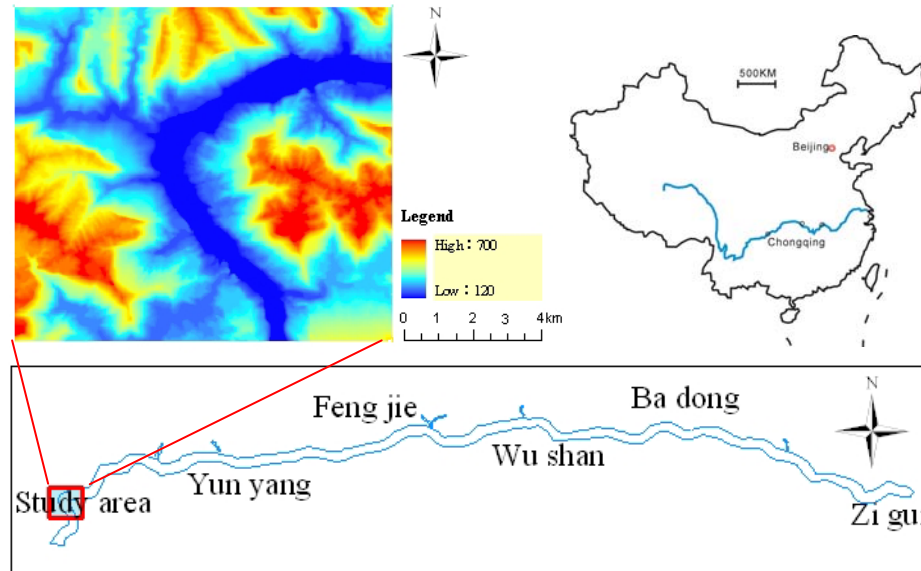


Figure.4 Location of the study area



Figure.5 Soft interlayer of mudstone with rich montmorillonite



Figure.6 Soft interlayer of amaranth mudstone with rich illite

Under the condition of geological structural stress and unloading, the integrity of the interlayer can be destroyed when the slope slips along the soft interlayer on bedrock. Several scratches in the layer are legible with eyes. Then underground water may penetrate into the interlayer through such fractures which has two effects in slope stability: (1) the shear strength decreases rapidly because of the expansibility; and (2) great hydrostatic pressure appears quickly. These have positive effects for landslide occurrences. With the industry development, landslides with different volume appeared in the geological conditions and they mainly distribute along the banks of the mainstream and branches of the Yangtze River (Fig.7). The landslide hazards range in elevation from 210 to 310m and more detailed information was shown in table 1.

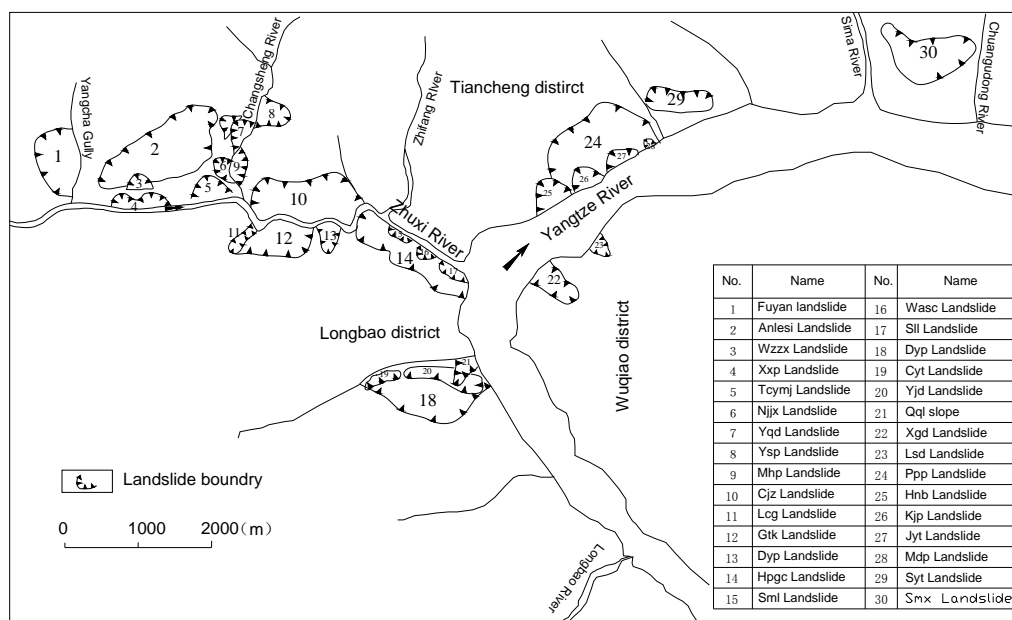


Fig.7 Landslide hazard distribution map of the study area

Table 1 Landslide hazards in the study area

Name of town	Name of block	Landslides			Unstable slopes		
		Numbers	Area (10 ⁴ m ²)	Volume (10 ⁴ m ³)	Numbers	Area (10 ⁴ m ²)	Volume (10 ⁴ m ³)
Tiancheng	Qingcaobei	6	76.3	1652.4	12	27.96	461.4
	Pipaping	11	147.2	4324	24	71.85	1129.5
	Caojiezi	8	73.5	2230.9	19	53.29	729.1
	Anlesi	6	181.6	4001.6	11	51.66	995.8
Longbao	Taibaixi	5	93.1	2048.6	9	3.64	236.2
	Diaoyanping	7	128.3	2792	8	11.16	395.9
	Taibaiyan	5	290.2	8877.3	14	48.54	1122.2
	Ersichang	4	49.3	1279.87	7	36.37	986
	Longbaohe	7	7.8	27.1	\	\	\
Wuqiao	Wanjiaba	9	206	3768.8	5	14.03	307.7
	Chenjiaba	6	187.3	1855.3	11	24.3	143.1

② Evaluation Factors

According to the geological environment of landslides by field inventory and laboratory test, seven factors are chosen to assess the susceptibility of the study area (Table 2). These factors are classified into two categories according to the principles introduced above. The controlling factors include slope angles, lithology, depth of deposit, river erosion and history hazards; and the triggering factors contain treatment project, uncontrolled settlement and agricultural activities.

Using the 1:10 000 scale topographical map of the area, a digital elevation model (DEM) was established and the slope angle was obtained. The slopes were classified into four categories: $<10^\circ$, $10^\circ\sim 25^\circ$, $25^\circ\sim 35^\circ$, $>35^\circ$. Geological map was used to obtain the distribution map of lithology, which were classified into three types: quaternary deposit, colluvial accumulation and bedrock. According to the data from boreholes, the thickness of deposit was classified into three categories: $<5\text{m}$, $5\sim 20\text{m}$, $>20\text{m}$. In addition, the influence of past landslide hazard presence and river erosion is also taken as variables. Land use type was classified into four categories: storages or ports, buildings, roads or bridges and green space. The presence of treatment project has great influence for landslide hazard reactivity. Slopes with no treatment project will be more probable to fail than those with treatment projects.

Table 2 Evaluation factors and relative information values

Factors	Secondary factors	Categories	Variables	Information value
Controlling factors	Slope angel	$<10^\circ$	X1	0.67
		$10^\circ\sim 25^\circ$	X2	-0.309
		$25^\circ\sim 35^\circ$	X3	-0.982
		$>35^\circ$	X4	-1.814
	Lithology	Quaternary deposit	X5	-1.211
		Colluvial accumulation	X6	2.545
		Bedrock	X7	-1.823
	Thickness of deposit (m)	<5	X8	-0.669
		$5\sim 20$	X9	1.376
		>20	X10	2.304
History landslides	Present	X11	2.688	
River erosion	Present	X12	1.691	
Triggering factors	Land use	Storages or ports	X13	0.365
		Buildings	X14	1.108
		Roads or bridges	X15	0.121
		Green space	X16	-1.393
	Treatment project	Present	X17	-2.25

With the help of GIS approaches, corresponding factor maps for hazard zonation were prepared, which include lithology map, slop angle map, river erosion map, land use map, history hazard distribution map, isoline map of deposit depth and spatial distribution map of treatment projects. These maps were over layered and 29 240 abnormality units were obtained.

③ *The application of information-ANN coupled model*

The combination approach of information and ANN model is applied in the study area. Both sides of the Zhuxi River bank were selected as the sample area because of the representation of hazards and abundance of past study work. According to the factors analyzed and prepared maps above, the information value of each factor was calculated by information model and was shown in table 2. After the normalized process, these values were input into the ANN model and a net work with a seven-node input layer, seven and five node hidden and a three-node output layer was constructed. The nodes of the input layer correspond to the seven factors. And the nodes of the output layer correspond to three stability categories: stable,

potentially unstable and unstable. Representative section in the sample area was selected and calculated for stability analysis, the coefficients of which were classified into three stability categories.

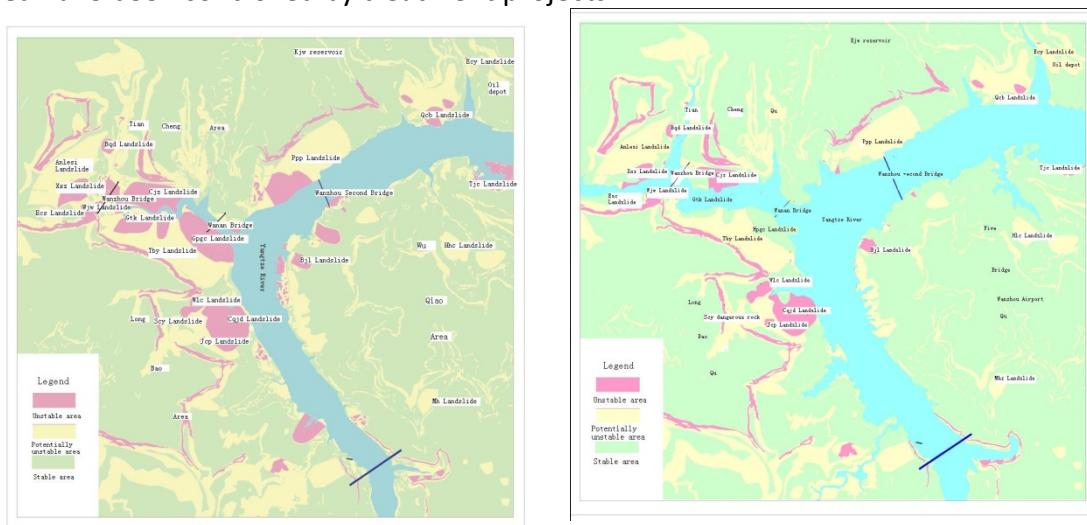
After 50 thousands of model training when network precision was satisfied, the network was constructed and applied to the whole area for hazard zonation. The zoning map was shown in Fig.8. It indicate that about 6% of the area, mainly along the river banks of Yangtze River and Zhuxi River, is unstable where ancient and new landslide or rockfall deposits mainly distribute and bedrock is buried deeply. The place is suggested to be the key area for landslide hazard prediction and controlling. About 13% of the area is potentially unstable where Quaternary deposits mainly distribute and it is suggested to be limitedly developed in future.

Considering that treatment works have been carried out for partial unstable slopes, a parameter reflecting this change should be added and the zonation assessment was done once again. The zones with different stability category were colored by red, yellow and green respectively. The map shows that:

(a) Stable area. It counts for 80% of the study area where is mainly composed of bedrock. In addition, there are no many more engineering projects in the steeper terrain.

(b) Potentially unstable area. It counts for 12% of the area which is suggested to be developed limitedly. The middle and front part of this area is mainly covered by deposits and ancient landslides. This zone is with flat terrain and the slop angle ranges from 10 to 30. Because of the deposit thickness, the foundation of the area is not good for building, except it is treated by some engineering works. Therefore, it is suggested that the area can be used for construction only after the place is assessed deeply by geologists and engineers.

(c) Unstable area. It counts for 8% of the area which is suggested to be the focus of hazard controlling in future. This zone mainly distributes along the sizes of Yangtze River and Zhuxi River, and is covered by landslide and alluvial deposits. Some unstable slopes or landslides in the area have been controlled by treatment projects.



(a) Before treatment projects

(b) After treatment projects

Figure. 8 The map of landslide hazard zonation in Wanzhou

(2) Landslide hazard zonation of Xunyang county of Shanxi province in China

① Geological settings

Xunyang county is located in south part of Shanxi province and has an area of about 100 km². The county is dominated by medium-low mountainous territory where deep gullies and valleys are present. The area is in the south of a Latitudinal structure belt with direction NWW-SEE. And the county is covered by Paleozoic metamorphic rocks and Quaternary deposits, mainly consists of sericite-chlorite quartz schist, sericite carbon quartz phyllite and thin bed crystalline limestone. Because of this special geological environment and severe folds and faults, high density landslides distribute in the area, including 200 rockslides and 10 deposit slides.

② Landslide spatial distribution characters

Landslides in the study area distribute in bands or in clusters due to the controlling of geological environment and special territory condition. And there are five hazard concentrate zones with the same direction of structure distribution. Some characters are shown by the statistical analysis:

(a) The schist and phyllite are very easy for landslide occurrence because phyllite mineral exists centrally and microscopic and macroscopic soft belts form in it which has the character of easily deformation. The rockslide area counts for 14.5% of the whole bedrock area and it also indicates that in such condition landslides mostly occur.

(b) Landslides distribute in cluster along faults. There are 36.8km faults in the area and 32 landslides occurred along these faults. The width of the landslides are about 7.05km and counts for 19% of all the fault length, which shows that faults have great effect for landslide.

(c) Landslides in the area are controlled severely by schistosity structure. The main direction of landslides are in NW340°- NE40° and SE160°- SW220°, which is in accord with the tendency of schistosity structure.

(d) The elevation of landslide toe ranges from 220m to 270m, which is close to the elevation of modern erosive datum plane (Fig.9).

(e) Landslides in the area mainly occur in slopes with gradient from 23° to 33° (Fig.10).

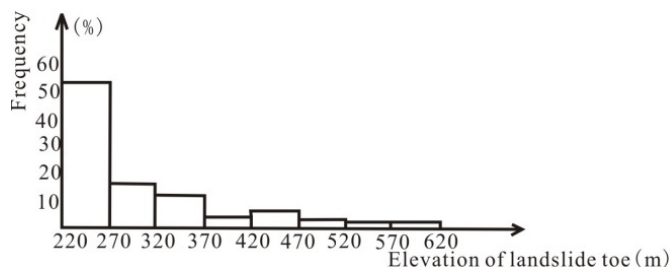


Figure.9 Histogram of elevation of landslide toe and frequency

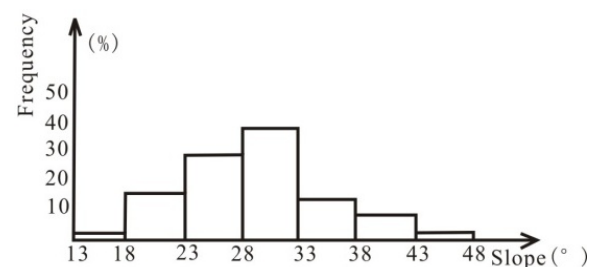


Figure.10 Histogram of slope and frequency

③ Mapping units and factors selection for hazard zonation

Polygon mesh units are used in this study on the basis of the landslide engineering geology map (1:50,000) and topographic map. The max width of landslides (500m) in the area is used as

slope unit width. And with the methodology of Polygon mesh units, 538 rock units and 108 deposit units are obtained in the area.

Five basic influencing factors are selected firstly, including lithology, faults, schistosity structure, shape parameters of slope and slope buttressing effect. According to the cross-correlation analysis of different factors and the analysis of landslides occurrence frequency and each factors, 24 variables for hazard zonation is finally chosen and the relative status for each variable is determined (Table 3).

Table 3 Variables and relative status for hazard zonation

Factors	Status	variables	Factors	Status	variables	Factors	Status	variables
Elevation of slope toe (m)	≤270	x ₁	Elevation difference (m)	241~360	x ₈	slope buttressing effect	The strata with slope buttressing effect	x ₁₅
	271~370	x ₂		101~340	x ₉			
	371~520	x ₃		≤100 or >340	x ₁₀	fault	Contrary to slope aspect	x ₁₇
	>520	x ₄		23~34	x ₁₁		present	x ₁₈
Aspect (°)	1~60	x ₅	Lithology	<23 or >34	x ₁₂	Angle between schistosity inclination and slope aspect (°)	0~20	x ₁₉
	61~180	x ₆		Sericite clorite Quartz schist	x ₁₃		21~65	x ₂₀
	181~240	x ₇		Carbonaceous sericite Quartz phyllite	x ₁₄	66~90	x ₂₁	

④ The application of information model and regression model

With the methodology of mapping units, 183 sample units and 355 prediction units are obtained. Two models of information model and binary status regression model are respectively constructed.

$$I_i = 0.264x_{i1} + 0.116x_{i2} + \dots - 0.100x_{i21} \tag{5}$$

and

$$P_i = 0.145x_{i1} - 0.021x_{i2} + \dots + 0.081x_{i21} \tag{6}$$

Where, I_i is predicted information value; P_i is regression coefficient; x_{ij} is the value of variable j in unit i , which is 0 or 1 ($i=1,2,\dots,j=1,2,\dots,21$).

The above two equations show that the slope may be more unstable when the value of I_i or P_i is greater. The information value and regression coefficient of each variable is depicted in Table 4.

Table 4 Information value and regression coefficient of variables

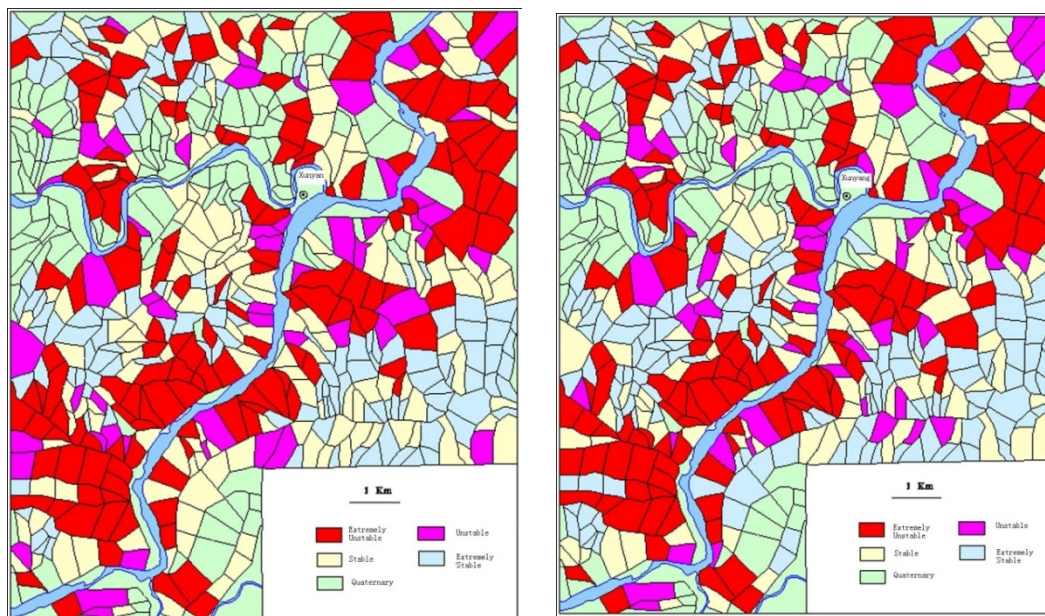
Variables	X ₁	X ₂	X ₃	X ₄	X ₅	X ₆	X ₇	X ₈	X ₉	X ₁₀	X ₁₁
Information	0.264	0.116	-0.353	-0.809	0.249	-0.148	0.211	-0.198	0.047	-0.135	0.05
Regression coefficient	0.145	-0.021	-0.232	-0.29	0.25	0.003	0.215	0.039	0.100	0.020	-0.071
Variables	X ₁₂	X ₁₃	X ₁₄	X ₁₅	X ₁₆	X ₁₇	X ₁₈	X ₁₉	X ₂₀	X ₂₁	
Information	-0.143	-0.143	0.032	-0.369	-0.030	0.054	0.225	0.22	-0.098	-0.100	
Regression coefficient	-0.088	0.062	0.042	-0.229	0.065	0.078	0.250	0.254	0.17	0.081	

To distinct landslides and stable slopes, the critical value for point e in former introduction of result precision evaluation should be found out. According to the histogram of information value -frequency or regression coefficient-frequency, point e is found out and thought to be the change-point. So I_{cr} and P_{cr} is 0.05 and 0.45 respectively for information model and regression model. To divide the slope into more stable classes except stable and unstable, the method of discriminate analysis is applied and more boundary values are obtained (Table 5).

Table 5 Critical and boundary values for landslide stability classes

Classes	Extremely stable	Stable	Unstable	Extremely unstable
Information model	$I < -0.75$	$-0.75 \leq I < 0.05$	$0.05 \leq I < 0.50$	$I \geq 0.5$
Regression model	$P < 0.19$	$0.19 \leq P < 0.45$	$0.45 \leq P < 0.69$	$P \geq 0.69$

To verify the results of the above two models, the precision is calculated by *Formula 3* and *Formula 4* respectively. The results show that the precision of information model is 69% and 70% and the precision of regression model is 71% and 80% respectively by the two formulas. And the results also indicated that the precision is almost above 70% which means that the constructed models can be used for hazard zonation in the prediction area. With the technology of GIS, landslide hazard zonation map is finally obtained (Fig.11).



A. Information model

B. Regression model

Figure.11 Landslide hazard zonation map of Xunyang county

5.4.2 Local scale landslide hazard zonation

(1) Anlesi landslide

① Geological settings

The landslide is located in the Wanzhou city, and it extends from the elevation of 240m to 325 m, with the length of 500m and the width of 200m (Fig.12). The area of the landslide is 1.01 km² and the volume is 24.86 millions m³. The terrain slope is smaller than 10° and the occurrence of bedrock is 150°∠4°~5°. The area is dominated by Jurassic sedimentary rocks, which mainly consists of siltstone with mudstone and the occurrence of which is 150°∠4°~5°.



Figure.12 General view of the Anlesi landslide

There are many deposit slides at the toe of AnLesi landslide, including Wzxx landslide, Ymj landslide, Njxx landslide and Yqd landslide (Fig.13). The depth of slip surface ranges from 10 m to 40 m, and is even 48 m at the crown of the slide. It is very special that the angle of the slip surface is close to horizontal. The soil of sliding belt is clay by boreholes and field investigation. The sliding zone has thickness of about 3.0 m which is composed of clay with 0.2-3 m thick grey sandstone rubble.

The thickness of landslide decreases gently from the rear to the front of the landslide. The elevation of slip surface ranges from 240m to 325m. The tendency of rock bed is south which is close to the aspect of slope. A gully develops along the main sliding direction in the middle of landslide, which drains the surface water to the ChangSheng River. Small debris flow occurred at the toe, when the slope encountered rainstorm, but the landslide is stable. The surface catchment area is very large, but there is only one longitudinal gully in the east, which is not enough to solve the drainage problem of the whole landslide. Many ponds distribute in the landslide irregularly. The groundwater depth ranges from 0m to 10 m and is higher than the sliding bed. The geological profile of the landslide is shown in Fig.14.

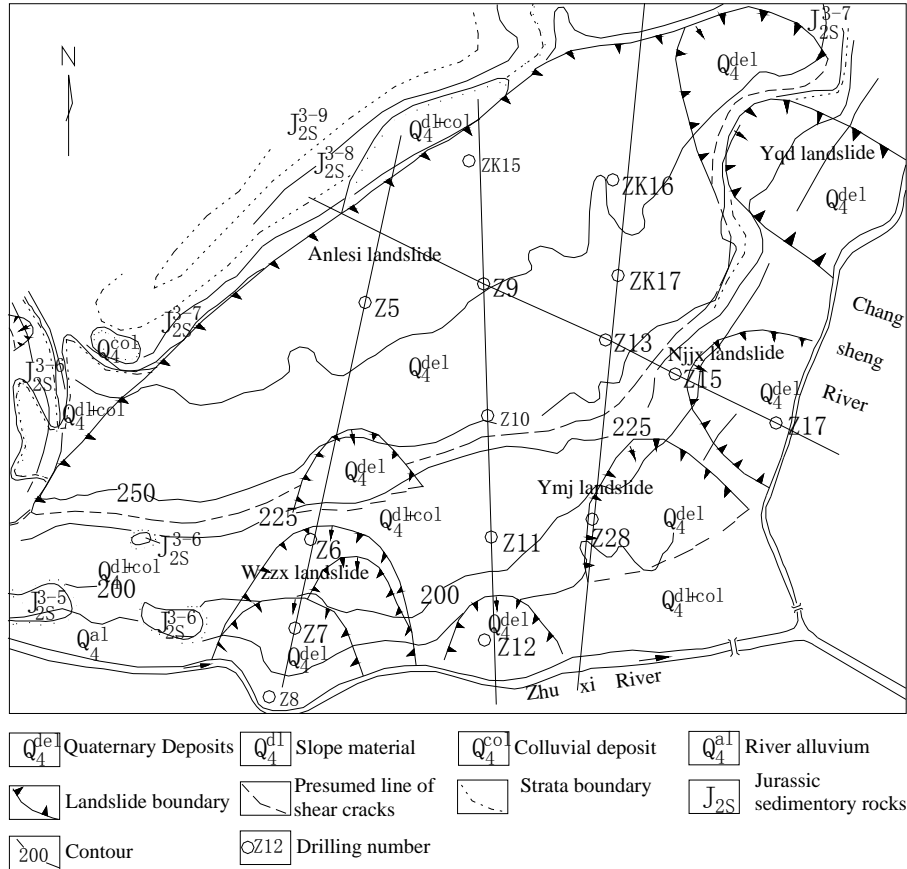


Figure.13 Engineering geological map of Anlesi landslide

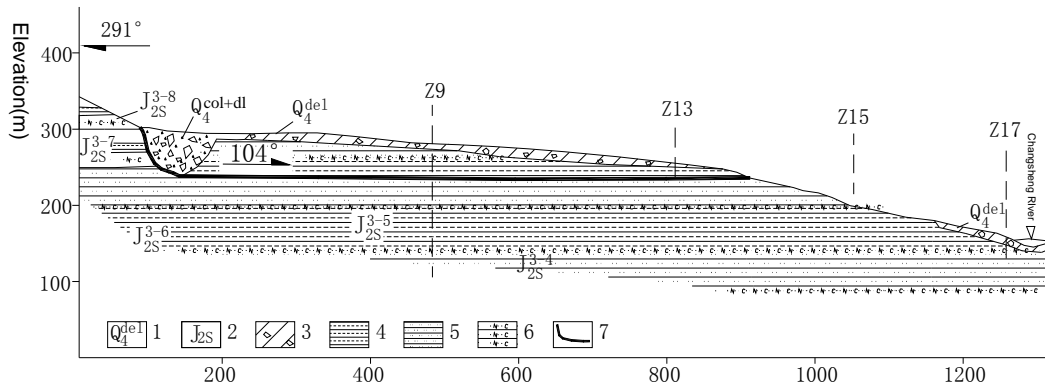


Figure.14 The geological section map of Anlesi landslide (Modified according to Cuizhengquan)

Influencing factors

Legend: 1. Landslide deposits; 2. Jurassic sedimentary rocks; 3. Clay with gravel; 4. Mudstone; 5. Sandstone; 6. Feldspar sandstone; 7. Sliding surface

The stability of landslide is influenced by many factors. According to the geological environment and landslide mechanism, eleven factors are selected as indexes for hazard zonation, which include slope, the relationship between slip surface angle and internal friction

angle of sliding zone, lithology, the thickness of deposit, permeability of rock and soil mass, slope structure, the influence of groundwater to sliding zone, history hazards, reservoir bank rebuilding, land use type and treatment projects (Table 6).

Table 6 Influencing factors of the Anlesi landslide

Factors	Status	Information value	variable		
Geological environment	terrain	<10°	-0.140	X1	
		10°~25°	0.601	X2	
		25°~35°	-1.321	X3	
		>35°	-3.702	X4	
	the relationship between slip surface angle (α) and internal friction angle of sliding zone (β)	$\alpha \geq \beta$	0.662	X5	
		$\alpha < \beta$	-0.505	X6	
	lithology	Surface petrofabric	Quaternary loose accumulation	1.741	X7
			Collapse slide accumulation	0.456	X8
		thickness of deposits	bedrock	-3.434	X9
			<5	-1.403	X10
			5~20	0.628	X11
			>20	1.454	X12
permeability of rock and soil mass			Strong permeability	1.741	X13
			Medium permeability	0.456	X14
	Weakly permeability	-3.434	X15		
geological structure	slope structure	Consequent slope	0.218	X16	
		Tangential slope	-0.070	X17	
		Reverse slope	-1.067	X18	
hydrogeology	the relationship between groundwater (Hw) to evaluation of sliding zone (Hs)	Hw>Hs	0.903	X19	
		Hw<Hs	-2.387	X20	
Dynamic geological process	development degree of existing geo-hazard	Relatively serious	2.591	X21	
	reservoir bank rebuilding	Present	1.710	X22	
Human engineering activity	landuse type	Building site	0.740	X23	
		Road and bridge	0.440	X24	
		Green space	-0.348	X25	
	governance engineering	Present	-2.221	X26	

② Mapping units and variables evaluation

The method of grid cell is adapted to this landslide. The size of cell is 25 m×25 m and the study area is divided into 7364 units. And then relative factor maps are also prepared, including slope map, isoline map of deposit depth, isoline map of groundwater depth, etc.. Spatial grid superposition function is used to evaluate the hazard, which is similar to the attribute function calculation of matrix. It is required that the study area and grid cell selection should be uniform.

③ Evaluation model establishment

(a) Establishment of information model

The information values of each variable are calculated and the evaluation model is built up by *Formula 2*. The result is shown in Table 7. Some variables with relatively large information values are indicted to be the important influencing factors which are in accord with field investigation. The variables are slope ($10^{\circ}\sim 25^{\circ}$), relationship between slip surface angle and internal friction angle ($\alpha \geq \beta$), quaternary deposits with depth greater than 20m, strong permeability, groundwater higher than sliding zone, serious history hazards and reservoir bank rebuilding. Then the information values are classified into four categories: *high* ($I \geq 1.4$), *medium* ($1.4 \geq I \geq -0.14$), *low* ($-0.14 \geq I \geq -1.24$), *extremely low* ($I < -1.24$). The model is used to evaluate the prediction area and the hazard zonation map is shown in Fig.15.

(b) Establishment of information-neural network model

Based on the field investigation and relative research work, the susceptibility of the area is classified into four categories, which means a 4-node output layer is determined. And according to the influencing factors that were analyzed above, an 11-node input layer is also confirmed. The hidden layer is thought to be 9 nodes and 7 nodes respectively. The value of input samples are information value obtained in the above analysis. And the value of output samples are the four susceptibility categories determined above. After 500 000 training until the results are very close to expected values, a neural network is obtained and used to the prediction area. The hazard zonation map is shown in Fig.16.

The area with extremely low susceptibility is 37 504 m², which covers around 14% of the study area and mainly distributes in the middle or at the toe of Anlesi landslide. The area with low susceptibility is 1 409 237 m², which covers around 53% of the study area and mainly distributes in the middle part of Anlesi landslide. The area with high susceptibility is 565 215 m², which covers around 21% of the study area and mainly distributes at the crown of Anlesi landslide. The area with extremely high susceptibility is 287 604 m², which covers around 11% of the study area and mainly distributes at the crown of Anlesi landslide.

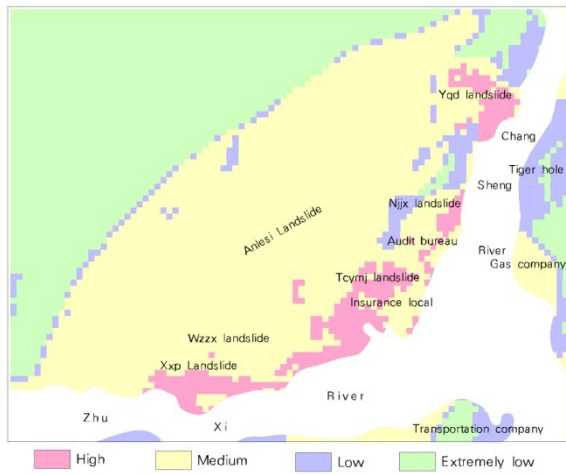


Figure.15 Hazard zonation map of study area (information model)

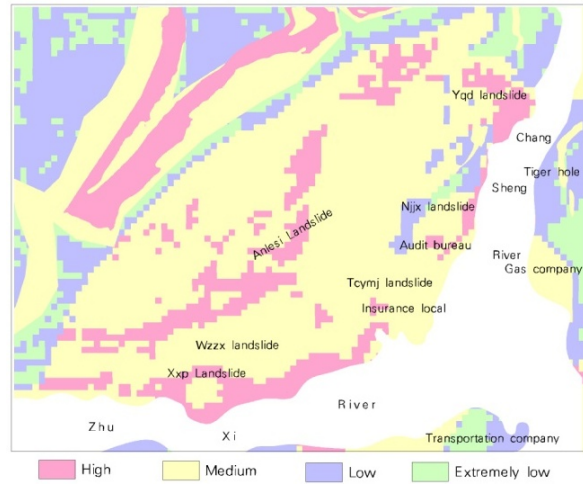


Figure. 16 Landslide hazard zonation map of study area (information-neural network model)

④ Comparison of different models

According to the hazard zonation maps obtained by two models mentioned above, it is known that the two models can reflect each other and the main difference centralizes on the area of low and extremely low susceptibility (Fig. 17 ,Fig.18), which has little influence on our recognition of the hazard. Based on the statistical relation of high and medium susceptibility areas with main prediction variables, it is known that the both models can reflect the influence of main controlling factors to landslides.

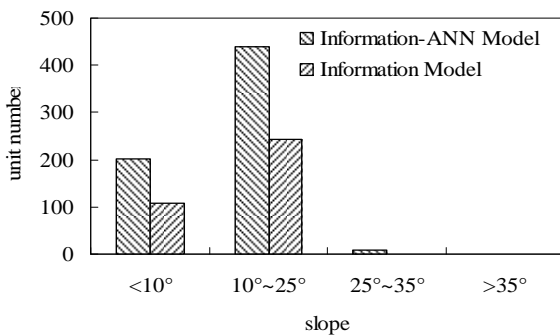


Figure.17 Histogram of slope-frequency in the area with extremely high susceptibility

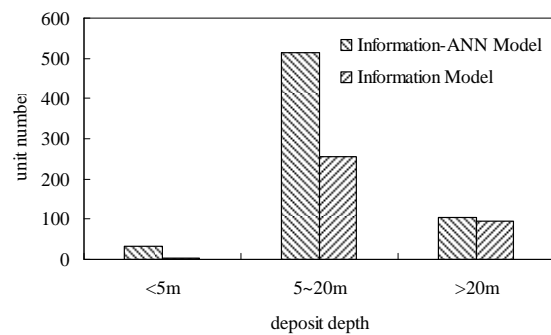


Figure. 18 Histogram of Deposit depth-frequency in the area with extremely high susceptibility

(2) Chonggang landslide

① Geological settings

Chonggang landslide is located in Chongqing province, China. It is on the left side of Yangtze River and is recognized as an ancient landslide. The slide is denudation and river erosion in geomorphology. Fig.19 shows the landslide distribution. It spread from east to west along the river, with a typically chair-shape terrain. The area is covered by Jurassic sedimentary rocks, which consist of sandstone, mudstone and Quaternary deposit. The soil of slide zone is

rich in montmorillonite with high expansibility, which is analyzed by Yin (1998) to be the most special factor for landslides in horizontal strata. The large landslide can be also divided into 5 parts: Gjl ancient landslide, Sjd ancient landslide, Cmc-smk new unstable slope, Bz new unstable slope and Sjd new unstable slope.

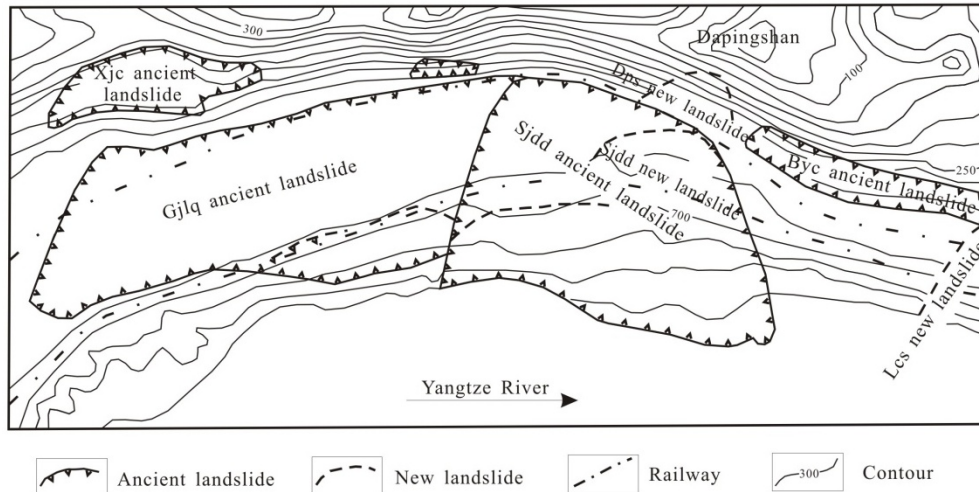


Figure.19 Distribution map of Chonggang landslide

② Mapping units and factors selection for hazard zonation

The method of polygon mesh units are applied in this study. The units are obtained according to the topography unit, lithology boundary and landslide boundary. Based on 1:2 000 topographic map, lithology map and landslide distribution map, a map with 323 units is obtained.

Generally, landslide is often caused by some controlling factors and inducing factors which include lithology, strata occurrence, slope gradient, slope aspect, river erosion, rainfall and human engineering activities. The factors of strata occurrence and rainfall have great influence to landslides, but they are not considered because they are not different in the relative small area. Therefore, some factors existing in all the units are not selected, but the factors that can express landslide macroscopical characters are taken into consideration. Finally, 10 factors are selected, including surface lithology, underground lithology, slope gradient, river erosion, depth of underground water, buildings loading, treatment projects, surface drainage, slope cut or loading and gradient of bedrock.

③ Application of information model

According to the information model, an evaluation model is constructed as:

$$I_i = 1.377x_{i1} + 1.517x_{i2} + 0.584x_{i3} + 0.472x_{i4} + 0.71x_{i5} + 0.326x_{i6} + 0.537x_{i7} + 0.786x_{i8} + 0.355x_{i9} + 0.757x_{i10}$$

Where, I_i is predicted information value; x_{ij} is the value of variable j in unit i , which is 0 or 1 ($i=1,2,\dots,j=1,2,\dots,21$).

With the help of histogram of information-frequency analysis, the critical and boundary values for landslide stability classes are obtained. And the susceptibility is classified into four categories: *extremely stable* ($I < 0.7$), *stable* ($-0.7 = I < 0$), *unstable* ($0 = I < 0.35$) and *extremely*

unstable ($I \geq 0.35$). Landslide hazard zonation map is shown in Fig.20. The precision is validated by landslide deformation through landslide monitoring and stability analysis.

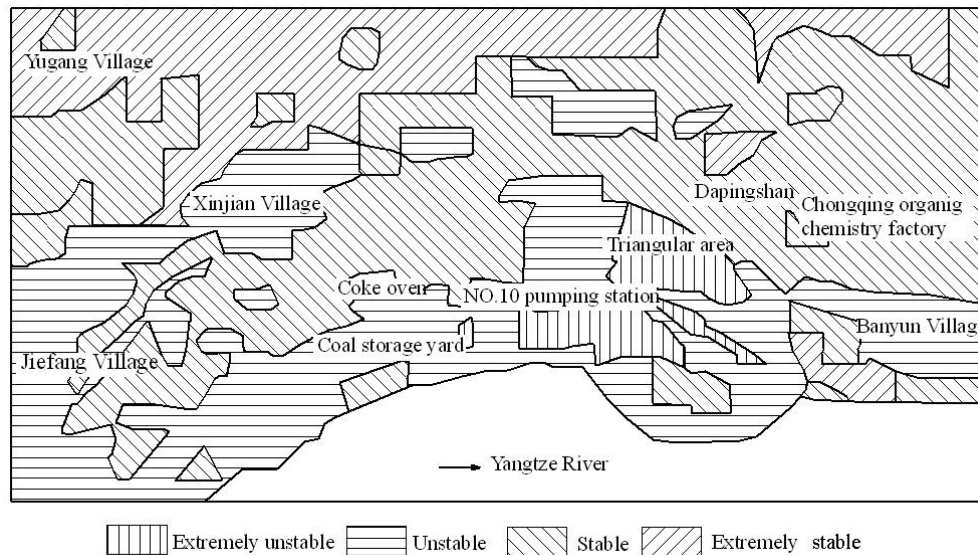


Figure.20 Large scale zonation map of Chonggang landslide

5.5 Conclusions

This research represents the basic terms and general methodology of medium and large scale landslide hazard zonation applied in China. An important assumption in this research is that slope failures in the future would be more likely to occur under the conditions which led to past and present slope movements. Therefore, the mechanism of landslide failure should be analyzed seriously before. And the influencing factors of landslides are considered to be two categories, controlling factors and triggering factors. To obtain satisfied hazard zonation results and work efficiently, the method of Polygon mesh units is thought to have more geological meaning and not loss calculation rates in GIS environment. In most general mathematical models, information model is thought to be an effective one that is widely used in China. And two methods for the evaluation of zonation precision are also interpreted in this study. To illustrate all the principles, methods and process more detailed, four cases with different scales and different landslide characters in China are studied, the results of which show good accordance with the factual hazard failures and can be good references for hazard risk management and control.

References

- Anbalagan, R., Landslide hazard evaluation and zonation mapping in mountainous terrain. *Engineering Geology*, 1992. 32(4): 269-277.
- Cascini, L., Applicability of landslide susceptibility and hazard zoning at different scales. *Engineering Geology*, 2008. 102(3-4): 164-177.
- Chung, C., A. Fabbri, and C. van Westen, Multivariate regression analysis for landslide hazard zonation. *Geographical information systems in assessing natural hazards*, 1995: 107-133.

- Corominas, J. and J. Moya, A review of assessing landslide frequency for hazard zoning purposes. *Engineering Geology*, 2008. 102(3-4): 193-213.
- Dai, F. C., Lee, C. F., et al.. Landslide risk assessment and management: an overview. *Engineering Geology*, 2002,64(1): 65-87.
- Dai, F., et al.. Assessment of landslide susceptibility on the natural terrain of Lantau Island, Hong Kong. *Environmental Geology*, 2001. 40(3): 381-391.
- Das, I., et al., Landslide susceptibility assessment using logistic regression and its comparison with a rock mass classification system, along a road section in the northern Himalayas (India). *Geomorphology*. 114(4): 627-637.
- Fell, R., et al., Guidelines for landslide susceptibility, hazard and risk zoning for land-use planning. *Engineering Geology*, 2008. 102(3-4): 99-111.
- Guzzetti, F., Carrara, A., et al.. Landslide hazard evaluation: a review of current techniques and their application in a multi-scale study, Central Italy, Elsevier. 1999, 31: 181-216.
- Hosmer, D.W., Lemeshow, S., 2000. *Applied Logistic Regression*, 2nd ed. Wiley, New York. 373
- Kamp, U., et al., GIS-based landslide susceptibility mapping for the 2005 Kashmir earthquake region. *Geomorphology*, 2008. 101(4): 631-642.
- Kunlong, Y., C. Lixia, and Z. Guirong, Regional Landslide Hazard Warning and Risk Assessment. *Earth science frontiers*, 2007. 14(6).
- Liu Chuanzheng, Li Tiefeng, Wen Mingsheng, et al. Assessment and early warning on geo-hazards in the Three Gorges Reservoir region of Changjiang River. *Hydrogeology and Engineering Geology*, 2004(4): 9-19(in Chinese).
- Saha, A., et al., An approach for GIS-based statistical landslide susceptibility zonation—with a case study in the Himalayas. *Landslides*, 2005. 2(1): 61-69.
- Sharma, V., Zonation of landslide hazard for urban planning: case study of Nainital town, Kumaon Himalaya, India. *Engineering Geology for Tomorrow's Cities*, Geological Society, London, Engineering Geology Special Publications, 2009. 22.
- Soeters, R., van Westen, C.J., Slope instability, recognition, analysis, and zonation. In: Turner, A.K., Schuster, R.L.(Eds.), *Landslides: Investigation and Mitigation*, Special Report 247, Transportation Research Board, National Research Council. National Academy Press, Washington, DC, 1996. 129-177.
- Van Westen, C., T. Van Asch, and R. Soeters, Landslide hazard and risk zonation—why is it still so difficult? *Bulletin of Engineering Geology and the Environment*, 2006. 65(2): 167-184.
- van Westen, C.J., Rengers, N., Terlien, M.T.J., Soeters, R., 1997. Prediction of the occurrence of slope instability phenomena through GIS-based hazard zonation. *Geologische Rundschau* 86, 404- 414.
- Varnes, D.. Landslide hazard zonation: a review of principles and practice. Published by the united nations educational scientific and cultural organization. Unesco, 1984.
- Wang Zhilu, Zhang Yan; Sun Chang. Study on Geology Disaster Weather Forecast and Forewarning Technique in Longnan Area. *Journal of Geological Hazards and Environment Preservation*, 2005 (1) :105-110(in Chinese).
- Xie Mingen, Cheng Jiangan, Fan Bo. The Cause of Meteorological Formation and Monitoring on Landslide and Debris Flow Disasters in Yunnan. *Journal of Mountain Research*, 2005(5):571-578(in Chinese).
- Xie Shouyi, Zhang Nianxue, Xu Bing. Probability analysis of precipitation-induced slide of typical

landslides in Three Gorges area of the YangZe river. *Journal of Engineering Geology*, 1995, 6(2): 60-69 (in Chinese).

Yin K.L., Liu Y., Systematic studies on landslide hazard zonation. *The Chinese Journal of Geological Hazard and Control*, 2000. 11(4): 28-32.

Yin, K.L., Zhu, L.F.. Landslide hazard zonation and GIS application. *Earth science frontiers*, 2001. 8(2): 279-284.

CHAPTER 6 METHODS FOR LOCAL SCALE HAZARD ASSESSMENT

Hengxing Lan^{1,2}, Hongjiang Liu¹, Shengwen Qi³

¹*LREIS, Institute of Geographic Sciences and Natural Resources Research, Chinese Academy of Sciences, Beijing, China, 100101*

²*Dept. of Civil & Environmental Engineering, University of Alberta, Edmonton, AB T6G 2W2, Canada*

³*Key Lab. of Geomechanics, Institute of Geology and Geophysics, Chinese Academy of Sciences, Beijing, China, P. O. Box 9825, Chaoyang area, Beijing, 100029, China*

6.1 Introduction

This chapter will mainly focus on introducing the rockfall hazard and risk assessment based on intensity and frequency using 3D spatial modeling. A case study of Du-Wen Highway in Wenchuan seismic area will be introduced.

The Wenchuan Earthquake on 12 May 2008 (seismic magnitude (Ms) 8.0; Mw 7.9 according to the USGS) triggered a great number of rockfalls. Du-Wen Highway was a major “life line”, during the earthquake and currently plays an important role in the re-construction in the earthquake affected area. It has been exposed to numerous types and magnitudes of natural ground hazards, with rockfall hazard a major concern in the operation of the highway system. In many situations rock fall hazards can not be eliminated, because the occurrence of these hazards vary both spatially and temporally, especially in areas with a high frequency of rockfalls such as the Du-Wen Highway.

Due to the high mobility of rockfalls, frequency-magnitude relationship, runout distance, kinetic energy, and the bouncing height of rocks are very important factors in assessing the hazard intensity and associated vulnerability for the elements at risk. Efficient risk assessment of rockfalls requires assessing these important physical characteristics of rockfalls. This paper discusses a risk assessment method for rockfall hazard using spatial modeling. Spatial modeling of rockfalls hazard was conducted using RockFall Analyst, a three-dimensional GIS extension, to determine the characteristics of rock blocks landing on or crossing over the highway in terms of traveling distance, velocity and volume. Enabling technologies such as LiDAR are also assessed in a number of sections.

The frequency-magnitude relationship in the threatened area has been established using LiDAR measurements of rocks in the deposition area. It is a good indicator of the characteristics of known rockfall activities. An exponential law has been found to describe the characteristics of the frequency-magnitude relationship of rockfalls in this granite area. Back calculation has been used to estimate the various consequences of different magnitudes of rockfall. For example, a rockfall with magnitude large than 5 m in diameter and velocity larger than 30 m/s can have catastrophic consequences, such as destroying a bridge.

Combined the hazard and vulnerability of highway transportation, risk assessment was performed on a section of Du-Wen Highway for differing rockfall scenarios, involving

combinations of various risks based on different types of consequences. Information on historical records of hazard events, frequency-magnitude and triggering mechanism provides additional insight to the recognition of risk sites and risk level. Further parameter calibration and expert judgment are required for practical risk management.

The development of a quantitative rockfall risk assessment (QRA) should include 1) assessment of the annual frequency of occurrence of rockfall events at different scenarios – temporal frequency; 2) assessment of the probability of rockfall reach at given location –spatial frequency; 3) rockfall magnitude (e.g. volume); 4) vulnerability assessment; 5) definition of the value of the Elements at Risk (Guzetti et al. 2002, 2003 and 2004; Aliardi and Crosta , 2003; Corominas et al., 2005; Australian Geomechanics Society,2007; Straub and Schubert, 2008; Agliardi et al., 2009).

Due to the complex mobility, rockfall-specific assessment should address various parameters including energy, frequency, block size, characteristics of the topography, uncertainty of all parameters, etc (Jaboyedoff et al. 2005). In many situations, rockfall hazards can not be eliminated because their frequency and intensity vary both spatially and temporally (Lan et al., 2007, 2010). Such spatial and temporal variability of the hazard and vulnerability of elements at risk result in difficulties in risk assessment for rockfall hazard.

Effective assessment depends on the frequency and intensity of the rockfalls. It requires assessing these important physical characteristics of rockfalls, such as runout distance, kinetic energy, and the bouncing height frequent-magnitude relationship (Hung 1997, Hung et al., 1999, Lan et al., 2007, 2010). This paper discusses the methodology for rockfall Rockfall hazard and risk assessment based on intensity and frequency using 3D spatial modeling, by taking into account these factors. Enabling technologies such as LiDAR are also assessed.

Combined the hazard and vulnerability of highway transportation, risk assessment was performed on a section of Du-Wen Highway in Wenchuan seismic area for differing rockfall scenarios. It involves the combination of various risks based on different types of consequences. Information on historical records of hazard events, frequency-magnitude and triggering mechanism provides additional insight to the recognition of risk sites and risk level. Further parameter calibration and expert judgment are required for practical risk management. It provides highway users and managers with insights into the estimation of the risks to lives, infrastructure damage and operational risk due to the rockfall events. It also can help prioritize the risk sites for defensive measures and risk-management plans.

6.2 Methodology

6.2.1 Risk model

Risk assessment refers to the determination of risk for a particular hazard. Risk (R) associated with hazard refer to potential undesirable consequences (or “loss”) associated with a particular hazard type as defined by International Society of Soil Mechanics and Geotechnical Engineering (ISSMGE, 2004). It is the combination of “hazard” (H) (i.e. potential occurrence of conditions that can produce undesirable consequences) and “vulnerability” (V) (i.e. undesirable consequences if a hazard occurs). Specific risk can be expressed by the equation:

$$R = H \times V \quad (1)$$

Fell et al. (2005) referred to the following model:

$$R = H \times V \times E \quad (2)$$

where E is the value of elements at risk.

The model can be improved by introducing the temporal and spatial probability of vulnerable elements being affected by the hazard event. For example (Morgan, et al., 1992; Dai et al., 2002):

$$R = P(H) \times P(S : H) \times P(T : S) \times V \times E \quad (3)$$

where

R = annual risk,

$P(H)$ = annual probability of hazardous event,

$P(S:H)$ = probability of spatial impact,

$P(T:S)$ = temporal probability of consequence,

V = vulnerability of the element at risk, and

E = elements at risk (e.g. individual, group, property).

It also worth noting that the total risk involves the combination of different types of risks:

$$R = \sum R_i \quad (4)$$

where R_i is the risk associated with certain consequence, e.g. risk to physical failure, risk to operation, risk to environment, risk to economy, etc..

6.2.2 Hazard spatial modeling

Spatial modeling of rockfalls hazard was conducted using RockFall Analyst (Lan et al., 2007), a three-dimensional GIS extension, to determine the characteristics of rock blocks landing on or crossing over the highway in terms of traveling distance, velocity and volume. The modeling procedure is shown in Fig. 1. It is mainly composed by three parts:

(1) Potential rockfall source areas were determined using detailed topographic data, such as LiDAR and high-resolution orthoscopic color aerial photographs and field observation data. The identification of source areas should take account of various features such as sharp topographic contrast, slope angle, terrain type and vegetation covering. For example, Guzzetti et al. (2003) used a DEM and thematic maps such as land use and soil types to identify potential rockfall sources. Enabling technologies such as LiDAR are also assessed.

(2) 3D rockfall trajectory simulation to calculate the entire rockfall process and obtain important physical factors in assessing the hazard frequency and intensity including runout distance, kinetic energy, and the bouncing height etc.

(3) Raster modeling for spatial distribution of rockfalls in terms of frequency and intensity. Because the spatial autocorrelation of factors affecting rockfalls (e.g. slope geometry, geology

and vegetation) exerts control on the distribution of rockfall events in terms of their runout extent, velocity and energy distribution, a geostatistical method is used to simulate and investigate spatial distribution of rockfall frequency, intensity, e.g. kinetic energy. This information plays fundamental roles in assessing the rockfall hazard and evaluating the risk to the infrastructure's operation (Lanet al. 2010). The rockfall event database, geological/geomechanical and morphologic/morphometric settings are required to deal correctly calibrate the modeling results.

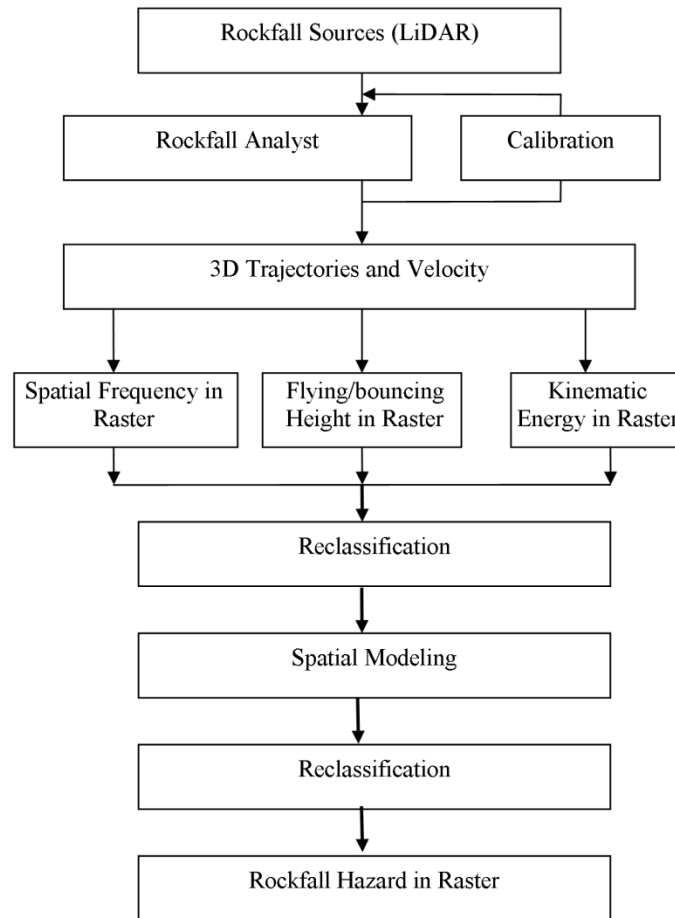


Figure.1 Modeling procedure using Rockfall Analyst

6.2.3 Hazard frequency-magnitude assessment

The hazard frequency assessment includes two parts: temporal frequency and spatial frequency. Temporal frequency is a likelihood characteristic of rockfall occurrence per unit of time period i.e. one year. It indicates the rock instability or failure in the source area. Temporal frequency can be inferred from historical catalogue or using relative rock failure rating system (Jaboyedoff et al. 2005). Distribution laws have been proposed for rockfalls based on statistical analysis of historical data sets to derive their recurrent probability (Dussauge et al.,2002, 2003).

Spatial frequency is a likelihood characteristic of rockfalls across certain position in space. It is a measure of how often the phenomena of rockfalls repeat per unit of area or distance. It is

corresponding to the physical process of rockfall propagation. Consider a reference period, the spatial frequency of rockfalls is obtained by (1) rockfall simulation and (2) field observation. It characterizes the probability of rock block propagation beyond a certain area. The propagation processes have been extensively studied (Guzzetti et al. 2002, 2003, 2004; Lan et al., 2005, 2010) and many models are available.

Using Rockfall Analyst, spatial frequency could be located directly from the raster modeling of rockfall frequency based on the runout simulation or the percentage of number of rockfall trajectories across certain area to the total rockfall trajectories. The spatial frequency of rockfalls is indicated by the geometrical patterns and geomechanical properties of the rock mass, with the strongest influence of existing discontinuities (Dussauge et al., 2002, 2003).

To further investigate the temporal and spatial probabilistic recurrent rate of an event at given size, the frequency-magnitude relationship needs to be established. Frequency-magnitude analyses are common approaches to characterize the occurrence of natural hazards. It provides the probability of occurrence of a given volume in a given time period in a given area and has been used for hazard assessment (Hungr et al., 1999, Dussauge et al., 2002, 2003). As for rockfalls induced by earthquakes, evaluating rockfall dynamics means analyzing the locations, size, and time patterns of rockfall events. Statistical analysis is used to derive the recurrence rate of an event of a given size to create the frequency-magnitude relationship.

To construct the spatial frequency-magnitude curves of rockfalls induced by the earthquake event, a LiDAR survey was conducted at numerous rockfall sites using ground-based LiDAR. In addition to capturing the 3D topographic data, the rock blocks at the foot of the slope and near the highway were also recorded. The survey has also to be performed on rock faces to estimate detached volumes. By comparing the information between rock face and the rockfall accumulations at slope toes, the studies on various important aspects can be carried out: 1) the possibility of accurately estimate volumes; 2) the influence of splitting/fragmentation on the frequency-magnitude distribution by estimating the volumes associated to single events, due to fragmentation;

The magnitude of rockfalls is usually expressed by the volume or diameter of the detached mass. The diameter of rock blocks at the slope toe was measured precisely using LiDAR data. The size of a block at the toe is usually much smaller than that of the detaching area because the discontinuous rocks break up on impact with the ground. The frequency has been calculated by considering the size range and the period of time. The magnitude-frequency of rockfalls along the highway characterizes the past rockfall activity and also serves as an important input in the risk modeling.

6.2.4 Grid computing for rockfall intensity

Hazard intensity represents the destructive capability to the element at risk. Uzielli et al. (2008) suggests using a composite intensity parameter to address the landslide intensity, accounting for kinetic and kinematic characteristics of the interaction between the sliding mass and the reference area.

As for specific rockfalls, the distributed parameters describing the destructiveness involve frequency-magnitude, spatial frequency, runout, kinetic energy and potential energy (bouncing

height) (Hungr 1997, Lan et al. 2007, 2010). A grid model is proposed to evaluate the important intensity of a rockfall acting on any vulnerable category as:

$$I = K_t \cdot K_s \cdot [r_K I_K + r_H I_H] \tag{5}$$

where

K_t is the temporal probability of rockfall occurrence at certain magnitude-temporal frequency; K_s is probability of the spatial impact by all rockfall events-spatial frequency; r_K is the kinetic relevance factor of the category, such as velocity; r_H is the potential energy factor of the category; I_K is the kinetic intensity parameter of the category denoted by the velocity of rockfall events; and I_H is the potential energy parameter of the category, which is indicated by height relative to the ground. The following constraint is imposed:

$$r_K + r_H = 1 \tag{6}$$

Table 1 shows an example of a possible set value for kinetic and potential energy factors.

Table 1. Example of possible sets of values for kinetic and potential energy factors

Category	Rockfall type	r_K (Kinetic)	r_H (Potential energy)
Highway	Rapid (i.e. $V > 10\text{m/s}$)	0.9	0.1
Highway	Slow ($V < 5\text{m/s}$)	0.7	0.3

All the parameters can be obtained from the spatial modeling and frequency-magnitude relationship. By detailed rockfall process simulation, the precise distribution of intensity-related parameters can be achieved by raster (grid) modeling, including the frequency, kinetic energy and potential energy. Using equation 5, the intensity of rockfalls can be evaluated by combining the temporal and spatial frequency with kinetic and potential energy of rockfalls. Figure 2 show an example of grid computing for rockfall intensity.

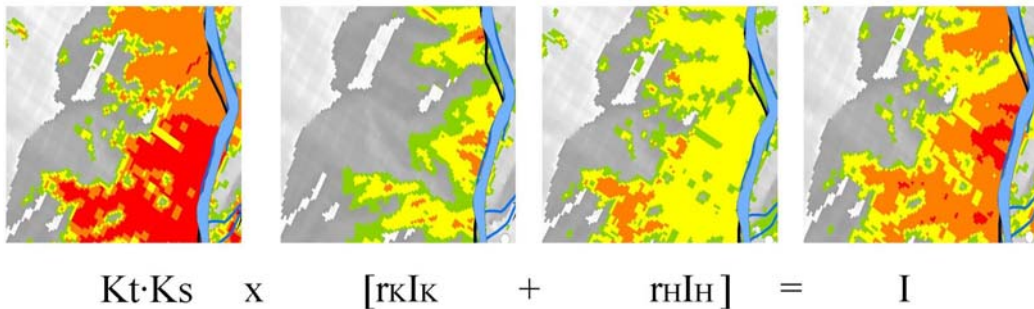


Figure 2. Example of computed grid map of rockfall intensities

Note: The $K_t \cdot K_s$ indicates the probability of rockfalls occurrence at a certain location for reference time period. The intensity of rockfalls is evaluated by combining it with kinetic and potential energy of rockfalls. The value for each parameter and final intensity ranges from 0 to 1. The highest value is represented by red color and lowest by green.

6.2.5 Vulnerability and Susceptibility of element at risk

The risk evaluation also includes the potential impact on vulnerable infrastructures (Wong et al. 1997). Vulnerability can be defined as the level of potential damage, or degree of loss, of a given element (0 to 1) subject to a hazard of a given intensity (Fell 1994). Vulnerability assessment therefore involves the interaction between a given hazard event and the element at risk. The vulnerability of element at risk can be expressed by (Uzielli et al., 2008; Kaynia et al., 2008):

$$V = I \times S \quad (7)$$

where V indicates vulnerability; I indicates landslide intensity (ranges from 0 to 1) and S indicates the susceptibility of elements at risk (0 to 1). Both intensity and susceptibility are dimensionless and at the same scale, which allows direct comparison between different sites and regions.

The elements at risk affected by rockfalls have particular characteristics, such as value, dimension and location. For the highway, the elements at risk can be divided into stationary vulnerable elements (e.g. the highway, bridges and other facilities) and non-stationary vulnerable elements (e.g. vehicles and people). Only spatial intersection between a hazard agent and stationary elements need to be considered, while both spatial and temporal interactions are needed for non-stationary elements. In this study, only stationary elements (the road and bridges) are considered. Susceptibility ranges and recommended values at three different level of consequence severity are listed in Table 2 (Finlay et al, 1999 ; Uzelli et al., 2008)

Table 2 Example of susceptibility range and recommended value for stationary vulnerable elements.

Case ID	Scenario	Highway		Bridge		Risk Type
		Range	Recommended	Range	Recommended	
1	Rock size >= 5m in diameter	0.6-0.8	0.7	0.8-1.0	1.0	Risk to infrastructure damage: High chance of bridge damage and road failure.
2	1m < Rock size < 5m	0.3-0.6	0.4	0.6-0.8	0.7	Risk to operation: traffic service disruption
3	Rock size < 1m	0-0.3	0.2	0.3-0.5	0.4	Risk to maintenance: minor damage to road and debris cleaning

6.3 A case study

6.3.1 Study area

The Wenchuan Earthquake on 12 May 2008 (seismic magnitude (Ms) 8.0; Mw 7.9 according to the USGS) triggered a great number of rockfalls. Du-Wen Highway was a major 'life line' during the earthquake and currently plays an important role in re-construction in the earthquake affected area. During the earthquake, a number of sections of the highway were

damaged. A new highway line has been designed and is under construction. It is exposed to numerous types and magnitudes of natural ground hazards, with rockfall hazard a major concern in the operation of the highway system.

Du-Wen Highway is located to the northwest of Chengdu, Sichuan province of China (Figure. 3). A great number of rockfalls were induced by the earthquake. These can be seen on the SPOT 5 satellite image taken several days after the earthquake. Rockfalls are still relatively frequent after the earthquake. The rockfalls shown in the lower right photo of Figure 3 occurred several months after the earthquake where a large block hit and destroyed the north part of the Chedi guan Bridge. The highway section from Tao guan to Chedi guan has been selected as a study area due to its high rockfall intensity. The bedrock of the slopes along this highway section is granite (Deng et al., 2006).

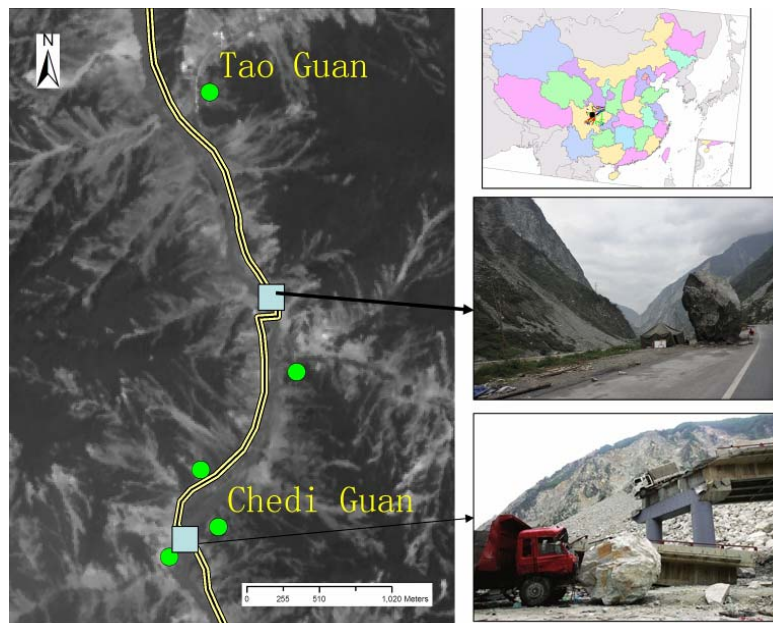


Figure.3 Study area. The section of Du-Wen Highway from Tao guan to Chedi guan. The underlying photo is a high-resolution SPOT 5 satellite image showing hazard phenomena after the 2008 Wenchuan earthquake. Two typical examples of rockfall damage are shown at the right.

6.3.2 Frequency-magnitude relationship

Several distribution laws for frequency-magnitude of rockfalls have been proposed, based on the statistical analysis of series of past events (Hungr et al. 1999). Many studies have shown that the frequency-magnitude distributions of rock falls from limited homogeneous areas are well fitted by a power law (Hungr et al., 1999 and Dussauge et al., 2002, 2003). Many studies use a logarithmic attempt.

The rockfall frequency-magnitude relationship induced by earthquake in the threatened granite area has been established. The returning time is corresponding to the returning time of the earthquake which is around 10 years. Nearly one thousand rock blocks at deposition areas were measured using LiDAR data at different failure sites. The frequency-magnitude

relationship of rockfalls detaching from the granite slopes is shown in Figure 4. For rockfalls induced by intensive earthquake in this study area, an exponential law of was captured with $R^2 > 0.9$.

It is a good indicator of the characteristics of known rockfall activities. Compared to logarithmic law, the exponential law might have advantage to reveal the intrinsic frequency-magnitude characteristics for the rockfalls in this granite area showing the local effect of earthquake. The frequency of rockfalls with rocks larger than 5 meters in diameter is relatively low, but falls of such large size rocks pose a huge threat to the highway and bridge. For example the rock block that damaged the Chedi guan Bridge has a diameter larger than 5 metres.

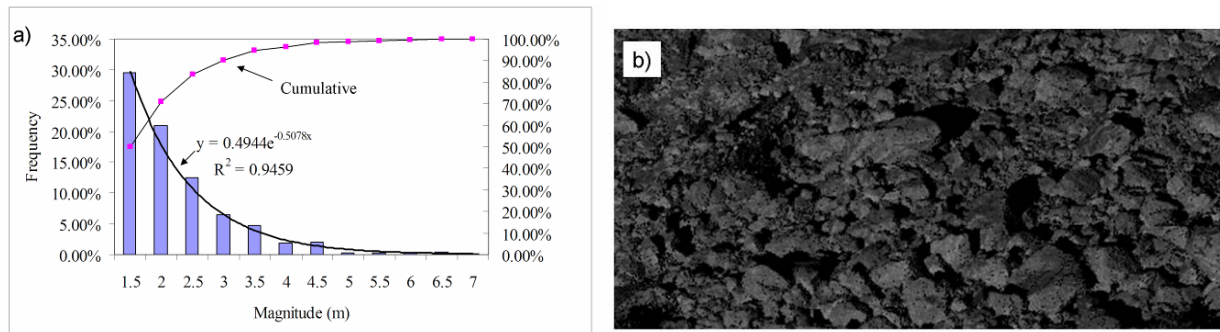
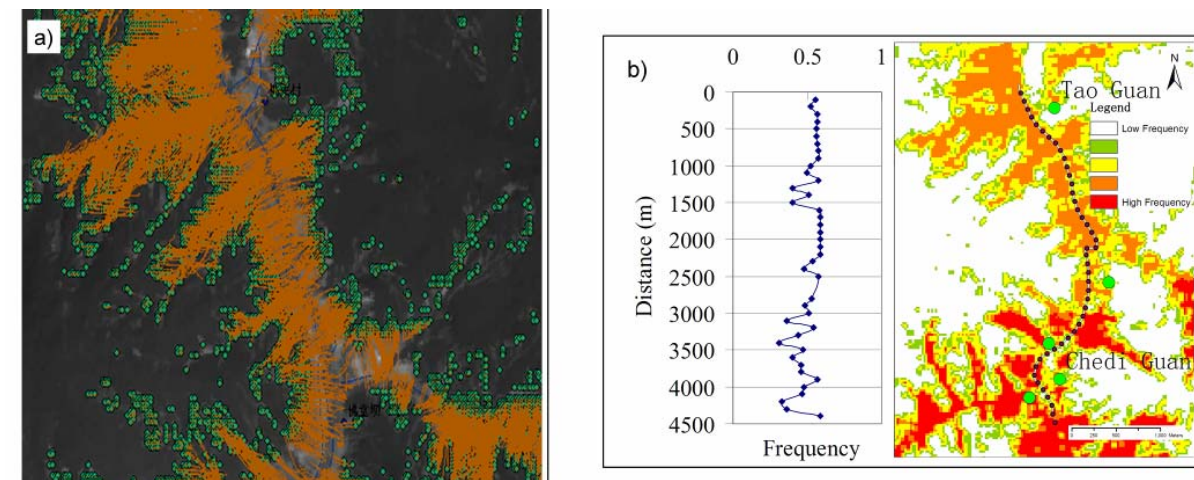


Figure 4. a) Frequency-magnitude relationship of rockfalls detaching from a granite slope along Du-Wen Highway; b) example of LiDAR data at rockfall deposition area

6.3.3 Hazard analysis

Spatial modeling using the Rockfall Analyst program was performed to evaluate the distributed parameters related to the rockfall hazard. Once the potential rockfall sources were identified, rockfall physical processes were simulated using Rockfall Analyst by considering ground topography and calibrated mechanical parameters (Fig. 5 a) (Lan et al., 2007,2010). The process involves rock detachment and fall, and subsequent bouncing, rolling, sliding and deposition. The subsequent raster images show rockfall spatial frequency (Fig. 5 b), kinetic velocity (Fig. 5 c) and rock bounce height (potential energy) (Fig. 5 d).



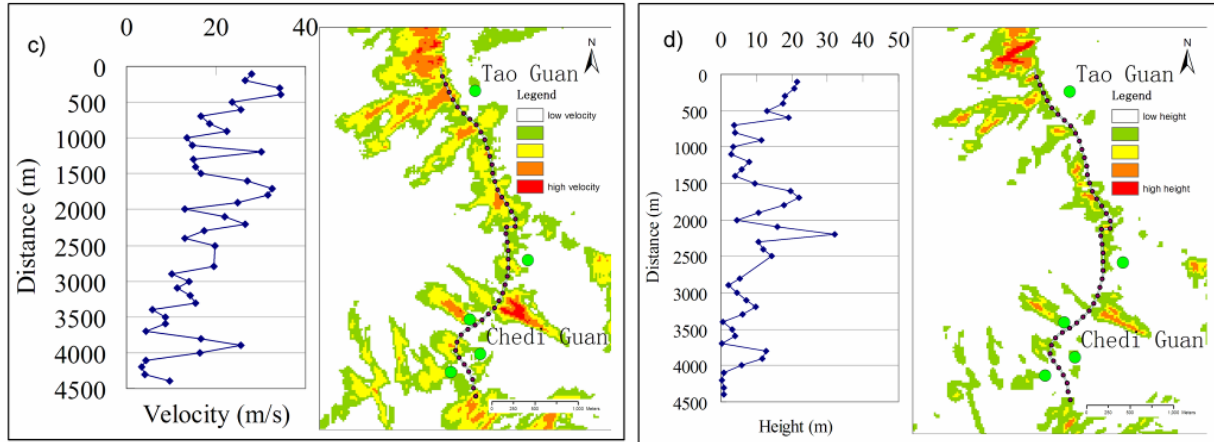


Figure 5. Hazard analysis using spatial modeling. a) Rockfall process simulation; b) Frequency distribution shows probability of spatial impact; c) Velocity distribution shows kinetic characteristics; d) Height distribution shows potential energy. The curve at left side of b-d shows the parameter distribution along the highway at intervals of 100 metres.

Spatial frequency is a characteristic of rockfalls that across position in space. The frequency is a measure of how often the rockfalls occur per unit of area. Simplest way is to calculate the percentage of all simulated trajectories that cross a point (2D) or an area (Crosta et al. 2001; Guzzetti et al., 2002, Jaboyedoff et al., 2005). It is normalized within the range from 0 to 1 to show the probability of spatial interception of rockfalls and locations. For example spatial frequency of 0.5 for highway indicates once rockfalls occur, they have 50 % of probability to propagate to highway.

The spatial frequency of rockfalls along the highway varies slightly. The high rockfall frequency along most parts of the Du-Wen Highway (i.e. larger than 0.5) implies a high probability of spatial impact by rockfalls. Kinetic velocity and rock bounce height relative to the ground vary dramatically from section to section at intervals of 100 metres. The velocity is related to the kinetic energy of rock blocks and rock bounce height to the potential energy. Both indicate the characteristics of interaction between the rock and ground. It accounts for the damage level when the rocks hit vulnerable elements. Based on back calculation for the case study of Chedi guan bridge, a rock block with magnitude larger than 5 metres in diameter and around 30 m/s velocity could destroy the bridge.

6.3.4 Risk Assessment

From field observation and case studies, the failure scenarios have been be divided into three groups based on the event magnitude: (1) blocks > 5 m diameter; (2) block >1 m but < 5 m diameter; and (3) block < 1 m in diameter. Each group represents a certain risk type which is shown in Table 2. From the frequency-magnitude relationship, the cumulative frequency for each group is:

$$\begin{cases} P(D \geq 5m) = 0.5\% \\ P(1m \leq D \leq 5m) = 79.5\% \\ P(D < 1m) = 20\% \end{cases} \quad (8)$$

The intensity map was generated using grid modeling described by Equation 5 (Figure. 5). It took into account all the important factors characterizing the rockfall events. Most of the slopes are in marginal condition due to the shaking by the 2008 Wenchuan Earthquake. The intensity curve at the left side shows the destructive potential for rockfalls at different locations on the highway.

From the historical earthquake data, the returning period for high intensity earthquake is around 10 years indicating the yearly probability of intensive rockfall hazard induced by an earthquake could be 10%. The result of risk assessment for each consequence group is shown in Figure 7. It can be seen from the risk distribution along the highway, the total section is subject to a high risk from rockfalls in terms of damage (magnitude of 10^{-4}), operation (magnitude of 10^{-2}) and maintenance (magnitude of 10^{-3}). The high risk for case 2 indicates the high operational risk for highway due to rockfalls activities. For all type of categories, bridges have a much higher risk than the highway itself. More attention should be paid to the proactive measures for protecting the bridges.

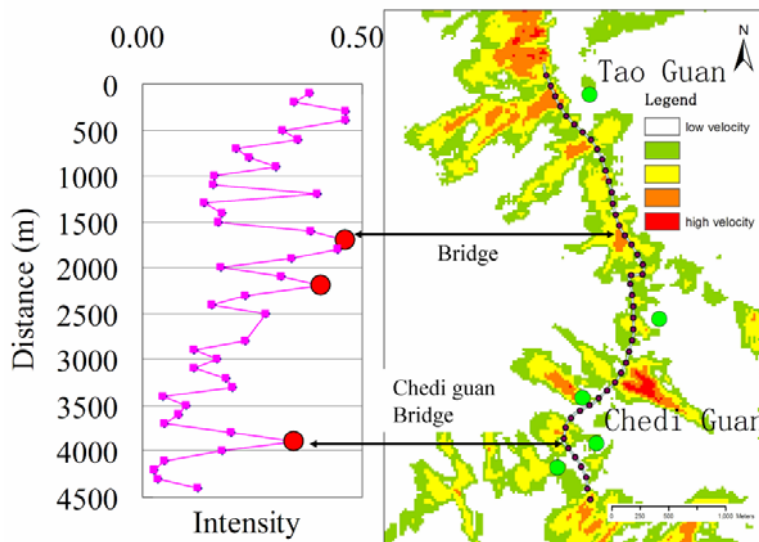


Figure 6. Intensity map. The large red dots indicate the location of bridges.

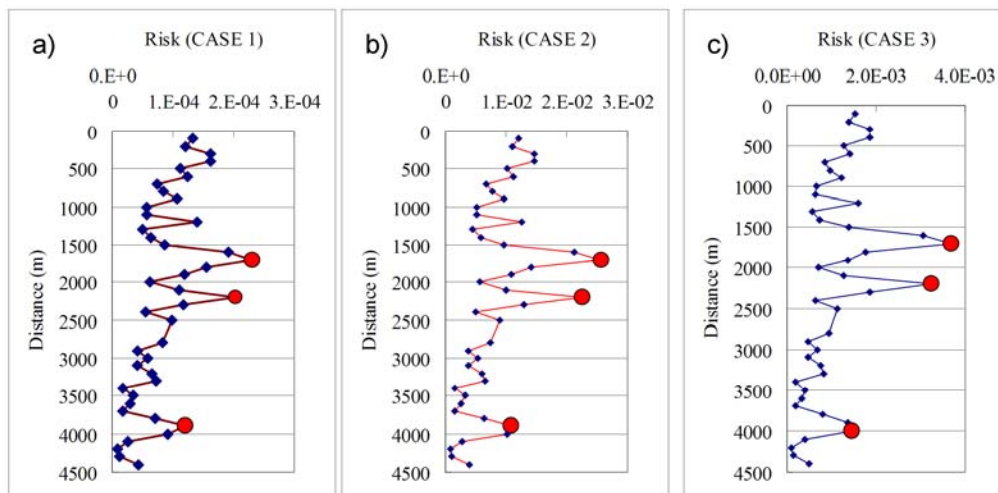


Figure 7. Result of risk assessment for three types of consequences. (1) risk of infrastructure failure with catastrophic consequences: i.e. bridge damage and highway failure; (2) the risk to operational serviceability (through temporary road closure); (3) risk to highway maintenance.

6.4 Conclusions and discussions

The high severity of rockfall hazard induced by earthquakes requires a practical and systematic method for risk assessment. It depends on the precise evaluation of the temporal and spatial frequency and intensity of rockfall events.

A methodology has been proposed for the rockfall hazard and risk assessment based on the frequency and intensity information. 3D spatial modeling and enabling technology, such as LiDAR technology help capture important physical characteristics of distributed parameters related to rockfalls intensity, such as runout and energy and facilitate addressing hazard variability and quantitative risk assessment.

The application of an effective risk assessment has been conducted in rockfall hazardous areas induced by earthquake, such as the Du-Wen Highway which is located in the area affected by the Wenchuan earthquake in 2008. It tries to answer the question “how safe is the highway”. It provides highway users and managers with insights into the estimation of the risks to lives, infrastructure damage and operational risk due to the rockfall events. It also can help prioritize the risk sites for defensive measures and risk-management plans.

The frequency-magnitude relationship established using LiDAR data shows a perfect exponential law. It is a good indicator of the characteristics of known rockfall activities. Compared to logarithmic law, the exponential law might have advantage to reveal the intrinsic rockfall dynamics in the homogenous area showing the local effect of earthquake.

Risk assessment involves a combination of various risks based on different types of consequences. Information on the historical record of hazard events, frequency-magnitude and triggering mechanisms provides additional insight for the recognition of risk sites and risk level. Further parameter calibration and expert judgment are required for practical risk management.

The uncertainties and risk criteria in the risk assessment methodology need to be more explicitly studied in the future. The uncertainties usually deals with the sensitivity of modeling parameters to the risk assessment results for different rockfall scenarios. The risk criteria needs to be established to assess the acceptable level of rockfall risk for different scenarios in seismic areas. This would lead to a better understanding of the risk variability of transportation for rockfall scenarios and related practical applications.

Acknowledgement

This research is supported by the One Hundred Talents Program of Chinese Academy of Sciences, and the National Key Technology R&D Program of China (2008BAK50B05), 973 Program (2008CB425802).

References

- Agliardi, F., Crosta, G.B., 2003. High resolution three-dimensional numerical modeling of rockfalls. *International Journal of Rock Mechanics and Mining Sciences* 40, 455 – 471.
- Agliardi, F., Crosta, G. B. and Frattini, P. (2009): Integrating rockfall risk assessment and countermeasure design by 3D modelling techniques. *Nat. Hazards Earth Syst. Sci.*, 9, 1059–1073.
- Australian Geomechanics Society (2007): Practice Note Guidelines for Landslide Risk Management. *Australian Geomechanics* 42, 1, 63-115.
- Dai F.C., Lee C.F. & Ngai Y.Y. (2002): Landslide risk assessment and management: An overview. *Engineering Geology*, 64 (1), 65-87.
- Deng, H., Huang, R. & Ju, N. (2006). Analysis of the deformation and failure mechanism of the Shawozi high rock slope near the Du-Wen highway. *Proceedings of the 10th IAEG International Congress, Nottingham, United Kingdom, 6-10 Sept.*, 7 p. (Paper number 569, available under <http://iaeg2006.geolsoc.org.uk/cd>).
- Dussauge, C., J.-R. Grasso, and A. Helmstetter (2003). Statistical analysis of rockfall volume distributions: Implications for rockfall dynamics, *J. Geophys. Res.*, 108(B6), 2286
- Dussauge-Peisser, C., Helmstetter, A., Grasso, J.-R., Hantz, D., Desvarreux, P., Jeannin, M., and Giraud, A. 2002. Probabilistic approach to rock fall hazard assessment: potential of historical data analysis, *Nat. Hazards Earth Syst. Sci.*, 2, 15-26.
- Finlay, P J , Mostyn, G R & Fell, R.(1999): Landslides: Prediction of Travel Distance and Guidelines for Vulnerability of Persons. *Proc 8th. Australia New Zealand Conference on Geomechanics, Vol 1*, 105-113.
- Fell, R. 1994. Landslide risk assessment and acceptable risk. *Canadian Geotechnical Journal* 31: 261–272.
- Fell, R., Ho, K.K.S., Lacasse, S. & Leroi, E. 2005. A framework for landslide risk assessment and management. In: Hungr, O., Fell, R., Couture, R., Eberhardt, E. (Eds.), *Landslide risk management, Proceedings of the International Conference on Landslide Risk Management, Vancouver, 31 May – 3 June 2005*. Taylor & Francis, London, pp. 3–25.
- Guzzetti, F., Crosta, G., Detti, R., Agliardi, F., 2002. STONE: a computer program for the three-dimensional simulation of rock-falls. *Computers & Geosciences* 28, 1079 – 1093.
- Guzzetti, F., Reichenbach, P., and Wieczorek, G. F. (2003). Rockfall hazard and risk assessment in the Yosemite Valley, California, USA, *Nat. Hazards Earth Syst. Sci.*, 3, 491-503.
- Guzzetti F., Reichenbach P. & Ghigi S. (2004). Rockfall hazard and risk assessment in the Nera River Valley, Umbria Region, central Italy. *Environmental Management*, Vol. 34:2, 191-208
- Hungr, O. 1997. Some methods of landslide intensity mapping. In: Cruden, D.M., Fell, R. (Eds.), *Landslide risk assessment — Proceedings of the International Workshop on Landslide Risk Assessment, Honolulu, 19–21 February 1997*. Balkema, Rotterdam, pp. 215–226.
- Hungr, O., Evans, S.G., Hazzard, J. 1999. Magnitude and frequency of rock falls and rock slides along the main transportation corridors of south-western British Columbia. *Canadian Geotechnical Journal* 36: 224–238.
- International Society of Soil Mechanics and Geotechnical Engineering (ISSMGE). 2004. Technical Committee on Risk Assessment and Management (TC32): Glossary of Terms for Risk Assessment.

- Jaboyedoff, M., Dudt, J. P., and Labiouse, V. (2005). An attempt to refine rockfall hazard zoning based on the kinetic energy, frequency and fragmentation degree, *Nat. Hazards Earth Syst. Sci.*, 5, 621-632.
- Kaynia, A.M., Papathoma-Köhle, M., Neuhäuser, B., Ratzinger, K., Wenzel, H., Medina-Cetina, Z. 2008. Probabilistic assessment of vulnerability to landslide: Application to the village of Lichtenstein, Baden-Württemberg, Germany. *Engineering Geology* 101: 33–48
- Lan, H., Martin, C.D., Lim, C.H. 2007. RockFall analyst: a GIS extension for three-dimensional and spatially distributed rockfall hazard modeling. *Computers & Geosciences* 33: 262–279.
- Lan, H. et al., Martin C.D, Zhou C.H., Lim C.H. 2010. Rockfall hazard analysis using LiDAR and spatial modeling. *Geomorphology*, doi:10.1016/j.geomorph.2010.01.002
- Morgan, G. C., Rawlings, G. E., and Sobkowicz, J. C. (1992): Evaluating total risk to communities from large debris flows, *Geotechnique and Natural Hazards*, 6–9 May 1992, Vancouver, Canada, 225–236.
- Uzielli, M., Nadim, F., Lacasse, S. et al. 2008. A conceptual framework for quantitative estimation of physical vulnerability to landslides. *Engineering Geology* 102: 251–256.
- Wong, H.N., Ho, K.K.S & Chan, Y.C. 1997. Assessment of consequence of landslides. *Landslide Risk Assessment*, Cruden & Fell (eds), Balkema, Rotterdam.

CHAPTER 7 LANDSLIDE EARLY WARNING AND MONITORING

Qiang Xu

State Key Laboratory of Geohazards Prevention, Chengdu University of Technology, China

7.1 Introduction

China is a country which has been suffering frequent geo-hazards and the consequent severe damages, especially in the western mountainous areas and central-eastern part of China, where the topographical and geological conditions are very complicated. Latest statistics show that there are millions of geo-hazards, including potential ones. Among them, more than 34 000 posed a severe threaten to people's lives and properties. Averagely, about 800 persons were killed or missed per year. More than 800 persons got injured. The direct economic loss can reach to 40 billion RMB (Chinese Yuan) (Table 1), while the indirect loss was underestimated, such as the loss caused by traffic interruption, the large factories, and lifeline infrastructure. Since 1980s, there are 100 landslides have caused more than 30 fatalities or tens of millions of economic loss.

Table 1 Statistics of geo-hazards and corresponding risk in China since the 21st century

Year	Amount (times)	Fatalities (persons)	Injured (persons)	Economic loss (unit:100 million RMB)
2001	5793	908	936	35
2002	48000	1016	470	51
2003	13832	868	3355	48.7
2004	13555	858	280	40.9
2005	17751	682	339	36.5
2006	102804	774	453	43.2
2007	25364	679	446	24.8
2008	26580	757	841	32.7
2009	10840	486	315	17.65
Average	29391	781	826	36.72

It is unpractical to carry out mitigation measures to every landslide, due to the great number and the extensive distribution. According to the situation in China, a geo-hazard prevention system with Chinese characteristics has been established, which is mainly composed of three types of landslide prevention measures as follows: (1) mitigation measure: this is applicable for the landslides that might cause severe damages to people's lives and property, and the evacuation is also impossible, or compared with evacuation, engineering methods have more technology feasibility and economic reasonableness; (2) evacuation plan: for the landslides that can not be treated by geotechnical methods; (3) monitoring & early warning. This chapter aims to introduce the early warning and monitoring methods that are commonly used in China.

7.2 Landslide monitoring in China

Landslide monitoring in China can be divided into two types: one is the public inspection & public prevention, the other one is the professional monitoring, which are described in the following text.

7.2.1 The characteristics of the early warning system in China

Since 1980s, the Chinese government started to pay special attentions to the landslide monitoring and early warning for the hazard reduction. A lot of funds were used to establish landside monitoring networks. However, around 90% of landslides happened every year are not covered by the monitoring network. Unexpectedly, the landslides covered by the monitoring network sometimes didn't happen, but those uncovered happened. This awkward situation might be explained by two reasons:

(1) The monitoring network only covers a small amount of potential dangerous landslides, because the professional monitoring is very costly, the government can't afford to apply professional monitoring to every landslides.

(2) A large number of landslides that were not monitored are small ones and have obvious deformation evidence. Thus, they are easily ignored by both local people and professional monitoring teams, but once these landslides happened, they can also cause serious damages. Instead, the monitoring network is mainly set on the landslides, which are large-scale and have serious displacements.

In China, Landslides widely distributed in the whole country and some of them are in the remote areas with very poor traffic condition, which make the professional monitoring very difficult. From the late 1990s till now, the government has been keeping on exploring an effective method for landslide prevention. Several steps have been taken: first, landslide survey need to be done, which provide us general information such as the location and the scale; secondly, based on the first step, different prevention plans were made for different landslides. For the large landslides that may cause serious damages, the mitigation and monitoring measures will be taken, while for other comparatively low hazard ones, simple monitoring will be done by local people who are trained by the professional monitoring teams. The monitoring groups are also organized by local people. The hazard office in the local government is in charge of the landslide monitoring and reporting to professional teams. They work with the local trained people together. In the raining season, they will go to the landslide site to check the deformation several times every day. This method actually is the combination of the public inspection & public prevention and the professional monitoring, but more focusing on the former one.

7.2.2 Public inspection & public prevention

The Public inspection & public prevention system was established based on three government levels: county, town and village levels. This system aims to call local people's attention to the potential landslides around them. Through the public training, they can accept the basic landslide knowledge and some simple monitoring method. Thus, they can monitor

landslides by themselves and try to reduce the hazards to the minimum. This system contains follow main measures:

(1) Appoint the persons who are capable of doing the landslide monitoring and determine the most dangerous landslides that need to be monitored. According to the guideline from the Chinese Ministry of Land and Resources, the local people who have good education backgrounds and have the sense of responsibilities can be appointed to take the local monitoring works. They will also be trained by the professional monitoring team. Everyone who is appointed has their own duty. The works are assigned to everyone.

(2) Geo-hazard knowledge training. The “Bring geo-hazard knowledge into tens of thousands villages program” was carried out in order to spread the geo-hazard knowledge into the masses by means of explanation, television, newspaper, posters etc.

(3) To implement the three policies: 24 h on duty policy, 24 h patrolling (inspection) landslide policy and immediate reporting system, during the raining season. The people who are in charge of landslide monitoring will work in turns for day and night. They checked around the landslide area and inspected the deformation evidence, such as the cracks on the slope, soil creeping, trunk tilting, abruptly rise of water level, abnormal behaviors of animals and ground sound etc. They will also make a record of the displacement measured by the simple monitoring device. Once they found very obvious evidence that indicate the landslide might become unstable, they will alarm other people and report the situation to local government, and assistant the government to evacuate people from the dangerous area.

(4) In order to protect people’s lives and properties, three methods can be applied: monitoring, early warning and emergent evacuation. For the slopes which have obvious deformation signs, simple monitoring methods such as using steel tape to measure the width of cracks can be used for detecting the slope deformation. The monitoring results can also help the geologist to understand the slope stability situation better and the authorities to make the right decision. When the situation became very serious, an emergent evacuation alarm will be sent. Then the local people will follow the pre-designed escape route to relocate in the safe place.

(5) Every year, the Chinese Ministry of Land and Resources will arrange the local government to make the pre-plan and specific practice procedures for the emergent evacuation and public inspection. After the pre-plan was made, the local government will inform the plan to the local people through multi-medias, like TV, broadcast, newspapers and internet. Every family will also received a kind of “landslide awareness card” with detailed evacuate plan, route, basic information of potential dangerous landslides. Through these ways, people are very clear about what they need to do, when facing to the disasters. Sometimes, rehearsals are also played for making sure that the pre-plan can work well.

(6) Local government will organize the local emergent rescue teams. The rescue teams are well trained and they can help the people to evacuate the dangerous place quickly.

(7) In order to make the monitoring and public inspection & public prevention work get good effect, the Chinese Ministry of Land and Resource should organize professional staff and experts to go to the local regions to supervise and evaluate the local activities and works.

The public inspection & public prevention has attained remarkable effects in China. According to the statistic data, since the 21st century, the public inspection and prevention network has predicted more than 5000 landslides successfully, and avoided 220,000 fatalities and injures, as well as about 4 billions RMB economic loss (as shown in Table 2).

Table 2 Effects of the public inspection & public prevention since the 21st century

Year	Number	Avoiding fatalities	Avoiding economic loss (unit: 10 000 RMB)
2001	231	4200	88600
2002	703	19120	24000
2003	697	29664	40000
2004	965	65561	86100
2005	500	11376	34100
2006	478	20566	23900
2007	920	37926	55000
2008	478	20709	32156
2009	209	14330	16353
In all	5181	223452	400209

7.2.3 Professional Monitoring

(1) Research and invention of professional monitoring equipments

In China, there are some organizations and institutes that are specialized in the research and development (R&D) of professional monitoring equipments. A lot of equipments have been invented for the monitoring & early warning of landslide, rockfall and debris flow (Table 3).

Table 3 Typical landslide monitoring & early warning equipments in China

No.	Name and Photo	Main application and index	Functions
1	<p>The early-warning extensometer for landslide</p> 	<p>Automatic monitoring landslide displacements, the measuring range is 0~300mm.</p>	<p>Without the function of recording and transmitting the displacement data, but it can send alarm automatically, once the displacement is larger than the pre-set threshold. It is made up of extensometer, cable(50m), alarm horn and rain proof equipment. The wireless remote alarm interface is prepared.</p>
2	<p>The crack alarm</p> 	<p>Automatic monitoring the development of micro-cracks in the landslide and buildings. Its monitoring method contains large-range contact form and small-range non-contact form.</p>	<p>Without the function of recording and transmitting the displacement data, but it can send alarm automatically, once the displacement is larger than the pre-set threshold. It is made up of alarm mainframe, rivet and</p>

			cable(30cm) and non-contact displacement sensor module.
3	<p>Four-circuit displacement monitoring and transmission instrument</p> 	<p>The monitoring & early warning of displacements, velocity and acceleration for landslide and collapse. The pull-rod displacement sensor has its measuring range of 150mm, and the pull-rope sensor has its measuring range of 1000mm.</p>	<p>Pre-sets the early-warning value and alarms directly. The monitoring data can be recorded and transmitted wirelessly.</p>
4	<p>Rainproof multi-functional alarm</p> 	<p>Hazard monitoring alarm, crack alarm and borehole water level monitoring instrument(pumping test)</p>	<p>1. Crack alarm's function: pre-sets the displacement early warning value, alarms directly.2. Rainproof alarm's function: can be used as an alarm for any geo-hazard monitoring instrument, and has the rainproof power. 3. When connected with the ruler cable, it can be used for pumping test.</p>
5	<p>Moisture monitoring & early warning instrument</p> 	<p>Used for the moisture monitoring & early warning in talus landslide and material source area of debris flow, its measuring range is 0~100.</p>	<p>Pre-sets the moisture early warning value, and when reaches the value, it alarms.</p>
6	<p>Digital hyetometer</p> 	<p>Transmits the rainfall data remotely.</p>	<p>Rainfall data's remote transmission and early warning.</p>
7	<p>The wireless remote early warning system of geo-hazards</p> 	<p>Mainly used for the abrupt geo-hazards' Remote wireless early warning. The direct alarm distance is 2000 m, when uses repeater, its range can reach to 5000m. Do simultaneous early warning for 50~250</p>	<p>When wireless emitter gets the alarm switch signal, the alarm signal is emitted immediately. Once the remote alarm mainframe receives the alarm signal and gives direct alarm. If there is nobody on duty, it will directly</p>

		circuits monitoring instruments	call the 6 cell-phones or fixed phones that prestored in it.
8	<p>Laser non-contact multi-point monitoring & early warning system</p> 	Large range, non contact, circulatory monitoring & early warning instrument for landslide and collapse.	Pre-sets the displacement early warning value, alarms directly. Also, the collected data can be transmitted wirelessly to the allopatry, which can replace the total station's hand monitoring work.
9	<p>Multi-parameter acquisition and transmission instrument</p> 	Multi-parameter monitoring & early warning and wireless data transmission for variety of rockfall, landslide, debris flow, ground collapse and other geo-hazards	Can be used to monitor collapse, landslide, debris flow, ground collapse, tailings dam-break and etc. The main parameters are displacement sensor, hyetometer, moisture meter, inclinometer, piezometer, etc.(16 channels in all). The monitoring data is transmitted wirelessly.
10		The GPS receiver composes the system's observation network. The static differential location technique is used to monitor the landslide displacements in mm precision.	GPRS network is used to realize the remote control and data transmission; The "solar cell plus battery" power supply scheme is adapted; The all-weather automatic real-time monitoring is carried out for the landslide deformation.

(2) Construction of professional monitoring & early warning demonstration region (station)

China Geological Survey has arranged more than 10 professional monitoring & early warning demonstration regions (stations) in China. According to the plan, there will be more than 30 regions till 2015. In order to take the initiative to prevent geological disasters in Three Gorges Reservoir area, the professional monitoring & early warning network was built.

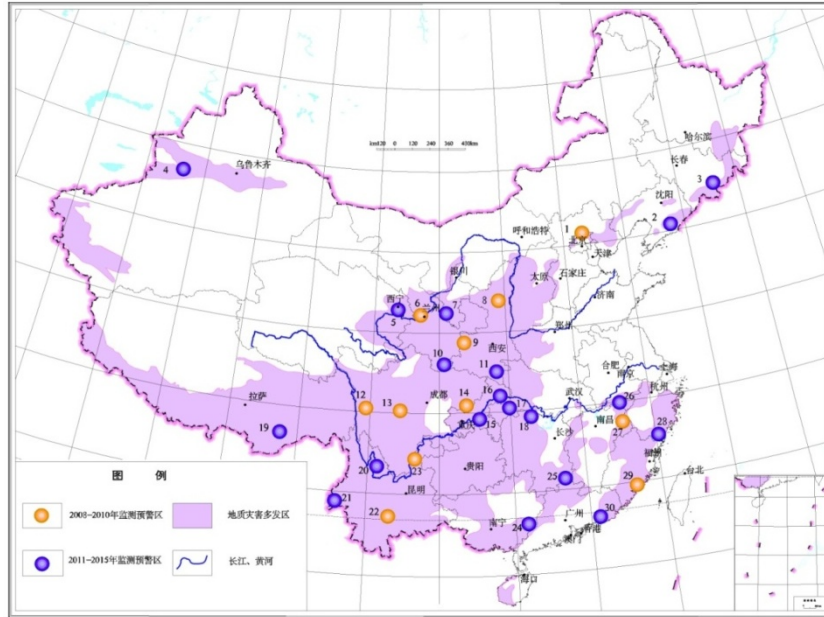


Figure.1 Planning map of the professional monitoring & early warning for geo-hazard in demonstration region, China

The professional monitoring of geological disaster in Three Gorges Reservoir area mainly relies on the means of GPS, RS, synthesis stereo monitoring (surface and deep displacement, deep thrust, underground water), macro-geological surveys. Meanwhile, based on the monitoring results, the geologists predicted the potential hazard that might be caused by the landslides. In addition, an early warning and forecast system are built.

According to geological and environmental conditions in the Three Gorges Reservoir area, GPS Monitoring Network (three-level) was built up to control the entire reservoir area (A-level control network, B-class benchmark network, C-level deformation monitoring), which can be seen in Figure 2 to Figure 4. Additionally, we can provide a basis for the discovery and forecast of the new landslides and bank collapse by establishing a remote sensing monitoring databases and regional monitoring system.

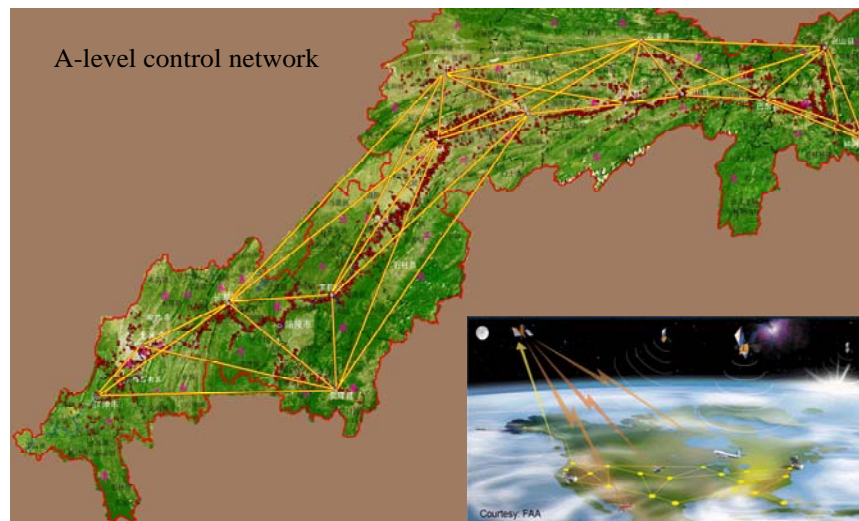


Figure .2 A-level control network in the Three Gorges Reservoir area

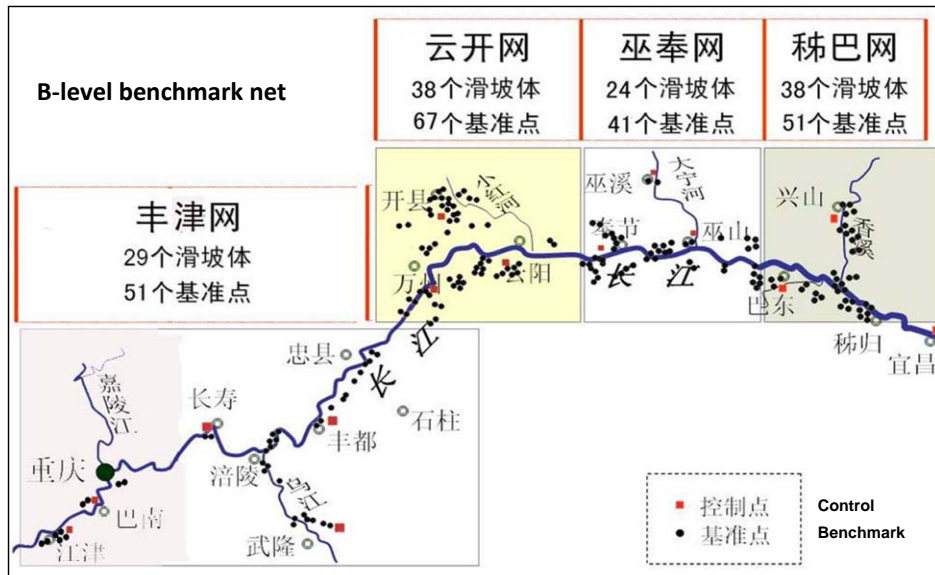


Figure.3 B-level benchmark network in the Three Gorges Reservoir area

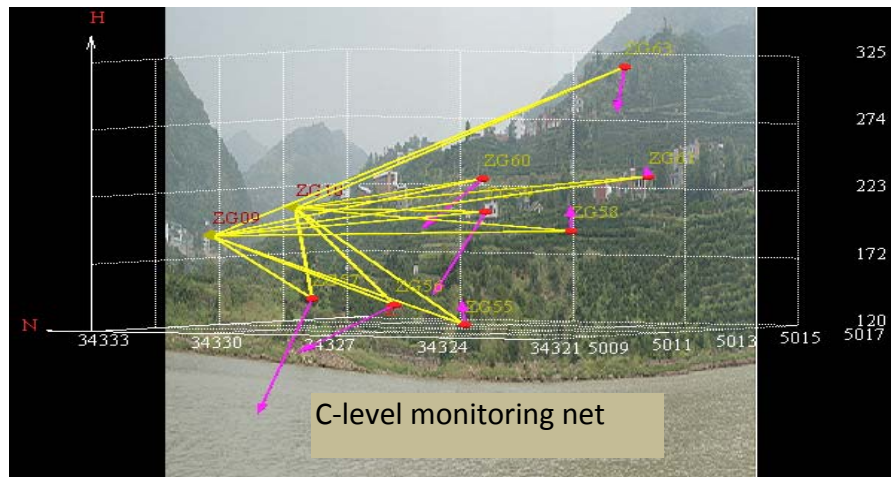


Figure.4 C-level deformation monitoring in the Three Gorges Reservoir area

Based on the public inspection & public prevention, professional monitoring is carried out for early warning of more than 200 landslides. The monitoring network is an integrated system, combining with remote sensing, GPS, deep displacement, landslide force, underground water, precipitation, water level fluctuation, geological inspection and etc.. The monitoring network is composed of over 3000 monitoring marks in total and uses over 500 sets of monitoring instruments and devices, making sure of catching the deformation signs and processing of landslides and providing the basis for early warning analysis by synthesis.

Professional monitoring methods of geo-hazards in Three Gorges Reservoir area include: GPS surface displacement monitoring, borehole inclinometer monitoring of deep displacement, underground water monitoring, landslide force monitoring, macroscopic geological inspection, relative displacement monitoring and so on.

In order to manage effectively the massive basic data and dynamic monitoring data, professional monitoring pre-alarm information system has been built up. The system uses application information technology as the major means and uses various types of networks and communications to transmit information about professional monitoring, public inspection & public prevention and pre-alarm commands. At the same time, the system created an integrated information platform with the monitoring, management and early warning functions, by making use of a distributing data acquisition system (collecting the geography, environmental geology, hazard survey, monitoring pre-alarm, mitigation measures, etc.). This system is very useful for data collection, processing, management and application. This network is used in inspecting the dangerous slides, evaluating their potential damages and quick response, therefore it can support the decision-making of different levels of governments and also provide concrete evidences and data for landslide mitigation, hazard relief and emergent measures.

For the early warning, the detailed investigation on landslide topography, lithology, slope structure and hydrogeology condition is the first step, which can help us better understand the scale, type, deformation and failure mode and genetic mechanism of landslides. Based on the above information, and also with the combination of monitoring data and deformation evidences, the deformation development and evolution status and stage can be analyzed. According to either the qualitative and quantitative model of landslide early warning, the temporal-spatial landslide deformation rules and trend can be attained. Therefore, with the previous information, we can do the early warning and prediction before-hand. According to the number of people who are threatened by landslides and need to be relocated, as well as the potential economic losses, the scale of landslide in the Three Gorges Reservoir area are ranked into four levels: catastrophic (super large) scale (*Rank I*), large scale (*Rank II*), medium scale (*Rank III*) and small scale (*Rank IV*), as shown in Table 4.

Table 4 Four-rank division of risk state in Three Gorges Reservoir area

Rank basis \ Rank	Especially large (<i>Rank I</i>)	Large (<i>Rank II</i>)	Middle (<i>Rank III</i>)	Small (<i>Rank IV</i>)
Water and land communication	Predict the landslide body into the Yangtze River may produce surge and the main stream needs closure of navigation	Predict the landslide body into the Yangtze River may produce surge, and the first-class tributary needs closure of navigation, or may cause large scale damage to main railways and roads (national roads), with long term interruption	May cause large-scale damage to provincial Roads with long term interruption	May cause damage to County and town roads with interruption
Number of people threatened and needing relocation	>1000	500-1000	100-500	<100
Potential economic loss	>100 million	50 -100 million	5-50 million	<5million

According to the deformation phases of rockfalls and landslides (steady deformation stage, early accelerated stage, middle and late accelerated stage and limiting equilibrium (near failure

stage)), the landslide early warning can be divided into four levels: attention (blue color), warning (yellow color), alert (orange color) and alarm (red color).

The monitoring & early warning network of geo-hazards in Three Gorges Reservoir area was built in two stages in 2003 and 2006, and put into operation. From 2003 to 2008, the Three Gorges Reservoir area suffered 5 times of flood seasons and 4 times of water storages (the water levels are 135m, 139m, 156m, respectively). During this period, the geo-hazards monitoring & early warning network played an extremely important role: the public inspection and prevention network observed 500 landslide sites having obvious deformation phenomena, while the professional monitoring network inspected 100 obviously deformed landslides with more than 40 reaching to the early watering level. Many landslides were successfully predicted, such as the Qianjiangping landslide, Nierwan landslide, Woshaxi landslide, Tongkouwan landslide, Liangshuijing landslide et al.. Around 7 000 people were evacuated, avoiding many fatalities and property losses. The shipping transportation of the Yangtze river was also protected to be interrupted.

7.3 Early warning of landslides in China

7.3.1 Early warning based on the meteorological forecast (regional early warning)

The Ministry of Land and Resources and Meteorological Administration in China signed an agreement of geo-hazard early warning system based on the meteorological forecast in 2003. Since 2003, the system has been carrying out geo-hazards early warning every year from May to September (flood period) in China. At present, all provinces and municipalities have launched a meteorological forecast of geo-hazards.

(1) Early warning region division

The landslide and debris flow hazards will be only triggered when the water content of rock and soil mass reaches to a certain threshold. Based on this statistical knowledge, the national or regional landslide and debris flow early warning can be carried out.

The state early warning division considered many factors, which are the national watershed or the snow line, regional climate, historical landslide and debris flow distribution density, geological environment, geotechnical properties of the slope and the average annual rainfall distribution. In China, from the Pamirs plateau to the sea continental shelf in the east is the largest slope, which can be divided into three categories.

① Watershed to the beach: the back border is from Yanshan mountain to Luerhushan mountain, the left border is Liao River, the right border is Yongding River or Hai River and the front border is the Bohai Sea;

② Areas bounded by mountains and rivers, such as the area enclosed by the Huai River, Yangtze River and Dabieshan mountain.

③ The margin areas around basins, the region around the Sichuan Basin.

China can be divided into 7 first-class, 27 second-class and 74 third-class early warning regions, according to the regional geology, topography and other factors (Figure 5).

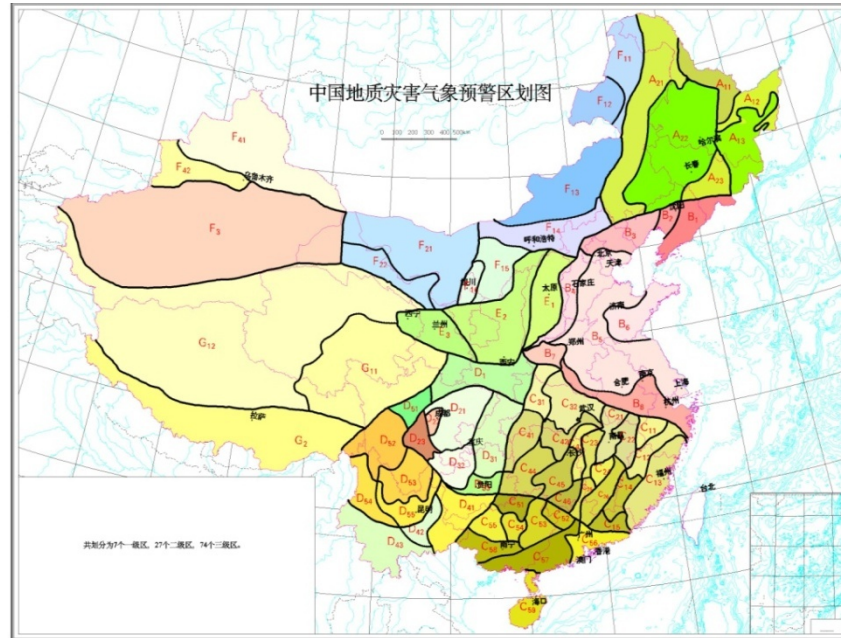


Figure.5 Zonation map of meteorological forecast of China

(2) Prediction chart based on the precipitation threshold

Based on the study and historical experiences, the occurrence of landslides and debris flows is not only related with the intraday rainfall, but also has close relationship with the rainfall amount before a event. We have made a statistical analysis on the process rainfall in different periods: 1, 2, 4, 7, 10 and 15 days. In this format, we expect to get a precipitation threshold for the landslide and debris flow occurrence.

The study on the rainfall threshold in a certain region is largely depends on the historical data of landslides and debris flows. The more relevant data and the longer time span, the more accurate results we can get.

According to the research on the relationship between landslides and debris flows and rainfall, we can make a scatter diagram, which reflects the relation of the landslides and precipitation threshold in different periods. We found the points distributed in a belt or cluster pattern. The upper bound can be expressed by α line and the β line represents the lower bound. Therefore, we can establish an early warning criterion model of landslides and debris flows, on the basis of the rainfall process in different period: 1, 2, 4, 7, 10 and 15 (Figure 6). In Fig.6 the horizontal axis represents the time (1-15 days), while the vertical axis represents the precipitation (mm). A-zone presents a comparatively safe zone (the first and second rank). If the data fits this zone, we don't need to send any warning signal, because it's difficult to triggerer a landslide or debris flow with a small amount of railfall. B-zone is located between $\alpha \sim \beta$ line. If the data is in this zone, a prediction signal needs to be published (the third and fourth rank). C-zone represents the relevant departments need to publish the red warning signal (the fifth rank).

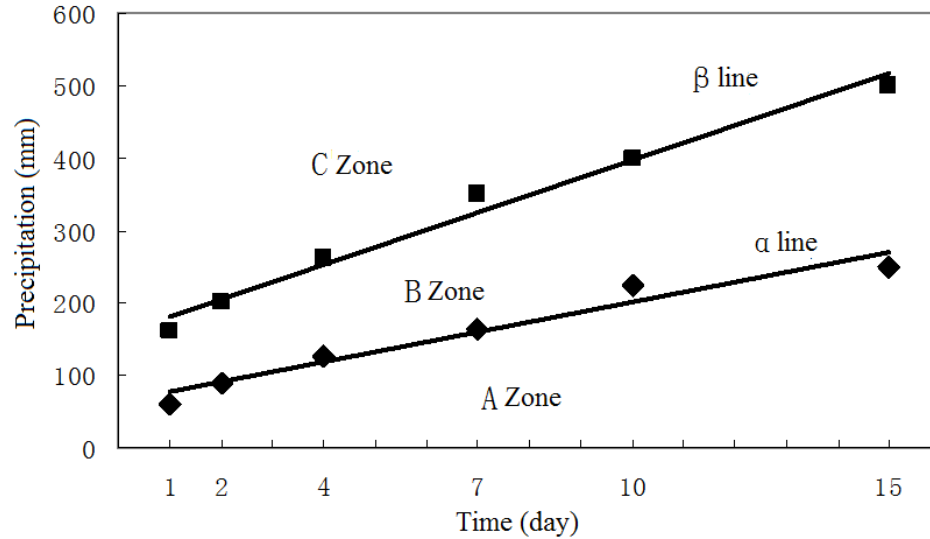


Figure. 6 Regional geo-hazards prediction model based on the precipitation threshold

A Zone—no need to send warning signal;

B Zone—Publishing prediction signal (yellow and orange);

C Zone—Publishing Red alarm signal;

α line — Prediction signal publishing envelop (boundary divided the second and third rank);

β line — Warning signal publishing envelop (boundary divided the fourth and fifth rank)

(3) Meteorological forecasting practice in China

The whole country has been divided into 7 regions, 28 early-warning zones in 2003. From 2004 to 2007, it has been subdivided into 74 early warning areas, based on the national scale (1: 6 000 000) geology data. According to the specific geological environment and climate in different areas, the regional geo-hazard criteria chart based on the precipitation threshold for different areas with specific geological characteristics can be developed.

① Early Warning Practice from 2003 to 2004

The national geo-hazard meteorological forecast products had been issued for 56 times in CCTV and 109 times in Geo-environmental Information Website in 2003, during the testing operation period. Based on incomplete statistics of intense rainfall-triggered landslide, we found that 264 events happened in China from June to September (the flood period) in 2003. Among them, there are 101 events were successfully predicted. The prediction success rate can reach to 38%.

In 2004, the national early-warning area was subdivided into 74 zones and the predictive criteria of landslides in different zones were established. The national geo-hazard meteorological forecast products had been published for 83 times in CCTV and 107 times in Geo-environmental Information Website in 2004 flood season (from May to September). According to the collected feedback, there were 382 geological hazards occurring in flood season, among which, 163 occurred within the early warning prediction region (Figure 7).

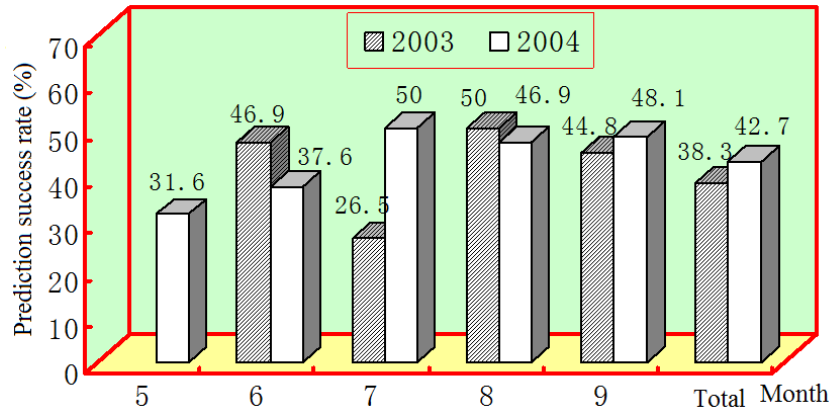


Figure. 7 Comparison between the geo-hazard prediction success rate in 2003 and 2004.

② Practice of early warning and monthly comparison in 2005

According to available statistics, 1399 landslides have been triggered by rainfall in 2005 in the flood season, 706 of which were successfully early warned. Based on the analysis of the occurrence of landslides and early warning situation, the prediction accuracy is lower in August and higher in July and September, and it is similar with the annual accuracy rate in May and June (Figure 8).

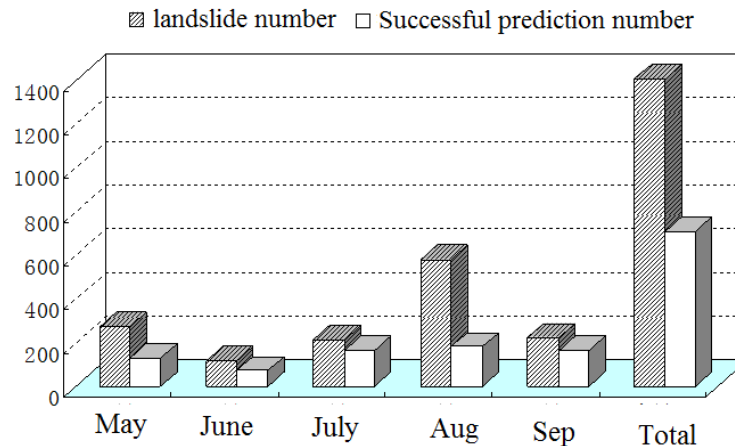


Figure.8 Monthly comparison of the prediction success rate in 2005

However, the meteorological forecast system has the following problems:

(a) The geo-hazard early warning based on the precipitation can not consider the changes of geological environment and the other key factors.

(b) There is no a standard method for evaluating the accuracy rate of landslide early warning.

(c) The mathematical analysis and quantitative classification of early warning ranks (levels) are still weak and are lack in therorical support.

(d) Without the detailed landslide investigation and good understanding of the landslide triggering factors and mechanism in the hazard-prone zones, it is very hard to attain some rules

of landslide temporal and spatial evaluation. In order to overcome the problems mentioned above, the researchers have developed a new meteorological forecast system.

7.3.2 Early-warning of individual landslides

The research of individual landslide prediction is a central issue concerned by researchers for a long time. Since the empirical predicting formula was suggested (Saito M., 1960), similar research has experienced several stages as followed through the persistently efforts of many scholars: the phenomenon and empirical formula prediction stage, non-linear prediction stage, comprehensive forecasting stage, real-time tracking and dynamic prediction and the list will go on. According to an incomplete statistics, more than 40 kinds of landslide prediction models, methods, and a range of prediction criteria had been put forward in the past few decades. But wide practice about landslide prediction indicate that the existing landslide predicting models and criteria can not make an accurate prediction for the deformation process and the specific time of landslide occurrence. The reason is mainly due to the strong specific traits of landslides, meanwhile, the deformation evolution behavior of landslides is closely related to their environmental conditions and geological structure. However, the existing predicting models are unable to consider the characteristics of every individual landslide, and mainly get the model by mathematical deduction which may be not suitable and accurate enough for prediction.

In order to get a breakthrough in landslide prediction, we had developed a series of key research on landslide monitoring & early warning technologies. A series of landslide hazard predicting systems have been put forward, which are based on the law of time-space deformation development and the relevance and sensitivity analysis of external triggering factors, as well as comprehensive time-space forecasting by carrying out the monitoring and predicting of Danba landslides in Sichuan Province, Baishi landslides in Beichuan County, Baishuihe landslide in Three Gorges and other tens of major landslide disasters. By this way, we had reviewed and summarized the temporal-spatial developing characteristics of landslide hazards, and then made an efficient combination of mechanism and prediction in recent year. The forecasting methodology technique has been applied and tested in the prediction an emergency management for several landslides occurred recently.

(1) The time-dependant development of slope deformation and failure

Extensive landslide monitoring data show the deformation evolution curve for rock and soil slopes has three stages (Fig. 9).

Stage 1 (A-B on Figure 9): Initial deformation stage. Deformation starts, cracks appear in the slope and the deformation curve is relatively steep. However, the deformation trends to a steady stage and the gradient of curve becomes moderate and shows an apparent decelerated deformation feature with time. This stage is often referred to be the initial deformation or decelerated deformation stage.

Stage 2 (B-C in Figure 9): Uniform-velocity deformation stage. The rock-soil slope continues to deform at a steady or uniform rate driven primarily by gravity. However, the deformation curve is likely to fluctuate as it is influenced by external factors such as rainfall and earthquake shaking, but the overall trend is for a relatively constant macro-deformation rate. This stage is often referred to as the uniform-velocity deformation stage.

Stage 3 (C-F on Figure 9): Accelerating deformation stage. When the slope deformation reaches a critical stage, the deformation rate will show an increase, accelerating continuously, and the curve will trend to the vertical until catastrophic failure occurs. This stage is defined to be the accelerating deformation stage.

Numerous examples of landslide and modern non-linear science research results indicate the arrival of accelerating deformation is the prerequisite for catastrophic landslide failure. Therefore, this stage is the most important for predicting catastrophic landslide failure. The accelerating deformation curve can be subdivided into three sub-stages, each with its own characteristics: the initial stage of accelerating deformation (C-D in Figure 9), the medium-term stage of accelerating deformation (D-E on Figure 9) and the surge stage of accelerating deformation (E-F on Figure 9).

The three-stage deformation process described above is universal for rock-soil slope deformation under the influence of gravity. Careful analysis is required to interpret slope monitoring data so the slope deformation stage is correctly assigned. And then, the appropriate mitigation measures can be taken to reduce the landslide potential hazard.

However, the slope deformation-time curve of Figure 9 is a representation of slope deformation and failure in an ideal situation without considering the external influences. Actually, almost all the slopes will be inevitably influenced by a variety of external factors (such as rainfall and human activities etc.). Consequently, the deformation-time curve will show some fluctuations from the ideal curve.

(a) Fluctuation type

If a slope is affected by some non-cyclical external factors (such as rainfall and human activities) during the deformation period, the slope deformation-time curve will contain some fluctuations with the wave-shape. Human errors of the monitoring data will also cause the similar

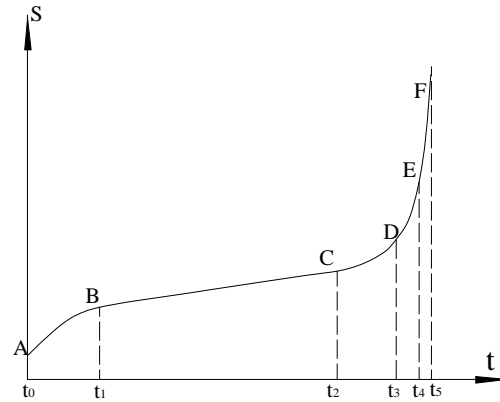


Figure.9 Sketch of three deformation stages of landslide

S: accumulative deformation t: time

AB: initial deformation phase BC: constant deformation phase CF: accelerated deformation phase CD: initial accelerated sub-phase DE: medium accelerated sub-phase EF: critical failure sub-phase

consequence. For example, the Longxi landslide which failed in 1985 had an deformation curve with a lot of fluctuations before the failure (Fig. 10).

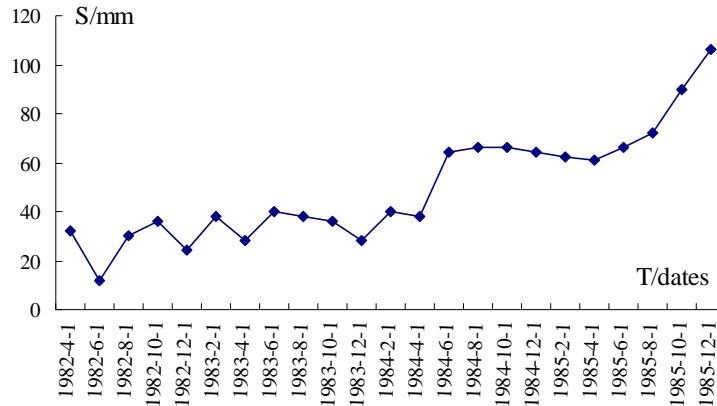


Figure.10 Deformation-time curve of Longxi landslide
S: the cumulative displacement T: date

(b) Staircase type

If the slope is influenced by periodic external factors during the deformation process, for example the regular rainfall in the flood season, or the annual change of the water level in a reservoir, the deformation-time curve might have the staircase shape. Figure 11 shows the Baishuihe landslide’s cumulative displacement-time curve in Three Gorges Area. Rainfall in the annual flood season causes a deformation increase, but after the rainfall the deformation will stop represented as a near horizontal segment of the curve (looks like a step). The whole curve shows a characteristic staircase-like evolution with the vertical changes corresponding to rainfall in the annual flood season. This type of curve is defined to be a staircase-deformation curve.

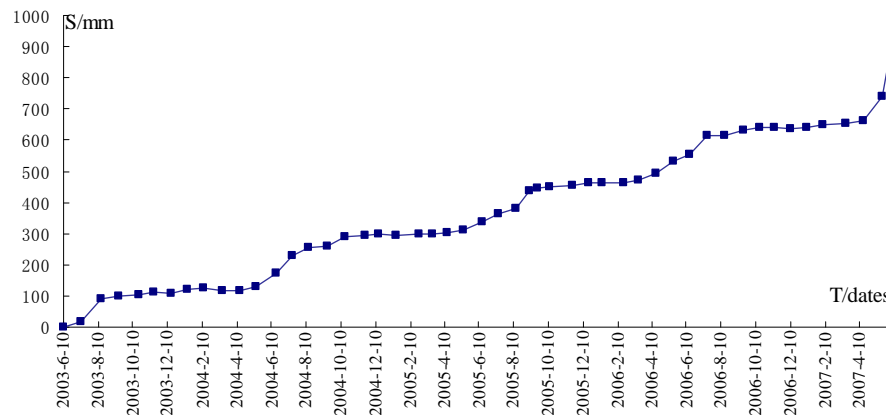


Figure. 11 Staircase-type deformation-through-time curve of the Baishuihe landslide
S: cumulative displacement T: date

(2) The Space development law of slope deformation and failure

The size, shape, or integrity will be changed when a slope accumulates a lot of stresses. If there is no significant change of the slope integrity, the slope is still in deformation process, otherwise, the slope is in the failure stage.

Generally, the slope will go through a long development process before failure. A large number of examples indicate that the landslides with different genetic mechanism will generate different stress concentration (tensile, compressive and shear stress) in different parts of the slope, corresponding to different types of cracks in the stress concentration place, due to various of mechanical properties. Meanwhile, these cracks fit the different deformation stages of landslide very well. For the landslides with the same genetic mechanism, there are some rules of the forming sequence, location and scale of cracks at different deformation stage. The generation and development of cracks in slope are not random. Both the temporal and spatial distribution of the cracks have some rules. With regard to the division of landslide genetic types, different people have different views. The most widely accepted genetic types of landslide are the advancing landslide (with the sliding force mainly from the rear part of the slope) and the retrogressive landslide. The characteristics of cracks evaluation and distribution pattern for these two types of landslides will be elaborated in the following text. Therefore, we will elaborate the stage and matching characteristics of cracks which were related to such two landslide mentioned above.

① Crack characteristics in different deformation periods for advancing landslides

Many case studies suggest that the slip surface of the advancing landslide usually has the gentle dip angle in front and steep dip angle in the rear of landslide. The middle and front part of landslides have the resistance sliding effect due to the near flat angle, while the rear part has the driving sliding effect, since mainly sliding force is from this part, due to the steep dip angle of the slip surface (Fig.12). Therefore, the tensile cracks and deformation will first appear in the rear part of the slope. And then the deformation and cracks will gradually develop to the front, lateral and deep part of landslides. Because the front part of slope has the sliding resistance effect, the slope in front will suffer the compression force. In this process, the ground cracks have following features (Fig.12):

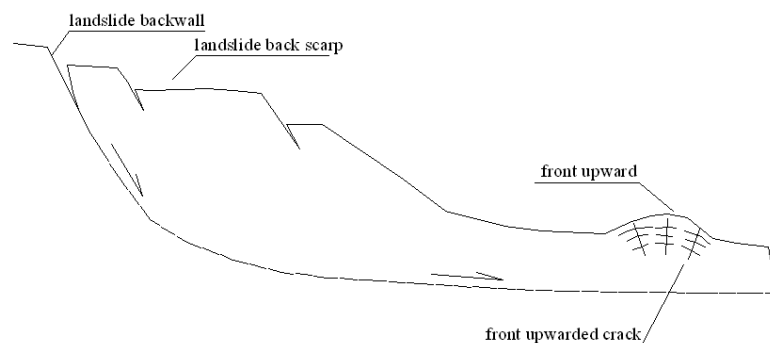


Figure.12 Typical cross section of advancing landslide

(a) Tensile cracks in the rear: the slope stability decreases under the effect of gravity or exogenous forces. Once the stability was reduced to a certain degree, deformation phenomena will appear in the slope. Usually, the sliding driven force form the rear part of slope is larger

than the sliding resistant force of the middle and front part of the slope. Thus, a tensile stress zone will be formed in the rear. Consequently, the horizontal component of sliding force will generate tensile cracks that are almost paralleled with the slope strike, while the vertical component will cause the vertical displacement of the slope in the rear, forming a series of small scarps. With the development of slope deformation, the number and extent of the tensile cracks will increase gradually. Finally these cracks will be connected with each other and form a long, deep, continuous arc crack in the rear. Meanwhile, multi-scarps will also be formed in the rear (Fig. 12 and Fig. 13).

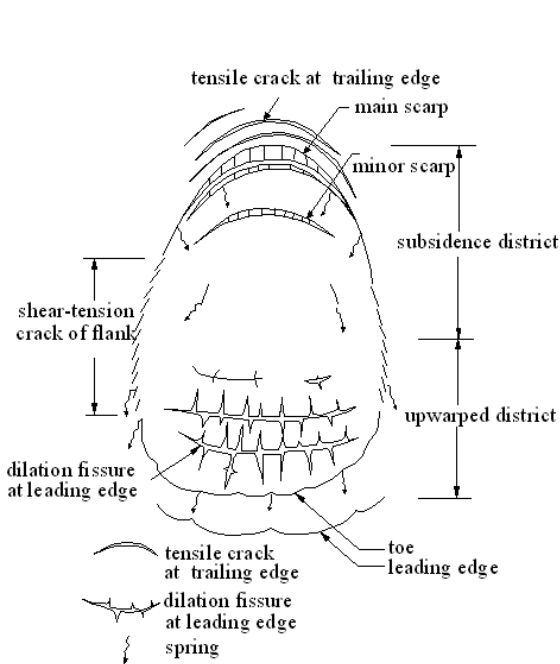


Figure.13 Crack development in different deformation periods for Advancing landslides

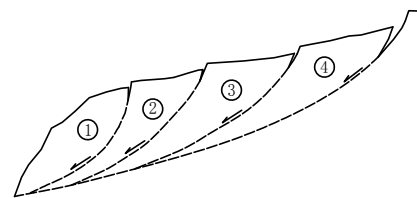


Figure. 14 Typical cross section of the Retrogressive landslide

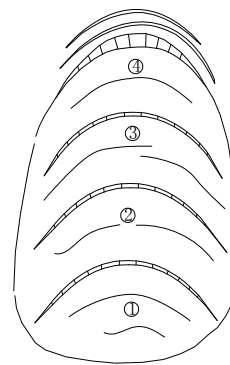


Figure.15 Crack development in different deformation periods for Retrogressive landslides

(b) The formation of shear and tensile cracks on the flanks of the central area of the landslide. The next step of the deformation development is the gradual deformation propagation to the front part of the slope. Due to this deformation propagation, the stress concentration will appear in the lateral flanks and the front part of slope, forming the lateral shear zones accompanied by the tensile shear cracks in these areas (Fig.13). The shear and tensile cracks on the flank will be enlarged and extend forward to the toe of the slope in an radial pattern. They always appear simultaneously and symmetrically on both sides of the landslide. If there is rotation generated in the process of sliding or if the slip rate is not uniform over the landslide, these cracks can also appear first in one flank and then in the other one.

(c) The formation of transverse fissures in the toe of the landslide. As the deformation accumulation in the slope, the rock and soil mass near the toe begins to deform. A raising ridge usually develops near the toe. A series of radial cracks are formed in the raising mass, while the fissures that are near perpendicular to the sliding direction will be formed in the toe of the slope, due to the bending deformation of the rock mass (Fig. 12, Fig. 13).

Once all these cracks become connected and enclosed, the slip surface becomes continuous, which indicates that the landslide will fail soon.

② Crack characteristics in different deformation periods for retrogressive landslides

For the slope with a uniform, gentler slip surface and also with a free face such as a steep cliff formed by water erosion, water level variation or manual excavation, the slope deformation under gravity will always occur in the front. A new free-face will be formed after the partial collapse and deformation of the toe of the slope. The landslide will deform retrogressively from the toe to the head of the slope (Fig. 14). The characteristics of cracks in different deformation periods for retrogressive landslides are as follows (Fig. 15):

(a) Tensile cracks will be first formed near the front free-face. When the slope is destabilized by some unfavourable factors, such as the influence of water erosion or manual excavation, a series of tensile cracks will appear near the toe of the slope, and propagate to the rear part, forming transverse tensile cracks.

(b) Partial collapse occurs in the front of slope, and the cracks extend to the rear part of the slope. With the development of the cracks in length, width and depth, the front sliding block will be formed. After the sliding of this block, a new free face will be formed (Fig. 14& Fig. 15). Due to the sliding of the first block, the rock and soil mass behind this block will lose the support (the resistant part). Therefore, new cracks will appear in the slope. When the deformation develops to a certain degree, the second sub-slide will happen in the same mode as the first slide. Gradually, the slope will fail from the front to the rear retrogressively. Multiple arc tensile cracks and minor scarps will be formed in the slope.

When the deformation develops a certain part of the slope, the slope will stop to develop retrogressively, due to the slope geological structure and material properties. Further deformation may result in several episodes of failure until the entire slope failed. If the slope has a steep slope angle, weak composition materials and resultant low slope stability, the slope will fail in the form of a series of sub-slides rather than sliding as an integrity.

Many landslide examples suggested that when the landslides are at the accelerating deformation stage, the cracks in the slope will start to connect with each other and become continuous and enclosed. However, because the slope deformation mechanism and process are very complex and different slopes have their own characteristics, the advancing the retrogressive slide modes may transform to each other.

Crack distribution patterns will also change temporally and spatially. Therefore, for the landslide prediction, we can not directly apply above methods without considering the special characteristics of the target landslide.

(3) An accurate landslide prediction method – the combination of the monitoring data and the slope deformation phenomena from the geomorphological view

Accurate early warning of landslide failure can only be achieved when the slope deformation stage is determined based on both the monitoring data and geomorphological deformation evidences. In order to determine the stage accurately, we need to consider both the slope deformation-time monitoring curve and the cracks development and distribution

pattern. If this method is not applied correctly, it will cause serious errors in the prediction results. Several large scale landslides have been successfully predicted by making use of this method. In the following text, two cases will be introduced.

(4) Case studies

① The Baishuihe landslide in Zigui County in the Three Gorges Reservoir Area

The Baishuihe landslide is located in a wide valley of the Three Gorges Reservoir Area along the Yangtze River, belonging to Zigui County. The topography of the landslide is high in the south and low in the north (Fig. 16). The landslide is developed on the western limb of the Zigui syncline. The strata is mainly consisted of medium to thick bedded sandstones inter-bedded with thin mudstone layer of the Xiangxi Group of Middle Jurassic System (J_{1X}). The dip angle of bedding varies from 15° to 36° . The back scarp of the landslide is composed of a rock cliff with a height of 410 m. The toe of the landslide is below water level, with an elevation of about 70 m. The lateral flanks of the landslide are bounded by ridges. The overall gradient of the slope is about 30° . The landslide is about 600 m long (from north to south) and 700 m wide (from east to west) with an average thickness of about 30 m. The volume is estimated as $12.6 \times 10^6 \text{ m}^3$. It is a large ancient landslide with loose accumulation layers. Monitoring results revealed that the deformation is mainly concentrated in the toe of the landslide, thus we paid special attention to this area, when we did the landslide monitoring (Fig. 16).

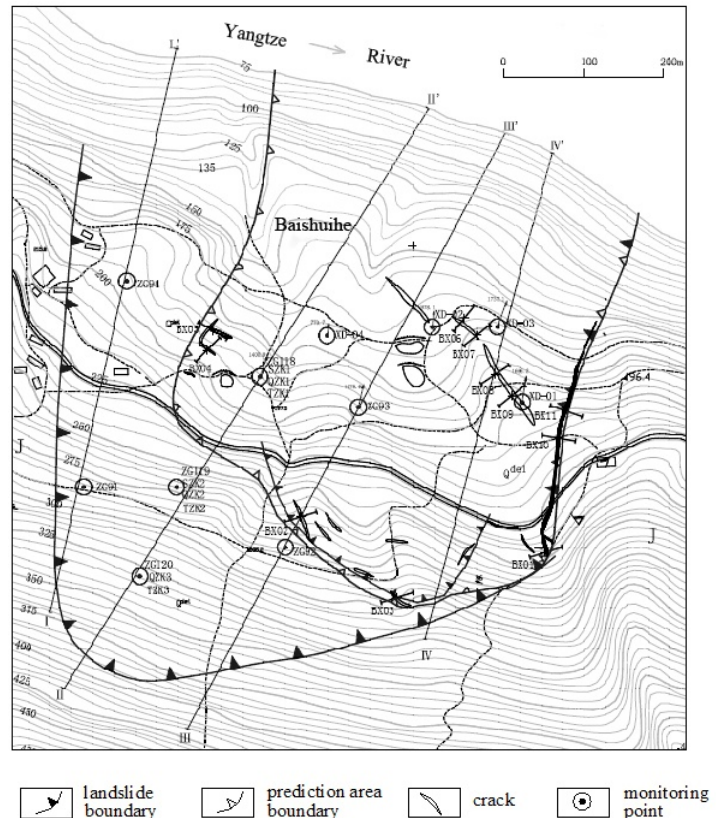


Figure.16 Plane graph and cracks distribution of Baishuihe landslide (2007)

According to monitoring data, significant deformation developed, when the Three Gorges Reservoir began to store water in 2003. A dramatic increase of deformation occurred in June 2007 (Figure 17). The annual cumulative horizontal displacement of 6 GPS monitoring points in the landslide increased from 928.2 mm on June 8 2003 to 1522.2 mm on July 12 2007. In July 2007, the monthly deformation rate was close to 600 mm, indicating that the landslide was reaching a "limited equilibrium" stage. The Three Gorges Area of Geological Hazards Prevention Leading Group Office organized an expert consultation meeting for the monitoring and early warning of Baishuihe landslide on July 13, 2007. The deformation stage of Baishuihe landslide was discussed and analyzed during and after the meeting. The results are as follows:

(a) Spatial evolution characteristics of the Baishuihe landslide

Continuous cracks were only found in the eastern (right) margin. In the rear of the slope, only discontinuous cracks were observed. The western boundary of the landslide is not so obvious. Thus according to the aforementioned crack development rules, till July 2007, the cracks in the landslide did not form a system yet, which are not developed enough to form the landslide boundary. Based on the spatial evolution of landslide deformation (the cracks), the Baishuihe landslide wasn't at the accelerating deformation stage at that time.

(b) Temporal evolution characteristics of the Baishuihe landslide

However, we still needed to explain the sudden increase of the displacement rate of the Baishuihe landslide in June 2007. Looking at the deformation-time curve deeply (Fig. 17), we can recognize it is a typical "staircase-type" deformation curve. We found that the landslide had an annual "step" from May to October each year since 2003. The timing of these steps have a good agreement with the rainfall season in each year (Fig. 17). Besides, the landslide deformation in 2007 was also impacted by the changes of the water level of the Three Gorges Reservoir, which decreased from 156m in March to 144m in May (Fig. 18).

By analyzing the landslide deformation curve and external factors, the sudden deformation increase in June 2007 was caused by the unfavourable rainfall and water level changes of the Three Gorges reservoir. Based on this explanation, the deformation rate of the landslide was supposed to be decreased, after the rainfall season and the reduce of the reservoir water level in 2007. This assumption was proved by the afterwards monitoring data. From Fig.19, we can see that the deformation-time curve measured by 6 GPS monitoring points became gentle and stable after August 2007.

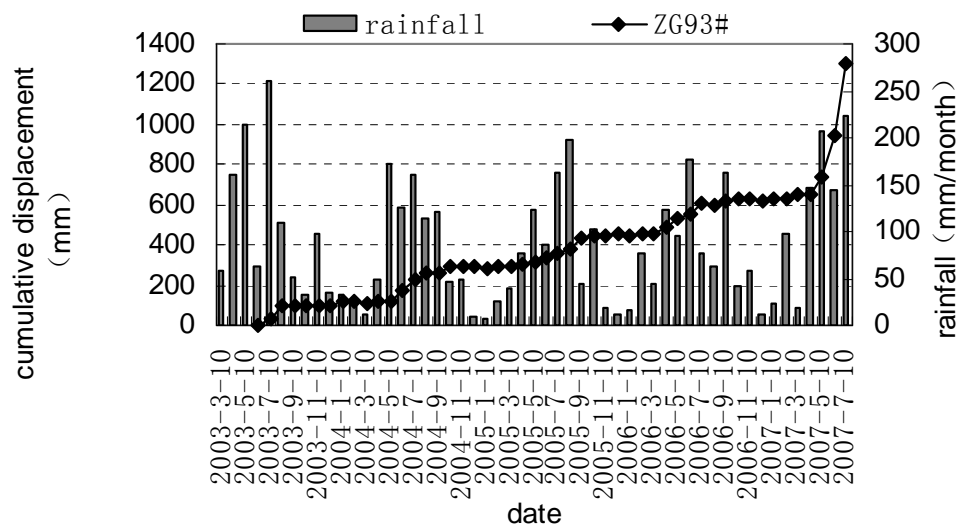


Figure.17 Correlation between deformation and rainfall for the Baishuihe landslide

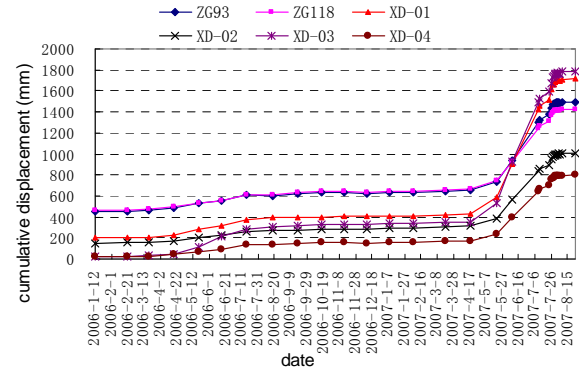
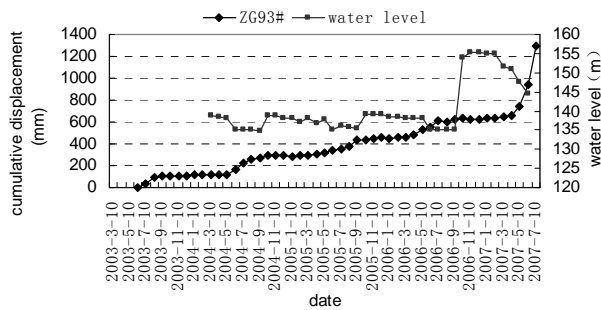


Figure.18 Correlation curve between cumulative displacement and reservoir waterlevel for the Baishuihe landslide

Figure.19 Curve of accumulating displacement over time for the Baishuihe landslide

② Baishi Village Landslide in Beichuan County, Sichuan Province

Baishi village landslide is located in Baishi Town, Beichuan County, Sichuan Province. The landslide is 350 m long, 400 m wide and 20 m thick on average. The volume is about $3.0 \times 10^6 \text{ m}^3$. The landslide developed in a deep slope about 500-700 m far from the valley. The landslide has posed a serious threat to lives and property of 695 rural people in the area. More seriously, if the landslide blocks the Baishuihe river, around 1 400 people in three villages at the upstream will be affected.

The Baishi Village landslide was reported by the local government on December 24th, 2006 and a team of landslide experts were sent to the field to carry out the on-site investigation. They found the vertical displacements in the back-scarp region was more than 10 m, multi-scarps and arc-shaped tensile cracks already appeared in the rear of the slope at that time. Meanwhile, small-scale rock falls also occurred in the toe of the landslide. Based on the deformation evidences and the crack development, most experts believe that the landslide was at the limited-equilibrium stage (near failure stage) at the end of 2006. The landslide deformation rate had reached tens of millimeters per day (Fig. 20) and the cumulative displacement was up to several meters. However, according to the monitoring data in early January 2007, as shown in Fig.20 and Fig.21, the displacement rate of the landslide was a constant value, which means that the landslide did not enter into the accelerating stage. Therefore, we supposed that we still have time to carry out some mitigation measure to reduce the potential hazard to minimum. In order to prevent the landslide forming a dam and submerging the upstream, a 678 m long drainage tunnel was constructed in advance to release the water. The construction was started on March 14th, 2007 and was finished on June 18th 2007. The landslide entered into accelerating stage in April 2007 and entered into near failure stage in July 2007.

A red alert warning was issued on July 26th, 2007, based on the analysis of the landslide monitoring data and the development of cracks in the slope. The slope failed catastrophically at 11:30 pm on 28th July 2007 (Fig. 22), and blocked the Baishuihe River, forming a barrier lake at 1:00 am on 29th July 2007. The water in the barrier lake was able to be drained through the tunnel, which significantly reduced the hazard of the landslide.

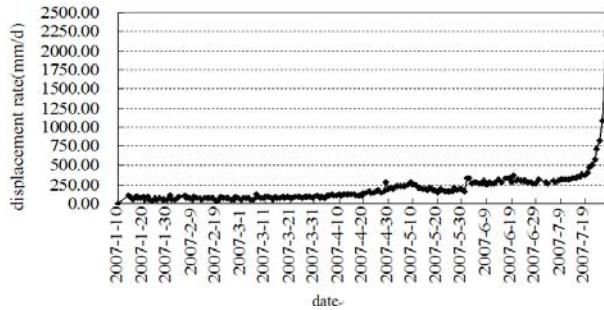


Figure.20 Discrete displacement rate-time curve for the Baishi landslide

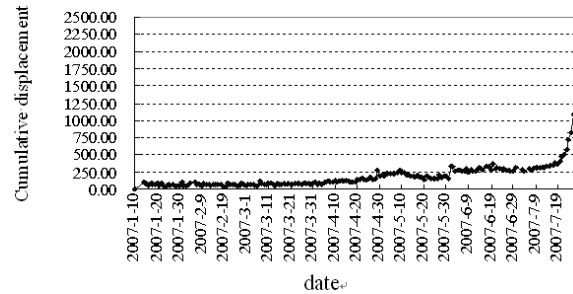


Figure.21 Cumulative displacement-time curve for the Baishi landslide



Figure.22 The Baishi landslide after catastrophic failure

7.4 Conclusions

Since 1980s, based on the national geo-hazard investigation, Chinese government has built up the geo-hazard prevention system with Chinese characteristics. The geohazard prevention methods such as the engineering measures, monitoring & early warning and evacuation have achieved remarkable effects. Combining Chinese reality, we establish the geo-hazard early warning system based on the regional meteorological forecast, the individual landslide early warning theory and techniques, as well as the public inspection & public prevention system. Series of geo-hazard monitoring & early warning instruments are developed for comprehensive monitoring & early warning of geo-hazards. Professional monitoring & early warning regions and demonstration stations were built in those areas where geo-hazards frequently occur. Till now, we have successfully forecasted several landslides triggered by strong rainfall, and have carried out the monitoring & early warning and emergency treatment for several tens of large scale landslides.

References

Three Gorges Project Committee of State Council, 2009.12. Analysis report for the Ecology and

- Environmental Monitoring System in Three Gorges Project - geological environment fascicule(in Chinese).
- Liu C.Z. & M.S.Wen.2004. Preliminary study on geo-hazard meteorological forecast in China. Geological Bulletin, 23 (4): 303 -309. (in Chinese)
- Liu C.Z.. 2009. Early warning method and application for regional geo-hazard in China, Beijing: Geological Publishing House. (in Chinese)
- Huang R.Q. & Xu. Q. 1997. Synergetic prediction model of slope instability. Mountain Research 15(1): 7-12.(in Chinese)
- Institute of Rock&Landslide of Hubei Province. 2007. Report on recent deformation for Baishuihe landslide in Three Gorges. (in Chinese)
- Li X.Z. & Xu Q. & Huang R.Q. (eds.). 2003. Research on prediction criterion for temporary prediction of landslide. The Chinese Journal of Geological Hazard and Control 14(4): 5-11(in Chinese).
- Liao Y. L. & Xie M.W. 1996. The grey forecast on monitoring displacement. Chinese Journal of Rock Mechanics and Engineering15(3): 269-274.
- Li T.B. & Chen M.D &Wang L.S. (eds.). 1999. Landslide real-time tracking prediction. Chengdu: Chengdu Scientific and Technical University Publishing. (in Chinese)
- S.G. Evans &J.V. DeGraff (eds.). 2002. Catastrophic landslides: Effects, Occurrence, and Mechanisms. The Geological Society of America, Reviews in Engineering Geology XV.
- Saito M. 1965. Forecasting the time of occurrence of a slope failure. In: Proceedings of 6th International conference: 220-227.
- State Key Laboratory of Geological Hazard Prevention and Geological environment Protection, Chengdu University of Technology. 2004. Research on prediction model and criterion of slope in Three Gorges. Chengdu: Chengdu University of Technology. (in Chinese)
- Siqing Qin & Jiu Jimmy Jiao & Sijing Wang, 2002. A nonlinear dynamical model of landslide evolution. Geomorphology 43: 77-85.
- Wang N.Z & Liu S.H. & Zeng S.W. (eds.). 1999. A study on forecasting method of the comprehensive analysis of macroscopic signs of landslide. Chinese Journal of Rock Mechanics and Engineering11(1): 34-38.(in Chinese)
- Wang S.Q. &Xu J.J. 2006. New method to monitor and forecast landslide disaster in short-term, Journal of China Three Gorges Univ. Natural Sciences 28(5): 385-388.(in Chinese)
- Xu Q. & Huang R.Q. & Li X.Z. 2004. Research progress in time forecast and prediction of landslides. Advance in earth sciences193: 478-483.(in Chinese)
- Xue Y. & Hu D. & Guo K. & Zhang J. 2007. Displacement forecast of slope deformation based on a new type of bionic and intelligent method . 29(5):446-449. (in Chinese)
- Yi S.M. 2007. Status and prospect of the temporal prediction of landslide activity. Chinese Journal of Engineering Geophysics4(2): 157-163. (in Chinese)
- Zhang B. & Men Y.M. 1998. Forecasting and prediction of landslides based on neural network. Journal of Xi'an Engineering University20(3): 67-69.
- Zhong Y.Q. 1995. Study of prediction method by synthetic information for Huanglashi landslide. The Chinese Journal of Geological Hazard and Control6(4): 67-74.(in Chinese)
- Zhang Z.Y. & Wang S.T. & Wang, L. S. 1992. Principle of engineering geology analysis. Beijing, China: Geological Publishing House

CHAPTER 8 NATURAL TERRAIN LANDSLIDE RISK MANAGEMENT- EXPERIENCE AND PRACTICE IN HONG KONG

K.C. Ng, K.K.S. Ho & T.H.H. Hui

Geotechnical Engineering Office, Civil Engineering and Development Department, Hongkong

8.1 Introduction

Hong Kong has a land area of only about 1,100 km² and a population of over 7 million. The terrain is hilly, with some 75% of the land steeper than 15° and over 30% steeper than 30°. Intense urban development has taken place in flat terrain and foothill areas, and is encroaching onto the rugged hillsides.

Much has been published in the literature on the geology of Hong Kong (e.g. Fletcher 1997, Fletcher et al. 1997, Davis et al. 1997, Sewell & Campbell 1997, Sewell et al. 2000). The two dominant rock types in the urbanized areas comprise granites and volcanic rocks. The small amounts of sedimentary and metamorphic rocks are of comparatively lesser importance as far as development is concerned. The granites and volcanic rocks have been deeply weathered, locally in excess of 60 m, or 100 m in more extreme cases.

The ground profiles are typically highly variable and heterogeneous. Corestones and coreslabs may be left behind in the saprolite which comprises a matrix of soil derived from in-situ rock weathering and retains the original rock texture, fabric and structure (e.g. relict joints). There are extensive bodies of colluvium over the lower hillslopes of Hong Kong, which comprise accumulations of debris from old landslides and mass movements up to about 30 m thick, commonly in the form of boulders, cobbles and gravel in a matrix of sand, silt and clay. Accounts of superficial deposits and rock weathering in Hong Kong are given in Fyfe et al (2000).

The climate of Hong Kong is sub-tropical, with the annual rainfall averaging about 2,300 mm, approximately 80% of which falls during the period of May to September. Rainfall intensities can be high, with 50 mm per hour and 250 mm in 24 hours being not uncommon.

Owing to the close proximity of developments to man-made slopes and natural hillsides (Figure 1), landslide is a common form of natural hazard in Hong Kong that can cause significant loss of life and socio-economical consequences. On average, some 200 to 300 landslides are reported to the Government every year. The scale of the problem is indicated by the fact that landslides have been responsible for the death of more than 480 people in Hong Kong since the late 1940s (Figure 2). In addition, there were many landslide cases that were classified as 'near-miss', which highlight the severity of the landslide risk to the community.

Hong Kong is probably unique in the world in terms of its combination of high seasonal rainfall, steep terrain in close proximity to dense urban development, a large stock of potentially substandard man-made slopes formed many years ago without geotechnical control, together with very high public expectation of slope safety.

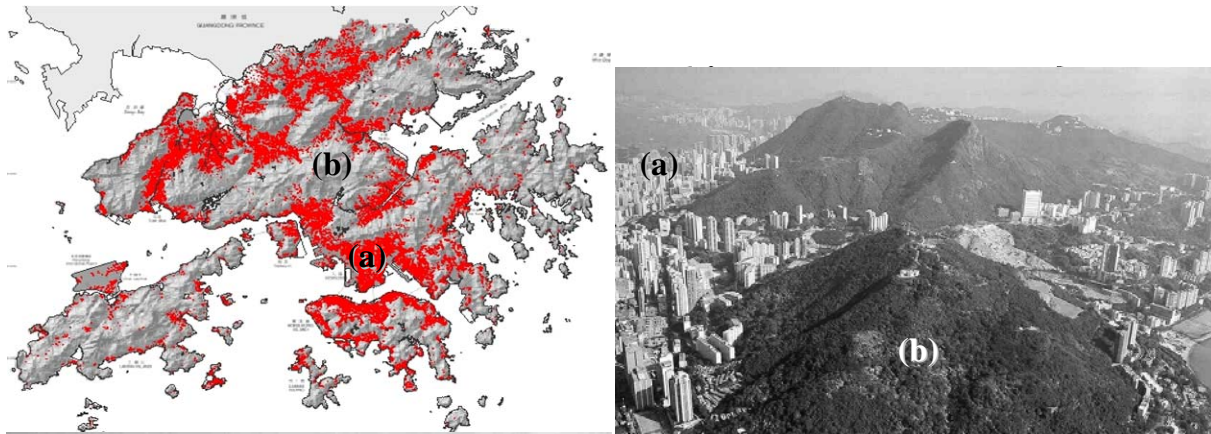


Figure.1 High concentration of urban developments in Hong Kong mingled with man-made slopes and natural hillsides (Note: urban development (a) fringing steep hillsides (b))

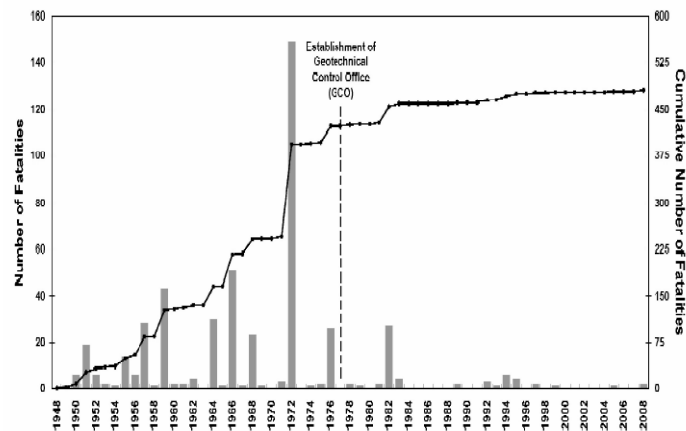


Figure.2 Known landslide fatalities in Hong Kong since the late 1940s

8.2 Hong Kong's Slope Safety System

Concerted efforts have been made by the Hong Kong Government over the past 30 years to manage and reduce landslide risk. In the aftermath of several landslide disasters with multiple fatalities that occurred in 1972 and 1976 (Figure 3), the Hong Kong Government created a central policing body, the Geotechnical Control Office (GCO, renamed Geotechnical Engineering Office, GEO, in 1991) in 1977, to regulate the planning, investigation, design, construction, monitoring and maintenance of slopes in Hong Kong.

A comprehensive slope safety system incorporating the application of fundamental risk management concepts at policy administration level has been developed and implemented by the GEO to combat landslide problems in a holistic manner (Chan et al. 2007, Wong 2009). The components of the slope safety system are shown in Table 1.



Figure.3a The 1972 Po Shan landslide in the Mid-levels district, which resulted in 67 fatalities



Figure. 3b The 1976 Sau Mau Ping landslide in the Kowloon foothills, which

Table 1 The key components of the Slope Safety System in Hong Kong (based on Malone 1998)

Slope Safety System Components	Primary Contribution by Each Component		
	To reduce landslide likelihood of landslide	To reduce consequence of landslide	To address public attitudes and tolerability of landslides risk
Policing			
• Checking new slope works	✓		
• Slope maintenance audits	✓		
• Recommending safety clearance of vulnerable squatters and unauthorized structures threatened by hillslopes		✓	
• Exercising geotechnical control through input to land-use planning		✓	
• Safety-screening studies and recommending statutory repair orders for private slopes	✓		
Works Projects			
• Retrofitting substandard Government man-made slopes	✓		
• Natural terrain landslide mitigation and boulder stabilization works	✓		
Research and Setting Standards	✓	✓	✓
Education and Information			
• Slope maintenance campaigns	✓		✓
• Risk awareness programmes and personal precautions campaigns	✓	✓	✓
• Information services	✓	✓	✓
• Landslip warning and emergency services		✓	✓

The slope safety system embraces a range of initiatives that serve to manage landslide risk in a holistic manner. The goals are: (a) to reduce landslide risk to the community through a policy of priority and partnership, and (b) to address public attitude and tolerability of landslide risk to avoid unrealistic expectations. The system also adds value to the community through averting potential fatalities and improving the built environment.

The recent development and application of Quantitative Risk Assessment (QRA) techniques has been instrumental in formulating the overall slope safety strategy for Hong Kong, as well as

managing the landslide risk at individual vulnerable sites (Wong 2005). This approach aligns slope engineering and landslide mitigation with other engineering fields that practise risk management in a more explicit manner.

The local slope engineering practice has evolved progressively over the years. Guidance on improved slope engineering practice is promulgated by the GEO in a series of Geoguides, technical reports and guidance notes from time to time. Over 250 of these documents are now available for viewing or downloading from the following website: <http://www.cedd.gov.hk/eng/publications>.

8.3 Landslide Risk Management

8.3.1 Landslides on Man-made Slopes

About 60,000 sizeable man-made slopes and retaining walls were formed as a result of urban developments. Since the establishment of the GCO in 1977, man-made slopes formed as part of new developments are required to be designed and built to the stipulated safety standards (GCO 1984). Old, substandard man-made slopes posing a significant risk to life are systematically studied and upgraded to the required safety standards under the Government's Landslip Preventive Measures (LPM) Programme, which was launched in 1977.

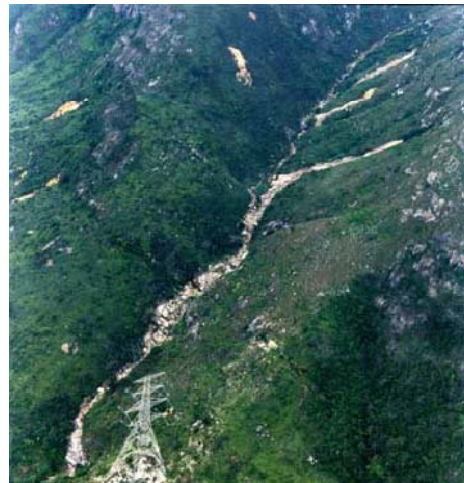
Implementation of the LPM Programme has reduced the overall landslide risk posed by man-made slopes in year 2010 to about 25% of that which existed in year 1977 (Lo & Cheung 2004, Cheng & Ko 2008). This strategy of systematically reducing landslide risk associated with sub-standard man-made slopes has proved to be appropriate and highly effective.

8.3.2 Landslides on Natural Terrain

Natural terrain covers over 60% of the total land area in Hong Kong (i.e. about 670 km²). Being shaped to its present form as part of the on-going natural geological, geomorphological and weathering processes, much of the natural terrain is often only marginally stable. The common forms of natural terrain landslides comprise open hillslope landslides (Figure 4a), channelized debris flows (Figure 4b), deep-seated slides (Figure 4c), rock falls and boulder falls.



(a) Open hillslope landslide



(b) Channelised debris flow



(c) Fault controlled deep-seated landslide

Figure 4. Common forms of natural terrain landslides

Hong Kong's natural terrain is especially susceptible to shallow (typically <3 m), small to medium-sized (typically several hundred cubic metres) landslides (Figure 5), which could develop into debris flows when the debris enters into drainage lines (Wong & Lam 1998, Wong & Ho 2000). Sizeable failures on steep open hillsides could also result in fast-moving landslide debris. The deep-seated failures are rare but when occurred, they are mostly related to the presence of adverse geological structures and adverse groundwater regimes. Should the debris reach densely developed areas, serious consequences are liable to, even if the volume of landslide is relatively small (Figure 6).



Figure 5. Landslide-prone natural terrain in Hong Kong



Figure 6. A relatively modest 50 m³ landslide in 1998 which resulted in damage to property

While the overall safety of man-made slopes has greatly improved with the progress of the LPM Programme, the risk of natural terrain landslides is on the rise due to continual increase in population and progressively more developments taking place close to steep hillsides. It was projected that, based on a quantitative risk assessment, the overall risk of landslides from natural terrain would be comparable to that from man-made slopes by the year 2010 (Wong et al. 2004a). This calls for an expanded effort to systematically combat and contain risk posed by natural terrain to a level that is as low as reasonably practicable, in order to discharge the Government's due diligence.

8.4 Landslide Inventories

As part of the hazard identification process, the GEO has compiled comprehensive information on past landslides on a GIS platform, as summarized below.

8.4.1 Natural Terrain Landslide Inventory

In the mid 1990s, the GEO compiled the Natural Terrain Landslide Inventory (NTLI), a Geographic Information System (GIS) based inventory of historical natural terrain landslides identified from interpretation of high-flight aerial photographs (2,400 m or above) taken since 1943 (King 1999). Figure 7 shows a graphical display of NTLI, including the identified natural terrain landslide crowns and debris trails. Up to the year 2000, the NTLI has catalogued some 30,000 landslides, about 11,000 and 19,000 of which are recent landslides (i.e. since about 1924) and relict landslides respectively. Factors such as photograph coverage, cloud cover, ground shadows, vegetation cover, and scale and resolution of the high-flight aerial photographs impose certain limitations on the dataset. Consequently, some landslides may have been missed, whilst some shown in the inventory may be other features mis-identified as landslides. Despite these constraints, the NTLI was one of the most comprehensive catalogues of historical natural terrain landslides that had been compiled at the time. It provided

important data for studies of natural terrain hazards, and was widely used by the local geotechnical profession until it was replaced by the Enhanced Natural Terrain Landslide Inventory (ENTLI) in 2007, as described below.

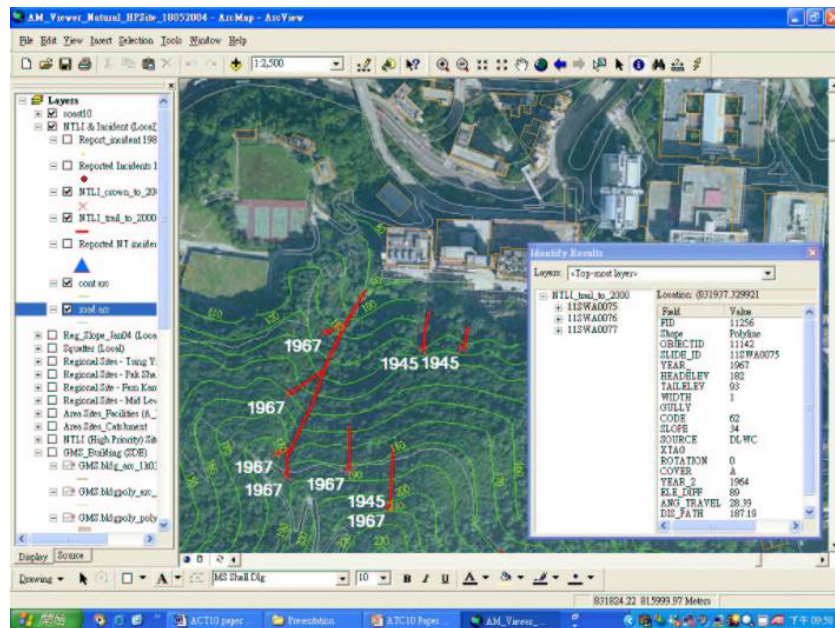
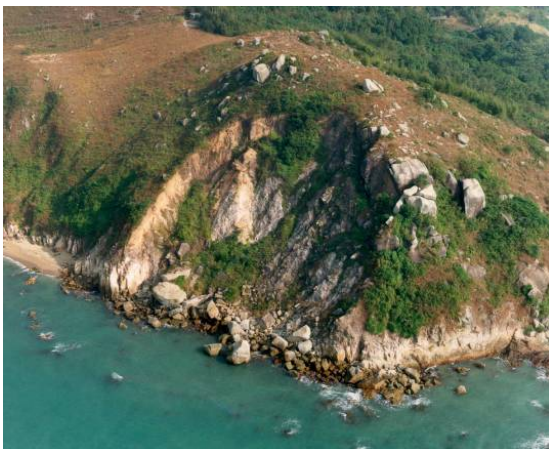


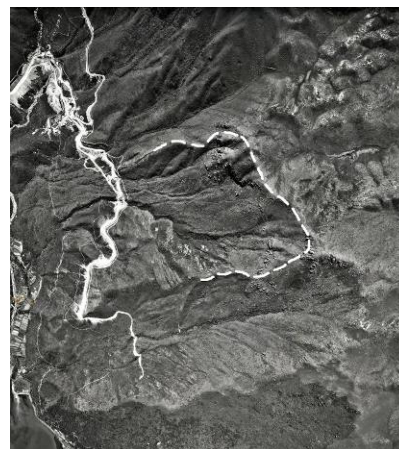
Figure 7. NTLI inventory comprising 30,000 natural terrain landslides - landslide source, trail and year shown on a geo-referenced, ortho-rectified infrared image

8.4.2 Large Landslide Database

A database of about 1,900 large natural terrain landslides was compiled based on the interpretation of aerial photographs and hillside geomorphology (Scott Wilson 1999a, b). These large landslides include large relict morphological features, as well as recent natural terrain failures with a scar exceeding 20 m in width. Some examples of the identified large relict landslides are shown in Figure 8.



(a) Large coastal landslide in Lamma Island



(b) Massive debris lobe at Sham Wat, Lantau



(c) Large relict landslide above Tung Chung Road

Figure 8. Examples of large relict landslide features

Studies were carried out by the GEO on the possible scale and age of some of the large relict landslides. For instance, the large coastal landslide on Lamma Island had an estimated volume of about 30,000 m³ and probably occurred within the last few hundred years based on a variety of dating techniques, including surface exposure (Cosmogenic Nuclide) and optically stimulated luminescence dating. The massive debris lobe at Sham Wat in Lantau covers a plan area of about 0.3 km². Age-dating revealed that the main body of the hillside probably failed some 30,000 years ago, but further sizeable detachments continued to take place and the youngest one was dated as only about 2,000 years old (Sewell & Campbell 2005). The large relict landslide scar that was left in place after a massive debris flow near the present Tung Chung Road was found to have occurred about 8,000 years ago. These landslides are relatively young in geological time scale and they could have implications to the assessment of the current landslide risk.

8.4.3 Enhanced Natural Terrain Landslide Inventory

In recognition of the limited resolution and temporal coverage of the high-flight aerial photographs, the GEO completed in 2007 a major enhancement of the NTLI to incorporate results from mapping of historical natural terrain landslides using the available low-flight (taken at less than 2,400 m) and high-flight aerial photographs (MFJV 2007a, Dias 2009). The improved inventory is known as the Enhanced Natural Terrain Landslide Inventory (ENTLI), which subsumes the NTLI. The ENTLI is presented in a GIS data format that contains the locations and attributes of all the 106,000 landslides identified on natural terrain up to 2006, about 16,000 and 90,000 of which are recent landslides and relict landslides respectively.

8.4.4 Historical Landslide Catchments

Based on the ENTLI, an inventory of hillside catchments with historical natural terrain landslides that occurred close to existing buildings and important transport corridors was compiled (MFJV 2007b). These vulnerable catchments, which are posing a notable risk, are denoted as Historical Landslide Catchments (HLC). The inventory comprises about 2,700 HLC, and is the basic dataset for planning the future priority ranking and implementation of risk mitigation works for vulnerable hillsides flanking existing developments in Hong Kong. The GEO

has completed a global QRA to evaluate the risk levels of the HLC, diagnosed their risk characteristics and projected the overall risk of natural terrain landslides in the whole of Hong Kong (Wong et al. 2004a). This provided key information for the formulation of the prevailing natural terrain risk management strategy. Using the global QRA results, a risk-based ranking system was devised for establishing the relative priority of the 2,700 HLC for systematic follow-up under the Landslip Prevention and Mitigation Programme (LPMitP).

8.5 Strategy Managing Natural Terrain Risk

The strategy for addressing natural terrain landslide hazards, including boulder falls, has evolved progressively with time. The current Government's strategy for dealing with natural terrain landslide hazards is aimed at keeping the natural terrain landslide risk to an as low as reasonably practicable (ALARP) level. It comprises two key components:

(1) New Developments

Contain the increase in the overall risk, through studying natural terrain landslide hazards and undertaking any necessary mitigation actions as part of the new developments that may be affected by such hazards. Avoid as far as possible new developments in vulnerable areas and on sites that are subject to the severe natural terrain hazards.

Whether a site may be affected by landslide debris depends on how close the site is to the hillside and how susceptible the hillside is to landsliding. To facilitate proper land-use planning and early identification of potential geotechnical constraints in planning stage, an initial hazard screening exercise is implemented, on a case-by-case basis, to examine whether a site may be subject to notable natural terrain landslide hazards and thereby require further hazard studies. Such screening needs to be carried out as early as possible in the land management process and project planning process. The screening should be efficient to carry out, and should give reasonably conservative results based on use of readily available data. For these purposes, the GEO has established a set of simple screening criteria (Ng et al. 2003) based on the analysis of debris runout data from historical natural terrain landslides in Hong Kong. In essence, the GEO would tender objection in-principle to proposals (i.e. the "In-principle Objection Criteria") where the zoning and disposal of a site is subject to severe natural terrain hazards (Figure 9). For a site that may be affected by natural terrain hazards but does not satisfy the "In-principle Objection Criteria", the "Alert Criteria" (Figure 10) are used by the GEO to determine whether or not a natural terrain hazard study (NTHS) is needed.

(2) Existing Developments

Undertake mitigation actions urgently where there exists an immediate and obvious danger (i.e. the 'react-to-known-hazard' principle). Study natural terrain landslide hazards only where there is reason to believe that a dangerous situation could develop, such as persistent landslides affecting an existing development, and undertake mitigation when considered necessary.

In 2007, the Landslip Prevention and Mitigation Programme (LPMitP) was endorsed by the Hong Kong Government as a long-term landslide risk mitigation initiative (Development Bureau

2007). The LPMitP has commenced in 2010 upon completion of the current LPM Programme, as a rolling programme. The annual output for the LPMitP would be: (a) to upgrade 150 Government man-made slopes; (b) to conduct safety-screening studies for 100 private man-made slopes; and (c) to implement risk mitigation works for 30 vulnerable natural hillside catchments.

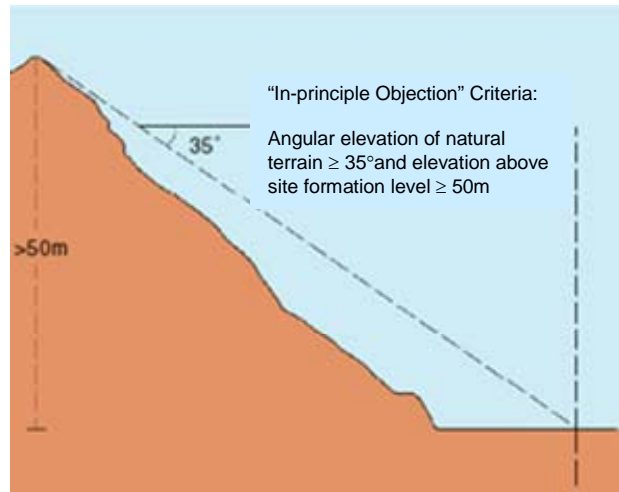


Figure 9. In-principle objection criteria for new development projects

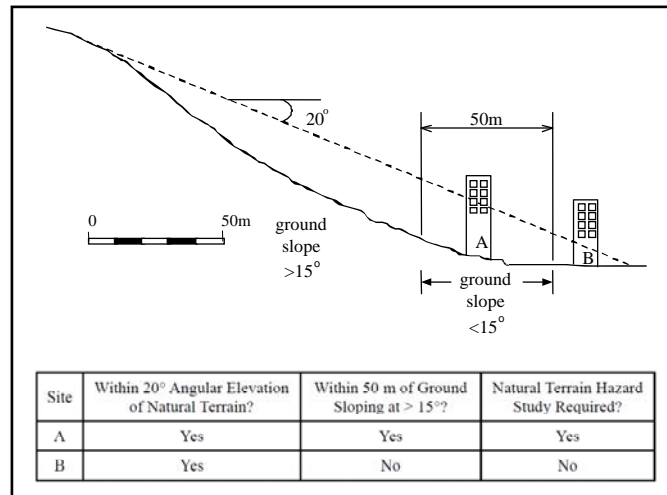


Figure 10. Screening criteria for assessing the requirement for NTHS in new development projects

The LPMitP marks a new chapter in Hong Kong's landslide risk management, by incorporating systematic study and mitigation of natural terrain landslide risk as an integral part of Hong Kong's long-term slope safety programme.

Research and development work carried out by the GEO over the past few years has led to an improved understanding of natural terrain landslide hazards. Methodologies for studying natural terrain landslide hazards are now in place. Pragmatic solutions for hazard mitigation have been developed and applied. The key technical criteria and guidelines for study and

mitigation of natural terrain landslides risk in Hong Kong are given in the following GEO publications:

- GEO Report No. 138 'Guidelines for Natural Terrain Hazard Studies' (Ng et al. 2003), which provides guidance on study and mitigation of natural terrain hazards. This includes recommended design standards and good practice in hazard mapping, risk assessment and risk mitigation. Guidance on maintenance of mitigation measures is also given.
- GEO Report No.75 'Landslides and Boulder Falls from Natural Terrain - Interim Risk Guidelines' (ERM 1998), which provides guidelines on the tolerable individual and societal risk criteria for the evaluation of QRA results.
- GEO Report No. 104 'Review of Natural Terrain Landslide Debris-resisting Barrier Design' (Lo 2000), which provides guidelines on the assessment of impact force and velocity of natural terrain landslide debris and design of debris-resisting barriers.

The development and advances in some of the key technical areas are discussed in the following.

8.6 Susceptibility and Hazard Zoning

Landslide susceptibility in the present context refers to the likelihood of the hillside to landslide occurrence, and excludes the consideration of debris runout and retrogression of the slope failure. Landslide susceptibility zoning usually involves classifying the terrain into different zones according to their landslide susceptibility.

Hazard is defined as "A condition with the potential for causing an undesirable consequence" in the Guidelines for landslide susceptibility, hazard and risk zoning for land use planning (JTC 2008), which would require the consideration of landslide runout as well as the outcome of susceptibility assessment.

8.6.1 Terrain Classification, Physical Constraints and Geotechnical Land Use Maps

Since the early 1980s, the GEO has been compiling regional terrain data and thematic maps that provide geotechnical information for use in land and project planning. A series of eleven 1:20,000 scale terrain classification maps covering the whole of Hong Kong were produced by the GEO in the 1980s. Based on the interpretation of topographical maps and aerial photographs, the terrain classification system recorded three attributes: (a) slope angle, (b) landform, and (c) instability and erosion. A total of 56,920 terrain classification units, each with an average map size of 1.9 ha, were delineated.

The terrain classification maps were used to create 1:20,000 scale thematic maps, e.g. Physical Constraints Maps and Geotechnical Land Use Maps (GLUM). Physical Constraints Maps present the major geotechnical constraints that may affect development, comprising zone of general instability, colluvium, flood plain, disturbed terrain, waterbodies, erosion areas, etc. In the GLUM maps, terrain units are categorized into four classes in respect of their suitability for development based on geotechnical considerations. An oblique aerial photograph on which the GLUM classes are shown is given in Figure 11.

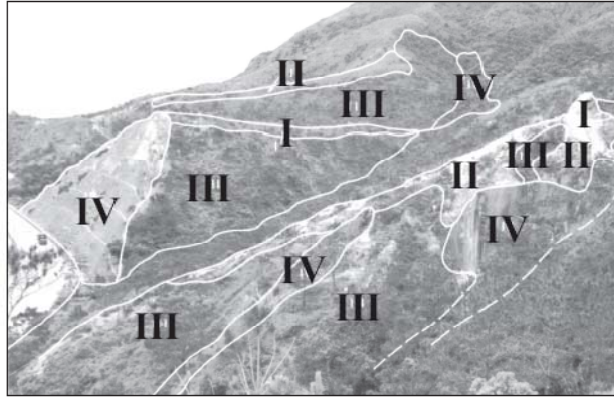


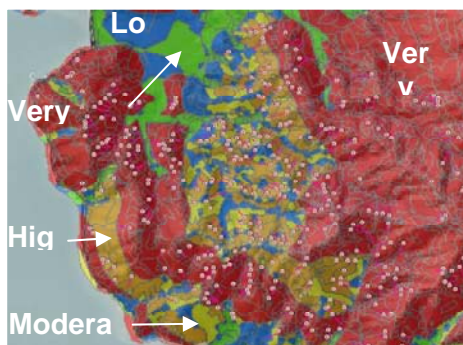
Figure 11. GLUM classes on suitability for development - I) High; II) Moderate; III) Low and IV) Probably Unsuitable

More detailed terrain classification and thematic mapping work was undertaken for selected regions. Maps at 1:2,500 scale were produced for nine catchments that contain extensive colluvial deposits, together with details of interpreted old landslide scars, in developed areas. Mapping was also completed for eleven 1:5,000 scale map sheets in the North Lantau area, where major infrastructure development was planned (Franks 1991 & 1992, Woods 1992).

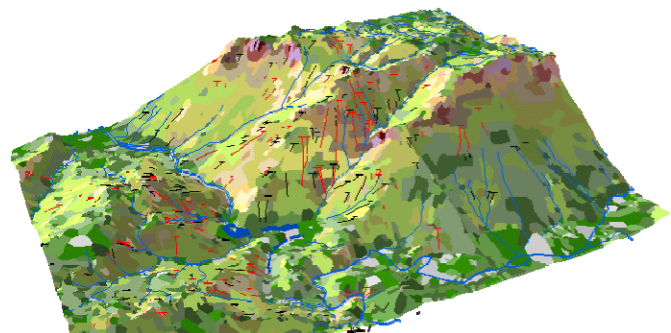
These thematic mapping products provide regional terrain classification and related geotechnical data, and are used by the Planning Department for general land-use planning and resources evaluation purposes.

8.6.2 Territory-wide Susceptibility Analysis and Zoning

Evans & King (1998) carried out a territory-wide landslide susceptibility zoning, based on correlation of natural terrain landslides (i.e. the Natural Terrain Landslide Inventory which was compiled in the mid-1990s) with slope angle and geology. Nineteen geological groups and thirteen slope angle classes were adopted, which resulted in 247 different types of terrain units. The Digital Elevation Model (DEM) was compiled from the 1:5,000-scale 10 m contour topographical maps, whereas the susceptibility zoning map was prepared in 1:20,000 scale. Based on the results of susceptibility analysis, terrain units are categorized into five susceptibility classes, with an average annual landslide frequency ranging from <1 per km² to >10 per km² (Figure 12).



(a) 2-D landslide susceptibility map



(b) 3-D presentation

Figure 12. Natural terrain landslide susceptibility classification

(Note: Very High = landslide frequency > 100 no./km²; High= landslide frequency 40 - 100 no./km²
 Moderate = landslide frequency 20 - 40 no./km²; Low= landslide frequency 10 - 20 no./km²
 Very Low = landslide frequency ≤ 10 no./km²)

Wong (2003) discussed the implications of the limited resolution in the calculated landslide frequency among the different susceptibility classes, which is only within about one order of magnitude between the least and most susceptible classes. Such a resolution is considered insufficient for differentiation of vulnerable hillsides, especially in view of the potentially high consequence of landslides given Hong Kong's dense urban development setting. From a different perspective, the low resolution probably demonstrates a lack of understanding of the combination of factors that control landslide susceptibility. It may also reflect the possibility that the natural hillsides in Hong Kong are generally susceptible to shallow failures, with a relatively small difference in the landslide susceptibility between the 'more problematic' and 'less problematic' terrain.

The accuracy of the susceptibility assessment in forward prediction was assessed by the GEO. It is noteworthy that the resolution of the assessment is scale dependent, and that the resolution was found to reduce if a smaller area was used in the analysis. The susceptibility classification in territory-wide scale may not necessarily be consistent with that in regional-scale or area-scale (Figure 13). In essence, whilst the results of the territory-wide susceptibility assessment may give an overall picture of the relative susceptibility to landslides, the resolution is such that they would not be adequate for the assessment of individual sites.

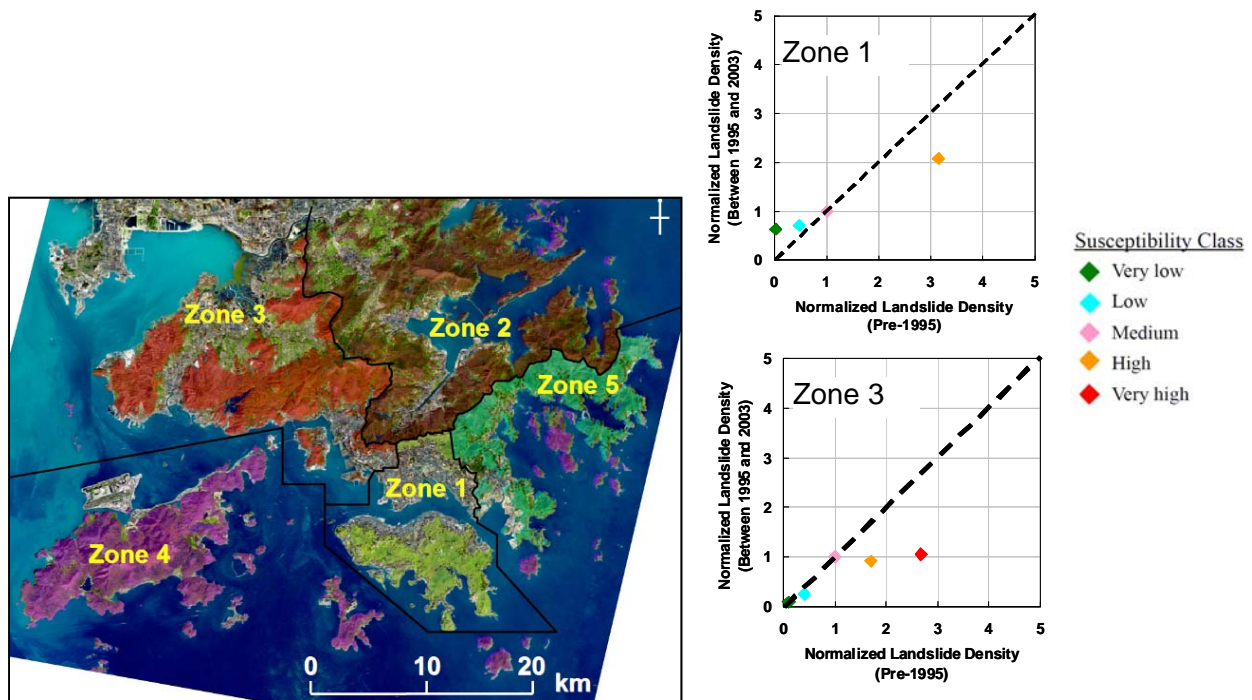


Figure 13. Consistency of susceptibility classification in smaller sub-regions

Some pilot coupled rainfall-susceptibility analyses have been conducted by the GEO, which showed that spatial and temporal variations in rainfall intensity could have a significant influence on landslide susceptibility. In particular, it was observed that at low rainfall intensity, landslides tend to occur predominately on the more susceptible terrain. However, given high rainfall intensity, even the relatively less susceptible terrain would suffer from failures. This reflects the fact that Hong Kong's steep hillsides are actively responding to heavy rain and are vulnerable to shallow slope failures.

8.6.3 Regional Susceptibility Analysis

(1) Lantau Island Susceptibility Analysis

A regional susceptibility analysis using the logistic regression technique was carried out at 1:5,000 scale on Lantau Island of Hong Kong, covering an area of about 140 km² (Dai & Lee 2002). Lantau Island was the largest outlying island in Hong Kong, with a history of natural terrain landslides. Previous field study and diagnostic analysis of natural terrain landslides on Lantau Island have identified landslide correlation with slope gradient, lithology and landform (Wong et al. 1998), as well as the importance of classifying the different landslide mechanisms and processes. In this regional susceptibility analysis, landslide susceptibility was assessed with the use of various terrain attributes including elevation, land cover and distance to drainage line in addition to slope gradient, lithology and landform. A GIS-based logistic regression model was used to relate combinations of terrain variables to landslide susceptibility, and to study the spatial distribution of landslide susceptibility (Figure 14). The model was found to have achieved a concordance rate of about 80% of the actual landslides being correctly classified with the use of a 50% probabilistic cut-off value.

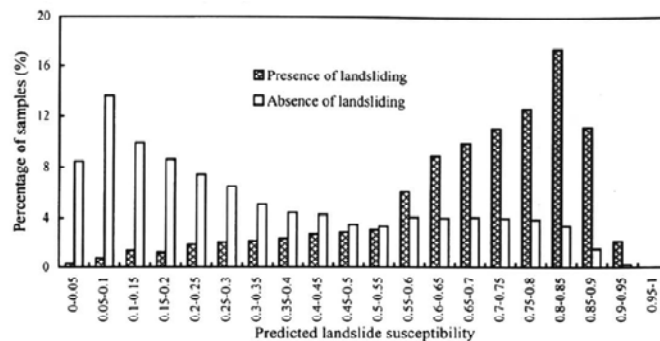


Figure 14. Comparison of predicted landslide susceptibility with actual landslides (based on Dai & Lee 2002)

The same methodology was also applied to a 13 km² zone in the Tung Chung area on Lantau Island. With the use of improved data quality (e.g. 1:5,000 geological data and 1:1,000 topographic data) and consideration of additional attributes (e.g. slope aspect, profile curvature and upslope catchment area), the concordance rate was improved to 87% (Dai 2002). Landslide susceptibility was zoned in terms of different classes, based on landslide probability predicted from the logistic regression model.

Another regional susceptibility analysis using the artificial neural network (ANN) technique was undertaken at 1:5,000 scale for the central part of Lantau Island, covering an area of about

45 km². The back propagation (BP) network method of ANN was applied, on a GIS platform. A total of 1,220 landslides were used as training samples to develop the trained network for the classification of landslide susceptibility. The model was reported to be able to predict 85% of the more recent landslides (Lee et al. 2002).

(3) Tsing Shan Area Susceptibility Analysis

An area-based susceptibility analysis of Tsing Shan Foothills of Hong Kong at 1:2,000 scale was completed, covering an area of about 10 km² with a history of failures. Positive correlation was established with three terrain attributes, viz. regolith type, lithological boundaries and proximity to the head of drainage lines, as obtained from detailed field mapping (MFJV 2003). As a result, an improved resolution was achieved in susceptibility zoning, which gives an average annual landslide frequency of >80 per km² at the most susceptible zone (Figure 15).

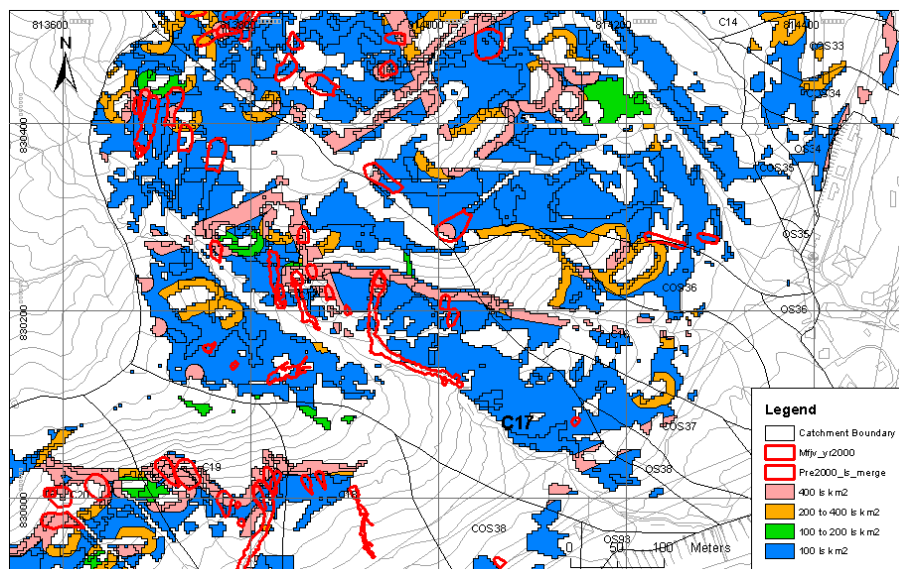


Figure 15. 1:2 000 susceptibility zoning from Tsing Shan study

8.6.4 Observations on Susceptibility Analysis

Wong (2003, 2009) reviewed the state of practice in susceptibility analysis and cautioned against the limited resolution and reliability achieved in susceptibility zoning, which affect its applicability to risk management. The key observations made are summarized as follows:

- Where data are available, it is practical to carry out susceptibility analysis to obtain insights on the correlation of landslide susceptibility with different terrain attributes, and to give broad categorization of landslide frequency and susceptibility zoning of terrain.
- Use of GIS technology greatly improves the capability and efficiency of susceptibility analysis and reduces human error. Statistical, probabilistic and ANN methodologies have proved to be useful tools for analyzing the data and developing landslide susceptibility models.
- Hong Kong is rich in landslide data at 1:20,000 to 5,000 scale. Regional analyses carried out at these scales gave reasonable statistical correlations and reasonable susceptibility

categorization. However, the resolution in respect of landslide frequency, which spans about one order of magnitude from the least to the most susceptible zone, is limited. Susceptibility analyses form an important part of the continued technical development work. However, given the low resolution in overall term, the derived zoning has not been directly applied to the management of natural terrain landslide risk under Hong Kong's slope safety system.

- The resolution and reliability of the susceptibility zoning can be improved in area-based studies at 1:2,000 to 1:1,000 scale, given the collation of supplementary information through field mapping. However, this requires considerable additional resources, which are costly particularly if a large area is to be covered. The work completed in Hong Kong to date shows that the resolution may be improved to cover about two orders of magnitude in respect of landslide frequency. Such improvement enhances hazard zoning and quantitative risk assessment work. However, susceptibility zoning with such a resolution is still of limited use for direct application to risk management in practice. As a comparison, it is not difficult to achieve a resolution better than three to four orders of magnitude in consequence assessments, for example, with the use of a generic consequence model (e.g. Wong et al. 1997). As a result risk zoning tends to be consequence-driven.

8.6.5 Engineering Geomorphological Assessment

The study of natural terrain hazards involves consideration of a given hillside in the context of its regional geological and geomorphological settings, any man-made influences that may have modified these settings, and the history of landsliding in the area (Ng et al. 2003). Geomorphology is the study of the forms of the surface of the earth. Their origins, the processes involved in their development, the properties of the materials which they are made of and predictions about their future form, behaviour and status (Brunsden et al. 1978).

Engineering geomorphological maps are a fundamental part of natural terrain hazard studies. By placing the hillside and its surroundings in a framework that integrates form, materials and process, the engineering geomorphological map helps the practitioners assess the influence of factors such as lithology, structure, materials and processes on past landform development, etc.

The main approach for the production of geomorphological maps in Hong Kong is a detailed aerial photograph interpretation, with an appropriate level of field verification. Aerial photograph coverage of Hong Kong is extensive. Aerial photographs covering the whole territory have been available since 1963. Repeated aerial photographs were taken annually to record the land use and development changes, as well as history of landslides.

Geomorphological mapping can be broadly divided into morphological (shape), morphographical (type), morphogenetic (origin) and morphochronological (age) components (Anon 1982), as follows:

- Morphological mapping involves the record of the detailed shape of the land surface, which can help identify landslide susceptibility areas, types of landslide hazard and possible extent of debris runout.

- Morphographical mapping has been used in Hong Kong in terms of regolith mapping, and is most applicable where there are lithological variations and significant elevation differences within the study area, resulting in a range of processes and hence regolith types. A regolith guide (available on <<http://hkss.cedd.gov.hk>>) was produced for the Tsing Shan foothills (MFJV 2002), where the regolith units were delineated based on a combination of topographical position, morphology, material type, vegetation cover and relative age.
- Morphogenetic mapping is mainly used where the landscape has been affected by different erosion and deposition processes.
- Morphochronological mapping is useful if a relative age relationship of landforms is discernible through aerial photograph interpretation. Improvements in dating techniques (e.g. Sewell & Campbell 2005) may facilitate further development of this type of mapping.

Different approaches to geomorphological mapping in respect of different terrain settings have been successfully adopted in some recent natural terrain hazard studies. A combination of approaches to geomorphological mapping is usually more beneficial when assessing natural terrain hazards. Useful results were reported with the use of engineering geomorphological (i.e. integration of engineering geology and geomorphology) assessments, e.g. Parry & Ruse (2002), HCL (2003), Mott Connell (2003) and OAP (2004).

(1) North-eastern Hong Kong Island Regional Study

In 2007, a pilot natural terrain hazard study was carried out for the north-eastern Hong Kong Island (MFJV 2009). The hazard maps produced take cognizance of the relationships between the information gathered from 1:2,500 scale engineering geomorphological mapping and the identified hazards (hazard type, location, volume range, etc.), together with consideration of historical landslide records and topographic data based on the results of the airborne Light Detection and Ranging (LiDAR) survey. The morphographic (i.e. type/regolith) information is also used in the hazard maps, typically to assess potential areas of erodible material (e.g. confined colluvium) along potential channelised debris flow paths.

The methodology adopted in the landslide hazard assessment considered the combination of hazard and proximity of the vulnerable facilities. Landslide hazard components include 'initiation' (potential source area location, magnitude and likelihood of occurrence), and 'mobility' (geomorphological setting, and drainage line characteristics, including entrainment potential).

The study provides an improved means of identifying natural terrain units that may be more susceptible to failure in general. It also offers insights that facilitate development of models for assessing where relatively rare but significant landslide hazards may be present, such as channelized debris flows originating on upper hillsides, with downslope cliffs along the drainage channel to boost the kinetic energy of debris, and entrainable materials along the streamcourse to significantly increase the debris volume (MFJV 2009).

(2) West Lantau Regional Study

In the West Lantau Study undertaken following the severe June 2008 rainstorm, a comprehensive engineering geomorphological mapping (AFJV 2010, Millis et al. 2010) was

carried out to extract relevant geological and topographical information of the natural terrain. The observations made during the API and field inspections indicated that the terrain within the study area could be broadly sub-divided into four 'Terrain Units' (viz. Incising Terrain Unit, Lower Terrain Unit, Middle Terrain Unit and Upper Terrain Unit) based on their regional scale, shape and form. These units reflect different stages and means of landscape evolution within the study area.

Landslide hazards within the study area were assessed based on the various components recorded within the engineering geomorphological maps, including the slope morphology, type and extent of superficial geological deposits, landform, drainage line characteristics and the 'Terrain Units'. The spatial distribution of the more hazardous zones was found to be in good agreement with the locations of both the historical landslide records and the June 2008 landslides (Figure 16).

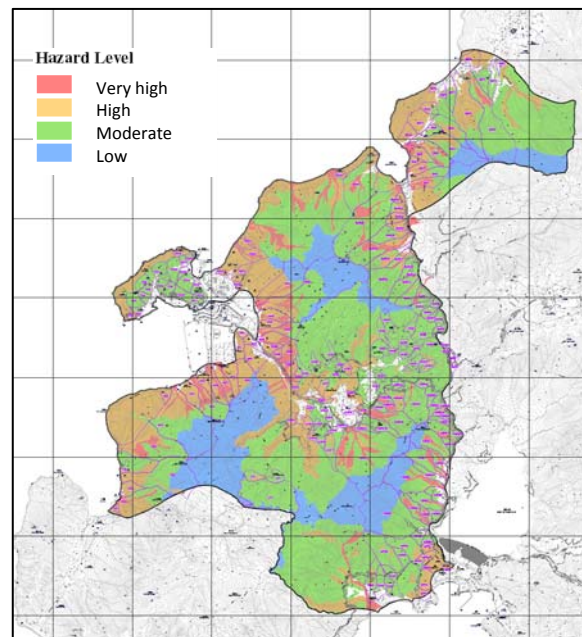


Figure 16. Landslide hazard map of the West Lantau regional study

The consequence of landslides within the study area has been evaluated based on two groups, viz. the occupied buildings within existing villages and selected transportation routes. By evaluating the relative landslide hazards in a given catchment against the corresponding landslide consequence, a risk matrix (Table 2) has been produced to allow screening and ranking of the hillside catchments.

Table 2a. Landslide risk assessment matrix for existing villages

HAZARD CONSEQUENCE	VERY HIGH	HIGH	MODERATE	LOW
VERY HIGH	VERY HIGH	VERY HIGH	HIGH	MODERATE
HIGH	VERY HIGH	HIGH	MODERATE	LOW
MODERATE	HIGH	MODERATE	LOW	LOW
LOW	MODERATE	LOW	LOW	LOW

Table 2b. Landslide risk assessment matrix for selected transportation routes

HAZARD CONSEQUENCE	VERY HIGH	HIGH	MODERATE	LOW
HIGH	VERY HIGH	HIGH	MODERATE	LOW
MODERATE	HIGH	MODERATE	LOW	LOW
LOW	MODERATE	LOW	LOW	LOW

8.7 Studies of Notable Natural Terrain Landslides

Landslide investigations have long played a key role in Hong Kong in advancing the profession's knowledge on slope performance and landslide mechanisms (Ho & Lau 2010). The systematic landslide investigation programme was launched by the GEO in 1997. The main goals of the systematic landslide investigation programme are as follows:

- (a) Identification of slopes in need of early attention under the slope retrofitting programme before the situation deteriorates to result in a serious problem;
- (b) Improvement in the knowledge on causes and mechanisms of landslides;
- (c) Auditing the performance of the Government's slope safety management system to identify areas that warrant improvement; and
- (d) Providing evidence in respect of serious landslides that may involve Coroner's inquests, legal action or financial dispute.

Since 1997, more than 3,000 landslide records have been examined, and around 200 landslide studies have been completed. In addition to the study reports on the individual landslides, thematic studies have also been carried out (e.g. review of soil-nailed slope failures, review of landslides during construction, etc.). The key findings and lessons learnt are uploaded to the Government's Slope Safety Website (<http://hkss.cedd.gov.hk>).

8.7.1 1990 and 2000 Tsing Shan Debris Flows

The 1990 Tsing Shan debris flow (Figure 17) is a significant landslide incident in Hong Kong and was studied in detail (Chan et al. 1991, King 1996). The landslide started off as a relatively modest debris avalanche of about 350 m³ at the landslide source. It developed into a 20,000 m³ mobile debris flow through material entrainment, with a total runout distance of about 1 km. This debris flow is regarded locally as an example of a low-frequency, large-magnitude landslide, and quoted internationally as a case that illustrates very high debris flow entrainment (Jakob & Hungr 2005). Before the debris flow, the planned development in the area was encroaching on the Tsing Shan foothills. The debris flow could have resulted in serious consequences if the site traversed by the debris flow had already been developed at the time. After the debris flow, the land use at the site was amended from residential development to a golf driving range in order to minimise the risk exposure. The case is a vivid illustration of the risk of debris flows and the importance of proper land-use and development planning in controlling undue increase in the risk of natural terrain landslides.

In 2000, another sizeable debris flow with a volume of about 1,600 m³ occurred on the adjoining area on the same hillside above Tsing Shan (King 2001). The landslide debris moved

down to a spur at mid-slope where it bifurcated to form channelized debris flows in the two downslope drainage lines (Figure 18). The golf driving range and the Light Rail Transit at the toe of the hillside were affected by the landslide mass and the subsequent outwash material.

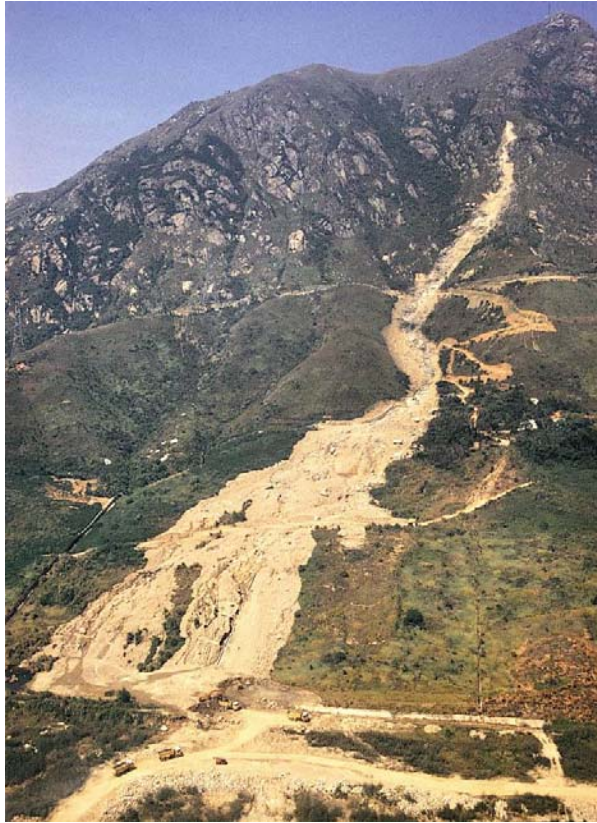


Figure 17. The 1990 Tsing Shan debris flow

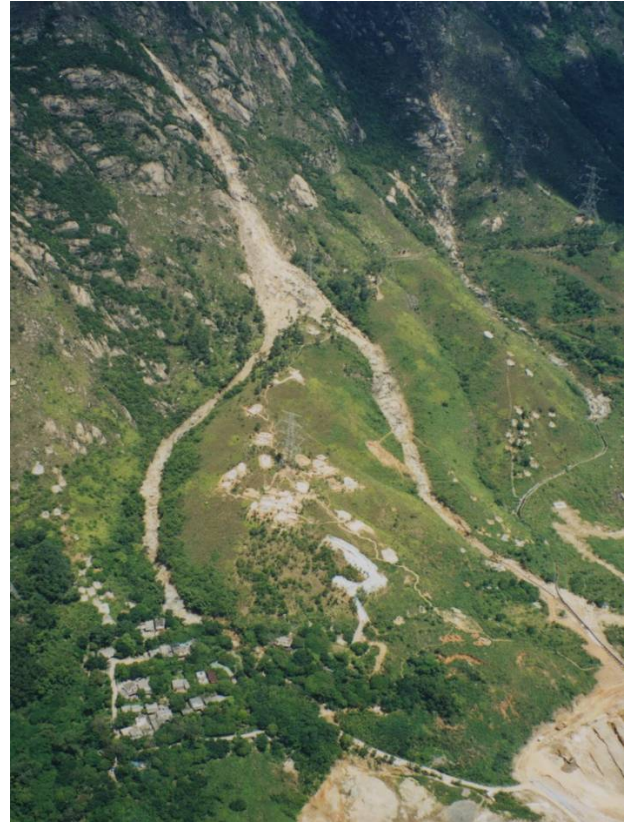


Figure 18. The 2000 Tsing Shan debris flow

8.7.2 1993 Natural Terrain Landslides on Lantau Island

Over 860 natural terrain landslides were triggered on Lantau Island (Figure 19) by the severe rainstorm of 5 November 1993. The landslides resulted in blockage of roads and catchwaters. As Lantau Island was largely undeveloped at that time, there were no landslide casualties. The landslides were mapped and the data collected were analysed (Wong et al. 1998). The study established that a high density of natural terrain landslides could be triggered in a severe rainstorm (about 7 landslides/km² in the region affected by high rainfall intensity in this rainstorm), and that terrain at a gradient of 30° to 35° underlain by volcanic rocks appeared to be particularly susceptible to failure.

Empirical assessment of landslide debris runout data showed that debris mobility was affected by the mechanism of debris movement, with channelized debris flows being more mobile than open hillslope failures. The study carried out by Franks (1998) on the 1993 landslides that flanked the Tung Chung New Town, which was being developed at that time, also arrived at similar observations.



Figure 19. The 1993 natural terrain landslides in Lantau Island

8.7.3 2008 Natural Terrain Landslides on West Lantau

A very severe rainstorm hit Lantau Island in June 2008 and caused about 2,400 natural terrain landslides (Figure 20). Some of the landslides were fairly sizeable by reference to the past landslides and resulted in a much greater runout distance than those that have previously occurred in Hong Kong. The 4-hour duration rainfall (with a rolling maximum of 384 mm) was the most critical (with a calculated return period of 500 to 1,000 years based on past rainfall statistics), which was more severe than that experienced in previous rainstorms. Detailed mapping of the landslides and related technical development studies have been initiated. The landslides serve as a vivid reminder of the risk associated with natural terrain landslides in the densely developed setting of Hong Kong. Some of the pertinent findings of the landslide investigations are as follows:

(a) natural terrain landslides predominantly involved shallow failures (typically within 1 to 2 m of the surface mantle), whereas deep failures rarely occur.

(b) the occurrence of natural terrain landslides is closely related to both 24-hour and 4-hour rolling rainfall, but it does not appear to be sensitive to shorter duration (e.g. 1-hour and 2-hour) rainfall. This finding is consistent with the observed shallow depths of failures caused by slope saturation and transient build-up of groundwater pressures as a result of direct infiltration and sub-surface seepage flows.

(c) the density of natural terrain landslides increases exponentially with rainfall intensity (Figure 21). In addition, the corresponding scale of failure and mobility of landslide debris also increase with the severity of rainfall. The above highlight that natural terrain landslide hazards are highly sensitive to climate change, which may result in more frequent occurrence of extreme rainfall conditions.

(d) the available landslide inventory covers the recent natural terrain landslides over the past few decades; this is a relatively short observation period and caution is needed as far as assessment of extreme events is concerned.



Figure 20. Landslides in Tai O, Lantau after the June 2008 rainstorm

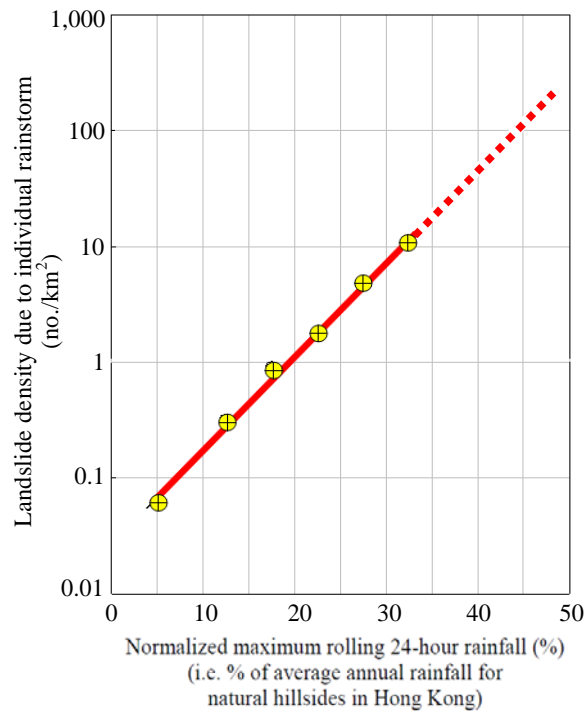


Figure 21. Rainfall-landslide correlation for natural hillside in Hong Kong

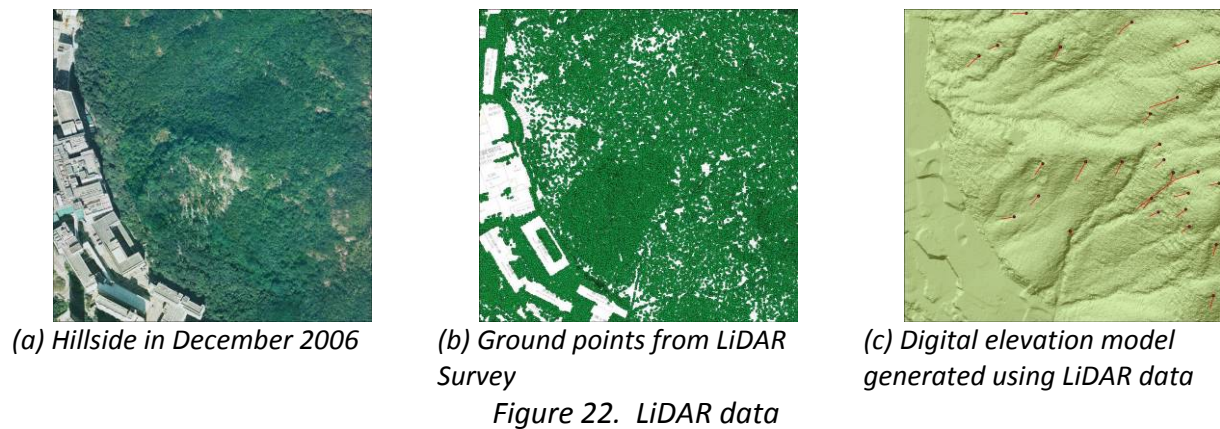
8.8 Rainfall-Landslide Correlations for Natural Terrain

The vast majority of landslides in Hong Kong are triggered by rainfall. Hong Kong has a dense network of automatic raingauges at strategic locations since the early 1980s. At present, there are a total of 110 raingauges that collate and transmit real-time rainfall data through wireless transmission technology (viz. General Packet Radio Service), at five-minute intervals round the clock.

Study of the correlations between the density of natural terrain landslides and rainfall intensity has provided insights into the effects of rainfall on natural terrain landslide occurrence and assisted in risk management and disaster preparedness. The study incorporated the use of GIS and statistical techniques to improve the assessment (Ko 2003, Wong et al. 2004a). The comprehensive inventory of historical natural terrain landslides and detailed rainfall records available in Hong Kong since 1985 provide the essential data for the diagnosis. The study showed that density of natural terrain landslides in Hong Kong increases exponentially with normalised rainfall intensity (i.e. normalised with the mean annual rainfall) (Figure 21).

8.9 Application of Digital Technology

Significant advances have been made in Hong Kong in the application of digital and remote sensing technologies to enhance the capability and efficiency of NTHS. Among these, digital photogrammetry, Geographic Information System (GIS), Global Positioning System (GPS), terrestrial and airborne LiDAR (Figure 22), Ground-based Interferometric Synthetic Aperture Radar (InSAR) (Figure 23) have provided promising results. A summary of the technological development and applications is given by Wong (2007). In addition, an improved capability in real-time slope monitoring has also been capitalised and applied in practice as one of the risk management tools (Lau et al. 2008, Solomon et al. 2008).



Multi-return airborne LiDAR survey has shown promising results in producing high resolution digital elevation models that can ‘see through’ vegetation to derive the ground profile (Ng & Chiu 2008). Landslide scars and geomorphological features on hillsides can be vividly recognised in the high-resolution digital elevation models derived from the LiDAR survey data.

Interferometric Synthetic Aperture Radar (InSAR) is an emerging remote sensing technology that could measure ground displacements with millimeter-level accuracy. Through repeated observations, it is possible to measure the surface displacement if ground movement has occurred over the observation period. In 2009, the GEO conducted a pilot trial of a ground-based InSAR system (Figure 23) to assess its performance in relation to the resolution, accuracy, range, line of sight and environmental conditions (high temperature and moderate to heavy rainfall). The results suggest that the ground-based InSAR technique is potentially a promising low cost, high accuracy remote sensing technique for geotechnical use, particularly for ground and rock slope movement detection (Hui in prep.).

The GEO has also continued to make progress in building up a GIS-based geotechnical information database (known as GInfo) and developing the corresponding web-based applications. A number of applications have been launched in 2009, including the digital Geotechnical Information Unit (GIU), GEO Raingauge System in the Internet and the ArcGIS browser. The ArcGIS browser (Figure 24) has been integrated with other existing GEO web-based information systems so that information from these systems could be retrieved through the ArcGIS browser. It has also been revamped to take advantages of the latest web technology and provide a rich internet application experience with fast retrieval of spatial data and efficient browsing to users. The capability of 3D web browser (i.e. ArcExplorer) will also be further explored.

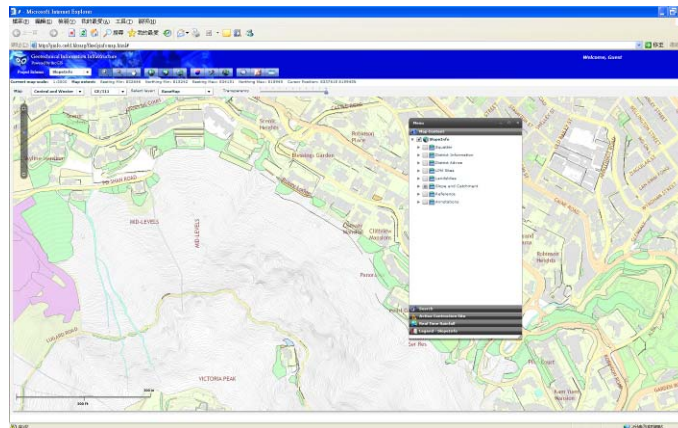


Figure 24. GEO web-based information system

While GIS data management and information services remain important, a notable recent trend is to adopt more advanced GIS functionality to address geotechnical issues in Hong Kong (e.g. search, browsing, analysis, modelling, mobile applications, 3-D visualization and virtual reality applications, etc.).

8.10 Natural Terrain Landslide Risk Assessment

One of the starting points of risk assessment is hazard identification and hazard study. The scope of a Natural Terrain Hazard Study (NTHS) comprises:

(a) the determination of the locations, types and magnitude of any natural terrain hazards that may affect the development of a site through a thorough engineering geological assessment, and

(b) where an identified hazard is deemed to affect the site of concern, determine the design event for such a hazard and formulate a mitigation strategy to reduce the risk it poses to the development.

Based on the information collected and interpreted, a geological and geomorphological model of current and past hillside processes in the study area should be developed. This will form a basis for assessing the likely sources, nature and volume of any instability that could affect the site. It is prudent to look beyond the hillside catchment boundary so as to observe processes and events in the adjacent or similar catchments that may be relevant for determining the possible hazards to the site.

The geological and geomorphological model should be specifically designed for each assessment and should combine the API with the engineering geological mapping. Historical landslide data often provide vital information for construction and calibration of the model. In the context of an NTHS, a representative geological/geomorphological model is essential for assessing the types of landslide hazards that may occur, the likelihood of their occurrence and the possible scale of failures.

8.10.1 Study Approaches

The insights gained on natural terrain hazards through the technical development work have resulted in the rationalisation of the appropriate technical approach for dealing with the hazards. In Hong Kong, three different approaches, viz., Factor of Safety, Design Event and QRA (Figure 25), are recommended for dealing with natural terrain hazards (Wong 2005).

The conventional Factor of Safety Approach aims to avert landslides by ensuring a prescribed margin of safety against slope failure. This is applicable to natural terrain if the design objective is to reduce the likelihood of slope failure, e.g. where developments are located above the natural hillside. However, it is often not suitable for use in dealing with a large area of natural hillside that poses a risk to facilities located at its toe. Given the large area of potentially unstable natural terrain involved, such landslide preventive works are likely to be exceedingly expensive and may not be justified. Also, widespread stabilisation works on natural terrain could cause considerable environmental problems and they are difficult to implement in practice.

The framework of the Design Event Approach (DEA) comprises a qualitative risk-based assessment (Tables 3 & 4) and is applicable when designers opt for mitigation of natural terrain landslide risk without carrying out a formal quantitative risk assessment (QRA). Under this approach, the required mitigation measures (e.g. debris-resisting barriers) to protect a development from natural terrain landslides are established by reference to an assessment of

the design landslide event, which is done in a semi-quantitative manner that may occur on the hillside and affect the development. Uncertainties are generally considered in an implicit manner through the direct assessment of the design event, e.g. a landslide of a certain size with a given degree of mobility. Where the debris thickness and spatial extent of the debris runout and deposition zones may be sensitive to the method of dynamic modelling or critical to the hazard/design assessment, sensitive analysis should be conducted as appropriate to address the possible uncertainties associated with the input data and assumptions.

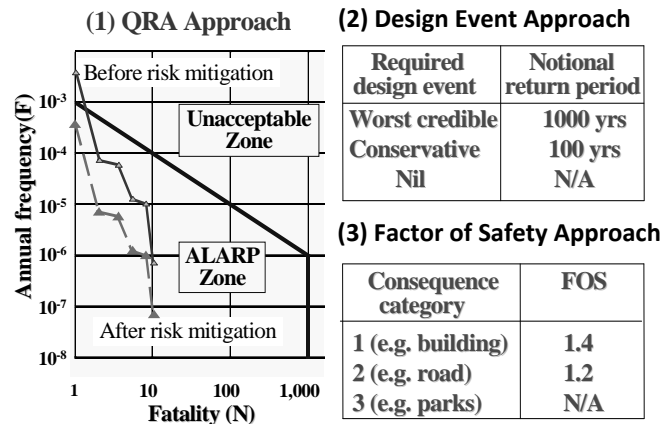


Figure 25. Different approaches adopted in the assessment and mitigation of natural terrain landslide hazards in Hong Kong

Depending on the potential landslide consequence and susceptibility of the hillside, the required design event may either be a 'worst credible' event or a 'conservative' event under the DEA framework, which correspond to a notional return period of 1,000 years and 100 years respectively. The DEA is relatively easy to apply, as it does not demand formal and rigorous quantification of risk, and is therefore favoured by many local practitioners. The approach has been used in the assessment for the Sham Tseng San Tsuen site (MGSL 2000) and hillside overlooking Shek Pik School and Hostel (Parry 2001). However, it should be noted that the DEA approach gives no provision for the consideration of practicality and cost-effectiveness of the proposed risk mitigation measures.

The QRA approach is applicable when designers opt for quantification and management of natural terrain landslide risk. Based on this approach, the designer can evaluate the risk of natural terrain landslides. The need for any necessary risk mitigation measures is assessed by reference to GEO's risk criteria (ERM 1998). The QRA approach entails a detailed assessment of the probability and consequence of natural terrain landslides, with account taken of the uncertainties in an explicit and systematic manner, and consideration of the tolerability of the assessed risk levels (both the individual risk and the societal risk). It may be considered as the most rigorous and comprehensive assessment. The assessment often requires expert input and may be fairly involved and costly. Further elaboration of the QRA approach is given in Section 12 below.

Table 3 Design requirements for Design Event Approach Table 4. Consequence classes

Susceptibility Class	Consequence Class				
	I	II	III	IV	V
A	WCE	WCE	WCE	CE	N
B	WCE	WCE	CE	CE	N
C	WCE	CE	CE	N	N
D	N	N	N	N	N

Notes:

(1) See Table 4 for definition of Consequence Class.

(2) Susceptibility Class as defined in Wong (2000), where:

A = Extremely susceptible; notional annual probability ≥ 0.1

B = Highly susceptible; notional annual probability 0.1 to 0.01

C = Moderately susceptible; notional annual probability 0.01 to 0.001

D = Low susceptibility; notional annual probability < 0.001

(3) WCE = Adopt a 'worst credible' event as the design event. A 'worst credible' event is a very conservative estimate such that the occurrence of a more severe event is sufficiently unlikely. Its notional return period is in the order of 1,000 years.

CE = Adopt a 'conservative' event as the design event. A 'conservative' event is a reasonably safe estimate of the hazard that may affect the site, with a notional return period in the order of 100 years.

N = Further study is not required

Proximity	Facility Group No.			
	1 & 2	3	4	5
Very Close (e.g. if angular elevation from the site is $\geq 30^\circ$)	I	II	III	IV
Moderately Close (e.g. if angular elevation from the site is $\geq 25^\circ$)	II	III	IV	V
Far (e.g. if angular elevation from the site is $< 25^\circ$)	III	IV	V	V

Notes:

(1) Facility groups are described in Table 10.

(2) For channelized debris flow, if the worst credible event affecting the site is judged to have a volume exceeding 2,000 m³, the angular elevation given in the above examples should be reduced by 5°.

(3) The above are for general guidance only. Other factors, such as credible debris path, topographical conditions and site-specific historical data, should also be taken into account in assessing the 'proximity' of the natural terrain to the site.

8.11 Qualitative Risk Assessment

Site-specific qualitative risk assessment embraces a broad range of qualitative and semi-quantitative approaches applied to analyze and manage the landslide risk at individual sites. The work is carried out with a resolution and reliability that are deemed to be adequate for use in making site-specific risk management decisions, without formally quantifying the risk.

A suite of methodologies have been developed and adopted in qualitative risk assessment. Examples include the Failure Modes and Effects Analysis (FMEA), Hazard and Operability Study (HAZOP) and Potential Problem Analysis (PPA). Among these methods, FMEA was commonly adopted in geotechnical risk assessment, e.g. geo-environmental risk management in mining projects (Dushnisky 1996), and dam risk management (Hughes et al. 2000, Stewart 2000). FMEA directs attention towards understanding the behavior of the physical components of a system, the possible failure modes, and the influence failure would have on each other and on the system as a whole. As noted by Vick (2002), it is usually used in two ways:

(a) to assist in hazard identification and risk screening, typically as a precursor to more detailed risk assessment; and

(b) to serve as a stand-alone preliminary risk assessment procedure.

A variety of qualitative and semi-qualitative risk assessment methods are available, including risk matrix, etc. A summary of which is given by Lee & Jones (2004). Many examples of site-specific application of qualitative risk assessment have been reported in the literature (e.g. Hutchinson 1992, Morgenstern 1995 & 2000, Vick 2002). Two cases are described below to illustrate its role and diverse range of applications in landslide risk management.

8.11.1 Shatin Heights

Table 5 shows an example of application of FMEA to assess the risk of natural terrain landslides in Shatin Heights, Hong Kong. The FMEA table was devised to address the specific circumstances of the site. The classification schemes that accompanied the FMEA are explained in Table 6.

The natural hillside at Shatin Heights is bounded by residential buildings at the crest and toe of the hillside (Figure 26). In 1997, a total of six landslides occurred on the hillside, and three of these developed into debris flows that ran into the buildings at the toe of the hillside. After the failures, the landslides were studied (GEO 1998b) and a Natural Terrain Hazard Study was carried out on the site (FMSW 2001). These provided data, which were incorporated into the FMEA for working out the semi-quantitative hazard and consequence categories in the FMEA table. The case study of using qualitative technique showed the following:

(a) The FMEA has facilitated hazard identification and provided a preliminary assessment of the risk. In this case, out of the 15 possible hazard scenarios, 5 were identified by FMEA as of risk concern and requiring further risk assessment. The likely order of risk of each of the five hazards was also estimated. Although these are not formal QRA figures, they give a preliminary indication of the possible level and severity of the risk.

(b) The availability of data and technical understanding of the landslide hazards at the site is a prerequisite for successfully using FMEA in site-specific qualitative risk assessment. Otherwise, the reliability of the assessment and its suitability for supporting site-specific risk management application are in question. In such cases, the FMEA assessment would practically be reduced to, at best, a relative risk rating process.

(c) The FMEA table can become very long (i.e. with many rows) when it is applied to a large site. Formulating a suitable FMEA table that addresses the particular circumstances of a site is important to the efficient and effective use of FMEA.

(d) The case also illustrates the use of a risk-matrix (Table 6) in evaluating the risk category and thereby providing a basis for hazard identification and risk estimation. The risk matrix combines different classes of the frequency and consequence of landslide, which may be aligned with some notional probabilities of failure and descriptions of the severity of landslide consequence respectively.

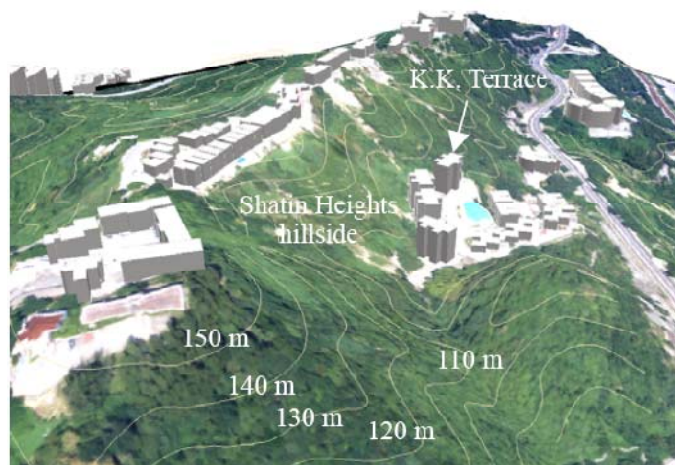


Figure 26. Shatin Heights, Hong Kong

Table 5 FEMA on Shatin Heights catchment No. 7

Component	Failure Mode (Notes (1))	Effects on K.K. Terrace	Likelihood Category			Loss of Life		Economic Loss & Disruption to Community		Risk Category (Proceed to detailed assessment?)
			Failure	Effect	Hazard	Consequence Category	Risk Category	Consequence Category	Risk Category	
Catchments 7a, 7d & 7h	Shallow landslide resulting in small-scaled open-slope debris slide/avalanche (SH1)	Debris run into and affect 1/F of K.K. Terrace	C to D	z	D to E	2	L to V	III	N	Low (Yes)
	Deep landslide resulting in medium- to large-scaled fast moving debris slide/avalanche (SH2 to SH3)	Debris run into and affect 1/F of K.K. Terrace	E	x	E	2	V	III	N	Very Low (No)
		Debris hit K.K. Terrace and result in building collapse or major structural damage		z	E-	1	V	II	N	Very Low (No)
Deep landslide resulting in medium- to large-scaled debris with limited mobility (SH2 to SH3)	Prolonged evacuation of K.K. Terrace	E	y	E-	5	N	II to III	N	Residual (No)	
Catchments 7b, 7e, 7f, 7i & 7j	Shallow landslide resulting in small- to medium-scaled debris flow without significant entrainment (TH1 to TH2)	Debris run into and affect 1/F of K.K. Terrace	D	x	B	2	H	III	L	High (Yes)
		Debris hit and affect the entrance to K.K. Terrace		y	B to C	3	M to L	IV	N	Moderate (Yes)
	Shallow landslide resulting in medium- to large-scaled debris flow with significant entrainment (TH2 to TH3)	Debris run into and affect 1/F of K.K. Terrace	D	x	D	2	L	III	N	Low (Yes)
		Debris hit and affect the entrance to K.K. Terrace		y	D to E	3	V to N	IV	N	Very Low (No)
Deep landslide resulting in medium- to large-scaled fast moving debris (SH2 to SH3)	Debris hit K.K. Terrace and result in building collapse or major structural damage		z	E	1	L	II	N	Low (Yes)	
Shallow landslide resulting in small-scaled debris with limited mobility (TH1)	Temporary evacuation of 1/F of K.K. Terrace	B	y	B to C	5	N	IV	V to N	Very Low (No)	
Catchments 7c, 7g & 7k	Shallow landslide resulting in small-scaled open-slope debris slide/avalanche (SH1)	Debris hit and affect the entrance to K.K. Terrace	C to D	z	D to E	3 to 4	V to N	IV	V	Very Low (No)
	Deep landslide resulting in medium-to-large scaled fast moving debris (SH2 to SH3)	Debris hit and affect the G/F of K.K. Terrace, including the entrance, G/F lobby, car park and drive way	E	x	E	2	V	III	N	Very Low (No)
		Debris hit K.K. Terrace and result in building collapse or major structural damage		z	E-	1	V	II	N	Very Low (No)
	Deep landslide resulting in medium- to large-scaled debris with limited mobility (SH2 to SH3)	Temporary evacuation of K.K. Terrace and the sole vehicular access to K.K. Terrace and Woodcrest	E	x	E	5	N	III	N	Residual (No)
Prolonged closure of the sole vehicular access to K.K. Terrace and Woodcrest		z		E-	5	N	II	N	Residual (No)	

Note: See Table 6 for the likelihood, consequence and risk categorization.

Table 6 FEMA categorization scheme

Risk Category		Risk to Life					Economic Loss				
		Loss of Life Consequence Category					Economic Loss & Disruption to Community Consequence Category				
		1	2	3	4	5	I	II	III	IV	V
Hazard Likelihood Category	A	H	H	H	H	R	H	M	L	R	R
	B	H	H	H	L	R	M	L	V	R	R
	C	H	M	L	V	R	L	V	R	R	R
	D	M	L	R	R	R	V	R	R	R	R
	E	L	V	R	R	R	R	R	R	R	R
	E-	V	R	R	R	R	R	R	R	R	R

Notes: PLL is the average number of fatalities per year. Risk Category is defined as follows:

Class	Descriptions (PLL for risk to life)	Further study
H	High – of major concern (notional PLL $> 10^{-3}$)	This failure mode should be examined with priority attention, to assess/verify the scale of the problem
M	Moderate – of considerable concern (notional PLL form 10^{-3} to 10^{-4})	This failure mode should be examined, to assess/verify the scale of the problem
L	Low – of some concern (notional PLL form 10^{-4} to 10^{-5})	It is advisable to examine this failure mode, to assess/ verify the scale of the problem
V	Very low – practically not a concern (notional PLL less than 10^{-5})	Further study not warranted except in special circumstances
R	Residual risk – no indication of risk problem	Further study not warranted

(a) Risk Category

Class	Failure Likelihood Category
A	Very high (notionally 1 in 10 years)
B	High (notionally 1 in 10 to 100 years)
C	Moderate (notionally 1 in 100 to 1,000 years)
D	Low (notionally 1 in 1,000 to 10,000 years)
E	Very low (notionally much less than 1 in 10,000 years)

Class	Effect Likelihood Category (likelihood of occurrence of the stated effects given the failure mode)	Adjustment on Failure Likelihood Category
x	Probable (notionally 0.5 or higher)	No change
y	Quite possible (notionally 0.1 to 0.5)	Downgrade by half a category
z	Possible (notionally < 0.1)	Downgrade by one category

(b) Likelihood Category

Class	Loss of Life Consequence Category
1	Very high chance of loss of life (PLL notionally > 1); multiple fatalities may occur
2	High change of loss of life (PLL notionally 0.1 to 1); low chance of multiple fatalities
3	Moderate chance of loss of life (PLL notionally 0.01 to 0.1)
4	Low chance of loss of life (PLL notionally < 0.01)
5	Very low chance of loss of life (PLL much less than 0.01)

Class	Economic Loss & Disruption to Community Consequence Category
I	Very high (severe structural damage to multi-story buildings; prolonged evacuation of multi-story building or a large number of houses; prolonged breakdown of transportation network)
II	High (severe structural damage to within a few flats or individual houses; prolonged evacuation of within a few flats or individual houses; prolonged closure of major road or important access; temporary breakdown of transportation network)
III	Moderate (some damage to properties; temporary evacuation of within a few flats or individual houses; temporary closure of major road or important access)
IV	Low (less serious than above)
V	Very low (much less serious than above)

(c) Consequence Category

8.11.2 Tung Wan, South Lantau

In 1999, two landslides occurred in natural terrain adjacent to a school and hostel at Tung Wan, Lantau (Figure 27). A natural terrain hazard study was carried out by the GEO, which comprises site-specific aerial photograph interpretation (API), engineering geological mapping, hazard identification and evaluation of the magnitude of the natural terrain landslides as design event for hazard mitigation (Parry & Wong 2002).

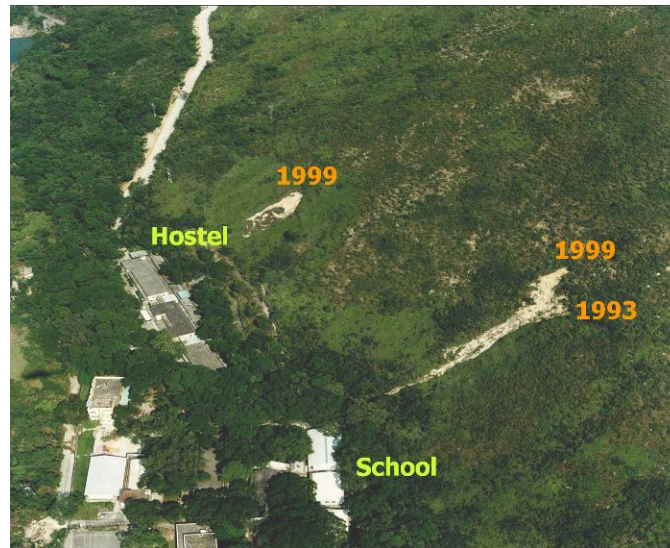


Figure 27. Open hillslope failure above the Hostel and channelised debris flow above the School, Tung Wan, South Lantau

Discrepancies were noted between the NTLI data and the site-specific API, particularly for relict landslides. Of the 70 NTLI relict features within the study area, only 33 could be confirmed by the site-specific API. This is probably the result of using low-flight aerial photographs in the site-specific API, whereas high-flight aerial photographs were used in compiling the NTLI database. Some well developed incised drainage lines were mis-identified as landslide scars in the NTLI.

In addition to the slope angle and solid geology, slope aspect was found to be a controlling factor for landslide susceptibility, with relatively high susceptibility between 330° to 120° (i.e. northwesterly to southeasterly facing). An examination of the structural data suggested that the high susceptibility aspect might be related to the dip directions of release surfaces.

Based on the results of the hazard assessment, the school and the hostel would be affected by open hillside failures and channelized debris flows respectively. The design event approach was adopted in the hazard assessment.

A design volume of 300 m^3 , corresponding to a 'worst credible' event, was recommended for open hillslope failures, based on consideration of the scale of historical failures and the geomorphological setting of the site. The study noted that caution should be exercised in using the frequency-magnitude relationship to estimate the landslide volume for different design events, as the relationship may not take into account of the geological setting of the site. Some

existing rock outcrops on slope would provide a constraint to uphill regression of landslide scar, thus limiting the size of the future landslide source volume.

Based on the findings of the field mapping along drainage lines, entrainment was considered to be negligible. Two design scenarios were recommended for the channelized debris flows:

- (a) A 300 m³ event, with landslide mobility more mobile than previous failures, and
- (b) A 600 m³ event (i.e. to account for the scenario of more than one failure occurring along a drainage line), with landslide mobility comparable with the recent failures.

8.12 Impetus to the Use of Quantitative Risk Assessment In Hong Kong

Hong Kong was amongst the pioneers to apply QRA techniques to help manage landslide risk, as well as to measure the performance of its slope safety system.

Since the mid-1990s, the GEO has steered the novel development and application of QRA in the formulation of slope safety policy (Ho & Ko 2007). The concepts, techniques and applications of landslide risk assessment have evolved with time and the developments at different times are summarised in a number of state-of-the-art papers, e.g. Wong et al. (1997), Ho et al. (2000) and Wong (2005).

QRA has been applied to two types of landslide risk assessment in Hong Kong:

(a) Global (or portfolio) QRA – this is used to assess the overall risk of certain types of landslide hazards posed to a given community. This can provide a useful and valuable reference for landslide risk management, in particular the consideration of the scale of the problem, resources allocation and formulation of risk management strategies. Notable examples of global QRA carried out in Hong Kong include the assessment of the overall risk from failures of registered man-made slopes, viz. comprising about 39,000 pre-GEO slopes and 21,000 post-GEO slopes (Wong & Ho 1998, Cheung & Shiu 2002, Lo & Cheung 2004), boulder fall risk (Reeves et al. 1998), risk of earthquake-induced landslides on man-made slopes (Wong & Ho 1999), risk of natural terrain landslides (Wong 2005) and risk of boulder falls (MGSL 1998).

(b) Site-specific QRA – this is to assess the natural terrain landslide risk at a given site. This is most useful for problems that may not be directly amenable to conventional slope stability analysis, or where a failure is liable to result in serious consequences. It facilitates the development of cost-effective mitigation strategy for management of the landslide risk on individual sites. Notable examples include those reported by Ho et al. (2000), Ho & Wong (2001), OAP (2003) and FSWJV (2006). Site-specific QRA may also provide a benchmark for calibrating the results of global risk assessments.

8.12.1 QRA Framework

Landslide risk is a measure of the chance of occurrence of slope failure causing a certain amount of harm (e.g. fatalities and economic losses), and can be quantified as the product of the probability and consequence of failure.

Risk = (Frequency of failure) × (Consequence of failure)

where

Frequency of failure = probability of occurrence of a given type of landslide hazard within a given area in a given time period (typically one year).

Consequence of failure = degree of damage in the event of occurrence of a given type of landslide hazard within a given area.

Landslide risk analysis in QRA is carried out through a systematic examination of the severity of the consequences and the probabilities for the various factors. The following key questions are addressed systematically under a risk-based framework:

- (a) What can cause harm? [Hazard identification]
- (b) How often? [Frequency assessment]
- (c) What can go wrong, how likely and how bad? [Consequence assessment]
- (d) What is the likelihood of damage? [Risk quantification]
- (e) What is the significance? [Risk evaluation]
- (f) What should be done? [Risk mitigation]

For QRA applications, an assessment of the frequency of different types of landslides is required, which can be assessed directly using past failure data. It is noteworthy that use of archived failure data is the norm in QRAs for major industrial hazards.

In a formal QRA, the findings of a risk analysis are to be presented in the following format:

(a) individual risk (which relates to the risk posed to a single person at a specific location), and

(b) societal risk (which relates to the risk posed to the affected population as a whole) – this is usually expressed as an F-N curve, i.e. a graphical representation of the cumulative frequency of N or more fatalities plotted against the number of fatalities (N) on a log-log scale, or as the Potential Loss of Life (PLL).

Results presented in the form of an F-N curve will allow an assessment of not only the average number of fatalities but also the full range of scenarios, including events that are liable to bring about multiple fatalities.

Risk tolerability criteria are defined separately for individual risk and societal risk (in terms of an F-N plot). The slope of the risk tolerability criteria defined in F-N curve reflects the aversion to high-fatality events, i.e. a steeper line represents a greater aversion to high-fatality incidents.

As noted above, the societal risk may alternatively be expressed in the form of a risk index known as Potential Loss of Life (PLL), i.e. annual fatality rates or average number of fatalities per year which is calculated as follows:

$$PLL = \sum(f_i \times N_i)$$

where

f_i = frequency of landslide incident i , and

N_i = estimated number of fatalities for landslide incident i

PLL is given by the area under the curve of frequency of occurrence of N fatalities plotted against N . It should be noted that PLL treat all fatalities as equally important, irrespective of whether they occur in the high-fatality range or low-fatality range.

Landslide risk management comprises an estimation of the landslide risk, deciding whether or not the risk is tolerable, implementing appropriate control measures to reduce the risk where the risk level cannot be tolerated (Figure 28). In a wider context, landslide risk management also embraces the systematic application of management policies, procedures and practice to the tasks of identifying, analyzing, assessing, mitigating and monitoring landslide risk.

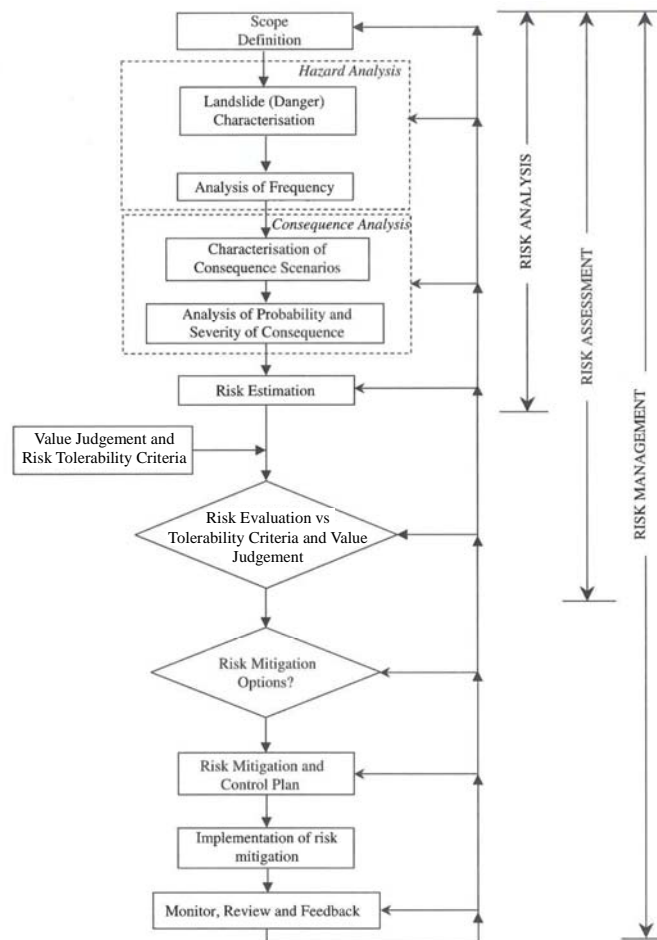


Figure 28. Flow chart for landslide risk management (based on Fell et al. 2005)

8.12.2 Risk Criteria

Risk criteria constitute an essential component of the quantified risk management framework and are used to evaluate the tolerability of the calculated risk levels. Based on benchmarking with the risk criteria adopted for major industrial hazards and dams in other countries, together with the risk criteria previously adopted for Potentially Hazardous Installations (PHI) in Hong Kong, the GEO formulated interim tolerable risk guidelines for natural terrain landslide hazards (ERM 1998). These criteria are defined in terms of Individual Risk and Societal Risk. The Individual Risk criteria relate to the annual probability of fatality for

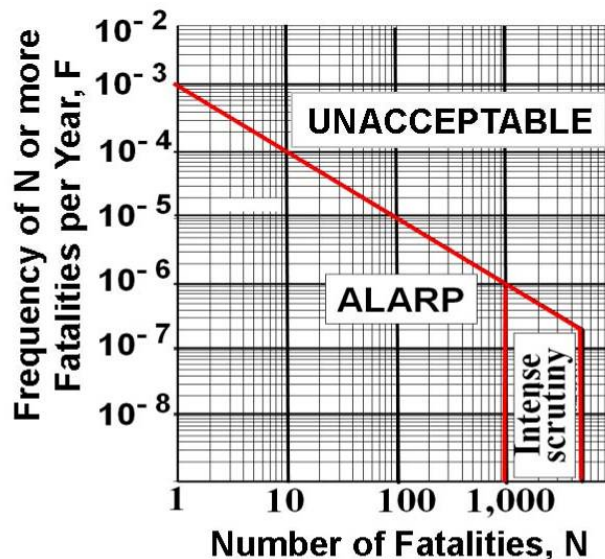
the most vulnerable person affected by landslide hazard (viz. Personal Individual Risk (PIR)), whereas the Societal Risk criteria relate to the total risk posed to the affected community, as expressed by means of an F-N plot (Figure 29).

Recently, GEO has conducted a comprehensive review of the new developments in risk criteria in other countries (Hui & Ho in prep.). The findings indicate that Hong Kong’s interim risk criteria for natural terrain landslides are appropriate and are not unduly conservative.

Individual Risk (IR)	New Developments	Existing Developments
Maximum Permissible IR*	10^{-5}	10^{-4}
Tolerable IR level*	$<10^{-5}$	$<10^{-4}$

* Apply to the most vulnerable person at risk (i.e. Personal Individual Risk)

(a) Individual risk tolerability criteria



(b) Societal risk tolerability criteria

Figure 29. Risk criteria adopted in Hong Kong for landslides and boulder falls from natural terrain

Note: The above societal risk criteria are to be used in conjunction with a reference toe length of the natural hillside of 500 m. Appropriate scaling of the risk criteria is done where the actual toe length is greater than 500 m (ERM 1998).

8.13 Assessment of Mobility of Natural Terrain Landslide Debris

Establishing the probable distance of debris runout is essential to the assessment of natural terrain landslide risk.

The GEO has commenced the empirical assessment of debris mobility since the study of the 1993 landslides on the man-made slopes in Lantau (Wong & Ho 1996), with the use of the

travel angle concept and taking due cognizance of the mechanism and volume of failures. However, the concept of the travel angle, which is appropriate for man-made slopes, is not suitable for use as an indicator of debris mobility in assessing the consequence of natural terrain landslides, because the facilities at risk are often not close to the source of the landslide and that the terrain between the facilities and the landslide source is steeply sloping. For natural terrain landslides, empirical correlations were made with 'proximity zones' that are defined by a combined consideration of debris travel angles and debris travel distance (Figure 30). These have been adopted in the global QRA and in site-specific NTHS (Wong 2005).

The 2-D dynamic analysis (DAN) model developed by Hungr (1995) was introduced for use in Hong Kong in the late 1990s (Ayotte & Hungr 1998). Subsequently, the GEO developed its own 2-D dynamic modelling algorithm, known as Debris Mobility Modeller (2d-DMM, Figure 31), based on a similar formulation and solution methodology (Kwan & Sun 2006).

Systematic back-analyses of about 130 selected long runout historical debris flows in Hong Kong were completed by the GEO. The results of the back-analyses indicate that the use of the Voellmy rheology is appropriate in simulating debris flows in Hong Kong. The probabilistic distribution of different sets of runout parameters for mobile debris flows is given in Figure 32, which provides a basis for predicting the debris impact zones under a probabilistic framework.

In recent years, there have been major developments of the 3-D dynamic continuum modelling capability (e.g. McDougall 2006, Kwan & Sun 2007). The key areas of development and performance of these 3-D algorithms are described in an expert panel review report on a recent international benchmarking exercise on debris mobility modelling organized by the GEO in 2007 (Hungr et al. 2007). The exercise revealed that a number of 3-D computer algorithms had the capability of simulating a wide range of landslide cases and achieving fairly consistent results.

The 3-D codes offer several distinct functionalities that can be important to risk assessment: (i) the debris runout path and lateral debris inundation zones are simulated in the 3-D modelling, instead of being subjectively prescribed in the 2-D codes; (ii) splitting and merging of debris during runout, which have occurred in actual cases, can be allowed for; and (iii) effects of entrainment, presence of debris diversion and retention facilities, debris flow depth, length of the debris flow mass, 3-D profile of debris deposition, etc. can be realistically simulated (Figure 33).

The development of 2-D and 3-D numerical modelling of debris movement has greatly enhanced the capability of assessment of debris influence zones and design of risk mitigation works.

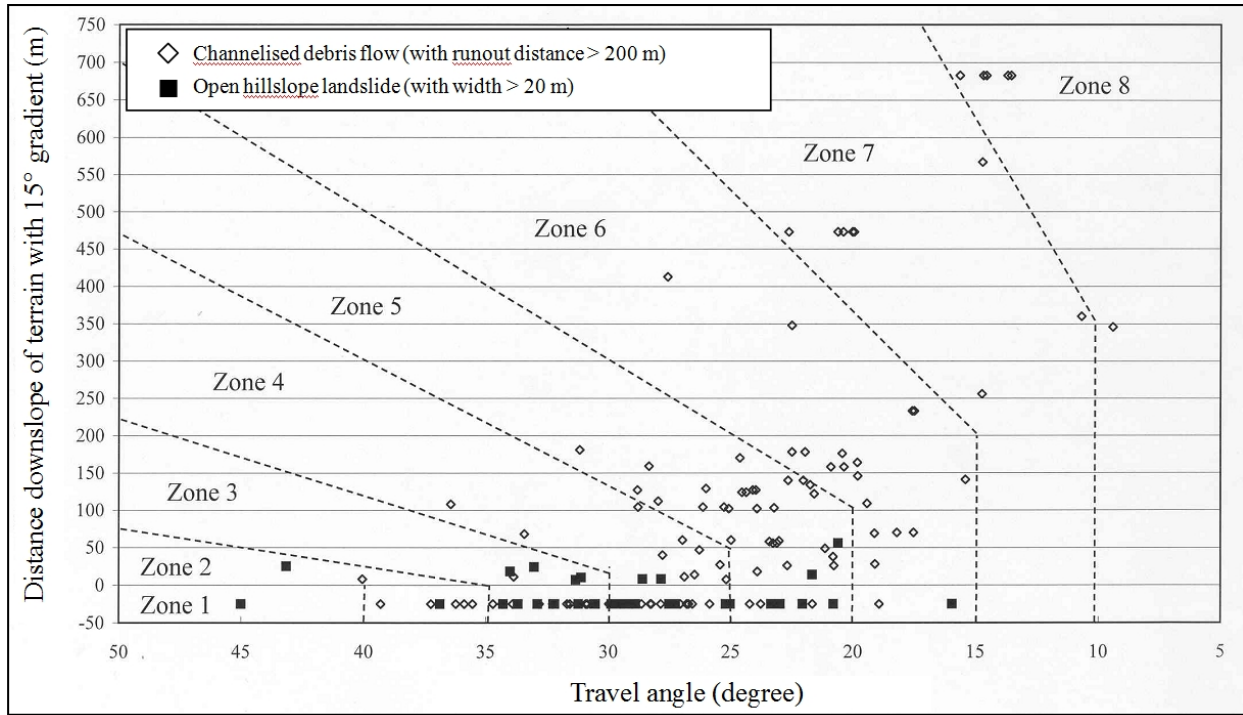


Figure 30. Data on debris mobility of natural terrain landslides and classification of proximity zones

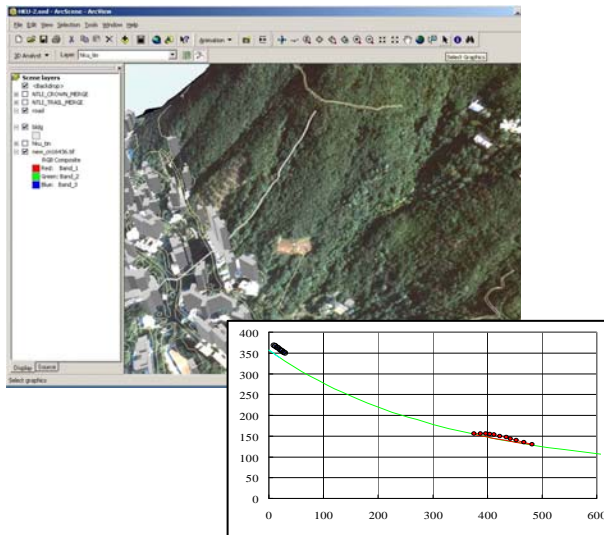


Figure 31. 2d-DMM debris runout modeling

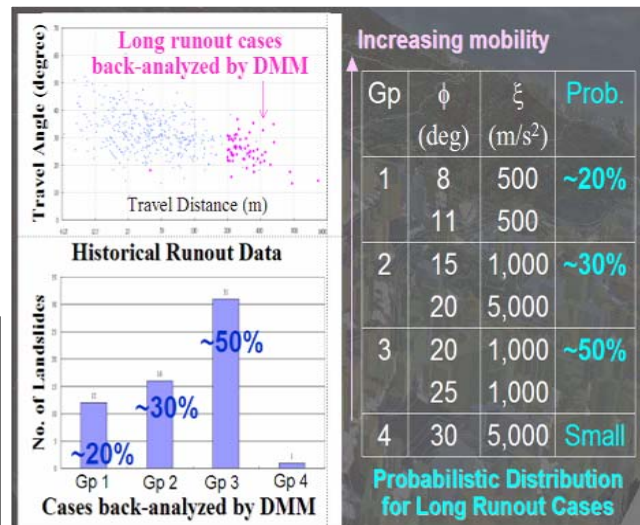


Figure 32. Probabilistic distribution of runout parameters for mobile debris flows based on back-analysis of historical long

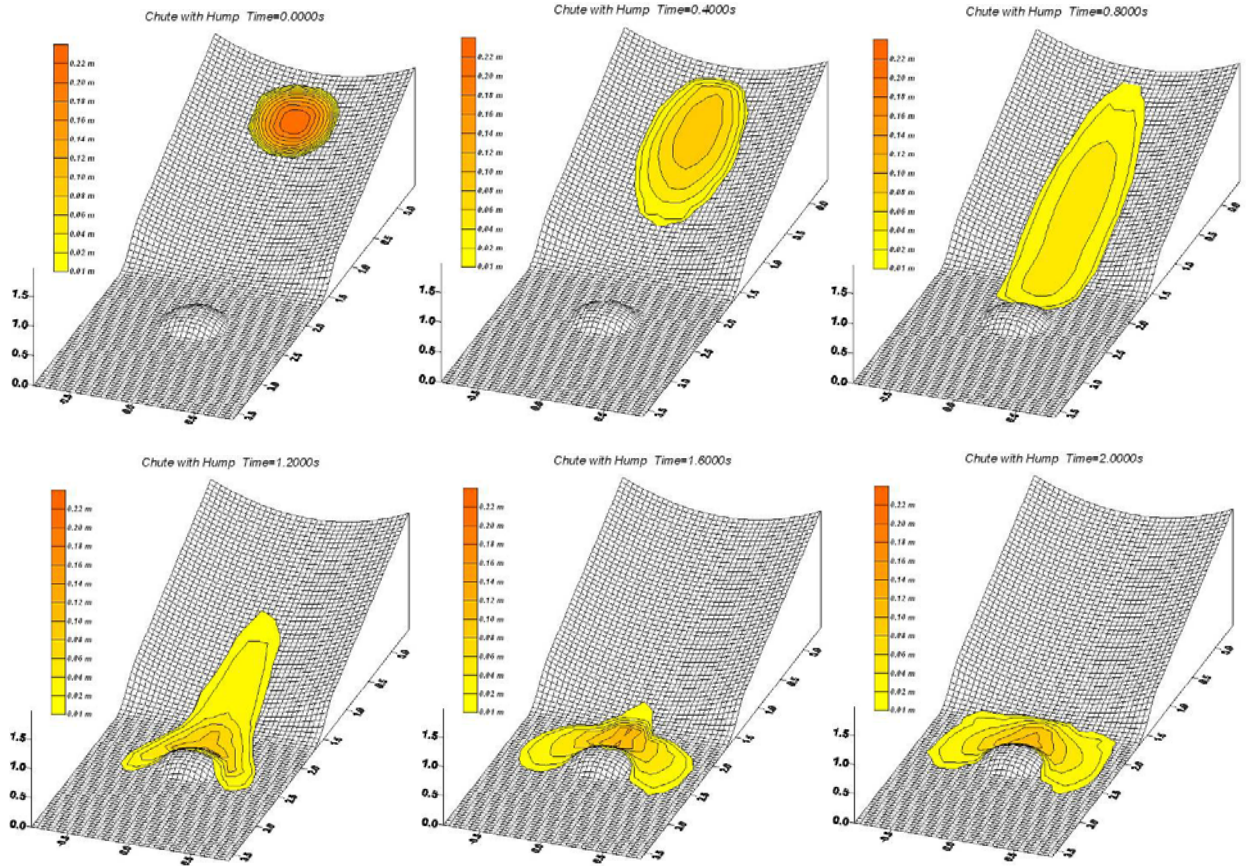


Figure 33. Simulation of frictional materials flowing down a channel obstructed by a hump (based on Kwan & Sun 2006)

8.14 Quantification of Landslide Consequence

The need to evaluate the consequence of failure for risk quantification poses a new challenge to the geotechnical profession. Where landslide consequence is assessed as part of a QRA, it is instructive to distinguish between the use and application of risk assessment at different scales, as this can have a bearing on the consideration of the appropriate approaches to be adopted for consequence assessments. For instance, the objective of a global QRA would be different from that of a site-specific risk assessment.

A generalized landslide consequence model has been developed which considers all the key factors affecting the mobility of landslide debris and the vulnerability of the affected facilities, including the type of facilities, temporal presence of population, mobility of landslide debris, scale of failure and the degree of protection afforded by the facility (Wong et al. 1997), which considers implicitly the intensity of landslide debris impact (i.e. the effect of depth and velocity of debris). Traditionally, the assessment of consequence is done either implicitly or qualitatively, largely based on subjective judgement.

With the improved capability of numerical modelling of debris runout that may be calibrated against field observations, a tailored-made consequence model was developed by

Wong et al. (2004a) for natural terrain landslides. The consequence of landslide not involving building collapse (denoted as CON1) can be assessed by the following equation:

$$\text{CON1} = P_n \times V_n \times S_n \times L_n$$

where

P_n = population at risk in the event of a direct hit by a natural terrain landslide hazard (a landslide of 10 m in width) but without building collapse

V_n = vulnerability factor

S_n = scale factor

L_n = location factor

This model also allowed the consideration of the possibility of building collapse due to landslide impact. The additional PLL, denoted as CON2, is assessed as follows:

$$\text{CON2} = P_{\text{collapse}} \times V_{\text{collapse}} \times L_{\text{collapse}}$$

where

P_{collapse} = additional population at risk due to building collapse

V_{collapse} = probability of building collapse

L_{collapse} = location factor for building collapse

The consequence model was calibrated against historical landslides in Hong Kong and gave reasonable estimates through application to case studies.

8.14.1 Type of Facilities

The type of facilities under consideration will affect the density of occupation and degree of usage. This directly affects the spatial and temporal distribution of the affected population. In addition, the type of facility will also influence whether significant secondary effects could occur, e.g. fire or explosion of dangerous goods caused by the impact of a landslide.

In general, two types of facilities, viz. (a) building structures and (b) transportation routes and mass transportation facilities, would be considered in the QRA. The corresponding population at risk, based on Wong et al. (2004a), is given in Tables 7 and 8.

Table 7 Population at risk for different types of building structures in case of full ground floor occupancy

Building Type	Description	Population at Risk (P_n) (No.)
B1	Individual houses or structures of one to three storeys	2
B2	Cluster of houses or structures of one to three storeys	4
B3	Buildings of four to ten storeys, including podium and similar area	6
B4	Multi-storey buildings of 11 to 20 storeys, including podium and similar area	6
B5	High-rise buildings of more than 20 storeys, including podium and similar area	6
B6	Sensitive structures that may involve severe consequence, including PHI, tunnel portal, petrol stations, railway platform, MTR exit	6

Note: Individual houses are not necessarily isolated houses. In the QRA, where data are available, some clusters of houses are assessed based on consideration of the risk on the individual houses that form the cluster.

Table 8 Population at risk for different types of sensitive routes and mass transportation facilities

Sensitive Route and Mass Transportation Facilities Type	Description	Population at Risk (P_n) (No.)
R1	Bus depots	0.25
R2	Bus routes	0.25
R3	Routes to vulnerable areas	0.5
R4	Pink routes	1
R5	Red routes	3
R6	Mass transportation routes, including MTR, railway, light rail, peak tram, tramway	6

The building structures are further categorized into ‘with protection’ and ‘without protection’, based on consideration of the type and strength of the building structures. For instance, building structures built of brick, stone and reinforced concrete are classified as ‘with protection’, while building structures built of wood and corrugated metal sheets are classified as ‘without protection’. Transportation routes and mass transportation facilities (such as railways, but excluding building structures) are taken as ‘without protection’. The assessment of the degree of usage for different buildings and roads is explained in Wong et al. (1997).

8.14.2 Assessment of Vulnerability

In the context of risk quantification, vulnerability may be defined as the level of potential damage, or degree of loss, of a given element at risk (expressed on a scale of 0 to 1), subjected to a landslide of a given intensity (Fell 1994, Leone et al. 1996). Vulnerability assessment therefore involves the understanding of the interaction between a given landslide and the affected elements. In essence, vulnerability (v) may be evaluated as follows (Fell 1994):

$$v = (v_s) \times (v_t) \times (v_l)$$

where

v_s = probability of spatial impact of a landslide on an element at risk

v_t = probability of temporal impact (e.g. that the element at risk is occupied during impact)

v_l = probability of loss of life or proportion of the value of the element at risk lost

In essence, the vulnerability of a given facility is related to the types of slope hazard taking cognizance of their different scales of failure and mobility and velocity of debris. In assessing vulnerability, account should also be taken of the type, proximity and spatial distribution of the affected facilities (e.g. whether they are within the crest area or toe area of a slope or hillside), population density, spatial and temporal distribution of population, degree of protection offered to persons by the nature of the facility, likely scale (i.e. volume) of the landslide, the degree of warning available to the affected persons (e.g. signs of distress prior to detachment of material, velocity of landslide debris, etc.) and their response (e.g. evacuation, precautionary measures taken such as avoiding the use of roads in a hilly terrain during heavy rainfall), etc.

8.15 Global QRA of Natural Terrain Landslides

In 2004, the GEO completed a global QRA of the overall risk of natural terrain landslides in Hong Kong (Wong et al. 2004a). An improved approach involving the application of GIS-based rainfall-landslide correlations in probabilistic terms (Ko 2003), which have been calibrated against historical natural terrain landslide data, was used to assess the landslide density. Different rainfall scenarios, together with their probability of occurrence, are considered to assess the likely landslide frequency. Allowance was made for the possible occurrence of extreme rainfall.

A series of sensitivity analyses were carried out to examine the reliability of the quantified risk results and their sensitivity to the assumptions made in the frequency and consequence models. The results of the global risk assessment were benchmarked against the findings of the site-specific QRA. The key findings of the global QRA are described below:

(a) The overall risk of natural terrain landslides, based on the state of development in Hong Kong as of 2004, was assessed to correspond to a PLL of about 5 per year. Parametric studies established that the overall risk might range from about 1 PLL to 10 PLL per year, with the best estimate being 5 PLL. The above range reflects the level of uncertainty of the assessment given the available data and technical know-how.

(b) In early 2007, the global QRA for natural hillsides was updated using the enhanced data in the newly compiled ENTLI. The estimated total natural terrain landslide risk is comparable to that established in 2004. The corresponding landslide risk profile in the year 2010 is shown in Tables 9 and 10. An important observation is that the overall landslide risk of natural hillsides will become comparable to that posed by the man-made slopes by 2010, hence the need to give due attention to both vulnerable hillsides and substandard man-made slopes in the newly launched LPMitP.

The results of the above global QRA were also used to formulate the priority ranking system for HLC for systematic follow-up action under the LPMitP.

Table 9 Landslide risk profile in year 2010

Type of slope		Approximate no.	Proportion of risk	Average PLL per no.	Relative risk-cost ratio
Natural hillside	Historical landslide catchments	450 catchments	~ 15%	3.3×10^{-2}	10
	Supplementary catchments	Many (exact no. not known)	~ 35%	Not known	Not known
Unengineered man-made slopes	Affecting Groups No. 2(b) & 3 facilities and unplanned structures	12,000 slopes	~ 25%	2.1×10^{-4}	1
	Affecting Groups No. 4 & 5 facilities	14,000 slopes	< 1%	$< 7 \times 10^{-6}$	0.03
Engineered man-made slopes	with old technology	10,000 slopes	~ 20%	2.0×10^{-4}	1
	with robust technology	20,000 slopes	~ 5%	2.5×10^{-5}	0.13

Notes: (1) See Table 10 for definitions of Facility Groups.

(2) Un-engineered man-made slopes affecting Groups No. 1 & 2(a) facilities would have been retro-fitted by year 2010, i.e. they become engineered slopes.

(3) In calculating the relative risk-cost ratio, it is conservatively assumed that the average cost of risk mitigating for a natural terrain catchment is 10 times as that for a man-made slope.

- (4) 'Old technology' slopes refer to slopes treated in the early years of setting up Hong Kong's Slope Safety System (typically in late 1970s to mid 1980s) based on the geotechnical knowledge and skills at the time. These are less robust than those treated using structural support or reinforcement, such as soil nails.

Table 10. Classification of facility groups (based on Wong & Ho 1995).

Facility Group No.	Facilities	Potential loss of life
1 (a)	Occupied buildings, e.g. residential building, school, etc.	3
1 (b)	Road with very heavy vehicular or pedestrian traffic density Sheltered public waiting area, e.g. bus shelter	3
2 (a)	Moderately-used built-up areas, e.g. indoor car park, temple, etc.	2
2 (b)	Road with heavy vehicular or pedestrian traffic density	2
3	Densely-used open space Road with moderate vehicular or pedestrian traffic density	0.25
4	Lightly-used open space Road with low vehicular or pedestrian traffic density	0.03
5	Remote area Road with very low vehicular or pedestrian traffic density	0.001

Note: (1) 'Potential loss of life' in this Table refers to the average number of fatalities in the event of a direct hit (i.e. 100% vulnerability) by a reference landslide of 10 m in width and 50 m³ in volume, as derived from formal consequence assessment (Wong et al. 1997).

8.16 Site-Specific QRA

Since 2000, a number of site-specific QRA have been carried out by the GEO. Typical examples include the Shatin Heights QRA (FMSWJV 2001, Pang et al. 2007), Pat Heung QRA (OAP 2003), Ling Pei QRA (Wong et al. 2004b), North Lantau Expressway QRA (OAP 2005), Po Shan QRA (FSWJV 2006) and Fu Yung Shan Tsuen QRA (Wong & Ko 2006). These involved hillsides of different nature in terms of geological, geomorphological and hydrogeological conditions, as well as different types of facilities at risk. Although the QRA generally followed similar principles with regard to the design of the hazard and consequence models, the QRA methodologies adopted were subjected to continuous improvement in order to enhance the accuracy of the results. As an illustration, three case examples are presented below.

8.16.1 Ling Pei QRA

In 2004, a land-use concept plan was drafted by the Planning Department of the Hong Kong SAR Government to guide the future development of the Ling Pei area in Tung Chung. The planned development was to comprise the construction of 76 nos. 3-storey houses at the toe of a hillside that flanks the existing Ling Pei village (Figure 34). Wong et al. (2004b) carried out a QRA to quantify the risk and evaluate risk tolerability.

As an attempt to standardise the QRA process and further improve the practice of QRA for natural terrain landslides, 16 standard modules of work were identified (Table 11). The Ling Pei QRA served as a reference case that was aligned with the above 16 modules of work.

Table 11 Key modules of work in natural terrain landslide Quantitative Risk Assessment

Module of Work	Scope
(1) Determine study objectives and approach	<ul style="list-style-type: none"> – Identify the background and purposes of the study, and any special requirements – Determine the objectives and the level of details required – Select the approaches to be adopted
(2) Delineate study area	<ul style="list-style-type: none"> – Identify the extent of the site that may be at risk from landslide hazards – Set out the extent of the study area
(3) Validate historical landslides	<ul style="list-style-type: none"> – Collate information on historical landslides based on documentary records, aerial photograph interpretation, and findings from field mapping and geomorphological assessment – Validate the data and compile a dataset of landslides and related attributes
(4) Examine rainfall records and effects	<ul style="list-style-type: none"> – Collate information on the rainfall history – Examine any relevant rainfall-landslide pattern/correlation – Establish any need to adjust figures on the historical landslide activity to account for rainfall effects
(5) Demarcate boundaries and types of catchments	<ul style="list-style-type: none"> – Delineate the boundaries of catchments – Sub-divide the catchments where necessary, e.g. based on topographic conditions and mechanism of debris movement – Match the catchments with the facilities at risk
(6) Identify facilities and population at risk, and their degree of proximity	<ul style="list-style-type: none"> – Identify the types and locations of the facilities at risk – Establish degree of usage and temporal distribution of population at risk – Examine degree of proximity with reference to GEO's screening criteria, empirical models, relevant historical runout data, etc.
(7) Geological assessment	<ul style="list-style-type: none"> – Carry out field mapping to establish the engineering geological and geomorphological conditions – Examine landslide processes and mechanisms, regolith type and distribution, signs of distress, and other relevant terrain attributes – Classify terrain, and develop geological and landslide process models
(8) Formulate hazard and hazard models	<ul style="list-style-type: none"> – Identify potential landslide hazards and the relevant hazard scenarios that require risk quantification – Formulate hazard models for use in QRA and in assessment of Design Events
(9) Identify possible debris runout paths and influence zones	<ul style="list-style-type: none"> – Divide potential landslide sources into cells – Identify possible debris runout paths for each cell – Match the cells with the facilities at risk – Assess the degree of proximity and the degree of damage to the facilities at risk
(10) Carry out frequency assessment	<ul style="list-style-type: none"> – Formulate frequency model – Establish the frequencies of occurrence of different types of hazard – Assess the spatial distribution of the landslide frequency, together with the use of susceptibility analysis and Bayesian methodology as appropriate – Assess the frequency of occurrence of special hazard scenarios, e.g. building collapse and events with knock-on effects
(11) Carry out consequence assessment	<ul style="list-style-type: none"> – Formulate consequence model – Assess the consequence of occurrence of different types of hazards – Assess the consequence of occurrence of special hazard scenarios, e.g. building collapse and events with knock-on effects
(12) Analyze risk	<ul style="list-style-type: none"> – Calculate the risk by integrating frequency and consequence models – Evaluate the distribution of risk – Carry out sensitivity analysis and examine the reliability of the findings of the risk analysis

Module of Work	Scope
(13) Assess design events	– Assess the magnitudes of Design Events
(14) Evaluate risk management strategy	– Compare risk results with risk criteria – Formulate possible risk management options – Evaluate the pros and cons of different risk management options and identify the preferred risk management strategy – Interact with and obtain feedback from stakeholders
(15) Draw conclusion and recommendation	– Conclude the findings of the study – Recommend risk management strategy and follow-up actions
(16) Document findings	– Document the findings of the study – Update the relevant documentary and digital records

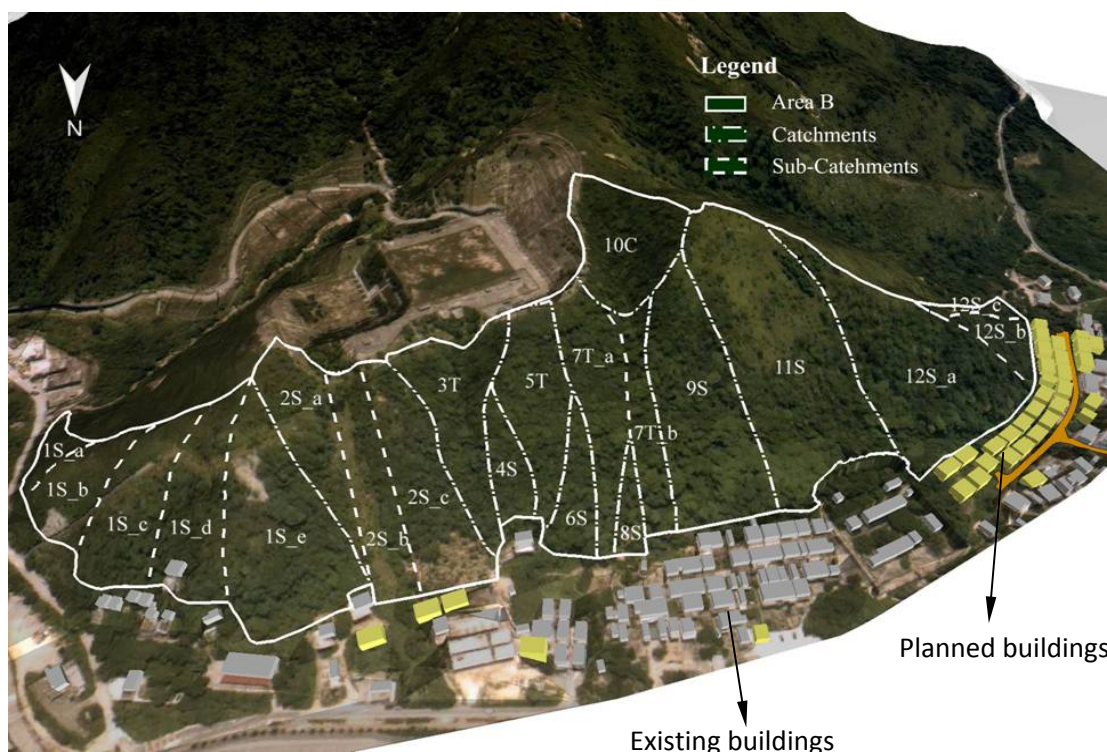


Figure 34. Catchments and sub-catchments in Area B, Ling Pei

Further enhancements of site-specific QRA techniques were made, such as consideration of the risk of occurrence of landslides, landslide-rainfall correlations, landslide mobility and consequence, etc. These helped to improve the rigor of the assessment and overcome some known technical problems that have been encountered in previous QRA. The procedures of the QRA and key findings are summarized below under the headings of the relevant modules of work:

(a) Study objectives, approach and area (Modules 1 & 2)

The study served to assess the risk on the planned development and guide the development strategy. The hillside that flanked the planned buildings is denoted as Area B in Figure 35. As a good practice in site-specific QRA of natural terrain landslides, a larger region

was studied for a thorough examination of the relevant landslide process and characteristics in the area (i.e. Areas A to D in Figure 35).

(b) Landslide history and rainfall effects (Modules 3 & 4)

Historical landslide activities and characteristics in the area were evaluated from an interpretation of all the available aerial photographs, ground-truthing through field inspections and geomorphological mapping. A total of 91 recent natural terrain landslides (five of which are in Area B) and five large relict landslide-related morphological features (none of which are in Area B) were identified (Figure 35). The correlations of natural terrain landslide density with normalized rainfall intensity in Hong Kong as established by Ko (2003) and Wong et al. (2004a) were applied to the site. The landslide and rainfall histories at the site were found to be broadly consistent with the Hong Kong-wide trend, and hence the available historical landslide data in Area B are considered to give a reasonably conservative baseline value for use in landslide frequency assessment.

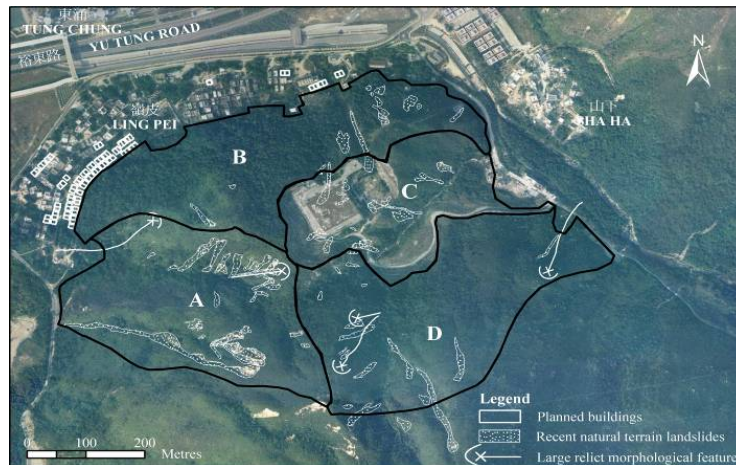


Figure 35. Historical landslides in Ling Pei

(c) Catchment and facility identification (Modules 5 & 6)

The topographic condition of the hillside was assessed with the use of a 2-m grid digital elevation model, together with terrain evaluation based on field mapping and interpretation of aerial photographs. This resulted in the hillside in Area B being demarcated into a total of 21 sub catchments (Figure 34), with account taken of the topography and layout of the planned buildings. The sub-catchments were classified into three types according to the mechanisms of debris movement, namely open hillslope failure, channelised debris flow and mixed debris flow/debris avalanche at a topographic depression (Table 12).

(d) Geological assessment and hazard identification (Modules 7 & 8)

The geological assessment comprised geological mapping, investigation and appraisal to establish the landslide processes at the site, examine the landslide mechanisms, classify the terrain, formulate geological models and identify possible landslide hazards. The work provided a technical basis for formulating the terrain and hazard models. Two types of terrain were identified at Ling Pei, namely Type A (with weathered rocks at a steep slope gradient located in the vicinity of heads of drainage lines or local topographic depressions where there is no

significant variation in slope gradient), and Type B (more irregular slope profile with colluvium overlying weathered rocks).

The hazard model entailed classification of landslide hazards according to the total volume of failure (i.e. 4 volume range classes) and mechanisms of debris movement.

Table 12 Hazard classification for the Ling Pei Quantitative Risk Assessment

Hazard	Classification	Definition
Mechanism of debris movement (as related to catchment characteristics)	C	Channelised debris flow
	T	Mixed debris flow/ avalanche along topographic depression
	S	Open hillslope debris slide/avalanche
Scale of landslide (different magnitude-frequency relationships have been derived for different types of catchments, viz. C, T and S)	H1a	20 m ³ to 60 m ³
	H1b	>60 m ³ to 200 m ³
	H2a	>200 m ³ to 600 m ³
	H2b	>600 m ³ to 2,000 m ³

(e) Debris runout path and influence zone (Module 9)

There are two main aspects to be considered in the evaluation of debris runout for the quantification of landslide consequence. Firstly, the mobility of the landslide debris has to be assessed. In the Ling Pei site, this was done by statistical analysis of the historical debris runout data. The empirical runout model entails the establishment of the worst credible runout distance for each of the hazard types and the assumption of a double-triangular probability distribution of debris mobility, based on the use of a mean runout distance that was taken to be half the worst credible runout distance.

Secondly, the debris runout path has to be predicted. To do this, sub-catchments in Area B were further divided into small hillside units (Figure 36). Each hillside unit has practically the same landslide susceptibility and debris runout path. Based on 3-D GIS analysis and terrain evaluation, the possible debris runout paths originating from each hillside unit were determined. Each unit was then matched with the segments of the lower boundary of the catchments, and with the existing and planned houses. An event tree methodology was adopted in the matching in order to cater for the uncertainties in predicting the debris flow paths where a hillside unit may result in more than one possible debris flow path.

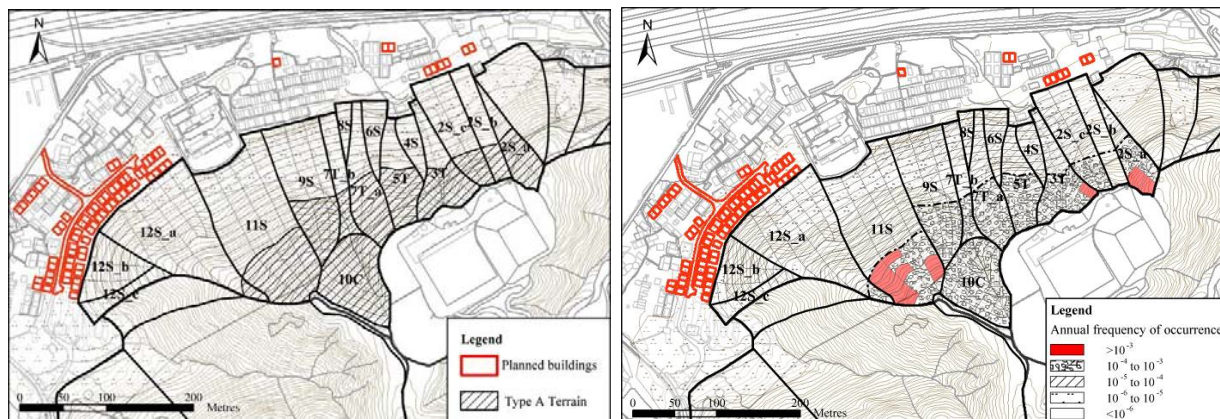


Figure 36. Hillside units (on the left)

Figure 37. Calculated annual frequency of landslide hazard H1a (20 m^3 to 60 m^3) (on the right)

(f) Frequency assessment (Module 10)

The frequency assessment was based on standard magnitude-frequency correlations and spatial distribution of the baseline landslide densities to each of the hillside units via a susceptibility analysis (Figure 37). In this QRA, different susceptibility models were adopted for the two different terrain types, in order to cater for the fact that their landslide processes were different. Bayesian updating of the theoretical landslide density was carried out to account for the actual performance of the hillside units in the past 50 years in order to derive the estimated landslide density for each hillside unit and hence the landslide frequency (which is equal to annual landslide density x plan area of the hillside unit). For each hillside unit, the frequency of occurrence of a given hazard type was calculated by applying the magnitude-frequency relationship to the estimated landslide frequency.

(g) Consequence assessment (Module 11)

An enhanced consequence model, which incorporated consideration of the hazard type, runout mechanism, runout path, debris mobility and vulnerability, was developed for this QRA. The relevant vulnerability factors for the buildings were derived by integrating the probabilistic function of debris runout distance for the different hazard type and degree of damage (as defined by a 'damage model'), which is a function of the distance that the distal end of debris would travel beyond the location of a building (Figure 38).

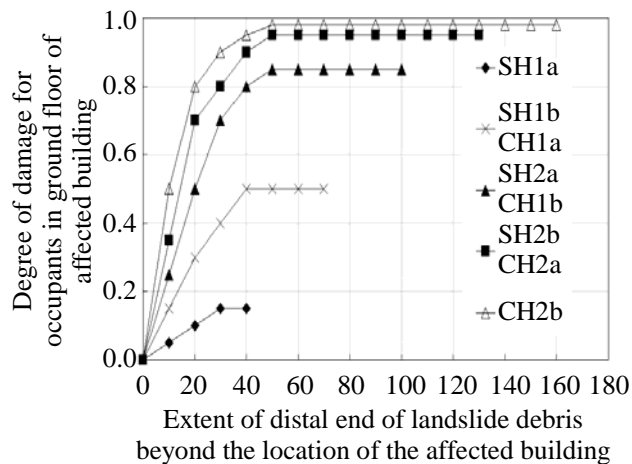


Figure 38. Degree of damage for occupants in ground floor of affected buildings

(h) Risk analysis and evaluation (Modules 12 & 13)

The assessments and risk integration were carried out on a GIS platform. The calculated PIR of an individual person in the planned buildings ranged from 3.3×10^{-7} /year to 8.9×10^{-6} /year (Figure 39), which was within the maximum permissible level of 10^{-5} /year for new developments (ERM 1998). The calculated societal risk for the planned houses was 1.8×10^{-4} PLL/year. The derived F-N curve (Figure 40) was found within the ALARP zone. In the assessment, allowance was made for the possibility of concurrent occurrence of landslides in Area B in the construction of the F-N curve. In view of the uncertainties in assessing the

probability of concurrent occurrence of landslides, the upper bounds of the two F-N curves were assumed in the evaluation of risk tolerability.

The PIR on the existing houses was also assessed and found to be within the maximum permissible level (i.e. 1×10^{-4} /year for existing buildings). The societal risk on the existing houses was 4.3×10^{-4} PLL/year. Hence, the planned development would result in more than 40% increase in societal risk. The F-N curve of the total societal risk for both the existing and planned houses was also within the ALARP zone (Figure 40).

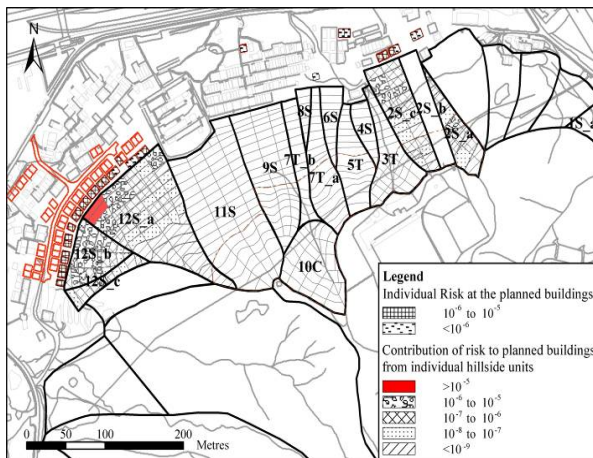


Figure 39. Individual Risk at planned buildings

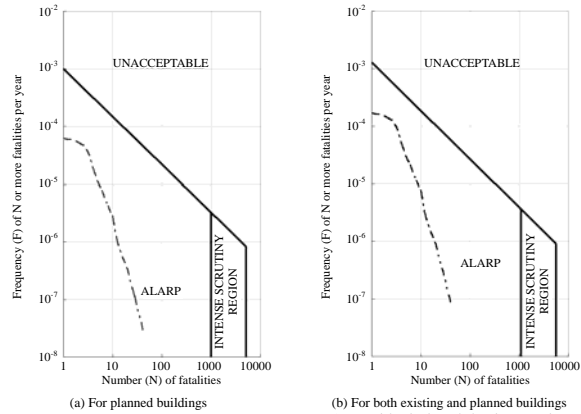


Figure 40. Calculated F-N curves for Ling Pei

(i) Risk management strategy (Module 14)

The maximum justifiable expenditure as calculated from the application of the ALARP principle in the cost benefit analysis (which equals $1.8 \times 10^{-4} \times \text{HK\$}33 \text{ million} \times 120 \text{ year design life for small house}$, with the HK\$33 million taken as the “value of a statistical life”) was found to be about HK\$0.8 million. With the adoption of maximum expenditure, extensive slope stabilisation measures (e.g. soil nailing) and provision of heavy-duty debris-retaining structures would not be practical. Two possible risk mitigation options were proposed (Figure 41): (a) provision of a flexible barrier along the toe of the natural hillside, and (b) adoption of a raised platform for the front row of the planned small houses bordering the natural hillside, both of which were within the order of the maximum justifiable expenditure. The total cost of the planned houses was assessed to be about HK\$250 million. Hence, the provision of landslide mitigation measures would only amount to about 0.3% of the total cost of the proposed development.

(j) Risk communication and documentation (Modules 15 & 16)

The QRA findings were presented to the stakeholders and the two possible risk mitigation options provide a guide for formulating the development strategy for the site. Details of the QRA are documented by Wong et al. (2004b).

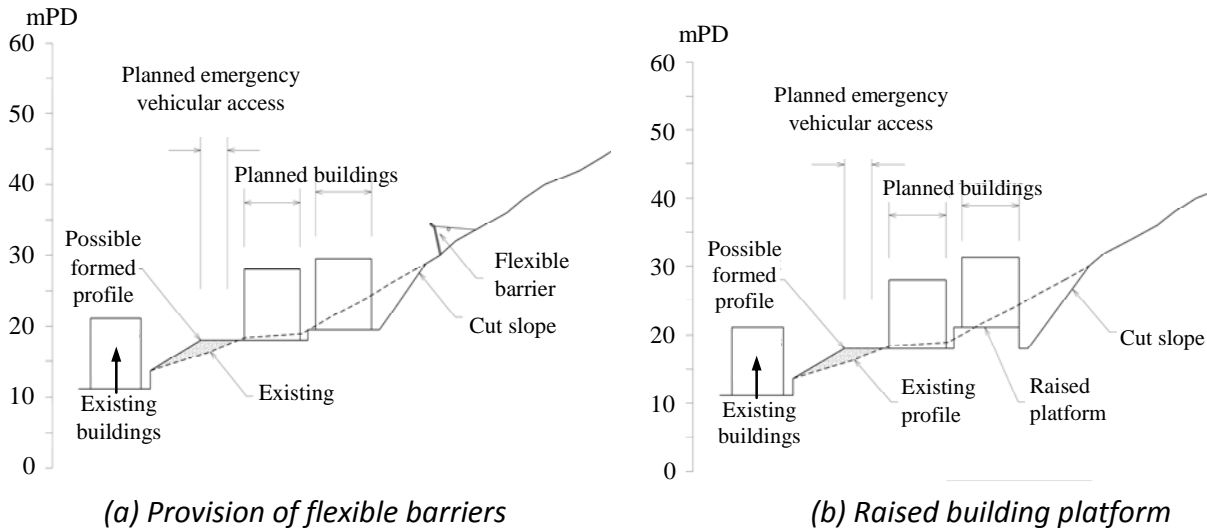


Figure 41. Risk mitigation options for Ling Pei

8.16.2 Po Shan QRA

The hillside catchment above Po Shan Road and the adjoining hillsides in the Mid-levels area of Hong Kong have a history of slope instability. A cross section through the catchment is shown in Figure 42. Some 70 horizontal drains of up to 90 m in length were installed in the mid-1980s to lower the main groundwater table and improve the stability against potential deep-seated failures. Long-term monitoring has shown that these drains have served their intended purposes in drawing down the main groundwater table, and no large-scale instability has occurred on the hillsides since. In recent years, however, the monitoring data revealed increased piezometric levels in local areas and that some of the horizontal drains exhibited a decreasing trend of outflow. These suggested a deteriorating drain performance. In addition, signs of deterioration of the hillside condition and degradation of the past failure scars were also evident from site inspections.

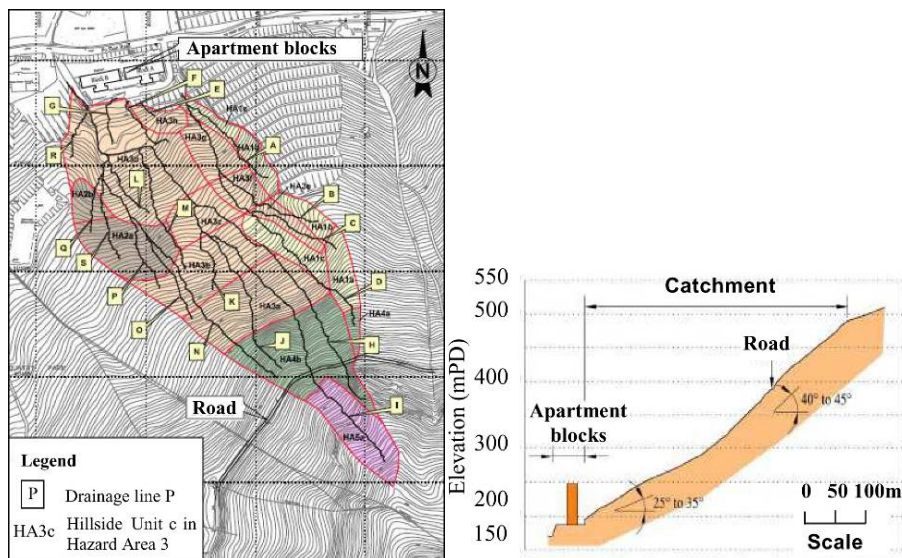


Figure 42. Hazard zones and hillside units of the catchment above Po Shan Road

In view of the above, the GEO decided to replace the horizontal drains with more robust landslide preventive works (i.e. drainage adits) to prevent deep-seated failures. A site-specific QRA was also carried out to assess the risk of shallow landslides. This QRA aims to quantify the landslide risk posed to the high-rise residential buildings and vehicular access at the foothill. Details of the QRA are documented in FSWJV (2006). The key findings are summarised below to illustrate how risk management decisions were guided by the results of the QRA.

(a) The PIR was generally in the order of 1×10^{-7} /year for users of Po Shan Road, while the PIR for carpark and driveway was of the order of 1×10^{-6} /year. The lobby of the residential buildings had the highest PIR of 2×10^{-4} /year due to the degree of exposure of the security guards because of a high temporal presence, which slightly exceeded the risk tolerability criteria. The Societal Risk for all the users of the affected facilities was found to be 3.9×10^{-3} PLL per year.

(b) The breakdown of the PLL showed that the landslide risk is unevenly distributed, with one of the five hazard zones on the Po Shan catchment contributing about 90% of the total PLL. With respect to the volume of failure, about 60% of the PLL is attributed to fairly sizeable landslide events (i.e. landslide volumes between 200 m^3 and 800 m^3).

(c) A notable share of the PLL (about 35%) is derived from the ground floor of the high-rise apartment block. The proportion of Societal Risk associated with the collapse of a portion of the apartment block due to landslide debris impact was only about 4% of the total PLL, i.e. it was not a major component of the overall risk.

(d) The calculated F-N curve (Figure 43) showed that the societal risk fell within the unacceptable zone. Mitigation measures were therefore necessary to reduce the landslide risk to within the ALARP region.

(e) In assessing the risk mitigation measures, account was taken of the capital cost, life-cycle cost, environmental and aesthetic considerations, long-term maintenance requirements, etc. The adopted solution comprised a combination of defensive measures (a series of flexible barriers) within the lower reaches of the catchment and local slope stabilisation measures (i.e. soil nails, rock slope treatment works and bioengineering measures) primarily within the hazard zone that gives the most significant contribution to the overall risk. The proposed risk mitigation was found to be justifiable from a cost-benefit analysis.

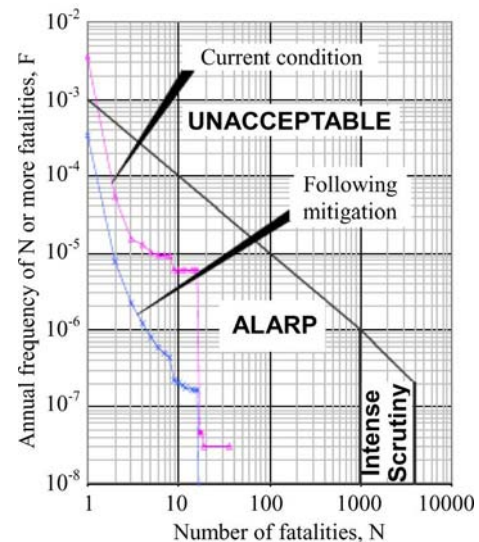


Figure 43. Calculated F-N curves for Po Shan

8.16.3 North Lantau Expressway QRA

The North Lantau Expressway is the sole vehicular access to the Hong Kong International Airport and the adjacent Tung Chung New Town in Lantau Island. It comprises a dual three-lane expressway that runs for about 20 km along the toe of the steep natural hillsides of north Lantau. The hillsides have numerous records of historical natural terrain failures, some of which reached the present alignment of the Expressway.

A qualitative hazard assessment was carried out by Ng & Wong (2002). This included a review of the historical landslide records, appraisal of the geological and terrain conditions, consideration of historical landslide activities, proximity of the Expressway to the hillsides and empirical debris runout data. On this basis, a 4 km long section of the Expressway near the Tung Chung New Town (Figure 44) was considered to warrant a further detailed study with the use of formal QRA technique. The findings of the QRA are documented in OAP (2005).

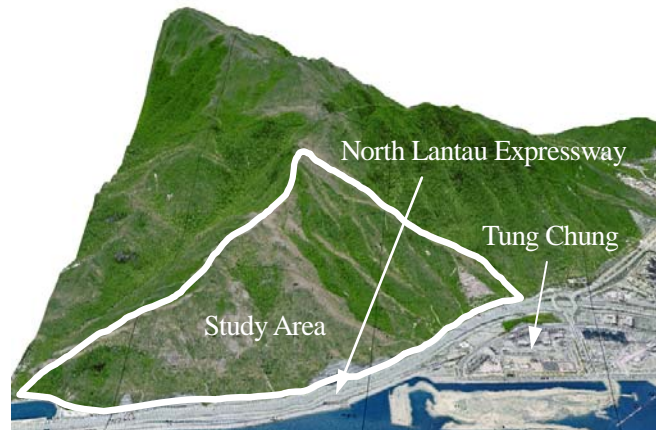


Figure 44. Natural hillside overlooking North Lantau Expressway

The QRA followed the procedures and techniques developed and adopted in previous QRA in Hong Kong. Three aspects of this particular QRA deserve special attention:

(a) The natural hillsides of concern covered a large area and involved variable geological conditions and landslide types. Hence, in this QRA, particular attention was paid to the rigour of the geological assessment of the terrain morphology and landslide processes, which formed an integral part of hazard identification and frequency assessment. The information was synthesized into detailed morphology-based regolith maps and landslide process models.

(b) The Expressway was located at some distance from the steep natural hillsides and was partly protected by buffer zones, which included open spaces, road reserves and drainage ditches and chambers. The QRA showed that both the calculated PIR and societal risk in terms of risk to life were not in the unacceptable zones. The PIR for the most affected persons (i.e. bus drivers) was found to be 1.7×10^{-7} /year, which was well within the acceptable limit of 10^{-4} /year for an existing facility. For societal risk, the total calculated PLL is 6.8×10^{-3} /year, which was derived principally from channelised debris flows. The F-N curves for the eight sections (each of 500 m length) of the Expressway all fell within the ALARP region (Figure 45).

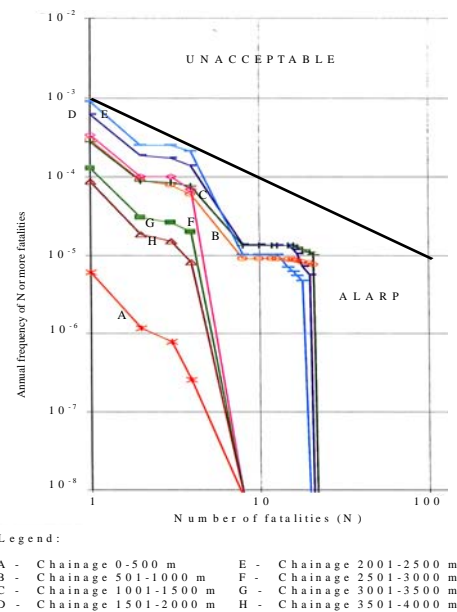


Figure 45. Calculated F-N curves for North Lantau Expressway

(c) While the risk-to-life was assessed to be in the ALARP region, it was perceivable that the potential economic losses arising from landslides could be very significant. This was confirmed by quantifying the risk in respect of different types of economic losses. The total potential economic loss was found to be about HK\$450 million over 120 years.

The preferred risk mitigation scheme comprised the provision of check dam basins at selected vulnerable debris flow channels. The cost of the proposed mitigation works was about HK\$30 million. Based on the ALARP principle, the maximum justifiable expenditure for mitigating loss of life alone was found to be within HK\$25 million, which was less than the cost of the preferred scheme. However, with account also taken of the significant potential economic losses, risk mitigation was considered justified. This case illustrates that for major infrastructure, potential economic losses due to landslides can be substantial and need to be properly considered in cost-benefit analyses.

8.17 Potential Effects of Climate Change

Global warming has now largely been recognized as a reality based on discernible scientific evidence and data. The warming alters the energy balance of the climate system. Scientists and meteorologists generally predict more frequent occurrence of more extreme weather in the 21st century, including droughts, heavy precipitation, heat wave and tropical cyclones. The implications and consequences could be very severe. In the context of geohazards, the extensive damage and loss of life brought about by landslide disasters that were triggered by the Typhoon Morakot on Taiwan in August 2009 are highlighted by Lee (2010).

Taking cognizance of the latest report on climate change released by the Intergovernmental Panel of Climate Change (IPCC), Wong & Mok (2009) conducted pilot studies of the long-term trend analyses of rainfall intensity and frequency associated with ambient air temperature, rainfall and wind speed in Hong Kong. It was found that the return periods for short duration rainstorms (e.g. 1, 2 and 3-hourly rainfall) had decreased significantly from 1885 to 2009. The return period for 1-hour rainfall greater than 100 mm had shortened from 37 years in 1900 to 18 years in 2000. In other words, heavy precipitation is becoming more frequent (Figure 46).

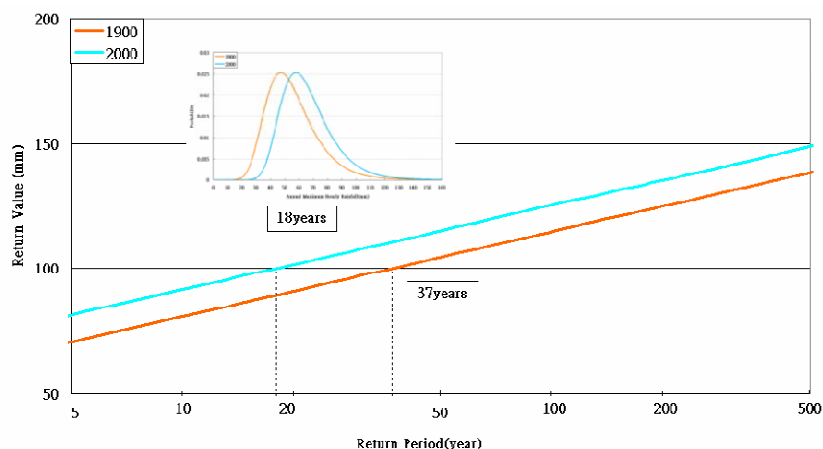


Figure 46. Change of return periods for annual maxima for 1-hourly rainfall in 1900 and 2000

Slopes that sustained past severe rainstorms would not necessarily perform satisfactorily under more extreme rainfall events, as the rain could surpass the historical high rainfall that the slopes had been subjected to. The potential increase in the frequency and severity of extreme rainstorm events would increase the landslide risk, particularly on natural hillsides.

Projections of future temperature trend and rainfall changes in Hong Kong are made by the Hong Kong Observatory (HKO) using the results of global climate models based on the Fourth Assessment Report (AR4) released by the IPCC (2007) and calibrated against measured rainfall in Hong Kong and south China through a technique known as statistical downscaling. The modelling suggests that extreme weather conditions would become more extreme. The number of heavy rains and thunderstorms will increase. There will be more extreme rainfall events with longer periods of little rain in between. Also, the year-to-year variability of rainfall and number of days with heavy rain will also increase. Further work is being carried out by the HKO to investigate the frequency and return period of extreme rainfall values. Climate change is liable to have major implications on slope safety management due to an increase in the frequency and the severity of extreme rainstorm events:

(a) There could be more erosion and wash-out type failures due to more frequent short-duration heavy precipitation. The design standard and detailing of drainage provisions for slopes may need to be reviewed and enhanced as appropriate.

(b) The frequency and scale of rain-induced slope failures may increase. Although the more extensive use of robust slope stabilisation measures (e.g. use of soil nails) and prescriptive subsoil drains as contingency measures could enhance the stability of man-made slopes under extreme conditions, the assessment of the design event for the assessment of risk mitigation measures for natural hillside may need to take cognizance of climate change effects; however, it is noteworthy that the uncertainties involved are considerable.

(c) GEO's studies on rainfall-landslide correlations for natural terrain revealed that the occurrence of natural terrain landslides would increase exponentially in extreme rainstorm events. In addition, the scale of failure and mobility of debris flows would also increase significantly with more extreme rainfall. The susceptibility of natural terrain to rain-induced failures is comparatively more sensitive to the effect of climate change than man-made slopes.

(d) The emergency preparedness set-up of the GEO would need to be reviewed in light of the projections of extreme rainfall.

(e) The understanding of the key factors and settings that could give rise to low-frequency large-magnitude landslides need to be further improved, together with the identification of the catchments and terrain that are vulnerable to such events.

8.18 Concluding Remarks

A new era of systematic natural terrain risk management has commenced in Hong Kong. This was made possible by the concerted efforts in research and development and technological advances made over the last 20 years or so by the geotechnical profession in improving our understanding. The uncertainties involved in natural terrain risk management are considerable. Further development work and field studies are called for. As the technical understanding of the subject is evolving rapidly, it is of the essence that the geotechnical

profession should keep abreast of the technical advances and get geared up to meet the challenges in discharging their enhanced responsibility.

ACKNOWLEDGEMENTS

This chapter is published with the permission of the Head of the Geotechnical Engineering Office and the Director of Civil Engineering and Development, Government of the Hong Kong Special Administrative Region. Many GEO colleagues have made significant technical contributions over the years on various subjects related to natural terrain landslides and risk management. These include notably HN Wong, Julian Kwan, Florence Ko, HW Sun, Edwin Chiu, Thomas Wong, Rod Sewell, Denise Tang, YM Sin, Jeffery Wong and Sammy Cheung. All contributions are gratefully acknowledged.

References

- AFJV (2010). Natural Terrain Hazard Review Report. Agreement No. CE 62/2008 (GE), Natural Terrain Hazard Mitigation Works, West Lantau, Geotechnical Engineering Office, Hong Kong, vols. 1 & 2.
- Anon (1982). Land surface evaluation for engineering practice. Quarterly Journal of Engineering Geology, vol. 15, p 265-316.
- Ayotte, D. & Hungr, O. (1998). Runout Analysis of Debris Flows and Avalanches in Hong Kong. Report prepared for the Geotechnical Engineering Office, Hong Kong, 90 p.
- Brunsdon, D., Doornkamp, J.C. & Jones, D.K.C. (1978). Applied Geomorphology: a British View. In: Embleton, C., Brunsdon, D. & Jones D.K.C. (Eds.), Geo morphology: Present Problems and Future Prospects. Oxford University Press, Oxford, p 251-262.
- Chan, R.K.S., Mak, S.H. & Au Yeung, Y.S. (2007). Partnering with the community to reduce landslide risk in Hong Kong over the past thirty years. Proceedings of the Seminar on Geotechnical Advancement in Hong Kong since 1970s. Hong Kong Institution of Engineers, p 183-196.
- Chan, Y.C., Lam, C.H., & Shum, W.L. (1991). The September 1990 Tsing Shan Landslide: A Factual Report (2 Volumes). Technical Note No. TN 4/91, Geotechnical Engineering Office, 91 p.
- Cheng, P.F.K. & Ko, F.W.Y. (2008). An Updated Assessment of Landslide Risk Posed by Man-made Slopes and Natural Hillsides in Hong Kong. Special Project Report No. SPR 7/2008, Geotechnical Engineering Office, Hong Kong, 44 p.
- Cheung, W.M. & Shiu, Y.K. (2000). Assessment of Global Landslide Risk Posed by Pre-1978 Man-Made Slope Features: Risk Reduction from 1977 to 2000 Achieved by the LPM Programme. GEO Report No. 125, Geotechnical Engineering Office, Hong Kong, 63 p.
- Dai, F.C. & Lee, C.F. (2002). Terrain-based mapping of landslide susceptibility using a geographic information system: a case study. Canadian Geotechnical Journal, vol. 38, p 911 – 923.
- Dai, F.C. (2002). A Spatial-temporal Approach to Landslide Hazard Modeling Using Multi-temporal Aerial Photographs and GIS Technology. Research Project Report, The Jockey Club Research and Information Centre for Landslip Prevention and Land Development, University of Hong Kong, 75 p.
- Dias, A., Hart, J. & Fung, E.K.S. (2009). The Enhanced Natural Terrain Landslide Inventory.

- Proceedings of the Seminar on Natural Terrain Landslides: Study and Risk Mitigation Measures, Hong Kong Institution of Engineers, p 71-78.
- Davis, D.W., Sewell, R.J. & Campbell, S.D.G. (1997). U-Pb dating of Mesozoic igneous rocks from Hong Kong. *Journal of the Geological Society, London*, vol. 154, p 1067-1076.
- Development Bureau (2007). Legislative Council Brief: Post-2010 Landslip Prevention and Mitigation Programme. Development Bureau, The Government of the HKSAR, November 2007, 11 p.
- Dushnisky, K. & Vick, S.G. (1996). Evaluating risk to the environment from mining using failure modes and effects analysis. *Uncertainty in the Geologic Environment*, Geotechnical Special publication No. 58, ASCE, vol. 2, p 848-865.
- ERM (1998). Landslides and Boulder Falls from Natural Terrain: Interim Risk Guidelines. GEO Report No. 75. Report prepared for the Geotechnical Engineering Office, Hong Kong, 183 p.
- Evans, N.C. & King, J.P. (1998). The Natural Terrain Landslide Study: Debris Avalanche Susceptibility. Technical Note No. TN 1/98, Geotechnical Engineering Office, Hong Kong, 96 p.
- Fell, R. (1994). Landslide risk assessment and acceptable risk. *Canadian Geotechnical Journal*, vol. 31, p 261-272.
- Fletcher, C.J.N., Campbell, S.D.G., Carruthers, R.M., Busby, J.P. & Lai, K.W. (1997). Regional setting of Hong Kong: implications of new gravity models. *Journal of the Geological Society, London*, vol. 154, p 1021-1030.
- FMSWJV (2001). Detailed study of the hillside area below Shatin Heights Road. Landslide Study Report No. LSR 4/1001. Reported prepared for the Geotechnical Engineering Office, Hong Kong, 204 p.
- Franks, C.A.M. (1991). Engineering Geology of North Lantau: Tsing Chau Tsai Peninsula to Ta Pang Po. Special Project Report No. SPR 4/91, Geotechnical Engineering Office, Hong Kong, 148 p. plus 9 drgs.
- Franks, C.A.M. (1992). Engineering Geology of North Lantau: Ta Pang Po to Tai Ho Wan. Special Project Report No. SPR 2/92, Geotechnical Engineering Office, Hong Kong, 109 p. plus 5 drgs.
- Franks, C.A.M. (1998). Study of Rainfall Induced Landslides on Natural Slopes in the vicinity of Tung Chung New Town, Lantau Island. GEO Report No. 57, Geotechnical Engineering Office, Hong Kong, 102 p.
- FSWJV (2006). Natural Terrain Landslide Risk Assessment for the Po Shan Catchment. Landslide Study Report No. LSR 4/2006, Geotechnical Engineering Office, Hong Kong, 319 p.
- Fyfe, J.A., Shaw, R., Campbell, S.D.G., Lai, K.W. & Kirk, P.A. (2000). The Quaternary Geology of Hong Kong. Hong Kong Geological Survey, Geotechnical Engineering Office, Hong Kong, 209 p. plus 6 maps.
- GCO (1984). Geotechnical Manual for Slopes. (Second edition). Geotechnical Control Office, Hong Kong, 295 p.
- Geotechnical Engineering Office (1998). Investigation of some selected landslide incidents in 1997. GEO Report No. 79, vol. 2, Geotechnical Control Office, Hong Kong, 142 p
- HCL (2003). Detailed Study of Selected Natural Terrain Landslides at Cloudy Hill. Landslide Study Report No. LSR 6/2003, Geotechnical Engineering Office, Hong Kong, vols. 1 to 3.
- Ho, K.K.S. & Wong, H.N. (2001). The role of quantitative risk assessment in landslide risk

- management. Proc. XIV Southeast Asian Geotechnical Conference, Hong Kong, vol. 1, p 123-128.
- Ho, K.K.S. & Lau, J.W.C. (2010). Learning from slope failures to enhance landslide risk management. Quarterly Journal of Engineering Geology and Hydrogeology, 43, p 33–68.
- Ho, K.K.S., Leroi, E & Roberds, W. (2000). Quantitative risk assessment - application, myths and future direction. Proc. The International Conference on Geotechnical and Geological Engineering GeoEng2000, Melbourne, vol. 1, p 269-312.
- Hughes, A., Hewlett, H.W.M., Samuels, P.G., Morris, M., Sayers, P., Moffat, I., Harding, A. & Tedd, P. (2000). Risk management for UK reservoirs. CIRIA C542, Construction Industry Research and Information Association, 213 p.
- Hui, T.H.H. (in prep.). Pilot trial of ground-based InSAR in Hong Kong.
- Hui, T.H.H. & Ho, K.K.S. (in prep.). Review of the risk acceptance criteria.
- Hungr, O. (1995). A model for the runout analysis of rapid flow slides, debris flows and avalanches. Can. Geotech. J., vol. 32, p610-623.
- Hungr, O., Morgenstern, N.R. & Wong, H.N. (2007). Review of benchmarking exercise on landslide debris runout and mobility modelling. Proceedings of the 2007 International Forum on Landslide Disaster Management, Hong Kong, vol. 2: p 755-812.
- Hutchinson, J.N. (1992). Landslide hazard assessment. Proceedings of the 6th International Symposium on Landslides, Christchurch, Australia, vol. 3, p 1805-1841.
- IPCC (Intergovernmental Panel on Climate Change) (2007). Climate Change 2007: The Physical Science Basis. Contribution of the Working Group I to the Fourth Assessment Report of the IPCC. Cambridge University Press, Cambridge, 996 p.
- Jakob, M. & Hungr, O. (2005). Debris-flow Hazards and Related Phenomena. Springer-Praxis, 739 p.
- JTC (Joint Technical Committee on Landslides and Engineered Slopes). (2008). Guidelines for landslide susceptibility, hazard and risk zoning for land use planning. Engineering Geology, vol. 102, Issues 3-4: 83-111.
- King, J.P. (1999) Natural Terrain Landslide Study – the Natural Terrain Landslide Inventory. GEO Report No. 74, Geotechnical Engineering Office, Hong Kong, 127 p.
- King, J.P. (2001). The 2000 Tsing Shan Debris Flow. Landslide Study Report No. LSR 3/2001, Geotechnical Engineering Office, Hong Kong, 54 p. plus 1 drg.
- Ko, F.W.Y. (2003) Correlation between Rainfall and Natural Terrain Landslide Occurrence in Hong Kong. GEO Report No. 168, Geotechnical Engineering Office, Hong Kong, 77 p.
- Ko, F.W.Y. & Kwan, J.S.H. (2006). Application of debris mobility modelling in landslide risk assessment in Hong Kong. Proc. International Conference on Slopes, Malaysia 2006, Kuala Lumpur, Malaysia, p 139-157.
- Kwan, J.S.H & Sun, H.W. (2006). An improved landslide mobility model. Canadian Geotechnical Journal, 43: p 531–539.
- Kwan, J.S.H. & Sun, H.W. (2007). Benchmarking exercise on landslide mobility modelling – runout analyses using 3dDMM. Proceedings of the 2007 International Forum on Landslide Disaster Management, Hong Kong, vol. 2: p 945–966.
- Kwan, J.S.H., Wong, T.K.C. & Ko, F.W.Y. (2007). Development and applications of debris mobility modelling in assessment of natural terrain landslide hazards. Proc. The Hong Kong Institution of Engineers Geotechnical Division Annual Seminar on Geotechnical

Advancements in Hong Kong since 1970s, p 241-248.

- Lau, K.W.K., Sun, H.W., Millis, S.W., Chan, E.K.K. & Ho, A.N.L. (2008). Application of innovative monitoring techniques at four selected natural hillsides in Hong Kong. Proceedings of the HKIE Geotechnical Division Annual Seminar 2008 – Applications of Innovative Technologies in Geotechnical Works. Geotechnical Division, The Hong Kong Institution of Engineers, p 161-170.
- Lee, C.F., Ye, H, Yeung, M.R., Chan, X. & Chen, G. (2002). Application of Artificial Intelligence to natural terrain landslide susceptibility mapping in Hong Kong. Proceedings of the Conference Natural Terrain – A Constraint to Development, Institution of Mining and Metallurgy – Hong Kong Branch, p 223 – 237.
- Lee, E.M. & Jones, D.K.C. (2004). Landslide risk assessment. Thomas Telford Publishing, London, 454 p.
- Lee, W.F. (2010). Geotechnical structure damages during the 2009 Typhoon Morakot. ISSMEG Bulletin, vol. 4, issue 1, p 25-35.
- Léone, F., Asté, J.P. & Leroi, E. (1996). Vulnerability assessment of elements exposed to mass movement: working towards a better risk perception. Proceedings of the 7th International Symposium on Landslides, Trondheim, Norway, vol. 1, p 263-268.
- Lo, D.O.K. (2000). Review of Natural Terrain Landslide Debris-resisting Barrier Design. GEO Report No. 104, Geotechnical Engineering Office, Hong Kong, 91 p.
- Lo, D.O.K. & Cheung, W.M. (2004). Assessment of Landslide Risk of Man-made Slopes in Hong Kong. Advisory Report No. 4/2004, Geotechnical Engineering Office, Hong Kong, 82 p.
- Lo, D.O.K. & Cheung, W.M. (2004). Assessment of Landslide Risk of Man-made Slopes in Hong Kong. Advisory Report No. 4/2004, Geotechnical Engineering Office, Hong Kong, 82 p.
- Malone, A.W. (1998). Risk management and slope safety in Hong Kong. Proc. The Hong Kong Institution of Engineers Geotechnical Division Annual Seminar on Slope Engineering in Hong Kong, vol. 1, p 3-17.
- McDougall, S. (2006). A New Continuum Dynamic Model for the Analysis of Extremely Rapid Landslide Motion across Complex 3D Terrain. Ph.D. Thesis, Department of Earth and Ocean Sciences, University of British Columbia, 253 p.
- MFJV (2002). Pilot Study Regolith Guide, Rock Guide and Field Mapping Proformas. Agreement No. CE 47/2000, Natural Terrain Hazard Study for Tsing Shan Foothill Area, Geotechnical Engineering Office, Hong Kong, 12 p.
- MFJV (2003). Natural Terrain hazard Study for Tsing Shan Foothill Area – landslide Susceptibility Analysis. Report to Geotechnical Engineering Office, Hong Kong, 71 p. plus 2 Appendices.
- MFJV (2007a). Final Report on Compilation of the Enhanced Natural Terrain Landslide Inventory (ENTLI). Agreement No. CE 15/2005 - Natural Terrain Landslide Identification - Feasibility Study. Geotechnical Engineering Office, Hong Kong.
- MFJV (2007b). Final Report on Compilation of the Historical Landslide Catchments Inventory. Agreement No. CE 15/2005 – Natural Terrain Landslide Identification – Feasibility Study. Geotechnical Engineering Office, Hong Kong.
- MFJV (2009). Approach to Hazard Mapping and Development of Hazard Models. Agreement No. CE56/2006 – Pilot Natural Terrain Hazard Review: North-eastern Hong Kong Island – Feasibility Study. Geotechnical Engineering Office, Hong Kong.
- MGSL (1998). Territory-wide Quantitative Risk Assessment of Boulder Fall Hazards (Vol. 1 to 3).

- Report to Geotechnical Engineering Office, Hong Kong.
- MGSL (2000). Detailed Design of Check Dam at Sham Tseng San Tsuen, Debris Flow Barrier (Check Dam) Design, vols. I & II, Report to Geotechnical Engineering Office, Hong Kong.
- Millis, S.W., Clahan, K.B. & Parry, S. (2010). Regional scale natural terrain landslide risk assessment: An example from West Lantau, Hong Kong. Proceedings of the 17th Southeast Asian Geotechnical Conference, Taipei, Taiwan, Vol. 1, p 322-325.
- Morgenstern, N.R. (1995). Managing risk in geotechnical engineering. The 3rd Casagrande Lecture. Proceedings of the 10th Pan American Conference on Soil Mechanics and Foundation Engineering, Guadalajara, vol.4, p 102-126.
- Morgenstern, N.R. (2000). Performance in geotechnical practice. Inaugural Lumb Lecture, Transactions of the Hong Kong Institution of Engineers.
- Mott Connell (2003). Tung Chung to Ngong Ping Cable Car Project - Stage 3 Natural Terrain Hazard Study Report.
- Ng, K.C. & Chiu, K.M. (2008). Pilot airborne LiDAR survey in Hong Kong – application to natural terrain hazard study. Proceedings of the HKIE Geotechnical Division Annual Seminar 2008 – Applications of Innovative Technologies in Geotechnical Works.
- Ng, K.C. & Wong, H.N. (2002). Review of Natural Terrain Hazards Affecting North Lantau Expressway. Geotechnical Engineering Office, 12 p. (unpublished internal document).
- Ng, K.C., Parry, S., King, J.P., Franks, C.A.M. & Shaw, R. (2003). Guidelines for Natural Terrain Hazard Studies. GEO Report No. 138, Geotechnical Engineering Office, Hong Kong, 138 p.
- OAP (2003). Natural Terrain Hazard Study at Pat Heung, Yuen Long. Advisory Report No. 1/2003, Geotechnical Engineering Office, Hong Kong, 266 p.
- OAP (2004). Natural Terrain Hazard Study at North Lantau Expressway – Final Report. Agreement No. CE 89/2002(GE), Natural Terrain Hazard Studies at North Lantau Expressway and Luk Keng Village, Geotechnical Engineering Office, Hong Kong, 73 p. plus drawings.
- OAP (2005) Natural Terrain Hazard Study at North Lantau Expressway. Report to Geotechnical Engineering Office, Hong Kong, 99 p.
- Pang, K.K., Koo, Y.C., Ho, K.K.S., Sun, H.W. & Hui, T.H.H. (2007). Quantitative risk assessment of a natural terrain catchment at Sha Tin, Hong Kong. Proc. of the First International Symposium on Geotechnical Safety and Risk, Shanghai, China.
- Parry, S. (2001). Natural Terrain Hazard Study Shek Pik. Advisory Report ADR 2/2001, Geotechnical Engineering Office, Hong Kong, 60 p. plus 3 drgs.
- Parry, S. & Ruse, M.E. (2002). The importance of geomorphology for natural terrain hazard studies. Proceedings of the Conference Natural Terrain – A Constraint to Development? The Institution of Mining and Metallurgy, Hong Kong Branch, p 89-100.
- Parry, S. & Wong, H.N. (2002). Natural Terrain hazard assessments: Observations from a pilot case study. Proceedings of the Conference: Natural Terrain - A Constraint to Development?, Hong Kong, p 173- 182.
- Parry, S., Ruse, M.J. & Ng, K.C. (2006). Assessment of natural terrain landslide risk in Hong Kong: an engineering geological perspective. Proc. X International Congress of the International Association of Engineering Geology on Engineering Geology for Tomorrow's Cities, Nottingham, England.
- Reeves, A., Chan, H.C. & Lam, K.C. (1998). Preliminary quantitative assessment of boulder falls

- in Hong Kong. Proceedings of the Seminar on Slope Engineering in Hong Kong, Hong Kong, A.A. Balkema Publisher, p 185-192.
- Scott Wilson (Hong Kong) Ltd. (1999a). Specialist API Services for the Natural Terrain Landslide Study - Potential Application of Remote Sensing Techniques for Identifying Areas of Seepage in Hong Kong. Report to Geotechnical Engineering Office, Hong Kong, 10 p.
- Scott Wilson (Hong Kong) Ltd. (1999b). Specialist API Services for the Natural Terrain Landslide Study - Task B Factual Report. Report to Geotechnical Engineering Office, Hong Kong, 9 p. plus 4 Appendices.
- Sewell, R.J. & Campbell, S.D.G. (1997). Geochemistry of coeval Mesozoic plutonic and volcanic suites in Hong Kong. *Journal of the Geological Society, London*, vol. 154, p 1053-1066.
- Sewell, R.J. & Campbell, S.D.G. (2005). Report on the Dating of Natural Terrain Landslides in Hong Kong. GEO Report No. 170, Geotechnical Engineering Office, Hong Kong, 154 p.
- Sewell, R.J., Campbell, S.D.G., Fletcher, C.J.N., Lai, K.W. & Kirk, P.A. (2000). The Pre-Quaternary Geology of Hong Kong. Hong Kong Geological Survey, Geotechnical Engineering Office, Hong Kong, 181 p. plus 4 maps.
- Solomon, I.J., Chan, W.M., Westmoreland, A.J. & Tang, E. (2008). Automated wireless groundwater monitoring system at Po Shan Road. Proceedings of the HKIE Geotechnical Division Annual Seminar 2008 – Applications of Innovative Technologies in Geotechnical Works. Geotechnical Division, The Hong Kong Institution of Engineers, p 251-262.
- Stewart, R.A. (2000). Dam risk management. Proceedings of the International Conference on Geotechnical and Geological Engineering GeoEng2000, Melbourne, vol. 1, p 721-748.
- Vick, S.G. (2002). Degree of belief. ASCE Press, Virginia, 455 p.
- Wong, H.N. (2003). Natural terrain management criteria - Hong Kong practice and experience. Proceedings of the International Conference on Fast Slope Movements - Prediction and Prevention for Risk Mitigation, Naples, Italy, vol. 2.
- Wong, H.N. (2005). Landslide risk assessment for individual facilities. Proceedings of the International Conference on Landslide Risk Management, Vancouver, Canada, p 237-296.
- Wong, H.N. (2005). Landslide risk assessment for individual facilities. Proceedings of the International Conference on Landslide Risk Management, Vancouver, Canada, p 237-296.
- Wong, H.N. (2007). Digital technology in geotechnical engineering. Proceedings of the Seminar on Geotechnical Advancements in Hong Kong since 1970s, p 157-168.
- Wong, H.N. (2009). Rising to the Challenges of Natural Terrain Landslides. Proceedings of the Seminar on Natural Hillside: Study and Risk Management Measures, Hong Kong Institution of Engineers, p 15-53.
- Wong, H.N. & Ho, K.K.S. (1996). Travel distance of landslide debris. Proceedings of the 7th International Symposium on Landslides, Trondheim, Norway, vol. 1, 143-188.
- Wong, H.N. & Ho, K.K.S. (1998). Overview of risk of old man-made slopes and retaining walls in Hong Kong. Proceedings of the Seminar on Slope Engineering in Hong Kong, Hong Kong, p 193-200.
- Wong, H.N. & Ho, K.K.S. (1999). Preliminary quantification of risk of earthquake-induced failure of man-made slopes in Hong Kong. Proceedings of the HKIE Geotechnical Division Seminar on Geotechnical Risk Management, Hong Kong, p 67-76
- Wong, H.N. & Ho, K.K.S. (2000). Learning from slope failures in Hong Kong. Proc. VIII International Symposium on Landslides, Cardiff.

- Wong, H.N. & Ko, F.W.Y. (2006). Quantitative Risk Assessment of Landslide Hazards at Fu Yung Shan Tsuen, Tsuen Wan. Landslide Study Report No. LSR 3/2006, Geotechnical Engineering Office, Hong Kong, 187 p
- Wong, H.N., Ho, K.K.S. & Chan, Y.C. (1997). Assessment of consequence of landslides. Proceedings of the International Workshop on Landslide Risk Assessment, Honolulu, Hawaii, USA, p 111-149.
- Wong, H.N., Ko, F.W.Y. & Hui, T.H.H. (2004a). Assessment of Landslide Risk of Natural Hillides in Hong Kong. Special Project Report No. SPR 5/2004, Geotechnical Engineering Office, Hong Kong, 115 p
- Wong, H.N. & Lam, K.C. (1998). The November 1993 natural terrain landslides on Lantau Island, Hong Kong. Proceedings of the Seminar on Slope Engineering in Hong Kong, A.A. Balkema Publisher, p 51-57.
- Wong, H.N., Lam, K.C. & Ho, K.K.S. (1998). Diagnostic Report on the November 1993 Natural Terrain Landslides on Lantau Island. GEO Report No. 69, Geotechnical Engineering Office, Hong Kong, 98 p. plus 1 drg.
- Wong, H.N., Shum, W.W.L. & Ko, F.W.Y. (2004b). Assessment of Natural Terrain Landslide Risk on the Planned Development in Ling Pei, Lantau. Advisory Report No. ADR 4/2004, Geotechnical Engineering Office, Hong Kong, 174 p.
- Wong, M.C. & Mok, H.Y. (2009). Trends in Hong Kong climate parameters relevant to engineering design. Proceedings of the HKIE Civil Engineering Conference 2009, in CD-ROM, 26 p.
- Woods, N.W. (1992). Engineering Geology of North Lantau:Tung Chung, vols. I & II. Special Project Report No. SPR 1/93, Geotechnical Engineering Office, Hong Kong, 94 p. plus 8 drgs.

CHAPTER 9 EARTHQUAKE INDUCED LANDSLIDES: THE CASE OF WENCHUAN EARTHQUAKE

**Cees van Westen¹, Tolga Gorum¹, Xuanmei Fan^{1,2}, Runqiu Huang², Qiang Xu²,
& Gonghui Wang³**

¹*Faculty of Geo-information Science and Earth Observation, University of Twente, Netherlands*

²*State Key Laboratory of Geohazards Prevention, Chengdu University of Technology, China*

³*Research Centre on Landslides, Disaster Prevention Research Institute, Kyoto University, Japan*

9.1 Introduction

On 12 May 2008, the M_w 7.9 (USGS, 2008) Wenchuan earthquake occurred in the Longmenshan region at the eastern margin of the Tibetan Plateau, adjacent to the Sichuan Basin (See Fig. 1). The area is characterized by elevations of up to 7500 m above sea level and by topographic variations of more than 5 km over distances of less than 50 km. The earthquake triggered a large number of landslides, rock avalanches, debris flows etc. Some of the landslides formed natural dams in the rivers, with the potential secondary hazard of the subsequent flooding. One third of the estimated 88,000 casualties of the earthquake were considered to be caused by landslides (Wang et al., 2009).

The present-day Longmenshan region is roughly coincident with the position of a Mesozoic collisional plate margin that developed during the closure of the Paleo-Tethys and the collision of the Qiangtang block with the North China-Kunlun-Qaidam and South China blocks (Li et al., 2003). Wang and Meng (2009) stated that the Longmenshan fault belt was first formed as an intercontinental transfer fault, partitioning the differential deformation between the Pacific and Tethys tectonic domains, initiated in the late Paleozoic-early Mesozoic period and continued to the Late Cretaceous. From the northwest to southeast, the eastern margin of the Tibetan Plateau is composed of three major tectonic units: the Songpan-Ganzi Fold Belt, the Longmanshan Thrust Belt, and the Longmenshan Foreland basin (Li et al., 2003). The southeastward extrusion of the Songpan-Ganzi block, which obliquely collided with the foreland basin, resulted in three large reverse thrust faults in the Longmenshan tectonic boundary: the Wenchuan-Maowen fault, the Yingxiu-Beichuan fault and the Pengguan fault (Wang et al., 2009) (See Fig. 1). These faults accommodated significant crustal shortening during the Late Triassic Indosinian Orogeny (Li et al., 2003), which has led to the identification of the Longmenshan region as a major thrust zone that was reactivated in the India-Asia collision (Xu and Kamp, 2000). During the collision, a complex package of rocks, including Triassic marine sedimentary rocks of the Songpan-Ganzi remnant ocean basin (Zhou and Graham, 1996), was thrust to the southeast over the margin of the South China block, creating a Late Triassic foreland basin. After the earthquake, extensive tectonic research was carried out in the eastern margin of the Tibet Plateau (Jin, et al., 2009; Zhang, et al., 2009; Tang et al., 2009; Wang et al., 2009).

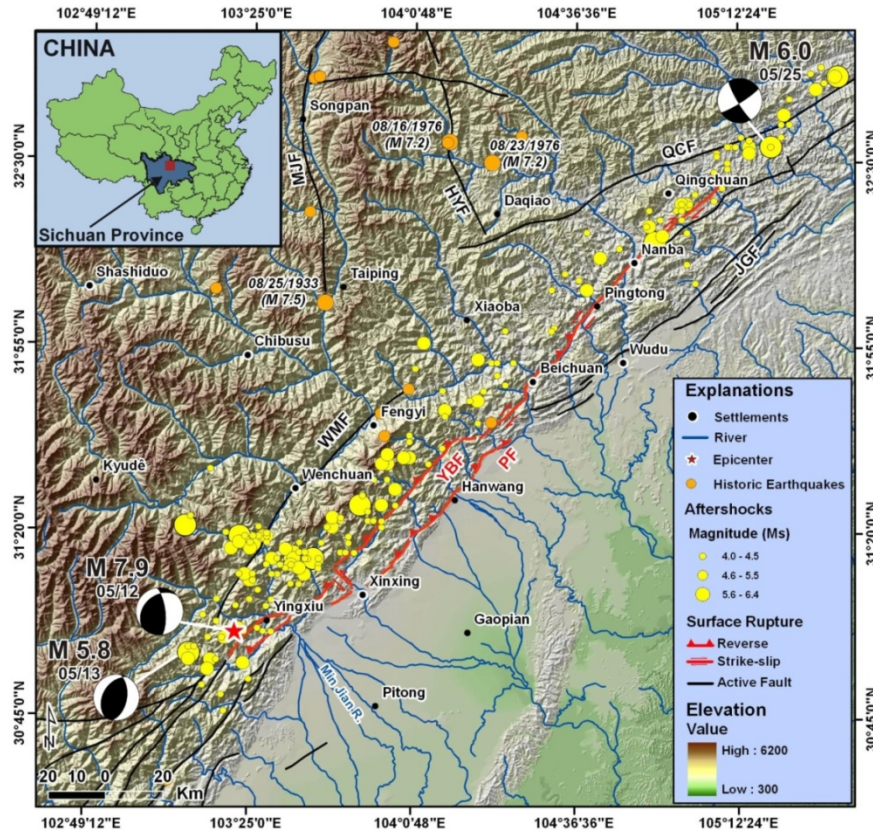


Figure 1. Location and 12 May 2008 Wenchuan earthquake fault surface rupture map, and focal mechanisms of the main earthquake (5/12) and two of the major aftershocks (5/13 and 5/25). Also the epicenters of historic earthquakes are indicated. The following faults are indicated: WMF: Wenchuan-Maowen fault; BF: Beichuan-Yingxiu fault; PF: Pengguan fault; JGF: Jianguyou-Guanxian fault; QCF: Qingchuan fault; HYF: Huya fault; MJF: Minjian fault Based on the following sources: (Surface rupture: Xu et al., 2009; Epicenter and aftershocks: USGS 2008; Historic earthquakes: Kirby et al., 2000; Li et al., 2008; Xu et al., 2009).

Densmore et al. (2007) and Li et al. (2003) indicated that the Longmenshan fault zone represents the features of thrusting and dextral strike-slip in late Cenozoic. The dextral strike-slip rate of the Yingxiu-Beichuan fault since late Pleistocene is less than 1 mm/year, and the thrust rate is 0.3-6 mm/year. Such low slip rates are consistent with GPS estimates of the shortening rate across the Longmenshan range of $< 3 \text{ mm yr}^{-1}$ (Shen et al., 2009; Xu et al. 2009).

Since 638 AD, there is historic information on 66 earthquakes with M_s larger than 4.7 that occurred in the eastern margin of the Tibetan Plateau, mainly concentrated on the Minjiang fault and the southern part of the Longmenshan fault zone (Li et al., 2008). For instance, in 1933, a strong earthquake (M_s 7.5) was induced by the tectonic activity along the Minjiang fault zone. Two earthquakes with Magnitude M_s 7.2 earthquakes occurred between Songpan and Pingwu on August 16 and 23, 1976 (See Fig. 1). Along the middle and southern part of the Longmenshan fault zone, three earthquakes were reported: in 1657 (Wenchuan with M_s 6.5), 1958 (Beichuan with M_s 6.2) and 1970 (Dayi with M_s 6.2) (Kirby et al., 2000; Li et al., 2008; Xu et al., 2009).

The Wenchuan earthquake, with a focal depth of ~14 km to 19 km, initiated close to the base of the Beichuan fault and propagated upwards. Seismological data indicate that the rupture initiated in the southern Longmenshan and propagated unilaterally toward the northeast, along a northwest dipping fault for about 320 km (Xu et al., 2009). The earthquake ruptured both the Beichuan (about 240 km long) and Pengguan faults (72 km long), which are linked by a short northwest-striking rupture zone at the southern end of the Pengguan fault through a lateral ramp, called the Xiaoyudong rupture zone. East of Yingxiu, the Beichuan fault branches into two segments. The largest surface slip (about 6.2m vertical and 4.5m right-lateral offset motion) is found near Yingxiu town and the branching point. Another peak of co-seismic surface offsets is found near Beichuan, located at a fault juncture, where the Beichuan fault bends about 25° clockwise and almost intersects with the Wenchuan-Maowen fault (Shen et al., 2009). The geometry of the fault changes along its length: in the southwest the fault plane dips moderately to the northwest but becomes near vertical in the northeast. Associated with this is a change in the motion along the fault from predominantly thrusting to strike-slip (Shen et al., 2009 and Xu et al., 2009). This is also illustrated in Fig. 1, where the aftershock of May 25 occurring in the NE part of the area has a clear strike-slip component.

After the Wenchuan earthquake, research was carried out on the seismic mechanism and characteristics of the Longmenshan fault zone (Bruchfiel et al., 2008; Wang and Meng, 2009), the location and offsets of the surface rupture, the slip distribution, the fault geometry, the slip rate and kinematic characteristics, based on field investigation and measurements, and the co-seismic deformation observed using GPS and InSAR (Xu et al., 2009; Shen et al., 2009; Li et al., 2008 and 2009). Research on landslide distribution and characteristics was carried out by several authors. Huang and Li (2009) studied the distribution of what they called “geohazards” triggered by the earthquake. They identified a total of 11,300 landslide initiation points on the basis of rapid inventory using air photos and satellite images. Sato and Harp (2009) carried out a preliminary study on landslides interpretation by using pre- and post-earthquake FORMOSAT-2 imageries. Wang et al. (2009) presented preliminary investigation results of some large landslides triggered by the earthquake. Yin et al. (2009) analyzed the distribution of earthquake-induced landslides and the characteristics and mechanism of some typical landslides, and assessed the hazards caused by some of the landslide dams. Tang et al. (2009) developed a numerical rating system, using five factors that contribute to slope instability to assess the landslide susceptibility in Qingchuan County, Sichuan. Studies on landslide dams induced by the earthquake were carried out by Cui et al., (2009) who listed more than 200 landslide dams in the earthquake-hit region and made a preliminary risk evaluation of some key landslide-dammed lakes. Xu et al. (2009) presented a statistical analysis of the distribution, classification, characteristics and hazard evaluation of 32 main landslide dams induced by the earthquake. Liu et al. (2009) studied the largest barrier lake, Tangjiashan, and presented a risk analysis, emergency planning and the effect of emergency measures.

9.2 Methodology and input data

The methodology used in this research, which is presented in Fig. 2, consists of two main steps. The first step is to generate the inventory of landslides triggered by the Wenchuan earthquake, and the second step is to correlate this with a series of parameters to investigate

the causal relationships. In the study, three different datasets were used: (1) Pre- and post-earthquake satellite images, (2) a pre-earthquake grid-based Digital Elevation Model (DEM) and DEM derivative factors (elevation, slope gradient, etc.) having a spatial resolution of 90m x 90m of the study area, (3) scientific papers, reports and maps which are related with the study area before and after the earthquake. In addition to these, a fieldwork was carried out in May and June 2009 to understand the general distribution pattern.

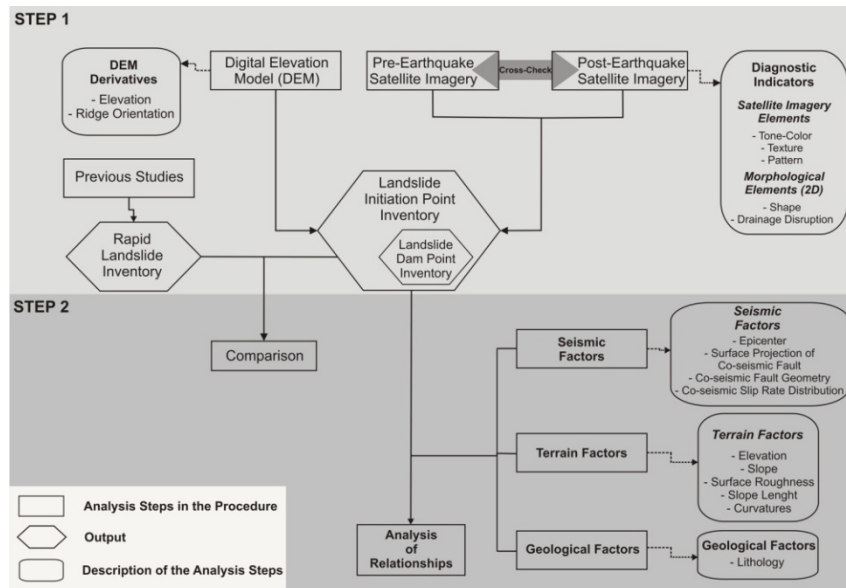


Figure 2. Flowchart indicating the method used for generating the event-based point inventory of landslides caused by the Wenchuan earthquake.

Geo-spatial and remote sensing data analysis was conducted with ArcGIS, SAGA, and ERDAS Imagine software. Remote sensing images have been extensively applied to landslide studies (Rengers et al., 1992; Mantovani et al., 1996; Metternicht et al., 2005; Weirich and Blesius, 2007). A landslide inventory is the simplest form of landslide mapping, which records the location, the date of event and types of landslides (Guzzetti, et al., 2000; Guzzetti, 2005; Van Westen, et al., 2008). Inventory maps can be prepared by different techniques, depending on their purpose, the extent of the area, the scales of base maps, satellite images and aerial photographs, the quality and detail of the available information, and the resources available to perform the work (Guzzetti et al., 2000). In this research, the spatial locations of the event-based individual landslide initiation areas were detected from the pre- and post-earthquake satellite images.

Fig. 3 indicates the spatial coverage of the satellite images that were collected for both the pre- as well as the post earthquake situation. A total of 52 satellite images were collected: 26 representing the pre-earthquake situation, and 26 of the post earthquake situation (See Fig. 3). The pre-earthquake images consisted of multispectral data such as ASTER (Advanced Spaceborne Thermal Emission and Reflection Radiometer-15 m spatial resolution) and ALOS (Advanced Land Observing Satellite- AVNIR-2 (10 m)) as well as panchromatic data from ALOS PRISM (2.5 m) and the Indian Cartosat-1 (2.5 m). Post earthquake images also included SPOT-5 (2.5 m) and IKONOS (2.5 m) data (Table 1). Most of the satellite images were chosen among the

images with low cloud-shadow coverage. The aerial coverage of the cloudy and shadow areas is 192.7km² in the total study area. This area corresponds to 0.5% of the total study area.

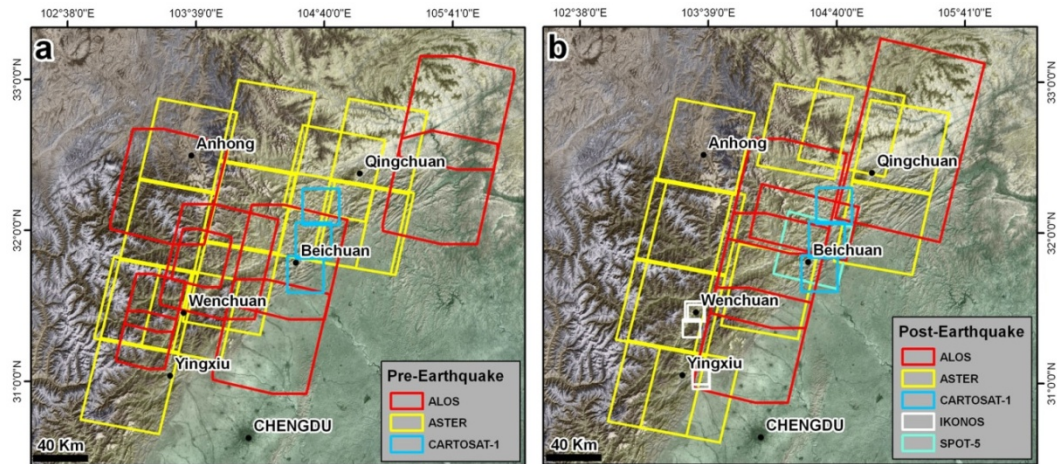


Figure 3. Pre- and Post-earthquake satellite image coverage.

Table 1. Satellite images data index table

Pre-Earthquake

Id	Date	Sensor	Resolution (m)	Spectral Information	Source	Production ID
1	02/19/03	ASTER	15	MS(VNIR)	Terra-ASTER	L1A0030219200303572803142003165639
2	02/19/03	ASTER	15	MS(VNIR)	Terra-ASTER	L1A0030219200303574603142003165712
3	02/19/03	ASTER	15	MS(VNIR)	Terra-ASTER	L1A0030219200303573703142003165656
4	08/30/00	ASTER	15	MS(VNIR)	Terra-ASTER	L1A0030830200004053101012003173757
5	03/31/06	ASTER	15	MS(VNIR)	Terra-ASTER	L1A0030331200603554504022006161342
6	09/05/02	ASTER	15	MS(VNIR)	Terra-ASTER	L1A0030905200203514109202002201647
7	06/14/01	ASTER	15	MS(VNIR)	Terra-ASTER	L1A0030614200103590706192001193607
8	06/14/01	ASTER	15	MS(VNIR)	Terra-ASTER	L1A0030614200103585806192001193546
9	06/30/01	ASTER	15	MS(VNIR)	Terra-ASTER	L1A0030630200103581907062001152354
10	04/18/01	ASTER	15	MS(VNIR)	Terra-ASTER	L1A0030418200104065501202004225713
11	08/27/02	ASTER	15	MS(VNIR)	Terra-ASTER	L1A0030827200203581210052002170010
12	02/19/03	ASTER	15	MS(VNIR)	Terra-ASTER	L1A0030219200303571903142003165623
13	08/30/00	ASTER	15	MS(VNIR)	Terra-ASTER	L1A0030830200004052201012003173741
14	08/30/00	ASTER	15	MS(VNIR)	Terra-ASTER	L1A0030830200004051301012003173724
15	03/31/07	ALOS	10	MS (AVNIR-2)	JAXA	ALAV2A062882960
16	03/31/07	ALOS	10	MS (AVNIR-2)	JAXA	ALAV2A062882970
17	04/17/07	ALOS	10	MS (AVNIR-2)	JAXA	ALAV2A065362960
18	01/02/07	ALOS	10	MS (AVNIR-2)	JAXA	ALAV2A054422950
19	11/28/07	ALOS	10	MS (AVNIR-2)	JAXA	ALAV2A098182940
20	11/28/07	ALOS	10	MS (AVNIR-2)	JAXA	ALAV2A098182950
21	05/06/08	ALOS	2.5	PAN (PRISM)	JAXA	ALPSMN121522965
22	05/06/08	ALOS	2.5	PAN (PRISM)	JAXA	ALPSMN121522970
23	08/30/06	ALOS	2.5	PAN (PRISM)	JAXA	ALPSMN031812960
24	04/19/07	CARTOSAT-1	2.5	PAN	ISRO	097027500102
25	04/19/07	CARTOSAT-1	2.5	PAN	ISRO	097027500202
26	04/19/07	CARTOSAT-1	2.5	PAN	ISRO	097027500302

Post-Earthquake

1	07/10/08	ASTER	15	MS(VNIR)	Terra-ASTER	L1A0030710200803570207152008112907
2	05/30/08	ASTER	15	MS(VNIR)	Terra-ASTER	L1A0030530200804024606022008170420
3	07/10/08	ASTER	15	MS(VNIR)	Terra-ASTER	L1A0030710200803565307152008112859
4	05/23/08	ASTER	15	MS(VNIR)	Terra-ASTER	L1A0030523200803570905282008121510
5	05/23/08	ASTER	15	MS(VNIR)	Terra-ASTER	L1A0030523200803565105282008121456
6	05/23/08	ASTER	15	MS(VNIR)	Terra-ASTER	L1A0030523200803570005282008121503
7	05/16/08	ASTER	15	MS(VNIR)	Terra-ASTER	L1A0030516200803504705192008111553
8	06/08/08	ASTER	15	MS(VNIR)	Terra-ASTER	L1A0030608200803571206112008121132
9	12/10/08	ASTER	15	MS(VNIR)	Terra-ASTER	L1A0031210200803504612132008113610
10	07/26/08	ASTER	15	MS(VNIR)	Terra-ASTER	L1A0030726200803564009262008160248
11	12/10/08	ASTER	15	MS(VNIR)	Terra-ASTER	L1A0031210200803505512132008113619
12	05/16/08	ASTER	15	MS(VNIR)	Terra-ASTER	L1A0030516200803502905192008111529
13	05/18/08	ALOS	2.5	PAN (PRISM)	JAXA	ALPSMW123272955
14	05/23/08	ALOS	10	MS (AVNIR-2)	JAXA	ALAV2A124002930
15	06/04/08	ALOS	10	MS (AVNIR-2)	JAXA	ALAV2A125752950
16	06/04/08	ALOS	10	MS (AVNIR-2)	JAXA	ALAV2A125752960
17	06/04/08	ALOS	10	MS (AVNIR-2)	JAXA	ALAV2A125752970
18	10/13/08	SPOT-5	2.5	PAN	Spot Image S.A	5261286/108/10/13
19	07/10/08	IKONOS	2.5+4	PAN+MS	Geo-Eye	325523
20	05/23/08	IKONOS	2.5+4	PAN+MS	Geo-Eye	325578
21	06/28/08	IKONOS	2.5+4	PAN+MS	Geo-Eye	325583
22	05/23/08	IKONOS	2.5+4	PAN+MS	Geo-Eye	325579
23	06/28/08	IKONOS	2.5+4	PAN+MS	Geo-Eye	325584
24	01/24/09	CARTOSAT-1	2.5	PAN	ISRO	097027500402
25	01/24/09	CARTOSAT-1	2.5	PAN	ISRO	097027500502
26	01/24/09	CARTOSAT-1	2.5	PAN	ISRO	097027500602

The interpretation of landslides was carried out using the pre- and post-earthquake satellite images and the DEM. The DEM was generated using digitized contour lines from 1:50,000 scale topographic maps with contour intervals ranging between 20 meters for low relief areas to 50 meters for mountain areas. The DEM was used to generate a derivative map showing the ridges and slope length. Fig. 4 illustrates some of the aspects that were encountered while carrying out the interpretation. Several areas presented landslides that were present before the earthquake. As can be seen in Fig. 4a and b some of these landslides were reactivated during the earthquake. In this case only the active landslides that were triggered by the earthquake were mapped. Fig. 4c and d show an example where a pre-existing landslide was not reactivated during the earthquake. In such cases the landslide was not included in the event-based landslide inventory.

The individual landslide initiation zones were indicated using points. The minimum size of landslide initiation area was determined as 600 m² and the areas below this value were not considered since the resolutions of the satellite images were not sufficient. In the case of complex situations where many landslides are interconnected, it was rather difficult to identify the individual initiation zones. This is illustrated in Fig. 4e to h. In such cases convergence index developed by Kothe and Lehmeier (1993) was used to produce ridge and valley orientations to get information for identifying the landslide initiation areas.

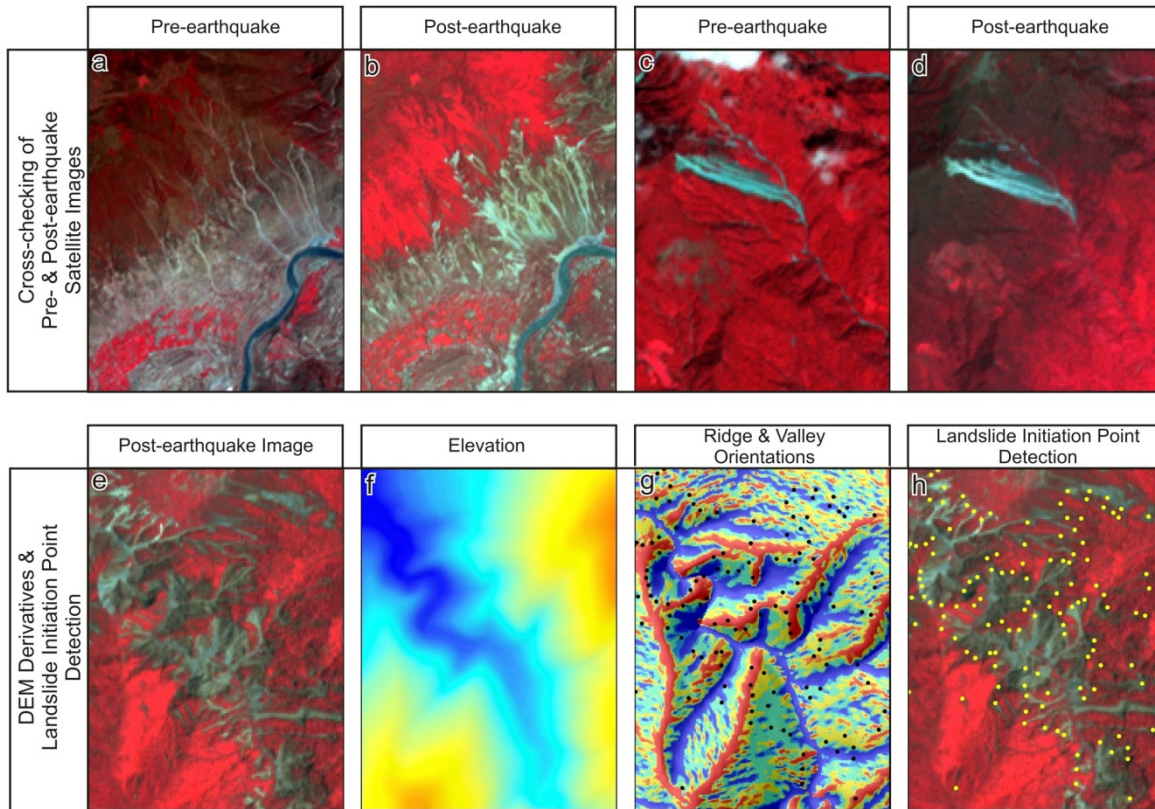


Figure 4. Examples aspects used in detection of landslide initiation points. Above: cross-checking of landslides with pre-earthquake imagery to avoid double counting of landslides. a: pre-earthquake image showing many landslides in the Wenchuan area; b: post-earthquake image of the same area. Only the new landslides were added to the database; c: Single large landslide existing before the earthquake in Wenchuan county; d: Post-earthquake image showing no major difference in landslide activity. Below: Use of DEM derivatives for detection of landslide initiation points. e: Post earthquake image showing complex landslide polygons that have merged. f: Digital Elevation Model; g: DEM derived map with ridges and valleys used for separating landslide initiation points; h: Final interpretation of landslide initiation points.

The visual landslide interpretation was made using false colour composites or panchromatic images, using monoscopic image interpretation. Although stereoscopic image interpretation would be better for optimal landslide interpretation, it was practically not possible to generate stereo images for such an extensive area. In the interpretation we made use of the following diagnostic features (See also Fig. 5):

- The tone, defined as the relative brightness in a black/white image, or the colour in the false colour composite allowed differentiating unvegetated areas that are most indicative for recent landslides. Fig. 5a and b show examples how differences in colour can be used to indicate different landslide initiation areas.
- Texture relates to the frequency of tonal change. It is the result of the composite appearance presented by an aggregate of unit features too small to be recognized individually. This is illustrated in Fig. 5c and d.

- Pattern refers to the spatial arrangement of features and implies a characteristic repetition of certain forms or relationships. Fig. 5e and f give an example how this was used for identifying a series of individual initiation points in a large unvegetated area.

- Shape or form refers to the geometric aspects of the object in the image, and association refers to the occurrence of the object of study in combination with other objects that makes it possible to infer about its function or meaning. Fig. 5g and h indicate how unvegetated landslide initiation points were differentiated from other unvegetated areas, related to urban areas.

- Drainage disruption and existence of lakes were used to identify landslides that have dammed the rivers (see Fig. 5i). These were mapped as a subset of the entire landslide distribution.

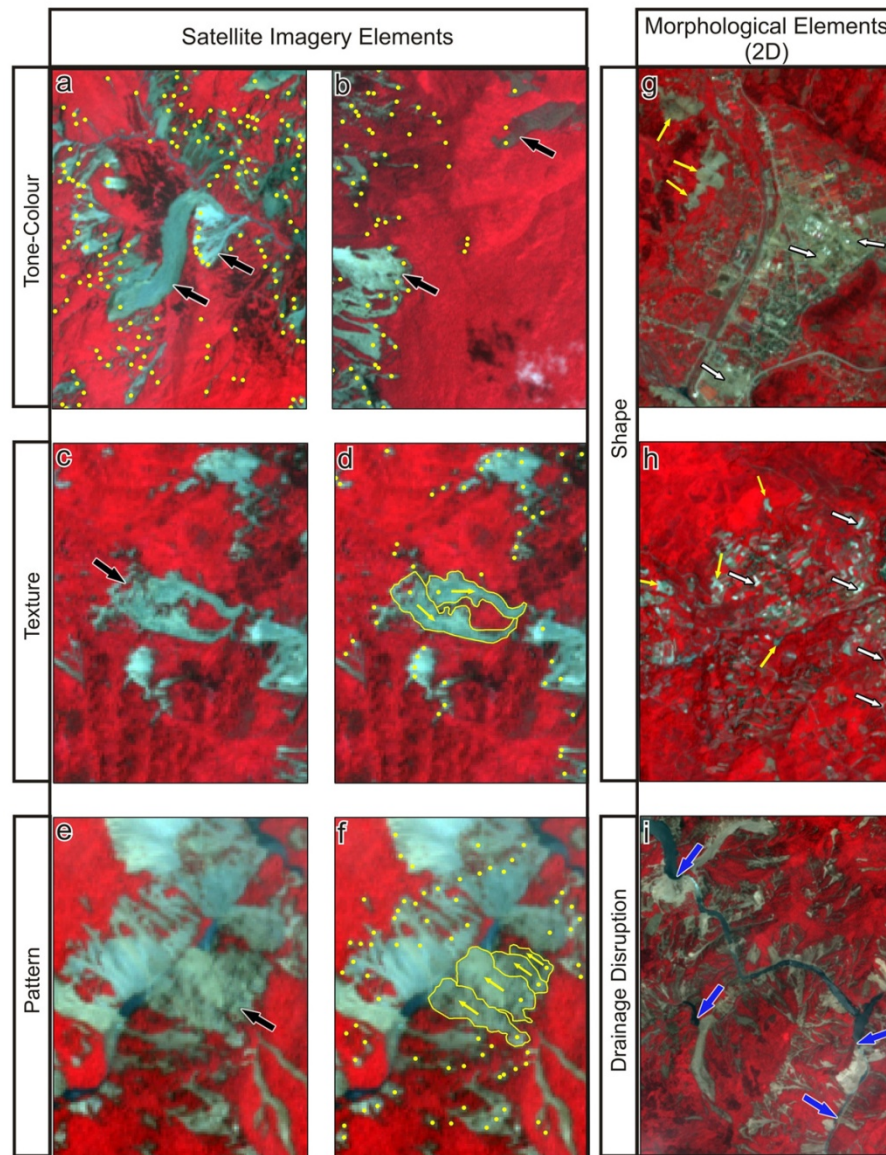


Figure 5. Use of image interpretation characteristics for the detection of landslide points. Initiation points are indicated with yellow points. White arrows indicate areas with high

reflectance values that are not considered as landslides. Yellow arrows indicated landslides direction, and black and blue arrows represent particular examples of satellite image and morphological (2D) elements. See text for explanation.

9.3 General Distribution Characteristics of Co-seismic Landslides

The Wenchuan earthquake produced landslides throughout an area of about 20,000 km², from which 8,000 km² was highly affected by landslides (Fig. 6). The landslide inventory map (See Fig. 6) shows a distinct pattern with higher landslide densities along the surface rupture of the faults and the banks of major rivers. The majority of landslides were concentrated on the hanging wall part of the Yingxiu-Beichuan fault and Pengguan fault, but with a higher density on the former.

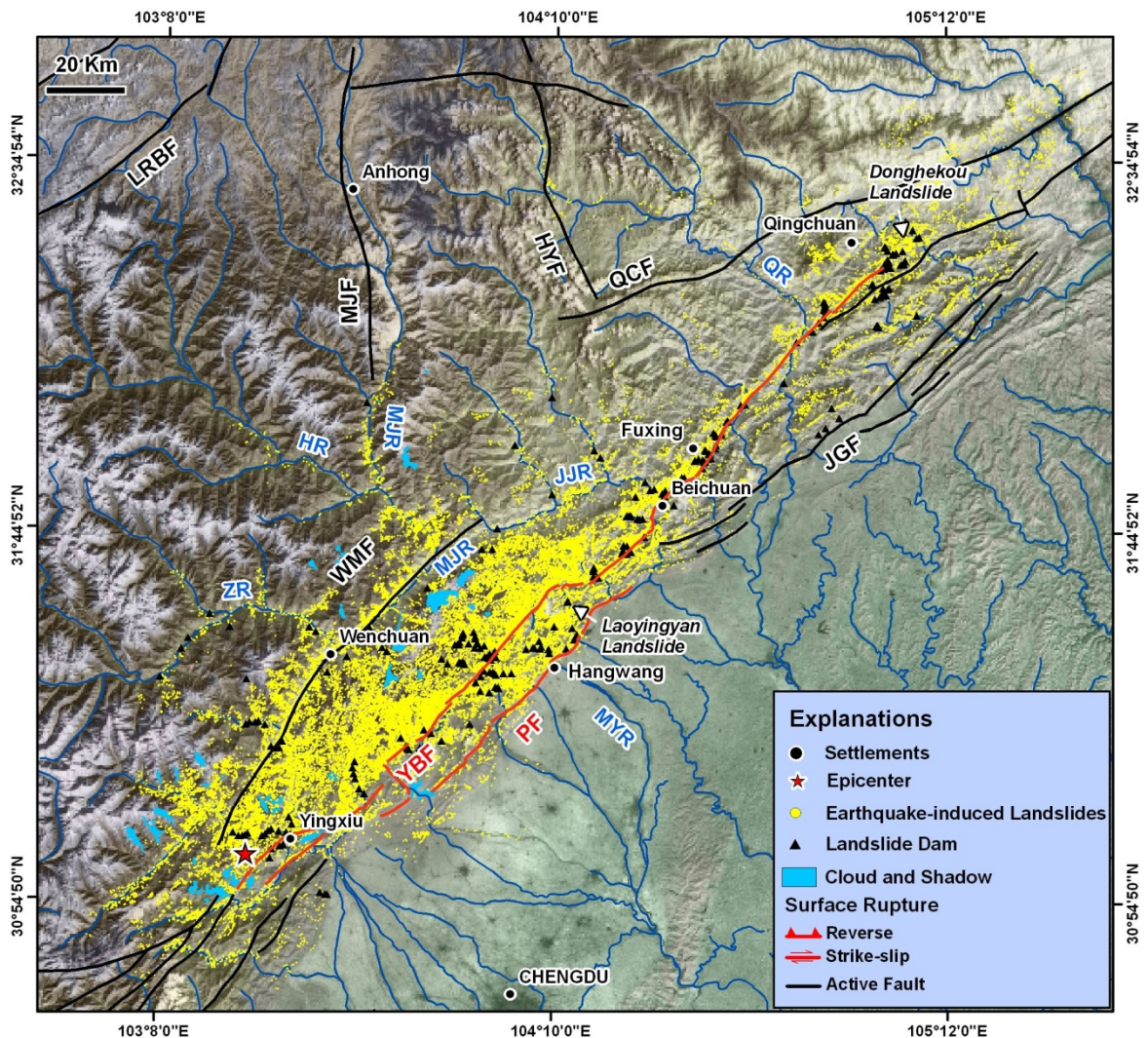


Figure 6. Landslide and landslide dam distribution map derived from this study. The map contains 60,104 landslide initiation points and 257 landslide dams. The following rivers are indicated: MJR: Minjiang River; ZR: Zagunao River; HR: Heishuehe River; MYR: Mianyuan River; JJR: Jianjiang River; QR: Qingzhu River. For fault names see Fig.1.

From the landslide inventory map, it can be observed that landslides are concentrated in a zone up to 100 km northeast of the epicenter, 15 km west and 4 km east of the fault rupture, and in a northeast-southwest direction along the co-seismic fault. Landslides are generally concentrated in the southwest and middle parts of the fault segments. More than 70 percent of the earthquake-induced landslides occurred in the area between Yingxiu and Beichuan towns, which is in agreement with the high vertical displacements measured by Xu et al. (2009) immediately after the earthquake. In addition, the distribution pattern of landslides was wider (~17 km) around the middle and southwest parts of the surface rupture (between Yingxiu and Beichuan towns) and became narrower (~3.5 km) after 10 km northeast of Beichuan (Fig. 7). Landslides are also frequent on the deeply incised valley side slopes along the Minjiang, Jianjiang, and Zagunao rivers. It is also remarkable how the landslide distribution patterns become much narrower after Beichuan (Fig. 6 and 7).

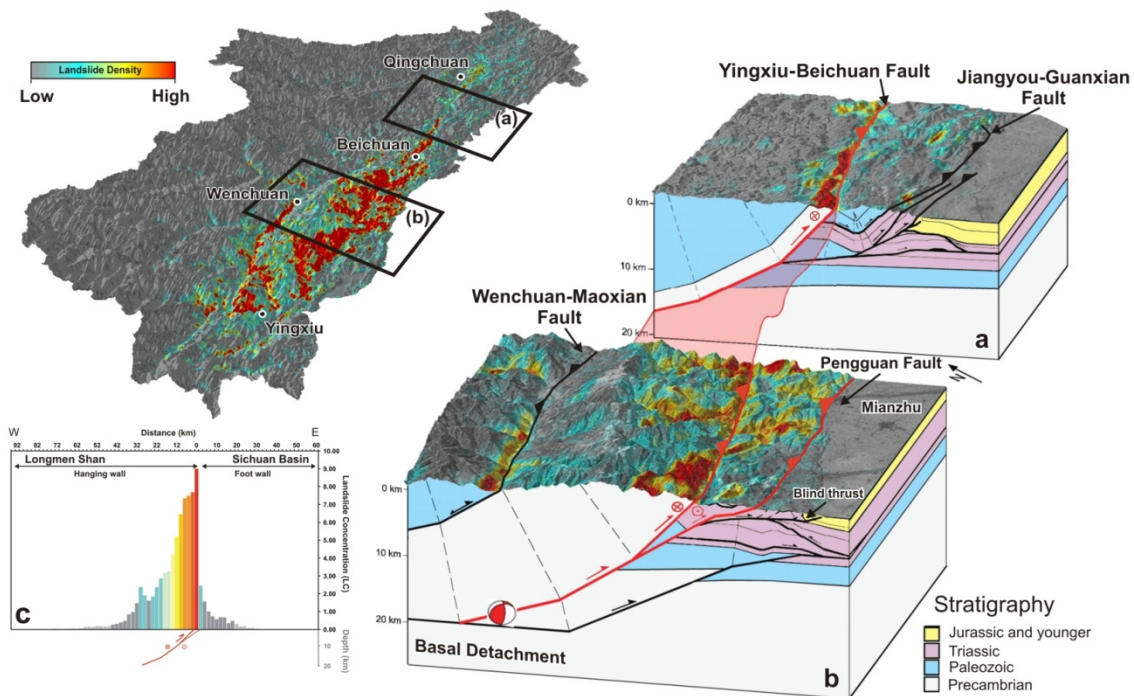


Figure 7. Three-dimensional model of co-seismic landslide distribution along the Longmen Shan mountain front. (a) Co-seismic landslide distribution pattern, fault geometry and lithology on the strike-slip segment of the fault, (b) Co-seismic landslide distribution pattern, fault geometry and lithology on the thrust segment of the fault (c) co-seismic landslide concentrations on hanging wall and foot wall areas. (Source of surface rupture, active faults and stratigraphy: Xu et al., 2009).

According to our field survey, most of the landslides are becoming smaller and shallower getting further away from the fault. This trend changes significantly around Wenchuan town and along Minjiang river (Fig. 6 and 7). On the other hand, the landslide density becomes considerably lower from East to West in the southwest section of the surface rupture and the density starts to increase again on both side slopes of the river. Similarly, the landslide density becomes less towards the side slopes of the Zagunao and Heishuihe rivers, which are tributaries

of the Minjiang River. The landslides along the Minjiang river show an asymmetric distribution pattern (Fig. 6 and 7). most of the landslides in this zone occurred on the hanging wall block of the Wenchuan-Maowen Fault, and from the image interpretation, using the pre-earthquake satellite images, it was determined that there were many active and dormant landslides before the earthquake (Fig. 8a and c). These landslides were re-activated by the Wenchuan earthquake (Fig. 8b and d). The presence of the Wenchuan-Maowen active fault (Densmore et al., 2007; Kirby et al., 2000) in this area and long-term tectonic deformation of this fault are considered to be the reason for this asymmetric distribution.

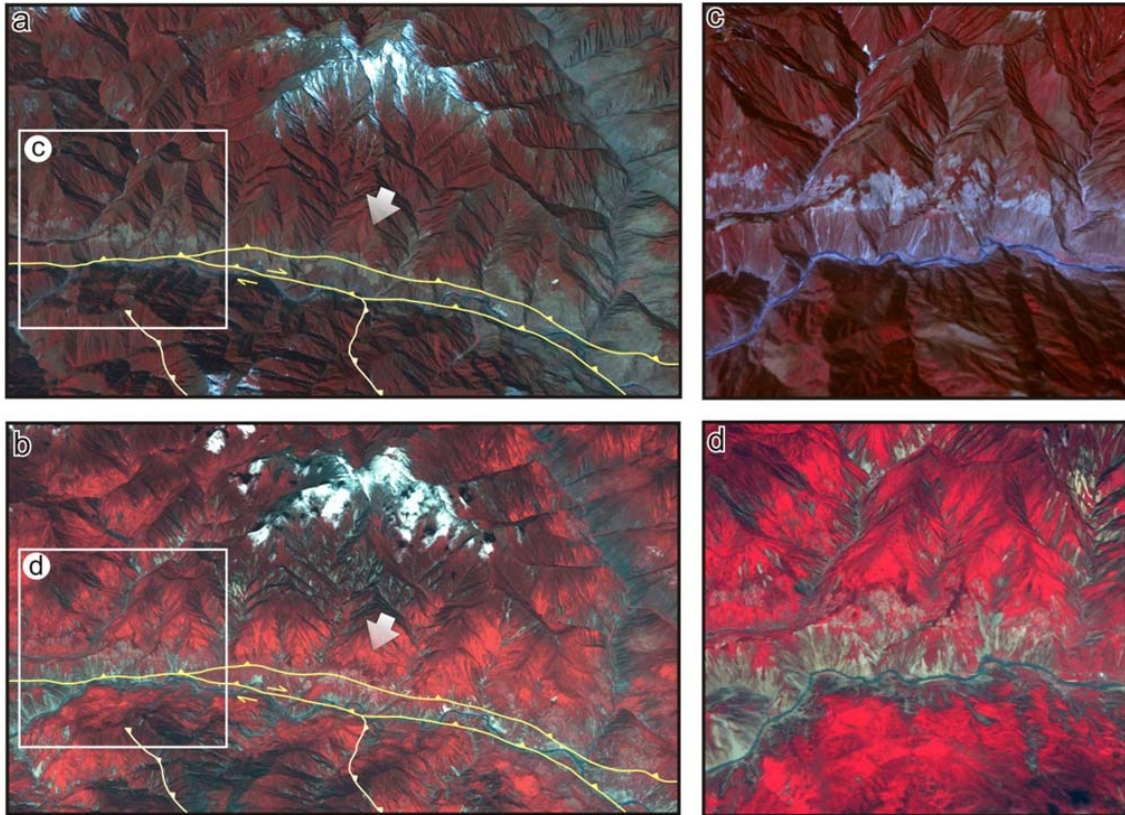


Figure 8. Pre- and Post-earthquake situation of the Wenchuan-Maowen active fault zone. (a) and (b) Pre- and Post-earthquake ASTER satellite images of the area, (c) and (d) Pre- and Post-earthquake detail view of the landslides along the Minjiang river.

The most common types of landslides were rockfalls, rock avalanches, and rock-debris slides in the area. Deep-seated large landslides were moderately common and these were abundant in the close vicinity of the fault rupture (Fig. 9). Most landslides were in highly fractured and jointed Precambrian aged crystalline and metamorphic rocks, weakly cemented and weathered Paleozoic aged sedimentary rocks and preexisting landslide deposits.



Figure 9. Examples of landslides triggered by the Wenchuan Earthquake. a: Large rockfalls and rock avalanches west slopes of the city of Hanwang; b: Large rockfalls (left and upper part of the tunnel) and multiple shallow narrow rock avalanches on steep (45-50°) slopes near to epicentral area (Yingxiu); c: Rockfalls and shallow to moderately deep rock avalanches and debris slides on the eastern side slopes of the Minjian River (Wenchuan County); d: Xiejadian rockslide-debris flow in the foreground and rock and debris falls in the background on the mountainous area; e: Large rock and debris slides, rock avalanches and shallow debris slides in Beichuan town. HW: Hanging wall, FR: Fault rupture trace.

The initiation parts for most of the landslides were very close to prolonged and narrow ridges. Areas with high internal relief show a larger landslide density than those with low relief. However, this difference generally varies depending on the distance to the fault and lithology.

Landslide density increases in areas where lithologies are highly susceptible to landslides, relatively close to the fault rupture, and with high relief and slope gradient. On the other hand, this situation changes 10 km northwest of Beichuan, where the co-seismic fault is transferred from a thrust component to a strike-slip component. Although the relief and slope gradient do not change significantly, the landslides are distributed in a narrow zone.

9.4 Analysis of Relations with Seismic and Geo-environmental Factors

The relation between the landslide distribution pattern was analyzed with three main types of factors: seismic (seismic source parameters and co-seismic slip), lithology and topographic factors. A statistical analysis was carried out using geologic maps digitally compiled by Chengdu Institute of Geology and Mineral Resources (2004) and a DEM produced by digitized contour lines from 1:50,000 scale topographic maps. In this study, the seismic factors were obtained from the China Earthquake Administration (CEA, 2008), Xu et al. (2009) and Shen et al. (2009), respectively.

The landslide concentration (C_L) index (Keefer, 2000; Wang et al., 2007) can be used to reflect the influence of landslide occurrence, which is defined as the number of landslides per square kilometer. Based on this definition, the analysis was conducted for an area of 34608.3 km² that contained 60,104 individual landslides. The average landslide concentration ($C_{L\text{ average}}$) in the study area was calculated and the result shows that it equals to 1.73/km² (60,104/34608.3 km²).

9.4.1 Relation with Seismic Factors

The relation of landslide (dam) concentration was investigated using three different seismic factors: the epicentral distance, the surface projection of the fault rupture (Xu et al., 2009), and the co-seismic slip (Shen et al., 2009). With the assistance of GIS, landslide concentration (C_L) and landslide dam concentration (C_{LD}) were determined for a sequence of concentric bands 2 km wide extending outward (buffer) from the source (epicenter and surface projection of the fault rupture).

Fig. 10a and b shows the variation of C_L and C_{LD} with epicentral distance. The highest C_L value was calculated as 8.4 landslides/km² in the area within 8 km from the epicenter. The highest C_{LD} value, 0.08 landslide dams/km², appeared in the area within 6 km from the epicenter. C_L values show significant peak values rather than decreasing gradually. These peaks are especially significant between the epicentral distances of 50-58, 80-96 and 224-230 km (Fig. 10a). Additionally, the standard error values of C_L and C_{LD} with epicentral distance are considerably high having values of 0.59 for C_L and 0.72 for C_{LD} respectively.

Contrary to other studies (Keefer, 2000; Khazai and Sitar, 2003; Wang et al., 2007) we found no obvious relation between the distance from the epicenter and C_L as well as C_{LD} (Fig. 10a and b). In other words, the landslide and landslide dam distribution are not controlled by the distance from the epicenter, and may be dominated by other factors.

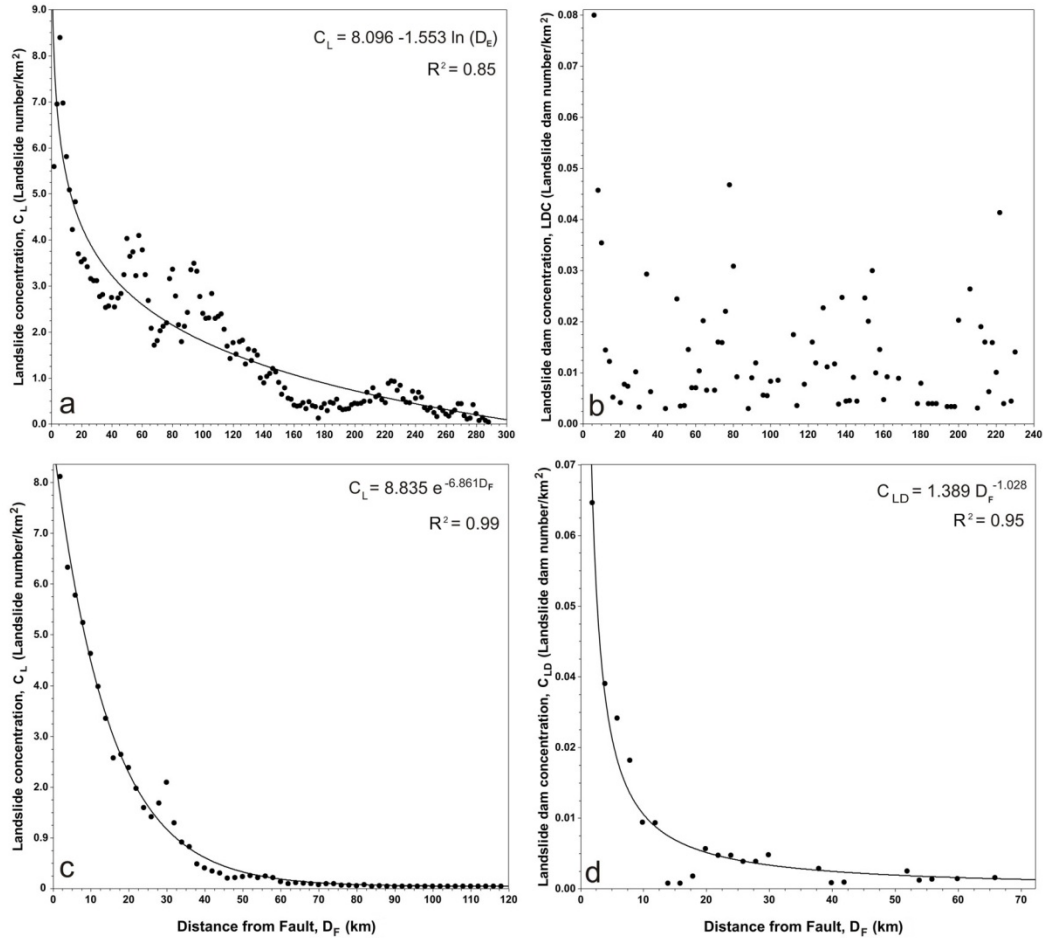


Figure 10. Relationship between landslide (dam) concentration and distance from epicenter and fault. a: Distance from epicenter for all landslides; b: Distance from epicenter for landslide dams; c: Distance from fault rupture for all landslides; d: Distance from fault rupture for landslide dams.

Fig. 10c and d show that the variation of C_L and C_{LD} has a strong inverse correlation with the distance from the surface rupture of the fault. C_L values descend from 8.0/km² at $D_F=2$ km to 5.2/km² at $D_F=8$ km, while C_{LD} values decrease from 0.066 landslide dams/km² at $D_F=2$ km to less than 0.012 landslide dams/km² at $D_F=10$ km. C_L and C_{LD} values are fitted best empirically with regression equations having an exponential form and power law form respectively, as shown in equation (1) and (2).

$$C_L = 8.835 e^{-6.861 D_F} \quad (R^2= 0.99, S=0.1801) \quad (1)$$

$$C_{LD} = 1.389 D_F^{-1.028} \quad (R^2=0.95, S=0.0029) \quad (2)$$

where, C_L and C_{LD} refer to landslides and landslide dams per square kilometer respectively, D_F is the distance to the surface projection of the fault rupture in kilometers, S is the standard error. Both the C_{LD} and C_L variation versus the distance from the ruptured fault show that the occurrences of landslides and landslide dams are strongly concentrated around the high seismic zone, near the ruptured fault zone. On the other hand, a peak of C_L is found at a distance of 28-

30 km from the surface rupture (Fig. 10c), corresponding to the Wenchuan-Maowen Fault Zone located along the Minjiang River. This is an active fault system at the western branch of the Longmenshan Thrust Fault, which is not ruptured during the Wenchuan earthquake. While the landslide density decreases gradually with increasing distance from the surface rupture, the density increases again in the 28-30 km distance band (Fig. 11).

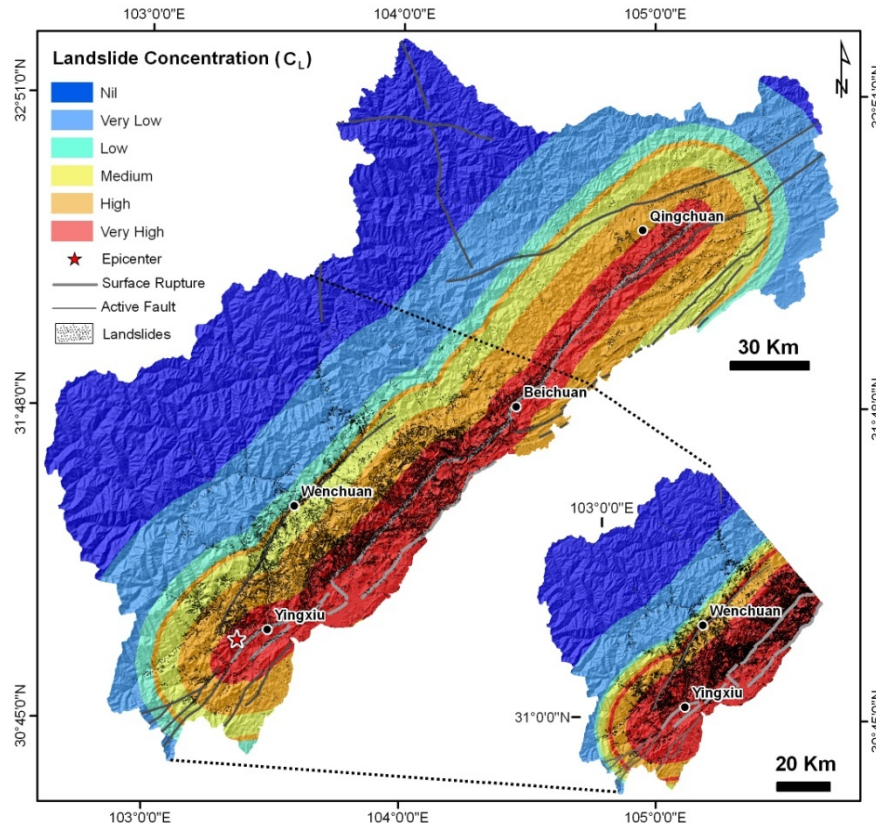


Figure 11. Landslide concentration in relation to the distance to the fault rupture.

For better visualization of this phenomenon, the map was cropped in the part where the Wenchuan-Maowen fault ends (NE). According to the map (Fig.11 inset map), C_L values are very high ($\sim 5.8/\text{km}^2$) up to 14 km distance from the surface rupture, while the C_L values decline to $\sim 3.6/\text{km}^2$ (High) between 14-26 km, and then increase again to very high C_L values in the 28 km distance band where Wenchuan-Maowen fault is located (Fig. 11). Besides the distance to the epicenter and surface rupture, the relation of C_L with co-seismic slip was investigated (Fig. 12). The landslide distribution pattern was compared with co-seismic slip values determined by Shen et al. (2009), which correspond with field measurements of slip-rate by Xu et al. (2009). Shen et al. (2009) have used Global Positioning System (GPS) and Interferometric Synthetic Aperture Radar (InSAR) data to infer fault geometry and slip distribution associated with the earthquake. Their study shows that the geometry of the fault changes from the epicenter to the Northwest. In the southwest part, the fault plane dips moderately to the Northwest but becomes nearly vertical in the Northeast. Associated with this is a change in the motion along the fault from predominantly thrusting to strike-slip. Peak slip along the fault occurs at the

intersections of fault segments located near the towns of Yingxiu, Beichuan and Nanba, where fatalities, damage, and landslides were highest (Shen et al., 2009).

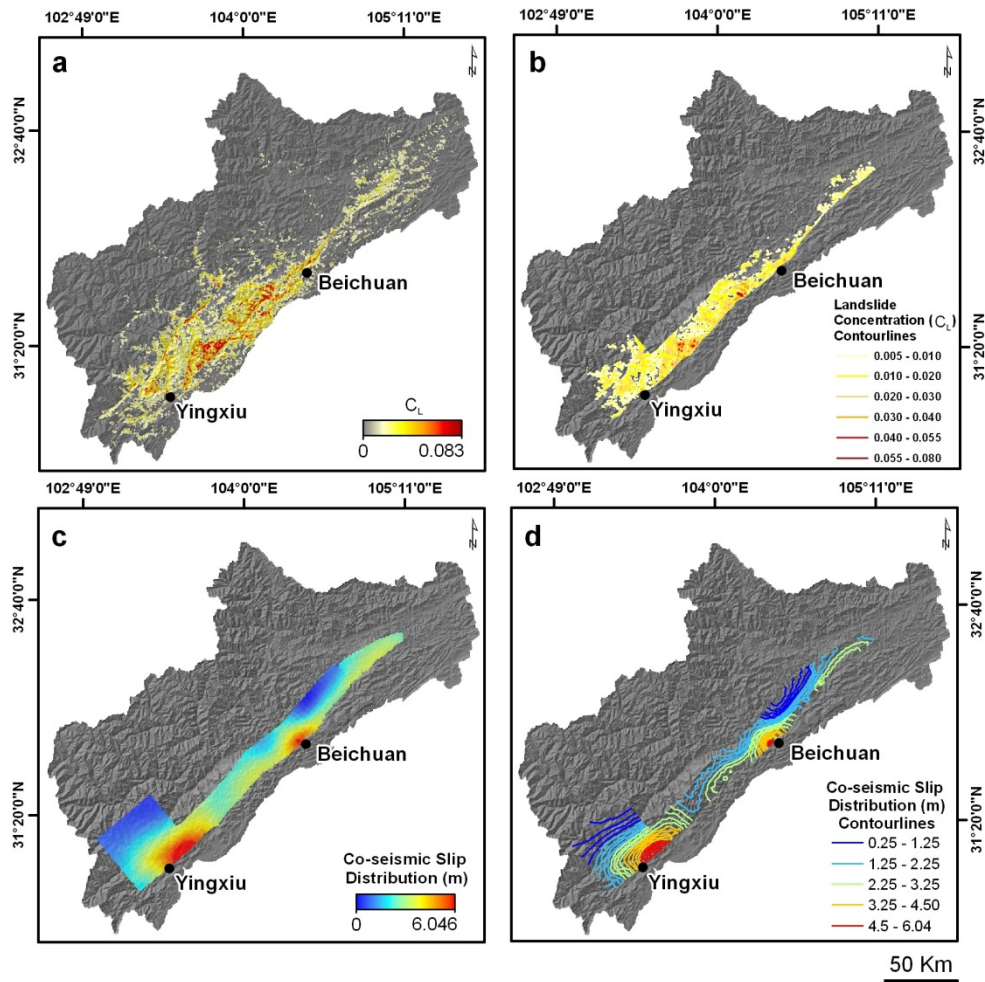


Figure 12. Landslide concentration in relation to the total co-seismic slip distribution of the fault rupture (co-seismic slip distribution model is from Shen et al. 2009). a: the landslide concentration; b: contour lines of landslide concentration clipped for the projected fault plane boundary; c: the co-seismic slip distribution; d: Contour lines of co-seismic slip distribution.

The co-seismic slip values determined by Shen et al. (2009) and the projection of co-seismic fault plane borders (surface and dip edge of Yingxiu-Beichuan fault rupture) were used in our study for the analyses of the landslide distribution pattern. C_L values which were calculated for the whole area (Fig. 12a) were clipped using the defined fault plane borders (Fig. 12b), and were depicted as isopleths. As a result, the C_L values range between 0.005-0.080 (Fig. 11b), with peak values at 35 km NE of Yingxiu and at 25 km SW of Beichuan town. When the results are compared with the co-seismic slip map (Fig. 12c), it is observed that these peak areas also correspond to the high co-seismic slip values. In addition, C_L values show a narrow pattern particularly in the zone starting 10 km NE of Beichuan town (Fig. 12c). There is a clear relation between the isopleths of landslide concentration and co-seismic slip values (Fig. 12d). As mentioned before, this area corresponds to the area where the fault geometry and the fault

plane dips degrees are almost vertical. Apart from this, in the SW part where the thrust component of the fault is high (Shen et al., 2009; Xu et al., 2009; Lin et al., 2009b), the fault plane dips is less steep and dips with an angle of 49° on average. In this zone landslides are distributed over a larger area as compared to the NE part. A statistical relation (Fig. 13) shows that landslide concentration increases with increasing co-seismic slip up to a certain maximum of 10 landslides/ km^2 .

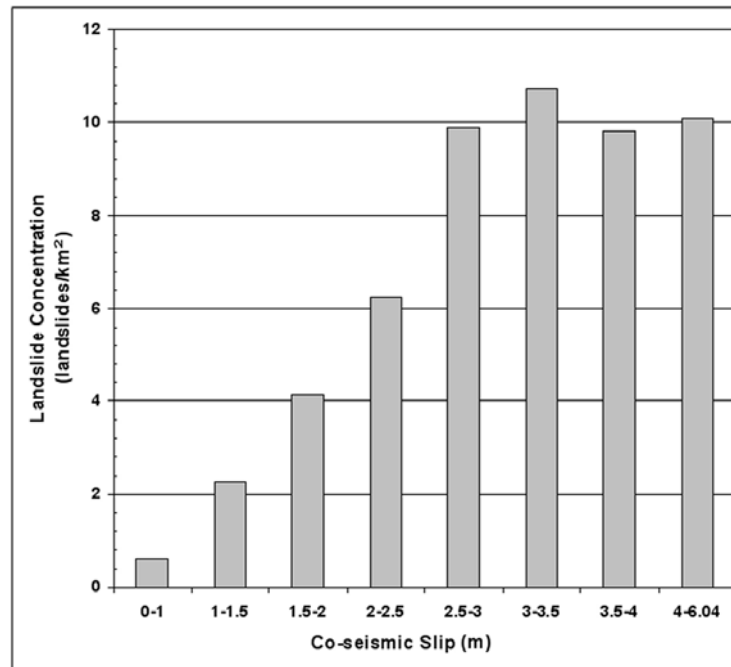


Figure 13. Relationship between landslide concentrations in relation to the total co-seismic slip.

On the other hand, it was observed that the landslide concentration is higher in the rate of $0.9/\text{km}^2$ in the class where the co-seismic slip is between 3-3.5m comparing to the other two classes where co-seismic slip is higher (3.5-4 and 4-6.04). The main reason for this difference is the high number of the landslides in the class of 3-3.5m co-seismic slip in spite of the small aerial coverage of these classes in the study area.

9.4.2 Relation with Lithology

For the analysis of the relation between landslides and lithology, the digitized geological map (1:250,000) compiled by the Chengdu Institute of Geology and Mineral Resources (2004) was used. The study area consists of seven main lithological units from the Mesozoic, Jurassic, Cretaceous, Paleozoic, Precambrian formations and three types of Quaternary sedimentary units (See Fig. 14). The rock masses along the ruptured fault are intensely fractured with a high joint density. Field investigation revealed that both the lithology and geological structure (joint density and the relation of discontinuity and slope orientation) play important roles in determining landslide types. For example, in Beichuan town, landslide types are mainly deep-seated rock slides in strongly weathered and fractured sandstone and mud-shale, while in Wenchuan town, the shallow rock slides in phyllite, limestone and granite are more common. Large rock avalanches mainly occurred in intensely cracked granite rock masses, such as in

Hongbai county in Shifang. The dominant types of landslides triggered by the earthquake are rock slides and rock avalanches, whereas soil slides were much less frequent.

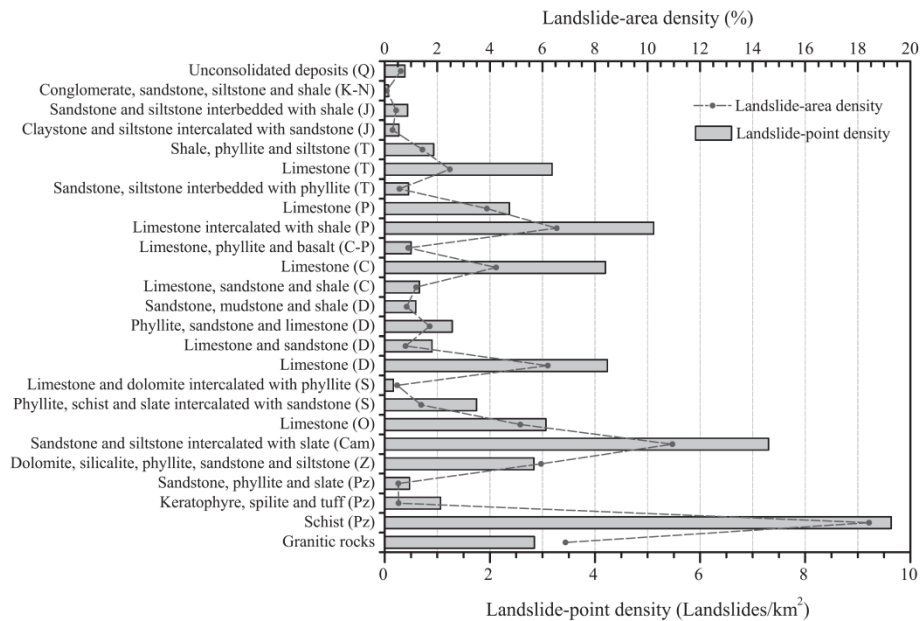


Figure 14. Landslide-point density and landslide-area density for lithological units (Dai et al., 2010).

As shown in Fig. 14, the area of mapped landslides covers lithology from Pre-Sinian rocks to Quaternary sediments. It can be found that slopes composed of Pre-Sinian schist, and Cambrian sandstone and siltstone intercalated with slate have the most concentrated landslide activity, followed by Permian limestone intercalated with shale and Devonian limestone (Dai et al., 2010). Pre-Sinian schist, or Cambrian sandstone and siltstone intercalated with slate generally have low shear strength and are heavily fractured, as observed in the field, resulting in most concentrated landsliding on those slopes consisting of these weak and fragmented rocks. Furthermore, slopes consisting of limestone, or limestone intercalated with shale, or granitic rocks are relatively more susceptible to earthquake-triggered failure. These rocks are generally hard, but rock mass is fragmented (Dai et al., 2010). The slopes composed of these rocks are generally steep, and prone to rockfall.

9.4.3 Relation with Terrain Factors

Three groups of terrain factors were considered for a descriptive statistical analysis of their relation with earthquake-induced landslides: altitude, slope gradient, and aspect. Detailed information on the generation of these factors from DEMs is provided by Wilson and Gallant (2000) and Hengl and Reuter (2009). Altitude does not seem to be an important factor for landslide occurrence. In the study area, altitudes vary between 500 m and 5940 m, whereas grid cells with landslides are observed between 600 m and 4900 m. While the mean altitude value of the area is calculated as 2361 m, on the grid cells with landslides the average value of this parameter is obtained as 1936 m. These simple descriptive statistics reveal that the landslides in the study area tend to occur on the moderately high mountainous terrains of the

Longmenshan range. The second terrain factor examined in this study is slope gradient. The mean values show a considerable dissimilarity between the grid cells with landslides and without landslides (30.76° and 26.19° respectively). Thus, it can be concluded that the recent landslides in the region commonly occurred on the grid cells having moderately high values of slope gradients.

Slope aspect may have an effect on landsliding because it is related to such factors as directional peak ground accelerations. It can be found that the eastern and southeastern facing slopes have relatively higher landslide concentration values than other directions. Li et al. (2008) found that peak ground accelerations in the EW direction are slightly higher than those in the NS direction. For example, the maximum accelerations recorded at the Wolong station, 18 km NWW of the epicenter, were 957.7 Gal, 652.9 Gal, and 948.1 Gal, for EW, NS, and UD, respectively, and accelerations at the Qingping station, 90 km NE of the epicenter, were 824.1 Gal, 802.7 Gal, and 622.9 Gal, for EW, NS, and UD, respectively (Li et al., 2008). This is in accordance with the preferred direction of landslide occurrence.

9.5 Discussion and Conclusion

This study aimed to generate a comprehensive data base of landslides triggered by the Wenchuan earthquake, based on multi-temporal image interpretation, and to correlate these with seismic and environmental factors. The landslide interpretation focused on the mapping of landslide scar areas in the very extensive area covering around 35,000 km². Unfortunately it was not possible to use stereo image interpretation techniques, due to time constraints and the unavailability of a high resolution DEM for generating the stereo images. Given the above mentioned constraints a database was generated containing more than 60,000 individual landslides (Gorum et al., 2010) with a total area of 811 km² (Dai et al., 2010), which were triggered by the Wenchuan earthquake. The main types of landslides include shallow, disrupted landslides, rock falls, deep-seated landslides, and rock avalanches. Most of the landslides occurred along the major surface rupture, and were concentrated on the hanging wall of the rupture.

The event might be one of the largest numbers of landslides triggered by a single earthquake event in historical times. Recent other earthquakes in mountainous areas triggered substantially less landslides: the Northridge earthquake (M_w=6.7, 1994) triggered around 11,000 landslides (Harp and Jibson, 1995), the Chi Chi earthquake (M_w=7.6, 1999) which caused 22,000 landslides (of which 9272 larger than 625m²) affecting an area of 128 km², and the Kashmir earthquake (M_w=7.6, 2005) caused only 2252 landslides (larger than 625 m²) (Dunning et al., 2007). The earthquake also triggered more landslides than the ones reported by recent hurricane events, such as Hurricane Mitch which caused over 9594 landslides in Guatemala, and comparable numbers in Honduras and El Salvador (Bucknam et al., 2001).

In our study we found that the distribution of earthquake-induced landslides for the Wenchuan earthquake is primarily controlled by the fault rupture. The landslide distribution shows a very distinct “hanging wall” effect, and most of events occurred within a 10 km range from the fault. It is observed that the 57% of all landslides occurred on the hanging wall of the Yingxiu-Beichuan fault and 13% on that of the Pengguan fault.

The distribution of landslides is within two main concentration zones; one is the area along the co-seismic rupture, and the other is along the deeply incised valley side slopes such as the Minjiang River. Besides of these, the landslide distribution patterns changes significantly NE of Beichuan town and has a narrowing pattern. This narrowing of the high density landslide area could be explained well with the change in fault geometry. The main thrust component transfers to a strike-slip component 10 km after Beichuan town (Xu et al., 2009; Lin et al., 2009b) and the fault dip angle changes from approximately 45° in the southwest to 65-80° after Beichuan town.

The landslides along the Minjiang River show a clear asymmetric distribution pattern. According to our field survey, most of the landslides in this zone occurred on the hanging wall block of the Wenchuan-Maowen Fault, and from the image interpretation, using the pre-earthquake satellite images, it was determined that there were many active and dormant landslides before the earthquake. These landslides were re-activated by the Wenchuan earthquake. The presence of Wenchuan-Maowen active fault (Densmore et al., 2007; Kirby et al., 2000) in this area and the long-term tectonic deformation of this fault can be considered as the reason for this asymmetric distribution. In this regard, long-term tectonic deformation characteristics and the existence of active faults, which were not ruptured during earthquake, are important in terms of earthquake-induced landsliding.

Although there is also a relation with lithology, the correlation of landslide concentration with lithology shows that slopes composed of Pre-Sinian schist, or Cambrian sandstone and siltstone intercalated with slate are most susceptible to earthquake-triggered failure.

Looking at the landslide distribution in terms of terrain factors, it is observed that 53.2 % of the earthquake-induced landslides occurred in the transition zone between highly dissected hilly topography and moderately high mountainous topography. This transition zone is observed between 1750-1950m and expresses moderately high topographic slope (30°-32°), convex slope and moderately rough characteristics in terms of terrain factors, curvature and terrain roughness values relatively. It was determined that the areas with such terrain values also relate with the high landslide density areas. More detailed analysis of terrain factors will be carried out after generating a DEM with a higher spatial resolution than the one used in this study which had a resolution of only 90 by 90 meters. We intend to use pre- and post earthquake DEMs in analyzing the volumes and sizes of the affected landslides. We also are currently working on the visual interpretation of the pre- and post earthquake images in order to characterize the landslides according to types and causal mechanisms.

Acknowledgements

This research was financially supported by the National Basic Research Program “973” Project of the Ministry of Science and Technology of the People’s Republic of China (2008CB425801), and by the United Nations University – ITC School for Disaster Geo-Information Management (www.itc.nl/unu/dgim). The authors acknowledge Prof. Li Yong, Dr. Liu Hanfu, Mr. Chen Wei and Mr. Li Weile from Chengdu University of Technology in China for their suggestions and supports during the fieldwork. We appreciate that the Japan Aerospace Exploration Agency (JAXA), GeoEye foundation, and Indian Space Research Organisation (ISRO) for providing the data for this research. We’d like to give our special thanks to Niek Rengers for his efforts on the

collaboration between ITC and the State Key Laboratory of Geo-hazard Prevention, Chengdu University of Technology, and to Oliver Korup for his constructive and helpful comments.

References

- Bucknam, R.C., Coe, J.A., Mota, A., Godt, J.W., Tarr, A.C., Bradley, L.-A., Rafferty, S., Hancock, D., and Dart, R.L.,(2001) Landslides triggered by Hurricane Mitch in Guatemala - Inventory and discussion: U.S. Geological Survey Open-File Report 01-443, 40 p., 23 plates.
- Burchfiel, B.C., Royden, L.H., van der Hilst, R.D., Hager, B.H., Chen, Z., King, R.W., Li, C., Lu, J., Yao, H., Kirby, E., 2008. A geological and geophysical context for the Wenchuan earthquake of 12 May 2008, Sichuan, People's Republic of China. *GSA Today* 18 (7), 4-11.
- China Earthquake Administration (CEA), 2008. Magnitude of the 12 May 2008 Wenchuan Earthquake and aftershocks.
http://www.cea.gov.cn/manage/html/8a8587881632fa5c0116674a018300cf/_content/09_02/02/1233562387132.html
- Chengdu Institute of Geology and Mineral Resources, 2004. Geological Map of the Qinghai-Xizang (Tibet) Plateau and Adjacent Areas, Map, Geological, Beijing.
- Cui, P., Zhu, Y.Y., Han, Y.S., Chen, X.Q., Zhuang, J.Q., 2009. The 12 May Wenchuan earthquake-induced landslide lakes: distribution and preliminary risk evaluation. *Landslides* 6 (3), 209-223.
- Dai, F.C., Xu, C., Yao, X., Xu, L., Tu, X.B., Gong Q.M., 2010. Spatial distribution of landslides triggered by the 2008 Ms 8.0 Wenchuan earthquake, China. *Journal of Asian Earth Sciences* (2010), doi:10.1016/j.jseaes.2010.04.010
- Densmore, A.L., Ellis, M.A., Li, Y., Zhou, R., Hancock, G.S., Richardson, N., 2007. Active tectonics of the Beichuan and Pengguan fault at the eastern margin of the Tibetan Plateau. *Tectonics* 26 (2007), p. TC4005, doi:10.1029/2006TC001987.
- Dunning, S.A., Mitchell, W.A., Petley, D.N., Rosser, N.J., Cox, N.J., 2007. Landslides predating and triggered by the 2005 Kashmir earthquake: rockfall to rock avalanches. *Geophys. Res. Abstr.* 9, 06376.
- Galli, M., Ardizzone, F., Cardinali, M., Guzzetti, F., Reichenbach, P., 2008. Comparing landslide inventory maps. *Geomorphology* 94, 268-289.
- Guzzetti, F., Cardinali, M., Reichenbach, P., Carrara, A., 2000. Comparing landslide maps: a case study in the upper Tiber River Basin, Central Italy. *Environmental Management* 25 (3), 247-363.
- Guzzetti, F., 2005, Landslide Hazard and Risk Assessment. Unpublished PhD Thesis, University of Bonn, November 2005, 389 pp.
- Harp, E.L. and Jibson, R.L., 1995. Inventory of landslides triggered by the 1994 Northridge, California earthquake, U.S. Geological Survey Open-file Report, 1995: 95-213.
- Harp, E.L. and Crone, A.J., 2006. Landslides Triggered by the October 8, 2005, Pakistan Earthquake and Associated Landslide-Dammed Reservoirs. U.S. Geological Survey Open-file Report, 2006: 1052-1065.
- Hengl, T., Reuter, H.I., (Eds.), 2008. *Geomorphometry : concepts, software, applications* Developments in soil science v. 33. Elsevier Science publisher, Amsterdam, 765 pp.
- Hsu, Y.J., Bechor, N., Segall, P., Yu, S.B., Kuo, L.C., Ma, K.F., 2002. Rapid afterslip following the

- 1999 Chi-Chi, Taiwan Earthquake. *Geophysical Research Letters* 29 (16) (2002), DOI:10.1029/2002GL014967.
- Huang, R.Q., Li, W.L., 2009. Analysis of the geo-hazards triggered by the 12 May 2008 Wenchuan Earthquake, China. *Bulletin of Engineering Geology and the Environment* 68, 363-371.
- Jibson, R.W., Harp, E.L., Michael, J.A., 2000. A method for producing digital probabilistic seismic landslide hazard maps. *Engineering Geology* 58, 271-289.
- Jin, W., Tang, L., Yang, K., Wan, G., Lü, Z., and Yu, Y., 2009. Tectonic evolution of the middle frontal area of the Longmen Mountain thrust belt, western Sichuan basin, China. *Acta Geologica Sinica* 83 (1), 92-102.
- Keefer, D.K., 1984. Landslides caused by earthquakes. *Geological Society of America Bulletin* 95, 406-421.
- Keefer, D.K., 2000. Statistical analysis of an earthquake-induced landslide distribution the 1989 Loma Prieta, California event. *Engineering Geology* 58, 231-249.
- Kothe, R., Lehmeier, F., 1993. SAGA – Ein Programmsystem zur Automatischen Relief-Analyse. *Zeitschrift für Angewandte Geographie*, 4 11-21.
- Li, X.J., Zhou, Z.H., Huang, M., Wen, R.Z., Yu, H.Y., Lu, D.W., Zhou, Y.N., Cui, J.W., 2008. Preliminary analysis of strong-motion recordings from the Magnitude 8.0 Wenchuan, China, earthquake of 12 May. *Seismological Research Letters* 79 (6), 844-854.
- Li, Q., Gao, R., Wang, H., Zhang, J., Lu, Z., Li., P., Guan, Y., Guan,Y. and He, R., 2009. Deep background of Wenchuan earthquake and the upper crust structure beneath the Longmen Shan and adjacent areas. *Acta Geologica Sinica* 83 (4), 733-739.
- Li, Y., Allen, P.A, Densmore, A.L. and Xu., Q, 2003. Evolution of the Longmen Shan Foreland Basin (western Sichuan, China) during the Late Triassic Indosinian Orogeny, *Basin Research* 15, 117-138.
- Li, Y., Zhou, R., Densmore, A.L., Ellis, M.A., Yan, L., Dong, S., Richardson, N., Zhang, Y., He, Y., Chen, H., Qiao, B., Ma, B., 2008. Geological background of Longmen Shan seismic belt and surface rupture in Wenchuan earthquake, *Zhongguo Lixue Wenzhai* 22 (4), 1-12 (in Chinese).
- Lin, A., 2009a. Geometry and Slip Distribution of Co-seismic Surface Ruptures Produced by the 2001 Kunlun, Northern Tibet, Earthquake. In: Fukuyama, E. (Ed.), *Fault-Zone Properties and Earthquake Rupture Dynamics*. Elsevier Academic Press, California, pp. 15-36.
- Lin, A., Ren, Z., Jia, D., Wu, X., 2009b. Co-seismic thrusting rupture and slip distribution produced by the 2008 Mw 7.9 Wenchuan earthquake, China. *Tectonophysics* 47, 203-215.
- Malamud, B.D. Turcotte, D.L. Guzzetti, F., and Reichenbach, P., 2004. Landslides, earthquakes, and erosion. *Earth and Planetary Science Letters* 229 (1-2), 45-59.
- Mantovani, F., Soeters, R. and van Westen, C.J., 1996. Remote sensing techniques for landslide studies and hazard zonation in Europe. *Geomorphology* 15 (3-4), 213-225.
- Martha, T.R., Kerle, N., Jetten, V., van Westen, C.J., Kumar, K.V., Characterising spectral, spatial and morphometric properties of landslides for semi-automatic detection using object-oriented methods, *Geomorphology* 116 (1-2), 24-36.
- Metternicht, G., Hurni, L. and Gogu, R., 2005. Remote sensing of landslides: An analysis of the potential contribution to geo-spatial systems for hazard assessment in mountainous environments. *Remote Sensing of Environment* 98 (2-3), 284-303.
- Rengers, N., Soeters, R. and van Westen, C.J., 1992. Remote Sensing and GIS applied to

- mountain hazard mapping. *Episodes* 15 (1), 36-46.
- Rodriguez, C.E., Bommer, J.J., Chandler, R.J., 1999. Earthquake-induced landslides: 1980-1997. *Soil Dynamics and Earthquake Engineering* 18, 325-346.
- Sato, H.P., Harp, E.L., 2009. Interpretation of earthquake-induced landslides triggered by the 12 May 2008, M7.9 Wenchuan earthquake in the Beichuan area, Sichuan Province, China using satellite imagery and Google Earth. *Landslides* 6 (2), 153-159.
- Shen, Z., Sun, J., Zhang, P., Wan, Y., Wang, M., Bürgmann, R., Zeng, Y., Gan, W., Liao, H., Wang, Q., 2009. Slip maxima at fault junctions and rupturing of barriers during the 2008 Wenchuan earthquake, *Nature Geoscience* 2, 718-724, DOI:10.1028/NGEO636.
- Tang, L., Yang, K., Jin, W., Wan, G., Lü, Z. and Yu, Y., 2009. Differential tectonic deformation of the Longmen Mountain thrust belt, western Sichuan Basin, China. *Acta Geologica Sinica* 83 (1),158-169.
- U.S. Geological Survey, 2008. Magnitude 7.9 - Eastern Sichuan, China, 2008 May 12 06:28:01 UTC. <http://earthquake.usgs.gov/earthquakes/eqinthenews/2008/us2008ryan/>
- van Westen, C.J., Seijmonsbergen, A.C., Mantovani, F., 1999. Comparing landslide hazard maps. *Natural Hazards* 20 (2-3), 137-158.
- van Westen, C.J., Castellanos Abella, E.A., Sekhar, L.K., 2008. Spatial data for landslide susceptibility, hazards and vulnerability assessment: an overview. *Engineering Geology* 102 (3-4), 112-131.
- Wang, F.W., Cheng, Q.G., Highland, L., Miyajima, M., Wang, H.B., Yan, C.G., 2009. Preliminary investigation of some large landslides triggered by the 2008 Wenchuan earthquake, Sichuan Province, China. *Landslides* 6 (1), 47-54.
- Wang, E. and Meng, Q., 2009. Mesozoic and Cenozoic tectonic evolution of the Longmenshan fault belt. *Science in China Series D: Earth Science* 52, 579-592.
- Wang, G.Q., Liu, F., Fu X.D., Li T.J., 2008. Simulation of dam breach development for emergency treatment of the Tangjiashan Quake Lake in China. *Science in China Series E: Technological Sciences* 51 (2), 82-94.
- Wang, H.B., Sassa, K., Xu, W.Y., 2007. Analysis of a spatial distribution of landslides triggered by the 2004 Chuetsu earthquakes of Niigata Prefecture, Japan. *Natural Hazards* 41 (1), 43-60.
- Weirich, F. and Blesius, L., 2007. Comparison of satellite and air photo based landslide susceptibility maps. *Geomorphology* 87(4), 352-364.
- Wilson, J.P., Gallant, J.C., 2000. *Terrain analysis principles and applications*. Wiley, Toronto Canada, 479 pp.
- Xu, G., and Kamp, P. J. J., 2000. Tectonics and denudation adjacent to the Xianshuihe fault, eastern Tibetan Plateau: Constraints from fissiontrack thermochronology, *Journal of Geophysical Research* 105, 19231-19251
- Xu, Q., Fan, X.M., Huang, R.Q., Westen, C.V., 2009. Landslide dams triggered by the Wenchuan earthquake, Sichuan Province, south west China. *Bulletin of Engineering Geology and the Environment* 68 (3), 373-386.
- Xu, X., Wen, X., Yu, G., Chen, G., Klinger, Y., Hubbard, J., Shaw, J., 2009. Coseismic reverse- and oblique-slip surface faulting generated by the 2008 Mw 7.9 Wenchuan earthquake, China. *Geology* 37, 515-518
- Yagi, H., Sato, G., Higaki, D., Yamamoto, M., Yamasaki, T., 2009. Distribution and characteristics of landslides induced by the Iwate-Miyagi Nairiku Earthquake in 2008 in Tohoku District,

Northeast Japan. Landslides (inpress), DOI 10.1007/s10346-009-0182-3.

Yin, Y., Wang, F., Sun, P., 2009. Landslide hazards triggered by the 2008 Wenchuan earthquake, Sichuan, China. *Landslides* 6 (2), 139-152.

Zhang, Y., Dong, S. and Yang, N., 2009. Active faulting pattern, present-day tectonic stress field and block kinematics in the East Tibetan Plateau. *Acta Geologica Sinica*, 83(4): 694-712

Zhou, D., Graham, S. A., 1996. Songpan-Ganzi Triassic flysch complex of the West Qinling Shan as a remnant ocean basin, in *The Tectonic Evolution of Asia*, A. Yin and M. Harrison (Eds.) 281-299, Cambridge Univ. Press, New York.

CHAPTER 10 DISCUSSION AND CONCLUSIONS

Runqiu Huang¹, Cees van Westen², Xuanmei Fan^{1,2}, Qiang Xu¹, Niek Rengers², Chuan Tang¹

¹State Key Laboratory of Geohazards Prevention, Chengdu University of Technology, China

²Faculty of Geo-information Science and Earth Observation, University of Twente, Netherlands

Landslides occur frequently in China. Especially, in the western part of China, large-scale landslides are notable for their scale, complex formation mechanism, and serious destruction. With this respect, carrying out landslide hazard and risk assessment with appropriate and effective method is extremely important for landslide prevention and management as well as development planning.

In the previous chapters, the experiences and practices in landslide risk and hazard assessment in the Mainland of China and Hongkong were presented. Since conclusions were summarized after each previous chapter, it's not necessary to repeat here. Instead, we would like to conclude the different aspects with Chinese characteristics, which are different from other countries, and the strong points and weak points of the method that we used in China. What should be improved in future is also an important issue that we should concern. During the workshop on "The state of art of landslide hazard and risk assessment" in Chengdu, a discussion section forum was organized. Some most important issues were discussed:

(1) Since China is a huge country, how to harmonize the landslide hazard and risk assessment methods used in China?

Nowadays, under the organization of China Geological Survey, Institute of Geology, Chinese Academy of Geological Sciences is creating a landslide risk assessment technical guideline. This guideline aims to standardize the methods used by different institutes and make people understand and do risk assessment better through following the procedures. The guideline will be completed in July, 2010. The guideline generally includes three levels (based on different scales) and four types of mapping (landslide inventory mapping, vulnerability, hazard and risk mapping). The three levels are:

① The first level is based on the scale of 1: 100 000. A national landslide inventory database was built up.

② The second level is based on the scale of 1: 50 000. This program was carried out by China Geological Survey.

③ The third level is based on the scale of 1: 10 000, mainly focusing on some specific areas with dense populations or important infrastructures and also threatened by landslides.

Once facing to the emergent situations, like very heavy rainfall and strong earthquakes, the pre-prepared emergent plan will be used.

The guideline also gives some typical examples of landslide risk assessment, presenting how to do it in practices by providing the practical procedures and the basic rules. For different scales landslide mapping, the guideline also recommends the suitable methods.

(2) With respect to the three levels (based on different scales) landslide mapping and inventory, nowadays which methods are used most commonly and effectively?

Up to date, for the first level landslide inventory (1: 100 000), because both the landslide number and inventory area are very large, it's not practical for the professional teams to map every one. Thus, landslides were first reported by local government to related geological institute with location, general size, damages etc, and then the professional team will go to field to check. At this scale, landslides are usually mapped as points. For the second level landslide inventory (1: 50 000), the method is quite different from the first level, it mainly depends on the remote sensing technique. Related satellite images were first collected. SPOT 5 are most commonly used for landslide interpretation. And then, geologists will go to field to check at least 70% of the interpretation results. At this scale, landslides are usually mapped as polygons. For the third level landslide inventory (1: 10 000), it mostly focuses on the densely populated counties, towns and cities, which are threatened by landslides. Detailed works are needed to be done, such as the drilling, field on-site and laboratory test, geophysical measures and so on.

(3) For the ancient landslides, how to get the information like the occurrence date, location, damages etc?

In China, plentiful of historical records and documents are available, which are managed by either the local government or the central government. Some of them can also be found in big libraries. In the national landslide database, around 40% of historical landslides have the accurate occurrence date record, which are very helpful for the landslide hazard assessment, regarding to the temporary probability.

(4) After the national landslide database was created, the database updating becomes an important issue. How is it practiced in China?

Unfortunately, the WebGIS is not so popularly used in China as in the European countries for the data updating. Due to the security concerns, any accurate location information is not allowed to publish on the website such as google earth in China, whereas Chinese government has its own way to solve this problem by taking advantage of the central governing policy. Every local government from the small village to big city has the strict responsibilities to report landslides to the higher level governments. Geo-hazard offices are set in all levels governments. The landslide first-hand information is usually collect by some well-trained people from the geo-hazard offices. Some of them are even professional geologists. They are also in charge of the database updating and using the database for managing the local landslide hazards. Besides, the provincial geological institute and universities are also involved in some programs, who are also invited to give the training courses on landslide inventory, early warning and simple monitoring methods to people work in the geo-hazard offices and others staffs, sometimes also to local people. Finally all the landslides should be reported to the highest ministry "Ministry of Land and Resources of the People's Republic of China".

(5) In China, especially after the Wenchuan earthquake, there are a lot of potential landslides, how the Chinese experts mapping these landslides?

The potential landslide inventory mapping actually is the landslide susceptibility mapping, which are commonly done by experts. They went to the field to collect information and

combined with some other previous information in the landslide area, such as geological, tectonic, hydrologic and historical data. Mostly based on their experience, sometimes also with assist of some models, they created the landslide susceptibility map. In fact, it is mainly based on the empirical method.

(6) What are other remote sensing data sources used in China?

High resolution satellite images are not commonly used in China for landslide mapping, again due to the security issues and poor data sharing condition. High resolution satellite images are seriously controlled by militaries, which are not open to even the researchers. Only for specific or small areas, high resolution images are available.

To summarize, landslide hazard and risk assessment in China have faced to a lot of challenges, because the large number of landslides, the huge area, the complex triggering factors and geological environments. Till now, Chinese government has finished the national landslide inventory and database creation at the 100 000 scale, which is the first stable step to the future detailed works on medium and large scale. There are both good experiences and lessons that we can obtain from China. The positive side is that Chinese government has more than enough power to fulfill a project or program from the central to the local government. Experienced experts support the government works very well. Public training and inspection played a very important role and also had good effect on landslide prevention and early warning. The negative side is that the very poor data shearing and too much concerns on security issues have made the work more difficult and less efficient.

ACKNOWLEDGEMENTS

The editors appreciate the State Key Laboratory of Geo-hazard Prevention (Chengdu University of Technology), Faculty of Geo-information Science and Earth Observation (University of Twente) and Norwegian Geotechnical Institute (NGI) for successfully organizing the workshop on “The state of art of landslide hazard and risk assessment in the P.R. of China” in Chengdu, China. We acknowledge all the Chinese experts who attended the workshop and contributed a lot for the chapter preparation for this report.

APPENDIX 1 OVERVIEW OF LANDSLIDE ORGANIZATIONS IN CHINA

Name	Address	Website
Ministry of Land and Resources of the People's Republic of China (中华人民共和国国土资源部)	Funei street, Xichenqu, Beijing, China (100812) 北京市西城区阜内大街 64 号	http://www.mlr.gov.cn
China Geological Survey (中国地质调查局)	45#, Fuwai street, Xichenqu, Beijing, China (100037) 中国北京市西城区阜外大街 45 号院	http://www.cgs.gov.cn
Institute of Geology and Geophysics, China Academy of Sciences (中国科学院地质与地球物理研究所)	19#, Beituxilu, Chaoyangqu, Beijing, China (100029) 北京市朝阳区北土城西路 19 号	http://www.igg.cas.cn 010-82998001
Chinese Academy of Geological Sciences (中国地质科学院)	16#, Baiwanzhuang street, Xichenqu, Beijing, China (100037) 北京市西城区百万庄大街 26 号	http://www.cags.ac.cn/ 010-68335853
Department of Geotechnical Engineering, China Institute of Water Resources and Hydropower Research (中国水利水电科学研究院)	20#, Chegongzhuang west road, Haidianqu (100044) 北京市海淀区车公庄西路 20 号	http://www.geoeng.iwhr.com/index.asp
Institute of Geology Chinese Academy of Geological Sciences (中国地质科学院地质研究所)	16#, Baiwanzhuang street, Xichenqu, Beijing, China (100037) 北京市西城区百万庄大街 26 号	http://igeo.cags.ac.cn/
Institute of Geomechanic, CAGS (中国地质科学院地质力学研究所)	11#, Education central university south road, Haidianqu, Beijing, China (100081) 北京市海淀区民族大学南路 11 号	http://www.geomech.ac.cn/ 010-68412303
Institute of Rock and Soil Mechanics, Chinese Academy of Sciences (中国科学院武汉沿途力学研究所)	2# Xiaohongshan, Shuiguohu street, Wuchangqu, Wuhan, Hubei Province, China 湖北省武汉市武昌区水果湖街小洪山 2 号	http://www.whrsm.ac.cn/
China Institute of Geo-Environment Monitoring (中国地质环境监测院)	20# Dahuisi, Haidianqu, Beijing, China (100081) 北京市海淀区大慧寺 20 号	http://www.cigem.gov.cn/ 010-62173424
Institute of Geology, China Earthquake Administration (中国地震局地质研究所)	Qijiahuozi, Deshenmengwai, Beijing, China (100029) 北京市德胜门外祁家豁子	http://www.eq-igl.ac.cn/ 010-62009001
Institute of Mountain Hazards and Environment, CAS (中国科学院水利部成都山地灾害与环境研究所)	9#, Renminnanlu, Chengdu, Sichuan Province (610041) 四川省成都市人民南路四段九号	http://www.imde.ac.cn/ 028-85228816
Institute of Geographic Sciences and Natural Resources Research, CAS (中国科学院地理科学与资源研究所)	11# Datunlujia, Chaoyangqu, Beijing, China (100101) 北京市朝阳区大屯路甲 11 号	http://www.igsrr.ac.cn/

Center for Earth Observation and Digital Earth Chinese Academy of Science (中国科学院对地观测与数字地球科学中心)	9#, Kediandasha, Zhongguancun Beiyitiao, Haidianqu, Beijing, China (100190) 北京市海淀区中关村北一条 9 号科电大厦	http://www.ceode.cas.cn/
School of Civil Engineering, Tsinghua University (清华大学土木水利学院)	Tsinghua Yuan, Beijing, China (100084) 北京市海淀区清华园	http://www.civil.tsinghua.edu.cn/ 010-62796770
State Key Laboratory of Geo-hazard Prevention and Geo-environment Protection, Chengdu University of Technology (成都理工大学地质灾害防治与地质环境保护国家重点实验室)	1# Erxianqiao Dongsanlu road, Chenghuaqu, Chengdu, Sichuan Province, China (610059) 四川省成都市成华区二仙桥东三路 1 号	http://www.sklgp.com/ 028-84073193
China University of Geosciences (中国地质大学)	388# Lumo road, Hongshanqu, Wuhan, Hubei Province, China (430074) 湖北省武汉市洪山区鲁磨路 388 号	http://www.cug.edu.cn/
Geological Society of China (中国地质学会)	26#, Baiwanzhuang street, Fuwai, Beijing, China (100037) 北京市阜外百万庄大街 26 号	http://www.geosociety.org.cn 010-68311539
Chinese Society for Rock Mechanics and Engineering (中国岩土力学与工程学会)	9825 Mailbox, Beijing, China (100029), TEL:010—82998163 北京 9825 信箱	http://www.csrme.com/CN/index.html

APPENDIX 2 LIST OF WORKSHOP PARTICIPANTS

Group photo



List of Participants

NO.	Name	Organization	Address	Email
1	Anders Solheim	Norges Geotekniske Institutt / Norwegian Geotechnical Institute (NGI)	P.O. Box 3930 Ullevål Stadion, 0806 Oslo	Anders.Solheim@ngi.no
2	Cees van Westen	UNU-ITC School on Geo-Information for Disaster Risk Management	University Twente, Faculty of Geo-Information Science and Earth Observation (ITC), PO Box 6, 75000 AA Enschede, The Netherlands	westen@itc.nl
3	Niek Rengers	The International Association for Engineering Geology and the Environment (IAEG)	Kortenaerstraat 15, 7513AC Enschede, the Netherlands	rengers@itc.nl

4	Tolga Gorum	International Institute for Geo-information Science and Earth Observation	7514 AE Enschede,P.O.Box 6,7500 AA Enschede,The Netherlands	gorum@itc.nl
5	WANG Gonghui	Kyoto University	Research Centre on Landslides, Disaster Prevention Research Institute, Kyoto University, Gokasho, Uji, Kyoto 611-0011, Japan.	wanggh@landslide.dpri.kyoto-u.ac.jp
6	HUANG Runqiu	State Key Laboratory of Geohazard Prevention and Geoenvironment Protection	1.Erxianqiao Dongsanlu, Chengdu University of Technology, Chengdu, 610059, Sichuan, China	hrq8037005@sohu.com
7	TANG Chuan	State Key Laboratory of Geohazard Prevention and Geoenvironment Protection	1.Erxianqiao Dongsanlu, Chengdu University of Technology, Chengdu, 610059, Sichuan, China	tangc707@gmail.com
8	CHEN Lixia	China University of Geosciences(Wuhan)	Room 601,School of Geophysics and Geomatics, China University of Geosciences, Hongshan district, Wuhan, Hubei province, China	ch_l_x@163.com
9	Fan Xuanmei	UNU-ITC School on Geo-Information for Disaster Risk Management	University Twente, Faculty of Geo-Information Science and Earth Observation (ITC),PO Box 6, 75000 AA Enschede, The Netherlands	fanxuanmei@gmail.com
10	HU Shiyou	Chengdu Center of China Geological Survey	2 Yihuanlu Beisanduan, Chengdu 610081, Chengdu , Sichuan, China	
11	LAN Hengxing	Institute of Geographic Sciences and Natural Resources Research, CAS	11 Datunlujia, Chaoyang District, Beijing 100101	lanhx@lreis.ac.cn lanhx@igsnr.ac.cn
12	SHI Jusong	Institute of Geology Chinese Academy of Geological Sciences	11 Nationality University Road, Haidian District, Beijing, China	shijusong@126.com
13	WANG Yingjie	State Key Lab. of Environment and Resources Information System Institute of Geographical Science & Natural Resources Research	11A, Datun Road, Chaoyang District, Beijing, 100101, China	wangyj@lreis.ac.cn

14	WU Shuren	Institute of Geology Chinese Academy of Geological Sciences	11 Nationality University Road, Haidian District, Beijing, China	shrwu@sohu.com
15	XU Qiang	State Key Laboratory of Geohazard Preverntion and Geoenviroment Protection	1.Erxianqiao Dongsanlu, Chengdu University of Technology, Chengdu, 610059, Sichuan, China	<u>xuqiang_68@126.com</u>